Quantifying Variability in Dynamic Cerebral Autoregulation in the Human Brain

DPhil Thesis

Department of Engineering Science

Linacre College

Thesis for the degree of

Doctor of Philosophy

Trinity Term 2023

Author

Yahya J Almuallem

Supervisors

Prof Stephen J Payne
Prof Alison Noble

Abstract

Introduction: The brain is a highly sophisticated system that operates dynamically which is in constant need of a continuous supply of oxygen and glucose via blood flow to sustain functionality and remain healthy. Despite changes in Arterial Blood Pressure (*ABP*), the blood pressure and flow are maintained at certain levels within the human cranium using a mechanism called dynamic Cerebral Autoregulation (dCA). The major challenge in this research thesis is that the dCA mechanism is a nonstationary process which means that measurements are varying over time. There are determinant physiological factors that make dCA a nonstationary mechanism including Carbon dioxide (CO_2), body temperature and Intracranial Pressure (*ICP*).

Aim: This work aims to quantify the variability found in dCA by applying Transfer Function Analysis (TFA) using the MATLAB platform on a univariate scale and multivariate scale. There are several input variables influencing the dCA mechanism and *HR* input will be included as a measure of sympathetic control in this research. However, CO_2 input is widely used in multivariate analysis where *HR* recordings were used for beat-to-beat averaging or filtering. Also, this thesis aims to examine and quantify the temporal variability of dCA which is found in measurement variability (across multiple recordings) and subject variability (across all recordings) on both univariate and multivariate scales.

Methods: The study included 20 subjects recording their vital signs during 5 visits for each subject at 3 conditions (normocapnia, hypercapnia and thigh cuff conditions), forming a dataset of 300 vital signs recordings of *ABP*, *CBv* (right and left sides), CO_2, and *HR* as well as mean recordings for *ABP* and both sides of *CBv*. Using univariate and multivariate techniques, this study will analyse measurements using the TFA technique. Then, apply reproducibility and covariance analyses where the first will measure ICC levels and the latter will quantify variabilities in measurement and subject variability recordings.

Results: For the univariate analysis, the results demonstrate different behaviours in coherence, gain, and phase for normocapnia, hypercapnia, and thigh cuff conditions under different frequency ranges (HF, LF, and VLF). Overall, the thigh cuff condition shows the lowest variation patterns, especially at the LF band. In the HF band, the thigh cuff condition shows low variation in gain and phase but not in coherence. However, the normocapnia condition shows different pattern of variation in the VLF band where normocapnia coherence and gain show narrower measurement variability (the variability between the different visits for each subject for each condition) but larger subject variability (the variability both within each subject 5 recordings, and between the overall subjects recordings for each condition) than hypercapnia and thigh cuff conditions. On the other hand, normocapnia VLF phase variations are significantly narrower in both measurement and subject variabilities compared to the other conditions. Besides, covariance results show that measurement variability are significantly smaller than subject variability in normocapnia, hypercapnia and thigh cuff conditions at all frequency bands.

For the multivariate analysis, using 2-inputs and 3-inputs in the TFA significantly increased coherence results compared to the univariate analysis results. Also, ICC results are significantly higher than the ICC results from the univariate analysis where the covariance results show measurement variability significantly smaller than subject variability at all physiological conditions across the frequency spectrum.

Conclusion: On a univariate scale, the thigh cuff condition at the LF band exhibits the lowest variation levels among both the right and left sides of the brain compared to the HF and VLF bands. However, the multivariate analysis shows that coherence results appear to improve TFA parameter results as well as ICC values, particularly, when using 3-inputs analysis where covariance results appear to be similar to those found from univariate analysis. Overall, adding *HR* ($Coh_{ABP+HR} = 0.685, \pm 0.160$, mean, ± Std) to the TFA appears to have more influence than adding CO_2 ($Coh_{ABP+CO2} = 0.676, \pm 0.137$) in increasing coherence results, which has not previously been shown ($Coh_{ABP+CO2+HR} = 0.732, \pm 0.128$).

Acknowledgement

I would like to thank my supervisor Prof. Stephen J. Payne for his elegant and professional supervision of my DPhil studies. With Prof Stephen I experienced prompt responses, thorough comments and valuable feedback throughout generating this thesis. This thesis was generated during difficult times (Covid-19 times), but with his continuous guidance and knowledgeable support, I was able to overcome and continue my research work. I can't thank him enough; I am looking forward to acquiring my DPhil thesis and I am eager to keep up to the level of meeting his expectations until and after completing my degree.

Moreover, I would like to thank Prof Alison Noble for Co-supervising me during the development of this thesis. Her follow-ups and genuine support are catalysing my educational journey here in Oxford. Prof Alison's supervision is a valuable enriching experience in my research work and certainly added informative knowledge to my academic experience. I profoundly and greatly appreciate her time and efforts while developing this thesis. Also, I would like to thank my colleagues in the research group for their support during my work and for providing me with quick ways to find my answers.

In addition, I would like to express my sincere gratitude to my employer, the Ministry of National Guard – Health Affairs (MNGHA) and King Abdullah International Medical Research Centre (KAIMRC), for funding my scholarship and granting me the opportunity to continue my DPhil studies at the University of Oxford. I would like to extend my thanks to the Saudi Arabian Cultural Bureau in the UK (UKSACB) for their continuous efforts in supporting my residence and studies at Oxford.

Remarkably, sincere and deep thanks to my parents and my siblings for their unconditional and boundless support during my studies. I also would like to extend my thanks to my wife, my beloved Sons (Jameel and Waleed) and my dearest Daughter (Rajaa) for their presence and for being part of my life here at Oxford.

Dedication

I am truly unable to fulfil my beloved family with what they deserve of thanks and gratitude, but I may use what I have learned from my life, education and professional experience to express my appreciation. In fact, I would like to dedicate this effort to my parents, my siblings, my wife, and my children. All the words found in the thesaurus and dictionaries can't express my gratitude as they are unwritable in all realms.

Table of Contents

1. Introduction

The human nervous system is the most delicate and complex in nature. This system comprises two major parts, the central nervous system which includes the brain and the spinal cord, and the peripheral nervous system which includes all nerve branches from the spinal cords and covers all body parts. The brain acts as the central engine for the entire human body which controls and monitors all body organs and systems including their movements and senses during humans' entire life.

The brain is a sophisticated system that operates dynamically which is in constant need of a continuous supply of oxygen and glucose via blood flow to sustain functionality and remain healthy. The brain is supported by the heart which pumps blood to the brain with every pulse, carrying oxygen and nutrients to the brain vessel network (cerebral vasculature) via the neck arteries that branch to reach all brain cells [1].

Despite changes in Arterial Blood Pressure (*ABP*), blood flow is maintained at certain levels within the human cranium using a mechanism called Cerebral Autoregulation (CA). CA mechanism protects the brain during any *ABP* alterations and ensures enough blood supply to the brain under all conditions according to a person's metabolism rate which is largely invariant from one individual to another. Meanwhile, metabolic wastes are transported out of the brain for reconditioning through the venous bloodstream. There is a significant relationship between blood supply and metabolism demands that is continuously adjusted by CA to keep the brain perfused with blood [1].

CA mechanism response can be categorized into two main types, static and dynamic response. Static CA denotes the changes in Cerebral Blood velocity (*CBv*) measurement in response to changes in *ABP* measurement at steady-state conditions. On the other hand, dynamic CA (dCA) denote the changes in *CBv* measurement in response to rapid changes in *ABP* measurement.

dCA could be triggered by altering the *ABP* using an external stimulus to increase blood pressure measurement. The blood pressure thigh-cuff and the Carbon Dioxide (CO_2) inhalation, which has independent direct response from *ABP*, are two examples of techniques used to alter *ABP* levels to trigger dCA [2].

Cerebral Perfusion Pressure (CPP) is a key parameter that represents the difference between the *ABP* and the Intracranial Pressure (*ICP*) which is the driving pressure to deliver the blood to the brain cells. The perfusion rate that supplies the vascular bed is controlled by cerebral vasculature resistance which is adjusted by three mechanisms, the myogenic response, the metabolic response and the sympathetic response. The myogenic response is ruled by CPP amount and CO_2 levels in the blood. The metabolic response is the supply of *CBv* containing oxygen and nutrients according to the metabolic demands. The sympathetic response results from the central nervous system reactions to autonomic responses. ***Figure 1-1*** is a schematic view of interactions among main cerebral variables [1].

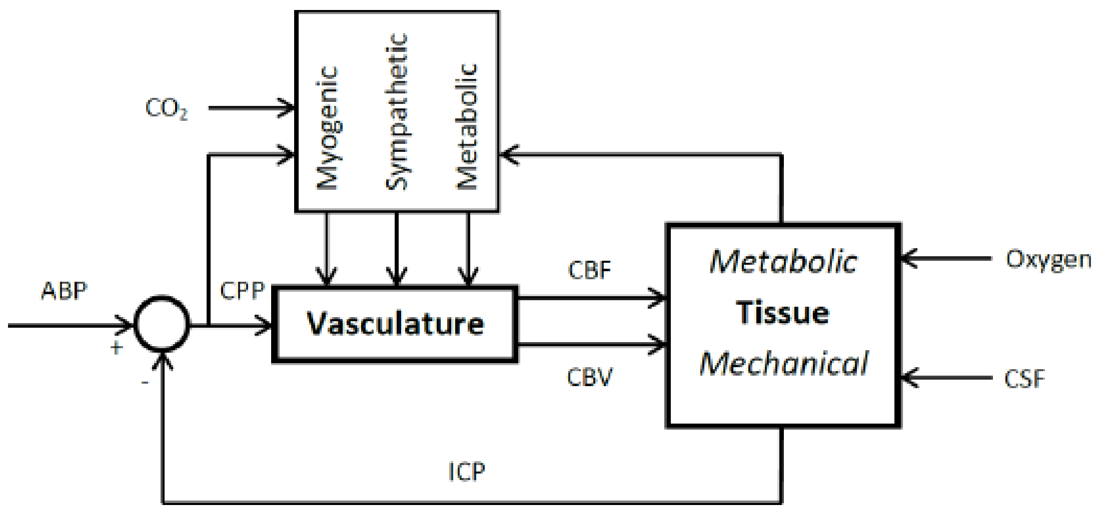

Figure 1-1: Schematic of interactions between main cerebral variables, reproduced with permission [1]

1.1. Context of the problem

Imaging technologies such as Computed Tomography (CT) and Magnetic Imaging Resonance (MRI) are used to provide in-depth details about pathological conditions in the brain. However, these technologies have limitations in terms of imaging magnification feature to capture the whole cerebral vasculature since the vessels in the brain branch from the main arteries in the neck to inside the brain and permeate at micro-levels (microvasculature) to supply brain cells with blood contents of oxygen and glucose. Using these technologies, imaging the complete cerebral vasculature is still a major challenge. Instead, mathematical modelling and computational techniques take place to calculate the cerebral vasculature geometries and properties inside the brain. The dCA mechanism is one of the key brain properties that need to be explored to understand the mechanism behaviours under different conditions. Some studies are proposing computational techniques to analyse the dCA behaviour over time [1] [3] [4] [5].

Deficiency in the dCA mechanism can lead to irregular blood perfusion rates within the brain which will affect the brain functionality and create unhealthy conditions. One of the diseases that are associated with a deficiency in dCA is stroke and almost 100,000 people are contracting the disease in the United Kingdom (UK) each year [1]. Stroke mainly has two types, ischaemic (vessel blockage) and haemorrhagic (vessel bleeding). Ischaemic stroke in major blood vessels will cause hypoperfusion in brain tissue in a region supplied by that vessel which will result in cell death if perfusion is not restored within a few seconds. Contrariwise, the haemorrhagic stroke results from blood leakage from the vessel (ruptured vessels) into the cranium interspace (e.g. bleed within the brain parenchyma or between the brain and the skull).

Stroke is a life-threatening disease that could lead to disability or death. In the UK, 100,000 cases are logged each year whilst nearly 17 million cases are logged each year globally. In fact, stroke is the leading cause of disability, the fourth leading cause of death in the UK and the second leading cause of death globally. There are noteworthy additional risk factors that are associated with a stroke which mostly are age, smoking, hypertension, diabetes, Atrial Fibrillation (AF) and high cholesterol [1].

However, a recent study conducted by Beishon et al. suggested that dCA impairment after ischaemic stroke (IS) may have significant suggestions for prognosis. Introducing the individual patient data meta-analysis (IPD-MA) international collaboration, the study aims to find a predictive model in IS by analysing changes in dCA data of post-IS patients in combination with their clinical history and neuroimaging. The study suggested exploring the temporal variations of dCA in IS patients in comparison with their baseline demographics, neuroimaging and variables of clinical outcomes using both the univariate and multivariate analyses [6].

Moreover, there is clinical interest in exploring dementia's impact on CA. Dementia is a term that refers to mental diseases that are marked as progressive neurological disorders which decline the brain's cognitive abilities and are more prevalent in elderly people. In the UK, dementia cases have surpassed cardiac cases in terms of mortality rate as the principal cause of death. In 2015, approximately 850,000 people contracted dementia in the UK where 60,000 have died in the same year compared to 35,000 deaths caused by cardiac diseases.

Specifically, Alzheimer's Disease (AD) is the most common type of dementia that is causing deaths in the UK. AD is a disease triggered by the formation of the amyloid plaques (protein formed around the nerves in the brain). ***Figure 1-2*** illustrates the death rate among men and women in the UK during the period 2001 – 2015. The declining graphs, ischaemic heart diseases, cerebrovascular diseases and other diseases, especially in men, show lower death rates than dementia and AD. However, during the period 2010 – 2015, there is a very clear increase in death rates caused by dementia and AD for both men and women. Also, there is an obvious trend similarity in men and women with evident differences in death rates in both which is partially caused by population demographic variation [1].

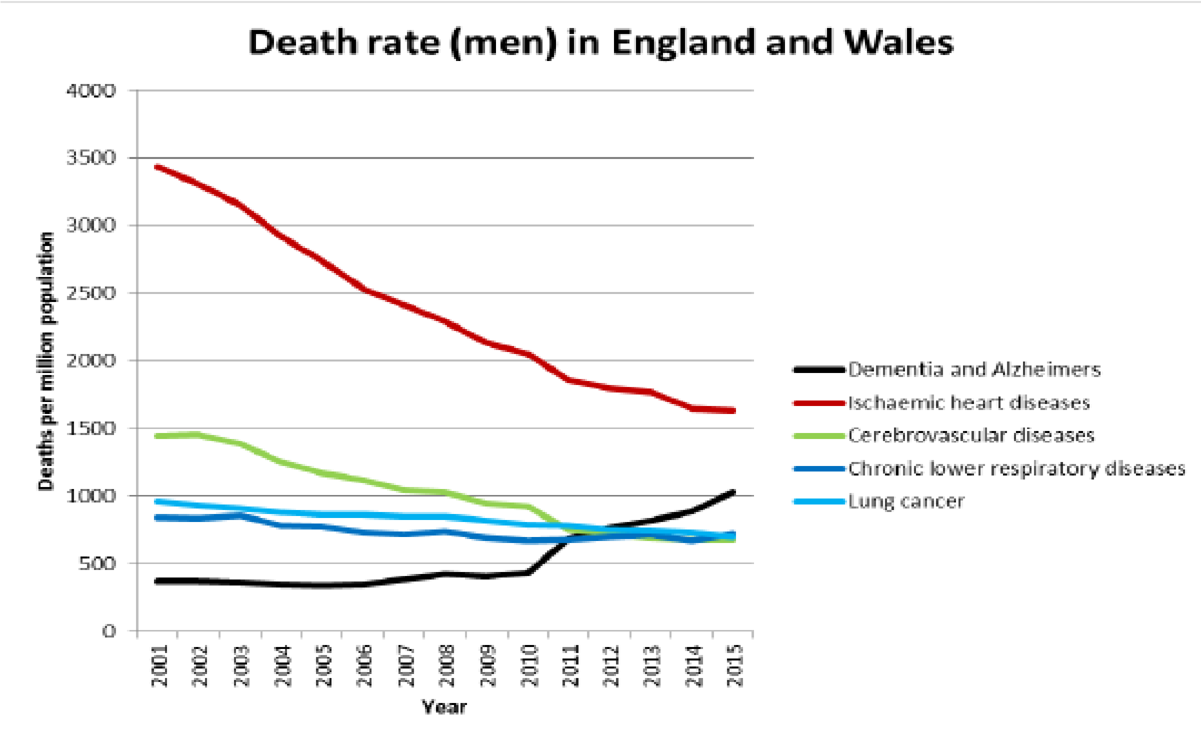

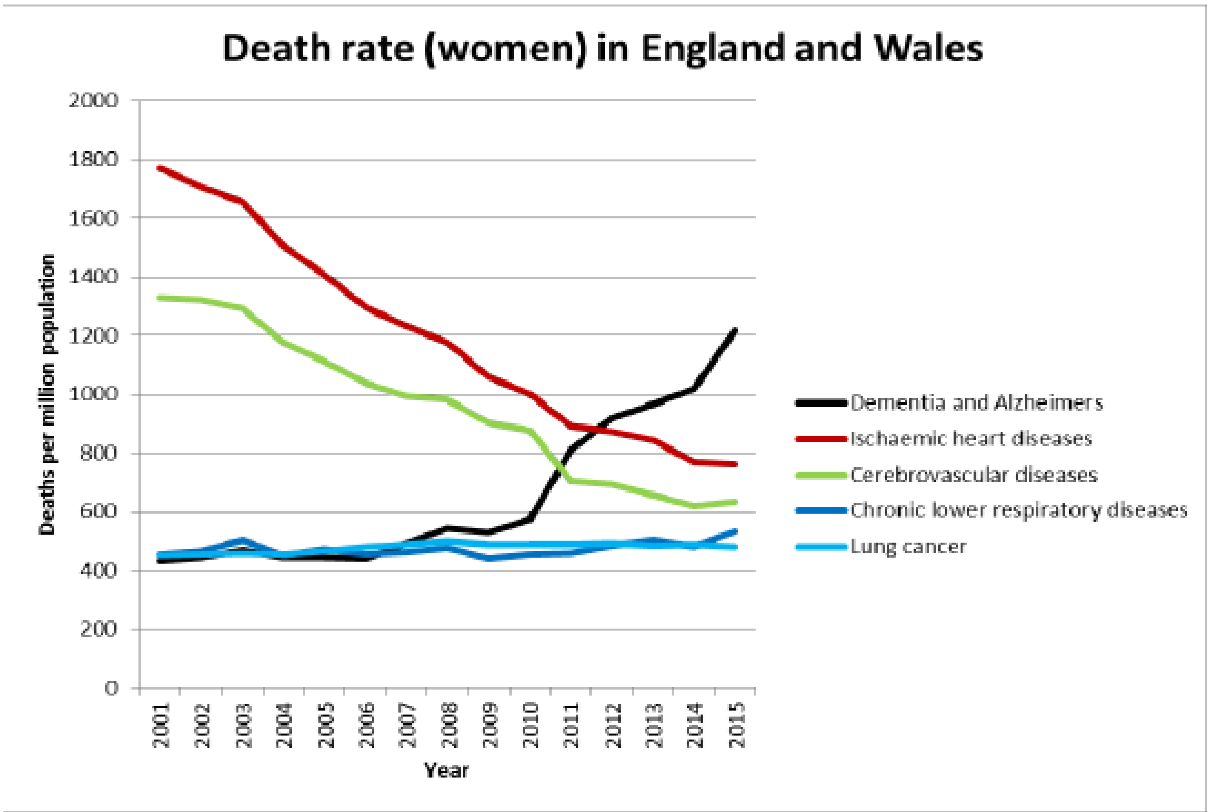

Figure 1-2: Death rates for the period 2001 – 2015 in the UK, reproduced with permission [1]

1.2. Dynamic CA assessment techniques

There are several techniques used to analyse dCA behaviour including mathematical modelling and computational techniques. These techniques are used to analyse dCA in order to visualize and interpret physiological parameters' behaviour over time. *ABP*, CO_2 and Heart Rate (*HR*) are measured by non-invasive monitors and the Transcranial Doppler (TCD) is used to measure *CBv* on both sides of the brain using non-invasive ultrasonic technology. These measurements are plotted in mathematical equations and computational platforms to draw the dCA mechanism and explore its behaviour under certain conditions.

Alternative technique is the 3-D modelling of the cerebral vasculature, which often uses imaging reconstruction software applications. This technique enables researchers to visualize the cerebral vasculature branching permeating the brain layers and study bifurcations morphology of both cerebral vasculature levels, macro and microvasculature. Still, imaging applications are limited only to the visible level of the cerebral vasculature whereas the lower levels of the brain at the microvasculature are usually built using mathematical modelling and computation techniques. Both imaging and computational techniques are utilized as an approach to simulate the complete cerebral vasculature, and then, verify the hypotheses by running the simulation to investigate the results of blood pressure and flow in all regions within the brain.

This thesis will focus on computational techniques to analyse the dCA mechanism. In particular, the thesis will explore measured vital signs parameters (*ABP*, *CBv*, *HR* and CO_2) behaviour that are acquired under different conditions, normocapnia (normal condition), hypercapnia (abnormally increased level of CO_2 in the blood stream), and thigh cuff (alternating pressure applied over one thigh) in order to evaluate dCA output at different physiological challenges. This should provide enlightenment on dCA mechanism behaviour at different conditions over time. Using a computational platform will provide an in-depth analysis of the acquired parameters and deliver a clearer understanding of dCA behaviour in the human brain.

Bearing in mind that a stationary process is defined as a constant statistical moment that doesn't change over time [4], the major challenge to be addressed in this research thesis is that the dCA mechanism is a nonstationary process according to several studies [1 3 4]. There are physiological factors that make dCA a nonstationary mechanism such as CO_2, body temperature and *ICP*. This means that dCA varies over time with the same person at a normal state. Since this work is analysing vital signs recordings, it is important to highlight the nonstationary behaviour of dCA as the study has suggested expecting nonstationary dCA as a normal one [4]. This highlights the need to apply multivariate time-varying techniques to explore dCA behaviours using new methods [4].

1.3. Aim

The work presented here aims to quantify the variability found in dCA by applying Transfer Function Analysis (TFA) using the MATLAB platform on a univariate scale (*ABP* as input and *CBv* as output) and multivariate scale (using multiple inputs, e.g. *ABP*, CO_2, and *HR*). It's worth noting that there are several input variables influencing the dCA mechanism and *HR* input will be included as an indirect measure of sympathetic control in this research. There are confounding factors linked to the dCA mechanism such as artefact, noise in the signal recorded, and input influence [4], however, CO_2 input is widely used in multivariate analysis where *HR* recordings are routinely acquired for beat-to-beat averaging or filtering [6].

These analyses will provide a better idea of dCA robustness as a measure and to visualize the coherence of measured blood pressure and blood flow parameters in the brain. However, quantifying the variability of the calculated results is a required precedent step which will contribute to the analysis and is essential to enable future work in quantifying the non-stationarity behaviour of dCA.

Moreover, this research will use TFA to measure and understand the variability of parameters across all datasets at different physiological challenges. Also, this thesis aims to examine and quantify the temporal variability of dCA which is found measurement variability (across multiple recordings) and subject variability (across all recordings).

Overall, the thesis aims to validate a previously developed univariate and multivariate time-varying techniques to explore the coherence using *ABP* only as input in the univariate analysis and multiple coherence functions of parameters using *ABP*, CO_2, and *HR* inputs in multivariate analysis and observe output (*CBv*) results in both analyses. This is to evaluate the relationship between them using linear methods, but as nonstationary variables. This will be accomplished by running these functions on datasets recordings of 20 subjects under different conditions. The results of these analyses will provide a quantification of the variability found in dCA mechanism in the brain.

Next, Chapter 2 will provide an overview of the literature and highlight previous studies findings to understand cerebral vasculature, dCA mechanism, and previous work in quantifying dCA. Also, to understand TFA, multivariate analysis and reproducibility notion. Chapter 3 will discuss the data used in this study including the study settings, data collection and pre-processing techniques. Chapter 4 will present methods, analyses (transfer function, reproducibility, and variability analyses) and results of the univariate analysis across different conditions on both the right and left sides. Then, Chapter 5 will present the results of the multivariate analysis using different combinations of inputs across same conditions and highlight few comparisons between univariate and multivariate results. Chapter 6 will present the results of each side (right and left sides separately) and their average across hypercapnia and thigh cuff conditions. Finally, the conclusion in Chapter 7 will provide a summary, suggesting recommendation for future work, discussing findings and limitations of this study.

2. Literature review

2.1. Introduction

This chapter will discuss previous relevant studies in the dCA mechanism field. The upcoming sections will look at the cerebral vasculature, dCA mechanism, dCA measurement, Quantifying dCA mechanism, transfer function analysis (TFA), time-varying multivariate analysis technique, and reproducibility using the Intraclass Correlation Coefficient (ICC). The cerebral vasculature section will explain the basics of the vasculature within the brain to visualize the anatomy and understand the underlying physiology. Then, the dCA mechanism section will review earlier studies and discuss their findings. Next, the dCA measurement section will discuss measurement techniques used to assess dCA variables. Afterwards, the quantifying dCA mechanism will review methods used to quantify dCA mechanism in both time and frequency domains. Subsequently, the TFA section will highlight scientific efforts in using this analysis technique. Likewise, the multivariate section will discuss the concept of this technique, former results, and future needs for further studies in this field. Finally, the reproducibility section will provide an overview of this concept and the most common method of measuring reproducibility.

2.2. Cerebral vasculature

The cerebral vasculature is a highly inter-connected network of blood vessels. Mainly, the brain is supplied by blood via four vessels which cover both the anterior and posterior sides of the brain. The vessels are right and left Internal Carotid Arteries (ICAs) as well as right and left Vertebral Arteries (VAs). Both VAs join together to form a bigger artery, Basilar Artery (BA) which is linked with ICAs through the circle of Willis. This circle acts as a hub that connects major vessels from both right and left sides and then branches to supply all areas of the brain. ***Figure 2-1*** shows a schematic of the circle of Willis and major blood vessels in the brain [3]

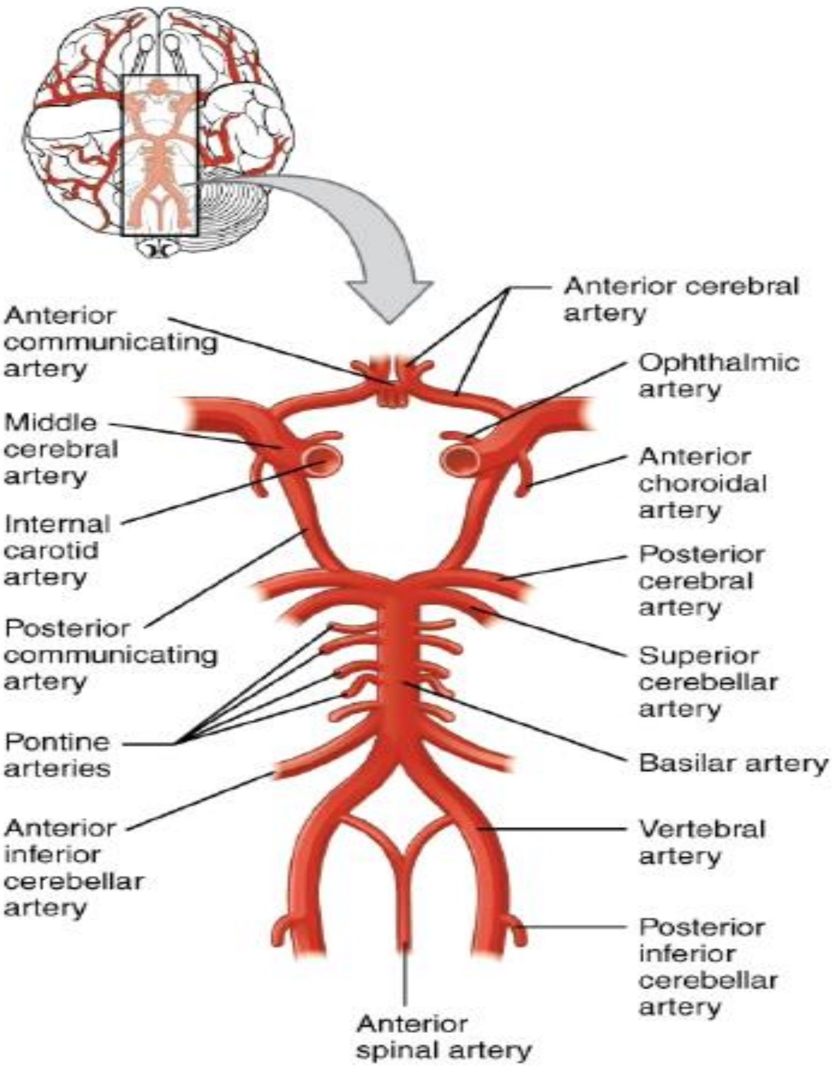

Figure 2-1: Schematic of the major arterial blood vessels in the brain, reproduced with permission [3]

Furthermore, there is a significant variation in the cerebral vasculature structure among people. It's important to acknowledge these variations and consider them when measuring *ABP* and *CBv* to quantify dCA. According to a study conducted in 1959 on 350 human brains diagnosed with atherosclerosis, only 52% of participants had a complete structure of the cerebral vasculature. A previous study conducted in 1963 on 994 subjects symptomatic with neural dysfunction presented that only 19% of the subjects had a complete circle of Willis.

A further study conducted in 2013 examining the variability of the circle of Willis among 500 participants found that almost 60% of participants had differences in the circle of Willis structure [3]. With such differences in circle of Willis structure a variation of blood flow in the brain is expected. A study investigated the variations of blood flow due to the absence of some arteries [7] and highlighted that structural variation happen in 10% of the people. The study suggested that variations in circle of Willis, and in case of occlusion or stenosis in artery, reduces the blood flow to the brain by almost 64% [7].

2.3. Dynamic dCA mechanism

The CA mechanism is normally considered in two ways: static CA and dynamic CA. Static CA is the mechanism that rules the steady-state behaviour of *CBv* in response to steady-state changes of *ABP*. This is normally considered as a normocapnia state which is the measurement of vital signs at normal CO_2 levels in the blood. This type requires a long time to measure, and participants are exposed to a recording period under normal conditions. Conversely, dCA requires external stimuli (e.g., thigh cuff) to happen by making a rapid change in *ABP* levels to evaluate *CBv* response at the time. This is a simpler and quicker method, but participants will be exposed to alterations in physiological conditions [3].

The dCA mechanism refers to the process of maintaining the perfusion of cerebral blood at proper levels by regulating the cerebral vasculature state. Under normal health conditions, the dCA mechanism operates when the mean *ABP* level ranges between 60 – 150 mmHg. *CBv* is regulated by dCA to ensure the normal functioning of neural activity. Several studies have revealed that dCA becomes impaired when patients contract haemorrhagic or ischaemic stroke as well as other diseases like epilepsy, AD and generalized anxiety. Moreover, many studies have shown that CO_2, Nitric Oxide (NO) [8] and levels of altitude impact the dCA mechanism [9].

There are several physiological challenges to stimulating rapid changes in *ABP* [4], but in this study two common types only will be considered, which are the thigh cuff and hypercapnia that will be used in the TFA technique. The thigh cuff technique is performed by wrapping a cuff around the participant's thigh that alternates between inflating and deflating the cuff to change the *ABP*. The hypercapnia technique is done by breathing air gas mixture with more than 5% CO_2 concentration than normal to the participant's airway for a certain period to induce changes in *CBv* level [3]. Both thigh cuff and hypercapnia techniques were used on the participants of this thesis [10]. The use of hypercapnia condition in this study is to compare results with thigh cuff condition and because hypercapnia coherence results appear higher than normocapnia coherence.

A study conducted by Panerai et al. in 2014 defines dCA as a temporary response of *CBv* to the rapid change in *ABP*. Due to the dynamic relationship between *ABP* and *CBv*, the study indicates that dCA is a nonstationary process and should be considered a normal one. However, the study listed some physiological determinants that impact dCA supported by evidence from the literature. These variables are CO_2, autonomic nervous system activity, neuronal activation, body temperature, *ICP*, intrathoracic pressure and blood rheology [4].

Nonetheless, it is worth noting that this study is using *HR* variable as input in the multivariate transfer function analysis. The *HR* variable is a marker of autonomic behaviour in this context which has not been discussed adequately in previous studies. There are only two studies [11] [12] that included *HR* as a 3rd input to MTFA. A study included *HR* input to assess *CBv* determinants at baseline and during squat-stand manoeuvre. The study compared the univariate coherence with the resulted partial coherences from autoregressive moving average (ARMA) model, a multivariate model using *ABP*, CO_2, and *HR* input. The study suggested that partial coherences resulted from the model are significantly lower when CO_2 and *HR* are included compared to univariate TFA coherence [11].

The other study included *HR* input in a nonlinear multivariate model (principle dynamic modes, or PDM) to examine *CBv* haemodynamics. The study suggested that the inclusion of nonlinear methods could cause reduction in significance results. Also, the study suggested, highlighting the influence of *ABP* fluctuations on *CBv*, there is a direct cardiac contribution which was demonstrated by *HR* influence in their results [12].

2.4. Dynamic CA measurement

In this section, the previous work on assessing dynamic CA in the literature will be reviewed. This thesis will highlight measurement techniques of *ABP*, *CBv*, CO_2, and *HR* as they form the variables in dCA assessment. A study published in 2016 suggested that dCA is crucial to sustain brain perfusion, supplying the brain with essential levels of oxygen and energy. Maintaining the brain perfusion with adequate levels is vital to reinforce normal functions of the brain [13].

The study overviewed cerebral blood flow measurement techniques including direct intravascular measurements, nuclear medicine, X-ray imaging, MRI, ultrasonic techniques, and optical methods. The study also overviewed *ABP* measurements techniques and CA assessment methods. The study suggested that optical techniques can deliver a noninvasively quantitative continuous monitoring of CA and listed methods used for measuring cerebral blood flow and the techniques used for each method. As well, the study listed methods used to measure *ABP* including the invasive arterial line, the non-invasive finger photoplethysmography, sphygmomanometers, and radial tonometry [13].

A study in 2010 discussed the techniques used to measure *ABP* [14]. The study mentioned that mercury sphygmomanometer is commonly known as the “golden standard” in measuring *ABP*. Currently in US hospitals, mercury devices are replaced with non-mercury and non-invasive devices where they become the preferred method in measuring *ABP*. The study overviewed different measurement techniques including auscultatory, oscillometric, ultrasonic, and finger cuff techniques discussing technical problems with each technique. Also, the study discussed *ABP* measurement in children, pregnant, geriatric, and bariatric populations [14].

Moreover, a study published in 2021 discussed the importance of accurate *ABP* measurement in healthcare provision [15]. The study compared between non-invasive and invasive measurement techniques listing the non-invasive techniques including, manometry, and oscillometry using inflatable cuffs as well as the invasive techniques including direct via transducer method using cannula transducers. Also, the study discussed the advantages and disadvantages of both invasive and non-invasive methods on continuous *ABP* measurement. The study suggested that radial, femoral, and brachial arteries are the most common arteries when measuring *ABP*. However, the study didn't recommend a method or technique but only discussed different techniques used in both invasive and non-invasive methods [15].

Reviewing previous work in measuring *CBv*, a study published in 1999 discussed measuring *CBv* using MRI techniques based on perfusion imaging method. The study suggested that dynamic tracking of paramagnetic contrast bolus and arterial spin labelling (ASL) techniques as the most successful methods in measuring *CBv* including the continuous arterial spin labelling (CASL), and the pulse arterial spin labelling (PASL) techniques. Each method was discussed in term of their principles, probable downsides, and their potential to quantify *CBv*. ASL has been used in investigating cerebrovascular disease and in functional brain mapping. Also, alternative approaches were presented to calculate the absolute value of *CBv* using MRI techniques [16].

A study published in 1999 investigated the use of contrast-enhanced CT to measure *CBv*. The study aims to develop a novel approach to correct the partial volume averaging in CT to accurately measure the intraarterial curves investigating the accuracy of *CBv* values resulting from CT scans. The experiment was conducted on rabbits scanning their basal ganglia regions. In conclusion, after validating the dynamic CT method, the study suggested that this technique could be used as an alternative approach to calculate *CBv* [17].

A study published in 2019 offer a new method to quantify *CBv* using near-infrared spectroscopy (NIRS). The new method is identified by new acronym NIRS-CHS which uses the coherent haemodynamics spectroscopy (CHS). The new method was tested on the prefrontal cortex of healthy subjects during induced mean *ABP* cycles at the thigh cuff condition. The study compared the results of NIRS-CHS with the results using diffuse correlation spectroscopy (DCS) technique which presented decent agreement of the CBv measurement in both results. In conclusion, the study suggest that the new method can deliver more precise measurement of *CBv* in comparison to previously reported method using NIRS [18].

Besides, a study published in 2018 compared results of a patient-specific lattice-Boltzmann simulation to transcranial doppler (TCD) *CBv* measurements of the middle cerebral artery (MCA). The simulation forecast the maximum *CBv* with less than 9% error where the error percentage increased as the velocity value was reduced in the simulation. The study concluded that using TCD could be used to measure *CBv*, recommending the discount of invasive procedure to measure blood flow [19].

A recent study published in 2022 introduced the 4D flow MRI to assess the intracranial haemodynamics. The study compared *CBv* measurement of the MCA from the 4D flow MRI with TCD attempting to overcome some of TCD drawbacks (such as operator error, low spatial resolution, and the likelihood of vessel diameter changes). The study highlighted the common use of TCD to obtain cerebral blood flow measurements which can provide real-time high temporal resolution measurement with low operational cost. The study concluded that there was excellent similarity of the assessment results between 4D flow MRI and TCD [20].

HR measurement techniques has developed over time. There are different techniques to monitor and record *HR* measurements from ECG to wireless monitoring, to *HR* variability (HRV) which is the time between R-R intervals [21]. A study published in 2002 compared finger plethysmograph (FP) with ECG in terms of providing accurate measurement for HRV for both conditions, at rest and at Stroop task. Both measurements recorded from both devices were highly correlated at rest, but the correlation decreased significantly at the Stroop task results. Additionally, HRV measurements were significantly higher using the FP. The study concluded that ECG is recommended for experimental use, but the FP could be suitable in determining HRV at rest condition [22].

A study published in 2014 inspected published work on non-contact physiological parameter measurement for human. The work was aiming to investigate measurement accuracy of HR and HRV. The study considered both conventional methods, ECG and photoplethysmography (PPG), and other non-contact experimental methods including ultrasound distance measurement, RGB camera, thermal imaging, and microwave distance measurement. The study compared different techniques discussing their advantages and disadvantages [23].

Furthermore, a study published in 2019 compared *HR* measurements from the in-ear photoplethysmography (PPG) with *HR* measurements derived from ECG devices. The aim of the study is to evaluate if the in-ear PPG could be used as a substitute approach to accurately measure *HR* instead of using ECG devices. The study concluded that in-ear PPG is a technology that has potential accuracy with imprecise ability in measuring *HR*. The study suggested that both accuracy and precision *HR* measurement is significantly dependable on the site of measurement and the stress state [24].

Besides, end-tidal CO_2 (or $etCO_2$) measurements are usually sampled using capnography device through mainstream or sidestream approaches. The mainstream approach is when an integrated sampling cell and CO_2 sensor placed between the endotracheal tube and the breathing circuit. The sidestream approach, on the other hand, is placing the CO_2 sensor on the monitoring device which the most common approach as it has the ability to sample from both intubated and non-intubated patients [25].

A study published in 2008 compared arterial CO_2 and proximal mainstream $etCO_2$ proposing a new method of distal $etCO_2$ capnography. The aim was to assess the proposed method by comparing results of proximal $etCO_2$ sampled through mainstream with arterial CO_2. The study concluded that results from the distal $etCO_2$ capnography show decent correlation with results sampled from the arterial CO_2. The study highlighted that distal $etCO_2$ capnography offered higher accuracy than the proximal mainstream $etCO_2$ [26].

A study published in 1994 compared the $etCO_2$ measurements with the measurements of arterial CO_2 in non-intubated patients. The aim of study was to evaluate whether $etCO_2$ measurements could reflect arterial CO_2 levels accurately. Each patient was asked to breath normally, collecting their capnography readings and had their blood sampled for arterial blood gas for arterial CO_2 measurement. The study concluded that $etCO_2$ measurements show a significant correlation with arterial CO_2 measurements. The study recommended the use of $etCO_2$ to avoid repeated blood sampling for the measurements of arterial CO_2 [27].

A study published in 2012 investigated the ability of mainstream $etCO_2$ measurements to forecast the arterial CO_2 levels in patients coming to the emergency department (ED). The aim was to evaluate the accuracy of mainstream $etCO_2$ measurements predictions of the arterial CO_2 levels. The study concluded that mainstream $etCO_2$ measurements can accurately reflect arterial CO_2 levels in ED patients, recommending further research to compare both mainstream and sidestream techniques [28].

A study published in 2020 investigated the new microstream technique and the mainstream $etCO_2$ technique with the partial pressure of CO_2 in the blood ($PaCO_2$) in intubated children. The study aims to assess the new microstream technique through comparison between $PaCO_2$

results with mainstream *$etCO_2$* results. In conclusion, both microstream and mainstream *$etCO_2$* techniques could predict *$PaCO_2$* results as there is a significant correlation between both techniques [29].

Importantly, a study conducted in 1992 examined the correlation of *$etCO_2$* with cerebral perfusion throughout CPR procedure. The study highlighted previous research work in learning the correlation of *$etCO_2$* with cardiac output, but the aim is to learn the correlation of *$etCO_2$* with *CBv* in cardiac arrest. In conclusion, *$etCO_2$* is significantly correlated with *CBv* changes which also could be relevant to changes in cardiac outputs [30].

2.5. Quantifying dCA mechanism

Dynamic CA quantification methods has developed over the years and the selection of a method to quantify dCA is up to researcher personal preference [5]. Mainly, there are few techniques that been employed to quantify dCA. These techniques roll around time-domain and frequency-domain, nonstationary, and nonlinear analyses [3]. In this section, these analyses will be overviewed on the following subsections highlighting attempts history to quantify dCA and techniques used in each analysis. It's worth noting that multivariate analysis will be discussed in Section 2.7.

2.5.1. Time-domain studies

In a study published in 1989 investigating cerebral autoregulation dynamics in humans. The Rate of Regulation (RoR) was first introduced as metric to quantify dCA subjecting participants to normocapnia, hypercapnia, hypocapnia, and thigh cuff conditions. Using the *ABP* and *CBv* measurements, the study calculated and introduced cerebrovascular resistance (*CVR*) variable. The study concluded that there is a highly significant inverse relationship between RoR and *CO_2* partial pressure [31].

A study published in 1995 compared the measurement of static and dynamic CA. The aim to compare results of both static and dynamic CA under normal and impaired states. This study estimated *CVR* from *CBv* and introduced differential equations to link *CBv* (output) changes following to *ABP* changes (input). Also, autoregulation index (ARI) was introduced from scale 0 – 9 where 0 represent no autoregulation, 5 represents normal autoregulation, and 9 represents the fastest autoregulation. In conclusion, the study suggests that results from the static CA is alike the results of dCA [2]. Later studies focused on improving the ARI assessment [32] and others focused furtherly on the intra-subject variability found in ARI estimation [33].

A study published in 2003 examined the intra and inter-subject variability to assess dCA using ARI. The study introduced an alternative method by using autoregressive moving average ARI (ARMA-ARI). The results of the introduced method display a highly significant stability and variability reduction compared to the ARI results. The study suggested that ARMA-ARI method could enhance the results of dCA estimation and improve temporal resolution [34].

A study published in 2002 analysed dCA using ARX model as a proposed method. The aim was to model a cerebrovascular system using the ARX model as a linear model. The study also used a non-linear system to test the performance of system in terms of input/output behaviour. The study suggested that dCA could be estimated using the introduced ARX model even when considering noise measurements [35]. Later study suggested that step response and phase shift at 1/12 Hz could be calculated from the ARX model and dCA could be estimated by one of the calculated results [36].

A study published in 1999 investigated the effect of CO_2 on dCA measurement using TFA and both impulse and step responses. The study calculated the TFA parameters, coherence, gain, and phase as well as the impulse and step responses of *ABP* (input) on the output (*CBv*). during hypercapnia, both coherence and gain significantly increased below 0.05 Hz where the phase decreased in 0.02 – 0.1 Hz. The results of both impulse and step responses suggest that dCA efficiency is decreased during hypercapnia condition [37].

Furthermore, a study published in 1996 explored monitoring CA in patients with head injuries. The study suggested that CA is reported to be unfavourable in head-injured patients. The aim is to examine if *CPP* could be used to reliably deliver information about CA mechanism. The study introduced the correlation coefficient (Mx) which is calculated from two samples in the time-domain. Mx varies from -1 to 1 where -1 represent negative correlation, 1 represents positive correlation and 0 means no correlation. In conclusion, calculating Mx display positive correlation between *CBv* and *CPP* indices which could be used to examine CA in head-injured patients [38].

It's worth noting that positive values indicate impaired autoregulation and zero value *CBv* is not resulted by *ABP*. The use of Mx is good instrument to monitor CA, but further improvements are needed for its specificity and sensitivity for reliable clinical practice [39]. Additionally, a study shows that calculating Mx in LF and HF bands has more significant results [40] then, a later study calculated Mx at 0.1 Hz found a time delay of -2 seconds in healthy participants only, agreeing to previous studies findings [41].

2.5.2. Frequency-domain studies

Mainly, TFA is identified as a reliable method in dCA quantification and is usually performed through either univariate or multivariate analysis. A study conducted in 1990 presents the attempt to estimate CA using TFA[3]. The study calculated coherence and gain in both healthy and unhealthy subjects (with subarachnoid haemorrhage). In conclusion, the study suggested that using *ABP* and *CBv* in TFA enable the measurement of CA temporal nature [42]. Then, following study published in 1997 examined *ABP* and *CBv* using TFA to calculate coherence and gain. In conclusion, coherence was less than 0.6 in healthy subjects and more than 0.6 in patients. The study suggested that using coherence could be used as quantitative index to assess CA which will be widely used [43].

A study published in 1998 examined TFA of dCA in humans. The study calculated TFA parameters coherence, gain, and phase in normocapnia, hypercapnia, and thigh cuff conditions across the 3 frequency bands, VLF, LF, and HF. In conclusion, the results suggest *CBv* changes in the VLF and LF bands highly correlate to changes in *ABP* [44]. A later study in 1999 displayed similar results in normocapnia condition and increased coherence and gain in hypercapnia condition. This following study investigated the effect of CO_2 on dCA measurements which calculated the TFA parameters and both impulse and step responses. In conclusion, the results suggest significant increase in coherence and gain and significant decrease in phase at the VLF band in hypercapnia condition. Also, impulse and step responses results suggest that hypercapnia condition diminish dCA mechanism efficiency [37].

A study published in 2014 discussing the use of TFA to assess dCA using *ABP* and *CBv* spontaneous oscillations. The study highlighted that TFA is widely used method to noninvasively quantify dCA and examined 113 publications to deliver an overview about dCA assessment techniques used in TFA. In results, the study indicated very few studies have reported TFA settings and standards but there is large disparity in TFA settings and criteria used in these publications which demonstrate that there is no gold standard for implementing and executing TFA. The study indicated that such diversity impedes the differentiation between normal and impaired dCA mechanism in different subject groups which make replication or comparison of these studies a challenging task. The study suggested the crucial need to unifying and optimizing TFA implementation techniques through developing international standards to implement TFA techniques and interpret results [45].

A study published in 2009 compared parametric with nonparametric estimations of dCA using spontaneous *ABP* oscillations in TFA. The study suggested that dCA impairment could be associated with cerebral ischemic risk in cerebrovascular disease. Both parametric and nonparametric TFA, autoregressive average model, and reproducibility analysis were performed in their methodology. The results demonstrated no significant variance between the 3 methods and obtaining dCA measurement could be stably achieved using any method [46].

A study published in 2011 investigated the effect of using the TCD and the Finapres (continuous non-invasive haemodynamics measurement device) combinedly. The study suggested that calibrating the Finapres could cause disruption in ABP recordings and TCD recorded signals could be lost because of probe movement. Using TFA, the study compared 5 minutes results with 1-minute outcomes. In conclusion, the study suggested that TFA estimates could be obtained accurately at the VLF band applying linear interpolation technique. The study recommended the use of 1-minute time series signals to obtain accurate results [47].

A study published in 1995 examined dCA using TFA to test the hypothesis about phase differences in induced ABP oscillations. The study calculated TFA results in normocapnia, hypercapnia, and hypocapnia conditions focusing on the results at 0.1 Hz. In results, the study reported phase shifts results as highly significant increase in hypocapnia condition and highly significant decrease in hypercapnia condition. In conclusion, the hypothesis made is supported by the reported results [48].

2.5.3. Nonstationary studies

The nonstationary analysis support exploring the nature of time-varying dCA and assist in understanding whether dCA mechanism is improving or deteriorating over time[3]. A study published in 2010 suggested tracking time-varying dCA results in response to changes in CO_2 partial pressure using adaptive time-varying filter to examine dCA. The study found that the suggested adaptive time-varying filter was able to track rapid changes in dCA. There was autoregulatory reduction in hypercapnia condition, but it increases in normocapnia condition. In conclusion the adaptive time-varying model displayed ability to track changes in dCA and hypercapnia condition impair autoregulation [49].

A study published in 2011 introduced a noninvasively nonlinear analysis to assess dCA. The study highlighted the unavailability of noninvasively nonlinear methods that can present an online estimation of dCA. The study introduced a nonlinear mathematical model using ensemble Kalman filter (EnKF) to estimate dCA mechanism. The suggested use of the introduced filter is for the parameter estimation from the introduced model which predict the results of *ICP* and *CBv* from *ABP* measurements [50]. An earlier study published in 2007 used the Wigner-Ville distribution in nonlinear model to calculate instantaneous TF in the LF band [51].

A study published in 2000 examined the dynamic analysis of cerebral blood flow regulation in humans. The study used *ABP* and $etCO_2$ fluctuations (2nd input) as inputs in a multivariate TFA in combination with least mean square finite impulse response filter to assess *CBv*. The results suggest that *ABP* input can significantly explain *CBv* variability with significant reduction in model error when including the 2nd input. In conclusion, 2nd input fluctuations explained the variability found in *CBv* [52].

A later study published in 2014 introduced time-varying multivariate nonlinear model as a novel method. The study suggested that the proposed method advances temporal resolution during the assessment of *ABP* and *CBv* dynamics with CO_2 variable. The study used the recursive least square (RLS) technique in the introduced model to repress CO_2 influence on *CBv*. The study used the phase difference calculated between ABP and CBv using mathematical transforms and filters to quantify autoregulation. The results show that the introduced model reduced phase difference influenced by CO_2 and time-varying autoregulation could be efficiently tracked. In conclusion, introduced method can rapidly track the dynamics of dCA in the presence of other covariates [53].

A study published in 2004 explored a multimodal pressure-flow (MMPF) method in assessing dCA in hypertension and stoke patients because of the nonstationary and nonlinearity nature of dCA mechanism. The study examined the influence of stroke in dCA on 15 normotensives, 20 hypertensives, and 15 stroke (minor) patients recording *ABP*, *CBv* from MCA while performing the Valsalva manoeuvre. In results *ABP-CBv* phase shift was computed from the minimum and maximum differences of *ABP* and *CBv* which show significant difference of *ABP-CBv* phase shifts between the 3 groups of patients. *ABP-CBv* phase shifts in stroke and hypertensive groups was significantly lesser than the normotensive group. In conclusion, the MMPF method demonstrates capability in evaluating the dynamics behind the autoregulation mechanism where change in mechanism behaviour is observed in hypertension and stoke diseases [54].

2.6. Transfer Function Analysis (TFA)

Transfer function analysis is a technique to study a linear system's behaviour between inputs and outputs. TFA is usually represented to study the relationship of inputs with outputs in the frequency domain. There are univariate and multivariate analyses that will be investigated to examine dCA behaviour under each type: *ABP*, alone in univariate, and CO_2, along with *ABP* and other parameters e.g. oxygen partial pressure (O_2), in multivariate analysis are considered as inputs whereas the output is the *CBv* of these analyses.

Mathematically, after applying the Fourier transform, *ABP* which is $P(t)$ in the time domain is denoted as $P(f)$ in the frequency domain and *CBv*, $V(t)$ is denoted as $V(f)$ in the frequency domain. The power spectrum of *ABP* is computed as [55]:

$$G_{pp}(f) = E[P^*(f)P(f)] \qquad (1)$$

Where $G_{pp}(f)$ is the power spectrum of *ABP* and $E[P^*(f)P(f)]$ is a complex product usually obtained by applying the Welch technique and 50% overlap Hanning window. Likewise, the cross-spectrum is computed as [55]:

$$G_{pv}(f) = E[P^*(f)V(f)] \qquad (2)$$

Where $G_{vv}(f)$ is the power spectrum of *CBv*. Then, the complex TFA function, $H(f)$, between *ABP* and *CBv* is [55]:

$$H(f) = G_{pv}(f) / G_{pp}(f) \qquad (3)$$

Thus, a function to estimate the univariate coherence is written as [55]:

$$r_p^2(f) = |G_{pv}(f)|^2 / G_{pp}(f)G_{vv}(f) \qquad (4)$$

Mainly, TFA is based on Fourier transform analysis of input and output signals by transforming the signals from the time domain to the frequency domain. This will give an in-depth visualization of signal properties such as amplitude (Gain), angle shift (Phase) and input-output relationship (Coherence). ***Figure 2-2*** shows the key steps of TFA transforming signals from time-domain to frequency-domain. The coherence is the ratio of output change which could be explained by input signal (i.e. amount of output caused by input). The coherence varies between 0 and 1, where 0 means no linear association and 1 means perfect linear association between input and output signals [5].

TFA is conventionally identified at 3 frequency periods ranging from 0.02 – 0.4 Hz. Very Low Frequency (VLF) ranges from 0.02 – 0.07 Hz, Low Frequency (LF) ranges from 0.07 – 0.2 Hz, and High Frequency (HF) ranges from 0.2 – 0.4 Hz [56]. These frequency ranges are somewhat arbitrary defined, but widely used by researchers in several studies which makes them conventional in the field [1 3 57 58 59 60].

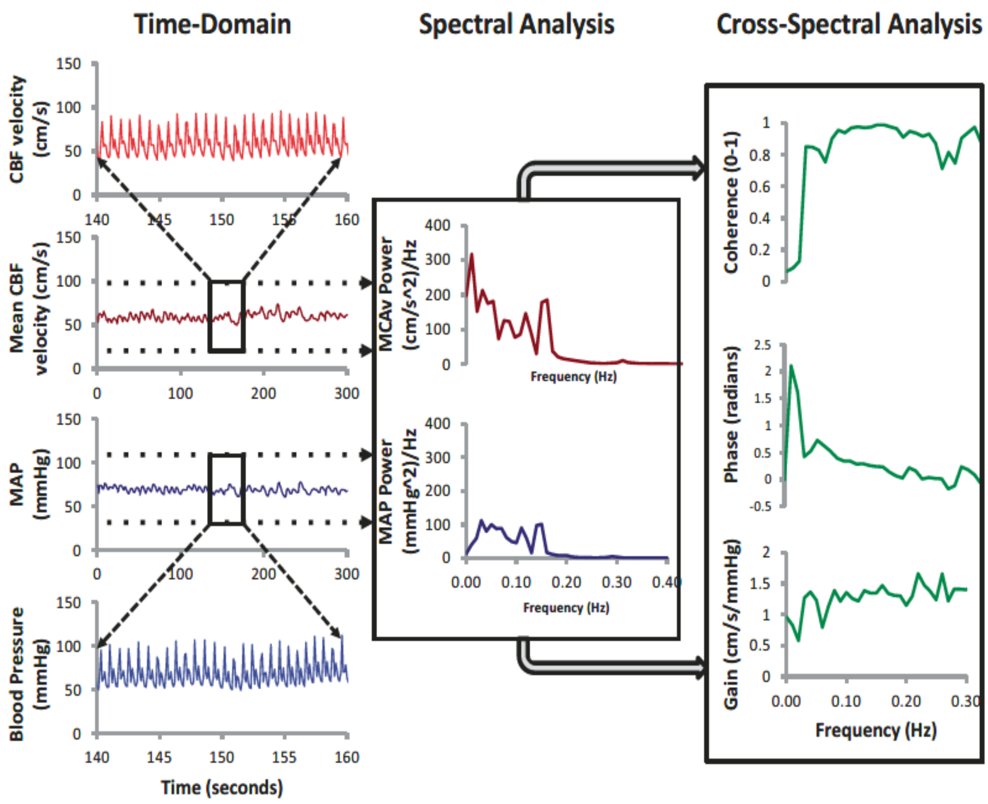

Figure 2-2: Basic steps of Transfer Function Analysis of a system from time-domain to frequency-domain, reproduced with permission [5]

In addition, a white paper was published in [5] on behalf of the Cerebral Autoregulation Research Network (CARNet) and additional update white paper published in [61] where both papers provided a brief background about TFA which is usually used to solve linear control systems. CARNet (http://www.car-net.org) is a community that gathers all researchers studying cerebral autoregulation around the world in annual meetings and combined research projects. The paper suggested that the aim of TFA is to evaluate parameters which reflect dCA behaviour across all frequency ranges. In fact, it should be borne in mind that assuming dCA as a linear system is considered only to simplify the assessment process. However, dCA is not a linear system in reality due to the varying physiological nature of inputs (*ABP* and CO_2) which alter output (*CBv*) levels where each has a separate influence on the dCA mechanism [5].

Moreover, the paper highlights that there is no universal standard that has been accepted in implementing TFA which makes the selection of a method to quantify CA a personal choice. Despite variations in results, the paper aims to provide a standard for the implementation of TFA since there is significant literature and findings using the implementation of this technique. Additionally, the paper supports the standardization of TFA implementation, proposes improvement on parameters settings and suggests recommendations to be considered when applying TFA [5].

2.7. Multivariate analysis

The multivariate analysis focuses on examining multiple inputs (*ABP*, CO_2, O_2… etc) in TFA and studying their influence on the output (*CBv*). This should provide an understanding of how these inputs react and impact the output over time periods and explain the variability found in the time scale. An early study conducted by Peng et al. in 2008, shows that CO_2 and O_2 can both change TFA between *ABP* and *CBv* at low frequencies. The study suggested identifying a multivariate system as a technique to include multivariable inputs of the TFA. The study presented a model to analyse a multivariate input signal to explore the impact of these inputs on the output, *CBv*. ***Figure 2-3*** shows multiple inputs to TFA to quantify output *CBv*. The result of this study shows a significant difference between the univariate (considering *ABP* only) analysis and the multivariate analysis when measuring *CBv*, and output spectral power in the frequency domain [55].

Figure 2-3 illustrates that inputs in the time domain are transformed to the frequency domain by TFA where H_{pv}, H_{cv}, and H_{ov} are the transfer functions of *ABP*, CO_2, and O_2 respectively. Each transfer function is computed by dividing the power spectrums of *CBv* and *ABP* (as shown in equation 3). This is done after calculating the power spectrum of each input and the output (as shown earlier in equations 1 and 2). Then, the multiple coherence is computed as shown in equation (5) where G_{YY} is the power spectrum of multiple inputs and G_{VV} is the *CBv* power spectrum [55].

$$r_{M2}(f) = G_{YY}(f) / G_{VV}(f) \qquad (5)$$

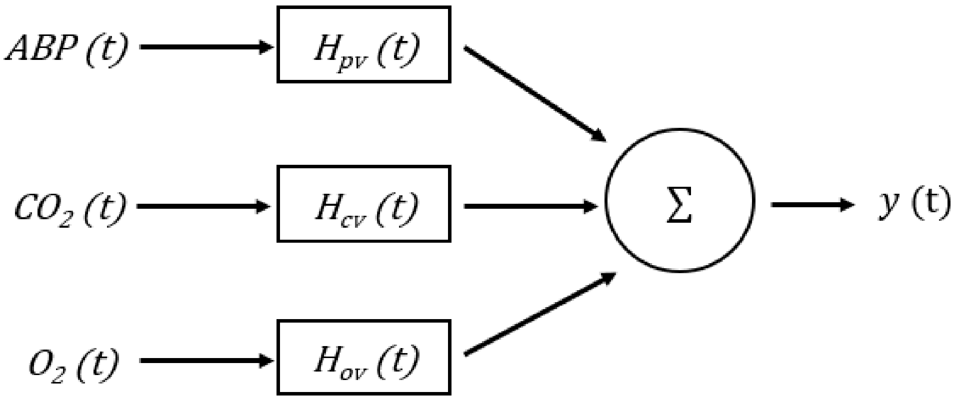

Figure 2-3: Schematic of multiple inputs system. *ABP*, CO_2 and O_2 pressures are model inputs and *CBv* as the output *y*(t), reproduced with permission [55].

Figure 2-4 shows the *CBv* spectrum of the residue (difference between measurement and system prediction) of both systems, univariate and multivariate. The low residue in the multivariate analysis (red dotted line) shows that combining other physiological parameters such as O_2 and CO_2 with *ABP* can better explain the multivariate system input and output [55].

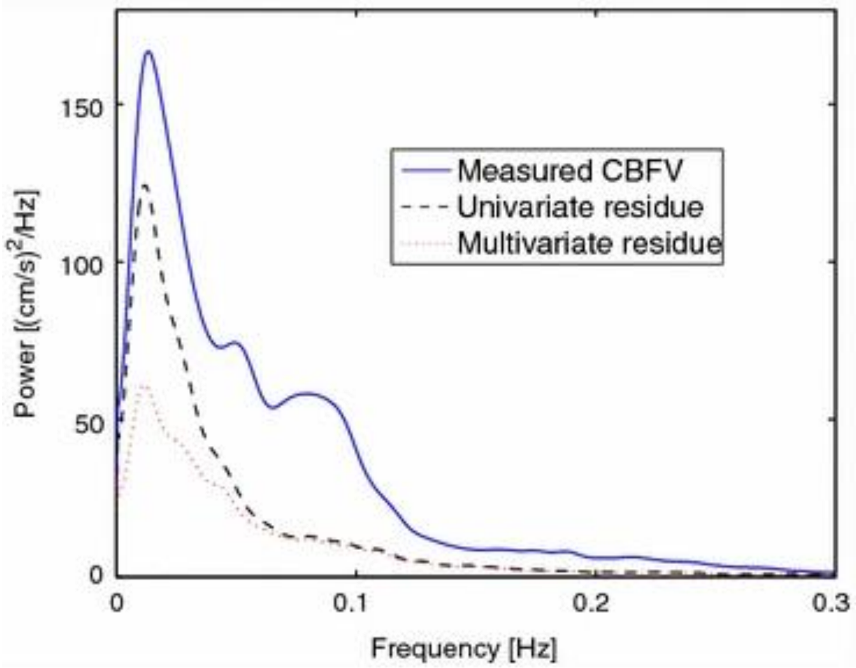

Figure 2-4: Spectra of measured *CBv* and model residue in both univariate and multivariate systems, reproduced with permission [55].

A recent study by Panerai et al. also included the neural stimulation with the *ABP* and CO_2 as inputs for TFA to assess changes in *CBv*. The study proposed a new approach for identifying the distinct contributions of BP and CO_2 by using a neural stimulation marker to observe *CBv* response in neurovascular coupling which is not a universally used marker and has a relatively limited or controversial influence on dCA mechanism. Neural stimulation was performed by repetitive passive elbow flexion of healthy subjects at a frequency of 1 Hz for one minute. The study suggested a dynamic multivariate model where neural stimulation, *ABP* and CO_2 are the inputs and *CBv* is the output of that model. This model is presented as a new approach to separately identify the contribution of each input to *CBv* response. The study highlighted that the suggested model has significant potential to quantify separate mechanisms implicated in *CBv* regulation and integrate these mechanisms [62].

Moreover, study conducted in 2022 [63] proposed that despite all the investigations aiming to improve clinical outcomes in post stroke patients, a large number of those patients still display no improvement, and some deteriorate. The study highlighted the development of the

INFOMATAS (Identifying New targets For Management And Therapy in Acute Stroke) project which is fostering interventions to better comprehend and advance cerebral haemodynamic features in acute cerebrovascular conditions. The review aims to summarize studies pertinent on dCA assessment in acute ischemic stroke, intracerebral haemorrhage, and subarachnoid haemorrhage patients to produce an investigation plan to enable bedside dCA information that will help in disease prognosis and perfusion interventions [63].

Furthermore, a study conducted in 2018 suggested that dCA is impaired in acute ischaemic stroke (AIS) patients. AIS patients were confirmed of contracting the disease through MRI and given a modified ranking scale (mRS) ranging from 0 – 3. Patients with favourable outcomes scores ≤ 1 and other scores ≥ 2 are defined as having unfavourable outcomes. The study investigated if dCA indices (coherence, gain and phase) could be used as a predictor of AIS in patients and applied multivariate analysis using TFA to assess dCA indices under unprompted hemodynamic oscillations. The study found that phase shift at VLF in favourable outcome patients is significantly better than in unfavourable outcome patients and conclude that phase shift value in the VLF range could be used as a predictor of AIS in patients [64].

Other studies have investigated dCA impairment after subarachnoid haemorrhage (SAH). The study was aiming to examine dCA relationship with some neurological and vascular impairments in patient with SAH, particularly, angiographic vasospasm (aVSP) and radiographic delayed cerebral ischemia (DCI). This was accomplished by studying 68 patients diagnosed with SAH using TFA method and multivariate logistic regression models. The study found that 62 % of the SAH patients have developed aVSP and about 19% have developed DCI. The study concluded that dCA is impaired in those patients especially in the early days after SAH onset [65].

On the other hand, a study researched the variability found on some short-term mechanisms regulating heart rate and blood pressure. The study employed autoregressive time-variant spectral estimation method that was extended to a multivariate approach to accommodate multiple processes and TFA. The results show that applying these methods have detected the dynamics that lies behind these signals. The study concluded that these methods establish new time series and define the underlying physiopathology of the cardiovascular control systems even the non-stationary periods [66].

Likewise, a study investigated the interactions between *HR*, *ABP*, and lung volume signals that have been previously described in bivariate models. The study introduced a trivariate autoregressive model to include all three signals simultaneously and calculate the transfer function between each pair of the signals and to compare the results of including all three signals in the analysis. The results have shown significant difference between the bivariate and trivarite analyses. The study suggested that using the trivariate expanded technique might provide a better understanding of some physiological mechanisms or specific pathological phenomena in cardiovascular control systems [67].

A study examined the time-varying feature of dCA by using multivariate analysis including CO_2 as an input with *ABP* to quantify both inputs' influence on the output (*CBv*). The study found nonstationary behaviour confirming earlier studies' findings of CO_2 impact on the dCA mechanism. Also, using CO_2 as an additional input to the model results in lesser time-varying approximations of the dCA compared to the univariate analysis using only *ABP* as the input [68].

2.8. Reproducibility

Reproducibility is the level of agreement between measured results and methods applied in analysing the data even if the results are extracted later by different individuals at different sites using different systems [69]. This means that a researcher should be able to replicate the results of previous studies using the same dataset that was used by the original researcher. Usually, reproducibility or reliability is tested to assess the reliability of devices used for measurement (instrumental reliability), reliability of observers and researchers (rater reliability), or reliability of measured parameters (response reliability) [70]. Reproducibility is essential in both research and in clinical practice to ensure that data can be quantified and replicated over time.

There are few common methods of quantifying reproducibility such as hypothesis test (e.g. using paired t-test), correlation coefficient (r), ICC, standard error of measurement (SEM), coefficient of variation (CV). The hypothesis testing provides estimations for systematic differences and don't not provide information about differences in individuals which necessitate the need to use alternative method to estimate these differences. For the correlation coefficient, the degree of association is detected but systematic errors are not which estimates the correlation between datasets but not the level of agreements. The ICC defeat some correlation coefficients limitations using single index to represent variance estimations between measurements. The SEM is oftentimes used with ICC to measure the absolute reliability, the greater the reliability the smaller SEM value which is not suitable for use with intervallic data [71].

For the CV, is mostly used in laboratory studies and expressed in percentage, some studies suggested that ICC should be used, and CV should not be employed to study reliability [71] [72] [73]. The ICC is the most common method used in measuring reproducibility and is widely applied in scientific research methods as it will be seen in the following paragraphs. There are 10 forms of reporting ICC and selecting the correct form depends on 3 main elements, the model (one-way random effect, two-way random effect, two-way mixed effect), the type (single rater or mean of k raters), and the definition (consistency, linearity of scores, or absolute agreement where different raters give same scores to subjects) [70]. This thesis is looking to correlation of results with previous studies using the same methodology/study data and will be using the Two-way mixed effects model as a single rater with absolute agreement, using the same recorded measurements to same cohort of subjects.

The ICC measurement describes the similarity of dataset recordings and how the outputs across all subjects have resembled each other. A study published in 2018 defines ICC as a measure of the reliability of different raters collecting measurements of subjects. ICC is mathematically expressed as [74]:

$$\text{ICC} = \frac{{\sigma_b}^2}{{\sigma_b}^2 + {\sigma_w}^2} \qquad (6)$$

where ${\sigma_b}^2$ is the variance subject variability and ${\sigma_w}^2$ is the variance measurement variability. The study suggested that ICC value ranges from 0 – 1 labelling values below 0.5 as poor reliability, from 0.5 – 0.75 as moderate reliability, from 0.75 – 0.9 good reliability, and above 0.9 as excellent reliability [74].

A study has suggested that ICC is scored by values between 0 – 1 where 0 represents "poor correlation" and 1 represents "excellent correlation" [59]. Alternative way of interpreting ICC is the indication of the reliability of measurement where values close to 0 indicate "no reliability" and values close to 1 indicates "high reliability". ICC measures values' stability of repeated measurements of the same subject and all subjects under the same settings [75].

A study conducted in 2010 suggested that dCA is lacking standards of measurement and analysis. The study proposed ICC as a quantification method to evaluate the different approaches to using TFA. The study proposed that only ICC values above 0.9 could be deemed reproducible. The study indicated a poor reproducibility of TFA indices due to the high variability of measured values [76].

An alternative study referred to reproducibility measurement as a prime assessment feature of any research method. The study researched dCA using TFA by analysing datasets consisting of 5 minutes recordings of baseline *ABP* and *CBv* signals from 14 centres with 75 healthy subjects. The study grouped the methods into 3 types: TFA, autoregulation index (ARI) and correlation coefficient. The study shows that TFA gain in the LF band has presented a decent reproducibility with ICC value ≥ 0.6 but lower reproducibility values in the VLF band. Therefore, the main reason behind poor dCA reproducibility is the physiological variability (nonstationary). The study concluded that the physiological nature of measurements significantly reduces the reproducibility of dCA, particularly when assessing data recordings in short periods and suggested that further study is required to understand physiological variability's impact on dCA reproducibility [59].

Likewise, a study conducted in 2018 reported that methods of calculating the reproducibility of dCA lack standardization and most available methods used to calculate dCA have limited reliability to be used in clinical practice. The study assessed systematic errors in data resulting from different modelling methods to evaluate the reproducibility of dCA parameters. This was approached by asking 14 different centres to analyse 22 datasets comprising repetitive measurements of *ABP* and *CBv*. The study investigated reproducibility through ICC analysis in 3 dCA methods; TFA, ARI, and correlation coefficient. As result, the TFA method shows decent ICC values at LF and VLF bands. The study underlined that ICC values are higher than reported in earlier studies for most methods [58].

Similarly, a study investigated *ABP* influence on dCA reproducibility by analysing mean *ABP*, *CBv* and CO_2 measurements which were taken twice from 75 healthy subjects. Fourteen different centres analysed dCA with a variety of analysis techniques. The study revealed that ICC values were significantly higher when removing gain, phase, and ARI parameters of subjects with low power spectral density of *ABP* values. The study reported that the ICC value for the gain at LF was the highest, tailed by phase at the same frequency band then gain at VLF. The study suggested that attaining good reproducibility of dCA could be achieved by increasing the measurement duration time to 35 minutes. The study concludes that increasing the measurement period and removing the low power spectral density of *ABP* can improve dCA reproducibility from poor to decent levels [60].

Furtherly, a study questioned dCA reproducibility when using TCD in the presence of CO_2 at high concentration levels. The study recorded *ABP* and *CBv* in 11 healthy subjects for 5 minutes in four settings, breathing air, 5% CO_2, 80% O_2, then mixed CO_2 and O_2. Using TFA, ARI was calculated for all recorded datasets, and it showed a significantly higher level of dCA reproducibility when using mixed gases. The conclusion indicates that ARI calculation and *CBv* measurement using TCD in the presence of mixed gas inhalation have resulted in an adequate level of reproducibility [77].

Obviously from these studies, when ICC values are above 0.9, they are deemed to be highly reproducible. ICC values reported in the LF band were the highest compared to HF and VLF bands. Also, the variability of physiological measurements has a significant impact on dCA reproducibility levels which could be improved by removing the low power spectral density from TFA inputs and increasing the measurement recording duration of subjects' vital signs.

2.9. Conclusion

In this chapter, earlier research efforts exerted in understanding and quantifying dCA were discussed to provide enlightenment about dCA variability. The first section viewed the cerebral vasculature and provided the basic anatomy of the circle of Willis and major arteries. The second section introduced the dCA mechanism and the underlying physiology. The third section presented measurement techniques to assess dCA. The fourth section provided an overview of methods to quantify dCA mechanism. The fifth section demonstrated TFA on dCA parameters and earlier scientific efforts in exploring different methods and finding a golden-standard approach. The sixth section offered the multivariate analysis concept and viewed research studies' endeavours and recommendations to apply further TFA considering multivariate methods. The last section explained the reproducibility concept using ICC analysis by exploring some studies methods and findings to have proper grounding for future works.

3. Study data

3.1. Introduction

This chapter will describe the dataset that will be used in the analysis of this study. The upcoming sections will describe the study settings, study population and data collection techniques. First, the study settings and population section will describe the study settings where the data collection took place and will describe the study subjects that will be considered in this thesis. Lastly, the data collection section will describe the sampling techniques used to collect the data from the participating subjects.

3.2. Study settings and population

Data collection took place at Southampton General Hospital (SGH), United Kingdom. The dataset is vital signs recordings of 20 healthy adult subjects (10 females) at 3 physiological challenges (normocapnia, hypercapnia and thigh cuff). The subjects were (25.5 ± 3.5 years, height 168.3 ± 12.3 cm, weight 64.5 ± 16.4 kg, body mass index 22.6 ± 4.5 kg/m^2, systolic BP 119.6 ± 15.4 mmHg, diastolic BP 70.5 ± 8.3 mmHg) recorded at rest during their visit to SGH. Each recording for each subject is 18.5 ± 1.1 minutes long at normocapnia and thigh cuff conditions whilst the recording last for 5 minutes in stimulated hypercapnia condition in order not to harm the subject's health. The dataset of 300 recordings represents 5 visits at 3 physiological challenges for each one of the 20 subjects where the recordings of each subject was taken in 5 separate times during almost a week (8.9 ± 6.4 Days) [57] [10].

During each visit, each subject is recorded to collect the *ABP*, *CBv* (right and left sides), CO_2, and *HR* parameters for a period of 18 minutes in normocapnia and thigh cuff conditions whilst the recording lasts for 5 minutes in the hypercapnia condition. Each recording includes the mean *ABP* as well as the mean *CBv* for the right and left sides measurements. It's worth noting that there are some missing visits from 2 subjects, a subject missing 3 visits in normocapnia recordings and one more subject missing a visit in hypercapnia. ***Figure 3-1*** shows a sample of a recording of one subject during a visit and displays input parameters that will be used in TFA [57].

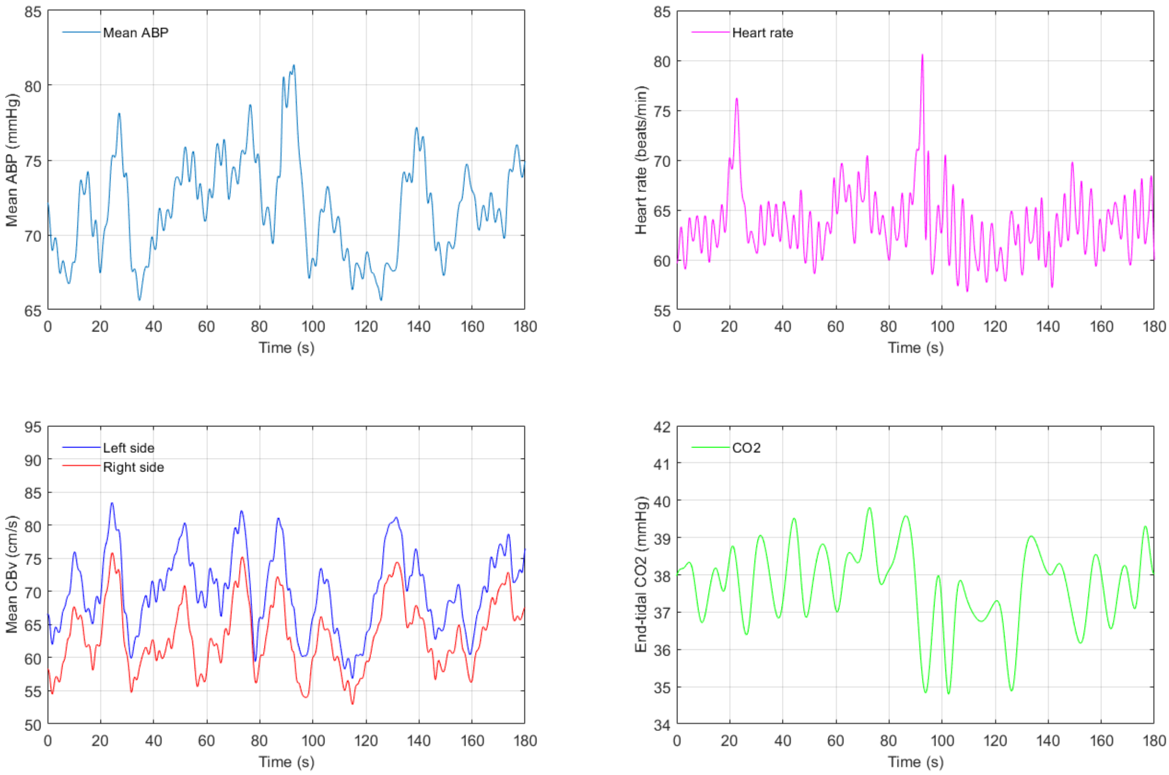

Figure 3-1: Sample of vital signs, mean *ABP*, right and left mean *CBv*, instant *HR* (inverse r-r interval) and CO_2 recordings of a subject in one visit at normocapnia

3.3. Data collection techniques

Datasets parameters are recorded using the devices described in the following sentences then exported and saved in MATLAB format to use in TFA in this thesis. However, 3 different devices were used to measure parameters from subjects. Finometer device, a non-invasive finger cuff device (Finapres 2300, Ohmeda) was used to measure *ABP* and mean *ABP*. Heart rate was measured using an electrocardiogram (ECG) device (Diascope1, Simonsen&weel) to detect heartbeat and compute average values of the signal. CO_2 was measured during normocapnia and hypercapnia using an infra-red technology (Capnocheck, BCI). Using TCD sonography, *CBv* was measured using Multidop-t, DWL system with a 2 MHz transducer to measure the blood flow velocity at the middle cerebral arteries (MCA) entering the circle of Willis from the right and left sides of the brain [57].

ABP, mean *ABP* and CO_2 partial pressure parameters are measured on an mmHg pressure scale whilst the *CBv* velocity is measured in cm/sec and *HR* is measured in beats/min. *CBv* and *ABP* are sampled at 125 Hz whereas CO_2 and *HR* are sampled at 10 Hz. Therefore, mean *ABP* and mean *CBv* need to be re-sampled at 10 Hz to unify the sampling rate of all parameters and be able to process them in TFA. The sampling frequency (10 Hz) refers to the number of instants recorded per second which are taken from the continuous input and then stored as numbers [5]. ***Figure 3-2*** shows samples of the *ABP* and mean *ABP* from the dataset that will be used in this study.

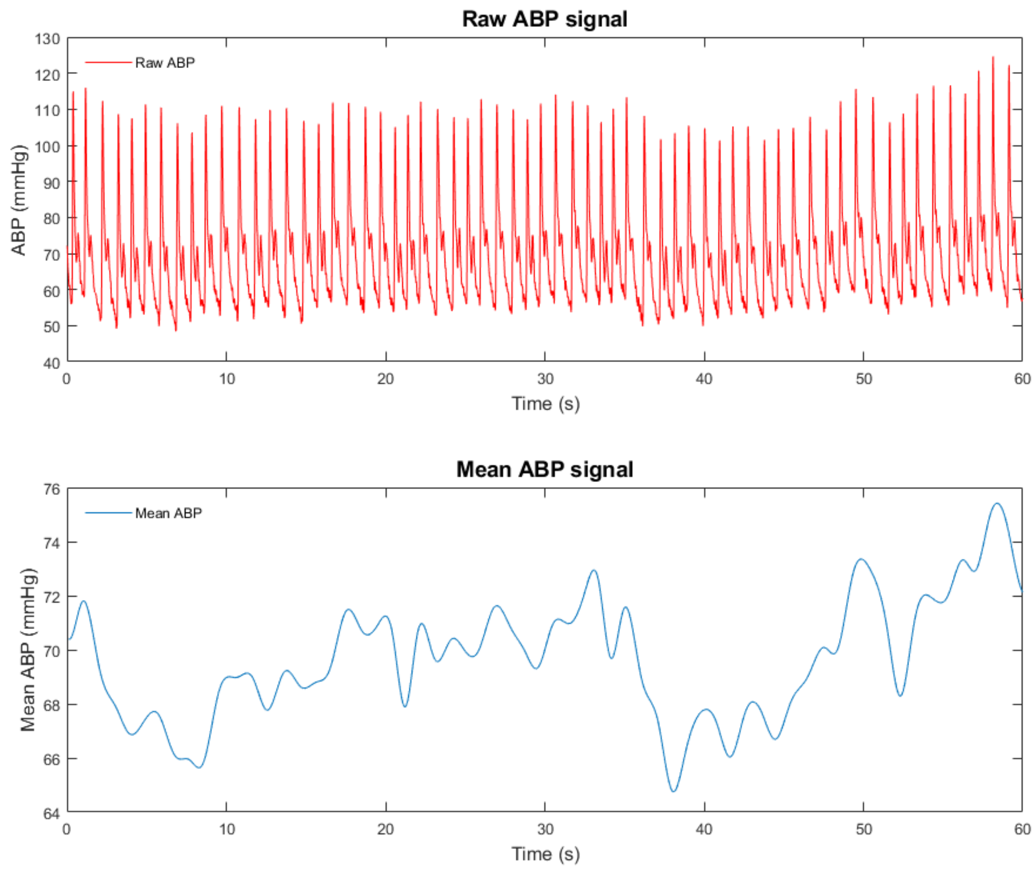

Figure 3-2: Sample of the raw *ABP* (top) and mean *ABP* (bottom) signals from the dataset

3.4. Univariate data pre-processing

Some recordings are missing values within the recording period. To overcome this challenge, linear interpolation was used to pre-process the dataset, fill gaps, and correct the error. This will generate new points within the recording period based on averaging values of the entire recording time. Sometimes, the missing values are present in the mean *ABP*, mean *CBv* right side and/or mean *CBv* left side. The missing values are labelled by NaN (Not a Number) fields within the recording.

Using MATLAB, algorithms were developed for each UTFA input variable (mean *ABP*, mean *CBv* right and mean *CBv* left). These algorithms find the missing values, correct the error by generating new values and inserting them into the recording and list both the percentage of missing values on the recording and the time points of the missing values. ***Figure 3-3*** shows a result of using the algorithm on the incomplete recording of the mean *ABP* signal. Pre-processing codes were developed and executed separately for each input variable. The result of executing linear interpolation code was deemed to be an effective approach to resolving the missing values problem and unifying the dataset fields to be ready for the UTFA.

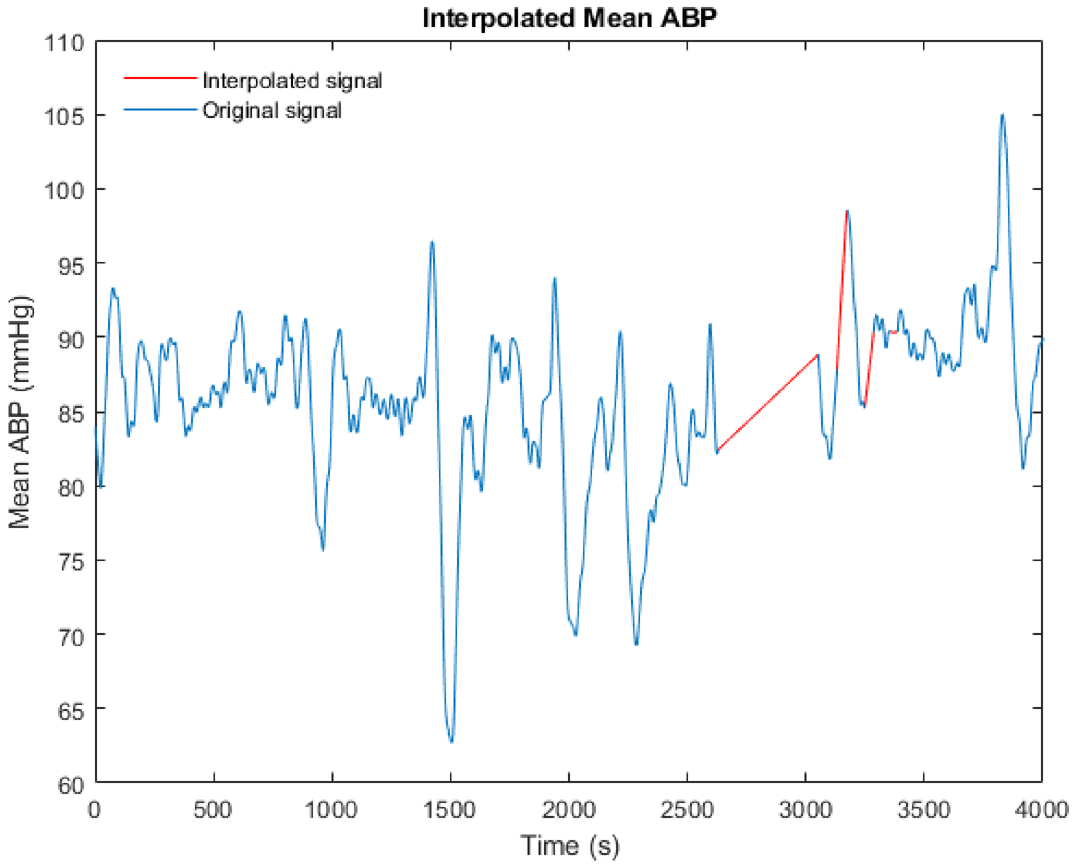

Figure 3-3: Example of linear interpolation on an incomplete recording of mean *ABP*

3.5. Multivariate data pre-processing

Using the same datasets described above, all multivariate TFA input variables (mean *ABP*, *HR*, CO_2, mean *CBv* right side and/or mean *CBv* left side) were sampled at 10 Hz where some recordings are missing values within recording period. To cope with this challenge, all multivariate TFA inputs were resampled to 1 Hz utilizing the cubic spline interpolation to pre-process the dataset, fill gaps and correct the error. The 1 Hz frequency is widely used in the literature when investigating dCA from the multivariate perspective [55].

Using MATLAB, algorithms were developed for each multivariate TFA input variable. These algorithms find the missing values and correct the error by generating new values and inserting them into the recording. ***Figure 3-4*** shows an example of an *ABP* time series after using the developed algorithms on an incomplete recording of an *ABP* signal. Reproducing the pre-processing approach of a study conducted in 2008, algorithms were developed and executed separately for each multivariate TFA input variable in this study. The result of executing the cubic spline interpolation code was found to be an effective approach to resolving the missing values problem and unifying the dataset frequency to be ready for the multivariate TFA [55].

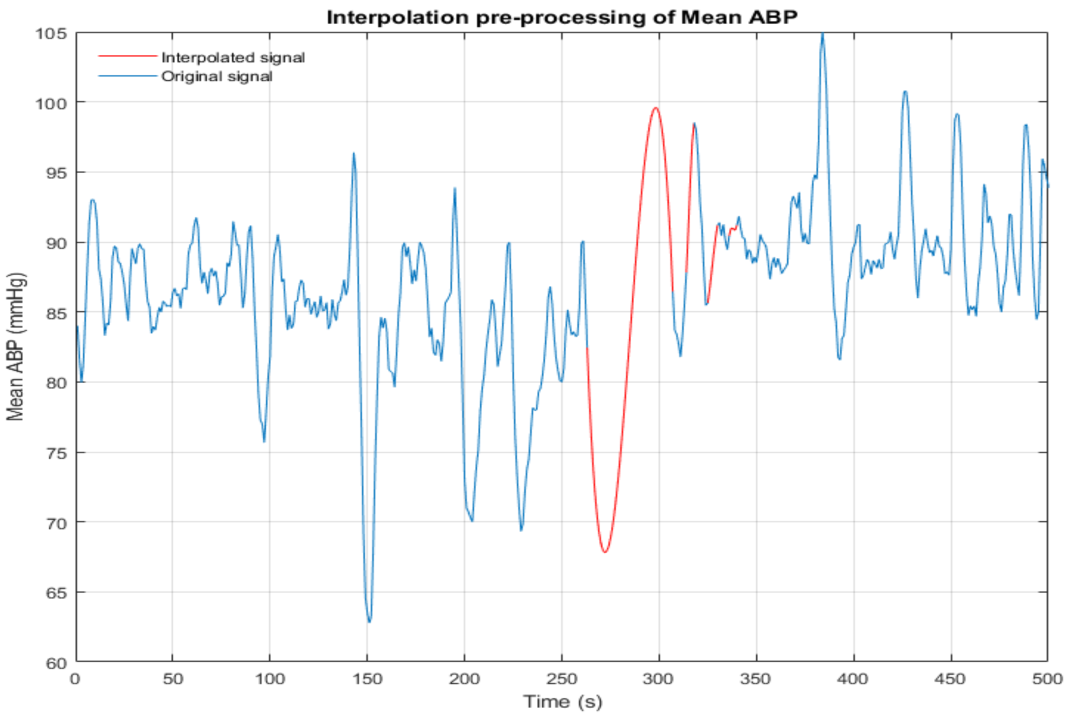

Figure 3-4: Example of a cubic spline interpolation on an incomplete recording of a mean *ABP*

3.6. Conclusion

In this chapter, study data including study settings and population were presented as well as displayed a sample of the subjects' measurements as shown in ***Figure 3-1***. Then, data collection techniques were discussed by describing equipment and tools used to collect participating subjects' measurements. Lastly, data pre-processing techniques were elaborated for both univariate and multivariate analyses.

4. Univariate Transfer Function Analysis

4.1. Introduction

This chapter will discuss the methods and materials used in the analysis processes of this study. There are 3 sections that will be covered within this chapter. First, methods will describe the approaches used to analyse the recordings datasets. Secondly, a brief explanation about the Univariate TFA (UTFA) outputs (UTFA parameters) analysis across frequency bands will be provided. The latter will outline the analysis on the datasets and the results extracted from this analysis. The results section will present the outcomes across the three different frequency bands as well as the outcomes of the reproducibility and covariance analyses.

4.2. Methods

In this chapter, the dCA assessment will be mainly based on beat-by-beat mean *ABP* (input) and mean *CBv* (output) measurements throughout the univariate analysis. Each dataset, as presented in Chapter 3, comprises a recording of *ABP*, *CBv* (right and left sides), CO_2, and *HR* as well as mean recordings for *ABP* and both sides of *CBv*.

Furthermore, the dataset in this study will be analysed using the UTFA technique. Then, Intra Class Correlation (ICC) analysis will take place on the UTFA outputs to evaluate the relationship between UTFA outputs within each subject's recordings and overall participating subjects. ICC results will show the strength level of UTFA outputs resemblances of each subject’s recording and overall subjects’ recordings. Afterwards, covariance analysis will be applied to measure variations of recordings of both groups, measurement variability and subject variability’ recordings.

4.3. Univariate Transfer Function Analysis (UTFA)

The UTFA analysis generates outputs (Coherence, Gain and Phase) at 3 frequency ranges, HF, LF and VLF. The results of UTFA analysis are listed in tables within MATLAB and plotted in figures as shown in ***Figure 4-1***. Each time series will result in coherences, gains, and phases in the form of 9 outputs at HF, LF and VLF ranges (3 outputs for each frequency range) for each subject at one visit on each side. Bearing in mind that there are 5 visits for each subject, this will result in having 18 outputs for each subject on each physiological challenge (e.g., normocapnia) on both the right and left sides across all frequency bands. The left plot shows the raw *ABP* (input) and *CBv* (output) signal in the time domain. The right plot shows the *ABP* (input) signal across the 3 frequency bands and *CBv* (output) line across these frequencies. The output is divided into 3 horizontal lines according to their measurements at each frequency band. The middle line represents *CBv* outputs (coherence, gain, and phase) in the LF band which will behave differently across subjects at different physiological challenges.

The next section will discuss the variability analysis that form the basis of the results. Subsequently, later sections will present variations of UTFA parameters in all 3 frequency ranges and normocapnia, hypercapnia and thigh cuff conditions. Then, the upcoming sections will present ICC analysis for all participating subjects as well as the covariance analysis of all subjects for all conditions.

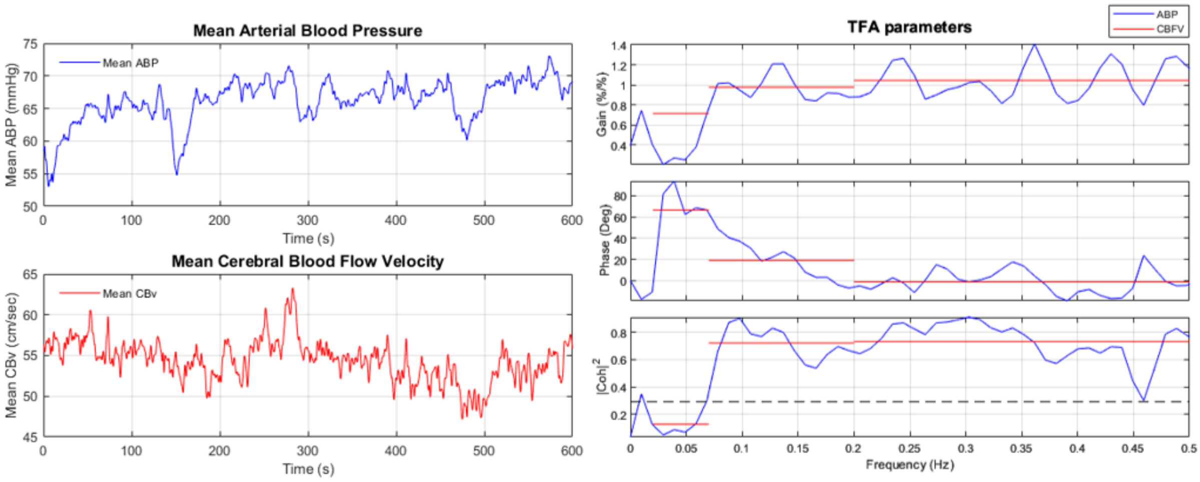

Figure 4-1: Sample of UTFA output plots for a subject evaluating the *ABP* and the right side *CBv*
Left plot – Raw recorded *ABP* and *CBv* on the right side
Right plot – Three curves represent Coherence (lower), Gain (upper) and Phase (middle) at HF, LF and VLF bands

4.4. Variability analysis

The variability of TFA outputs in terms of both the measurement variability, MV, defined here as the variability between the different visits for each subject for each condition, and the Subject Variability (SV), defined here as the variability both within each subject 5 recordings and between the overall subjects recordings, including MV, for each condition. The variability is calculated here by comparing the measurements made in both right and left sides using the plot shown in ***Figure 4-2***. This approach assumes that the differences between these two measurements represent the true variations between measurement variability and subject variability, as the two hemispheres of the brain are driven by the same systemic challenges. In the absence of any measurement variability, it would be expected that all data points would lie on the line of equality with the variance along this line representing the subject variability. Thus, any divergence from this line of equality is taken to represent measurement variability and the variability between hemispheres is assumed to be negligible in comparison to the other forms of variability. In another word, the variabilities on each side is assumed to be equal to other side (left and right sides). This is an important assumption that will be discussed further later. Under this assumption, conceptually the variability perpendicular to the line of equality can be assumed to be the measurement variability and the variability along the line to be the sum of the measurement and subject variabilities.

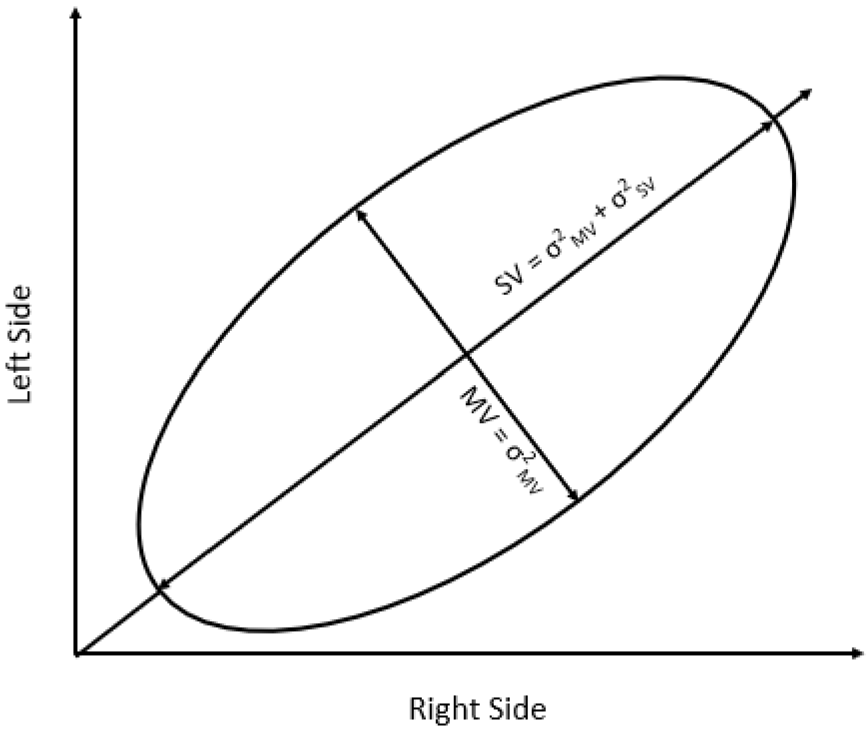

Figure 4-2: Measurement Variability (MV) and Subject Variability (SV) recordings of both right and left sides
MV is the variability in each subject recordings (5 visits per subject)
SV is the variability across all subjects including the variability of each subject (MV)

To estimate the different variabilities, it has been assumed that the two recordings (left side and right side) can be expressed as the sum of the true value (i.e., the population-average) with variability on both recordings that reflects first the subject variability, $\varepsilon(i)$, and then additional variability that depends on the subject and that reflects the measurement variability, $\varepsilon_L(k)$ and $\varepsilon_R(k)$, i.e.:

$$y_L(i,k) = \bar{y}_T + \varepsilon(i) + \varepsilon_L(k) \qquad (7)$$

$$y_R(i,k) = \bar{y}_T + \varepsilon(i) + \varepsilon_R(k) \qquad (8)$$

where the noise sources are assumed to have zero mean and variances σ_{SV}^2 and σ_{MV}^2 respectively (i.e., between subject and within subject). Then, calculate the covariance matrix of the recordings, $cov(\mathbf{Y})$, where the left and right recording values are given by $\mathbf{Y} = [y_L \quad y_R]^T$. Assuming that the noise terms are independent, then the covariance matrix straightforwardly becomes:

$$cov(\boldsymbol{Y}) = \begin{pmatrix} \sigma_{MV}^2 + \sigma_{SV}^2 & \sigma_{MV}^2 \\ \sigma_{MV}^2 & \sigma_{MV}^2 + \sigma_{SV}^2 \end{pmatrix} \qquad (9)$$

This explains the shape of the plot in ***Figure 4-2***, where the data points are plotted both individually and in terms of an ellipse that includes 95% of the covariance. This plot also provides a physically intuitive visualization of the variability in different TFA parameters under different conditions and physiological challenges. Note that this approach allows the computation of both variabilities and to 'compensate' for the different variabilities, thus providing a more robust measure of both variabilities. Calculation of the measurement variability from a set of single recordings from different subjects will not represent the true measurement variability, rather the sum of the subject and the measurement variabilities (Equation 9).

To compute the two measures of variability from this plot, a covariance matrix is computed for each of the TFA parameters in each condition using equations (7), (8), and (9). The covariance matrix is computed from all subjects' TFA parameters outputs in each condition which result into a 4 by 4 matrix. Then, the matrix is factorized, using singular value decomposition, which results into 2 eigenvalues. The larger value, corresponding to the major axis on this plot, is the sum of both measurement variability and subject variability variances, and the smaller one is purely the measurement variability variance. The points that are closest to the reference line represent the lowest variability of the subject's TFA parameters between the right and left sides of the brain. Conversely, the points that are far from the reference line represent a higher variability of the subject's TFA parameters between the right and left sides of the brain.

4.5. Results

First, the results from TFA across all recordings in normocapnia, i.e., coherence, gain, and phase have been compared in all three frequency bands, as shown in ***Figure 4-3.*** As can be seen, there is no discernible difference between left and right sides values. Statistical testing shows no statistically significant differences in any parameter values under any of the three conditions. This is as would be expected in a healthy population and supports the analysis that is performed to quantify variability.

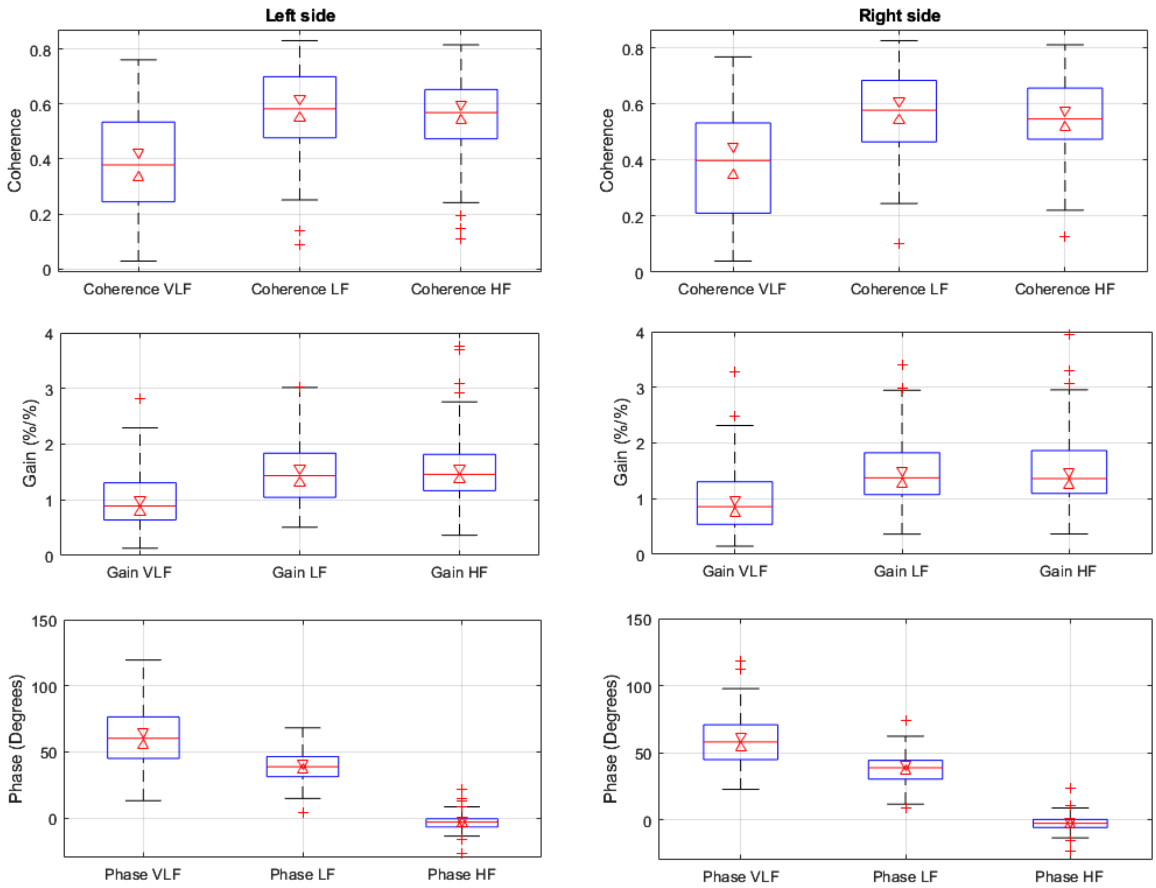

Figure 4-3: Boxplot of TFA variations over frequency bands under normocapnia condition

Reproducibility analysis was next performed to calculate ICC values for all subjects in normocapnia, hypercapnia and thigh cuff conditions. The result shows moderate reproducibility levels across all subjects in thigh cuff and normocapnia conditions, and poor reproducibility level in hypercapnia condition, with ICC values ranging from 0.43 – 0.53, as shown in ***Figure 4-4***. Normocapnia has an ICC value of 0.517, hypercapnia has a value of 0.433, and the thigh cuff condition has a value of 0.531. The thigh cuff test produces the greatest value of ICC, with hypercapnia yielding the lowest value; however, the results are moderately reproducible across all conditions except the hypercapnia, again supporting the analysis that will be performed next.

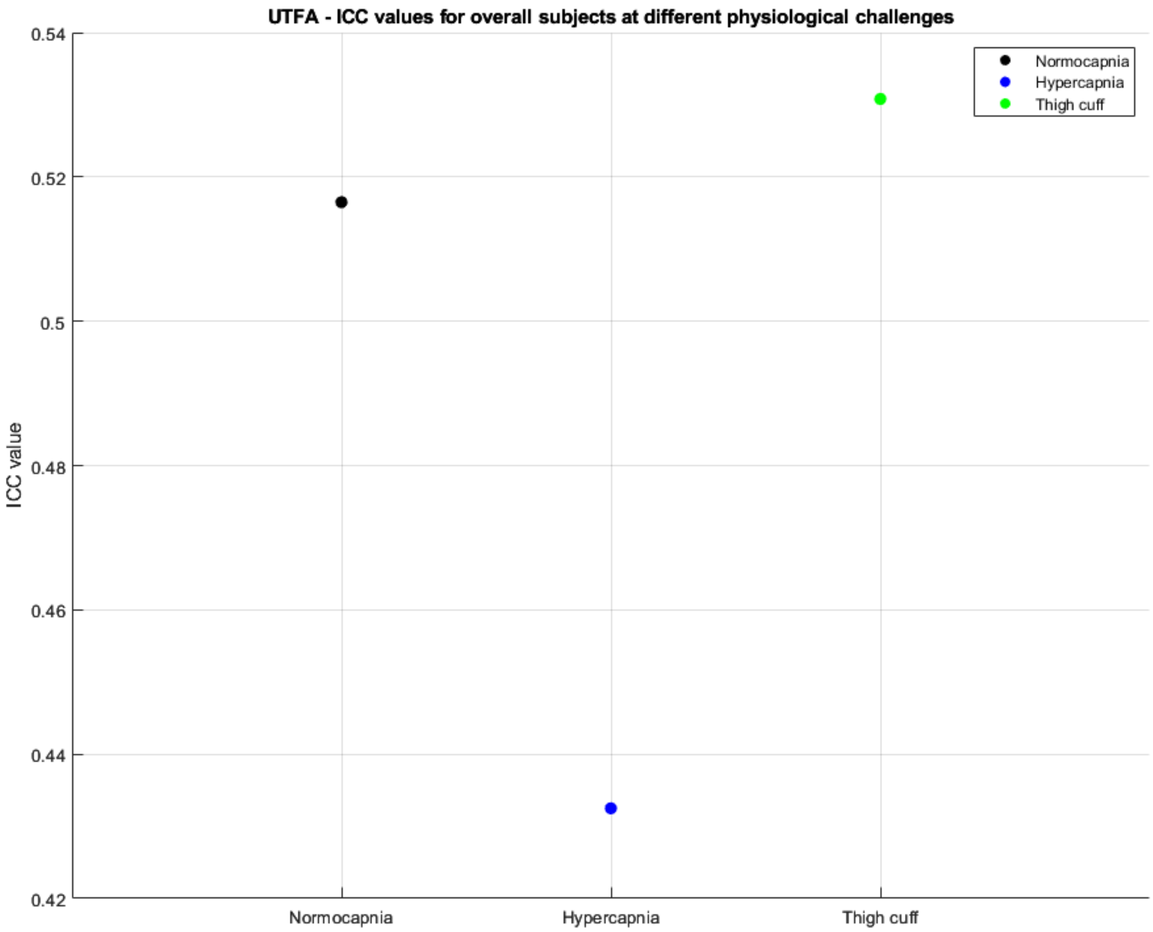

Figure 4-4: Scatterplot shows total ICC values for all subjects at different physiological challenges

The newly proposed covariance analysis was next performed to calculate both measurement variability and subject variability levels in all parameters at all physiological challenges. In addition, to help to quantify the reliability of the results, an additional assessment was conducted by removing one subject from the dataset and recomputing the values of variability. This procedure was repeated 20 times (removing one subject each time) as a simple way of providing 20 estimates of the computed variability values, allowing the provision of both a mean and standard error for each value. This analysis was carried out for all measurements at all frequency bands in all physiological challenges.

Figure 4-5 shows an example of the TFA results that shows the LF phase values for all recordings for all subjects in normocapnia (black dot), hypercapnia (blue dot) and thigh cuff (green dot). The ellipses for 95% confidence intervals are also plotted, based on the calculation of the covariance matrix. As expected, the LF phase decreases in conditions of hypercapnia (blue ellipse) compared to normocapnia (black ellipse), with a greater variability being shown in the thigh cuff condition (green ellipse). Note also that the ellipses for all three conditions lie close to and along the reference line, supporting the proposed analysis (similar behaviour is exhibited for the other eight plots, results not shown for reasons of space).

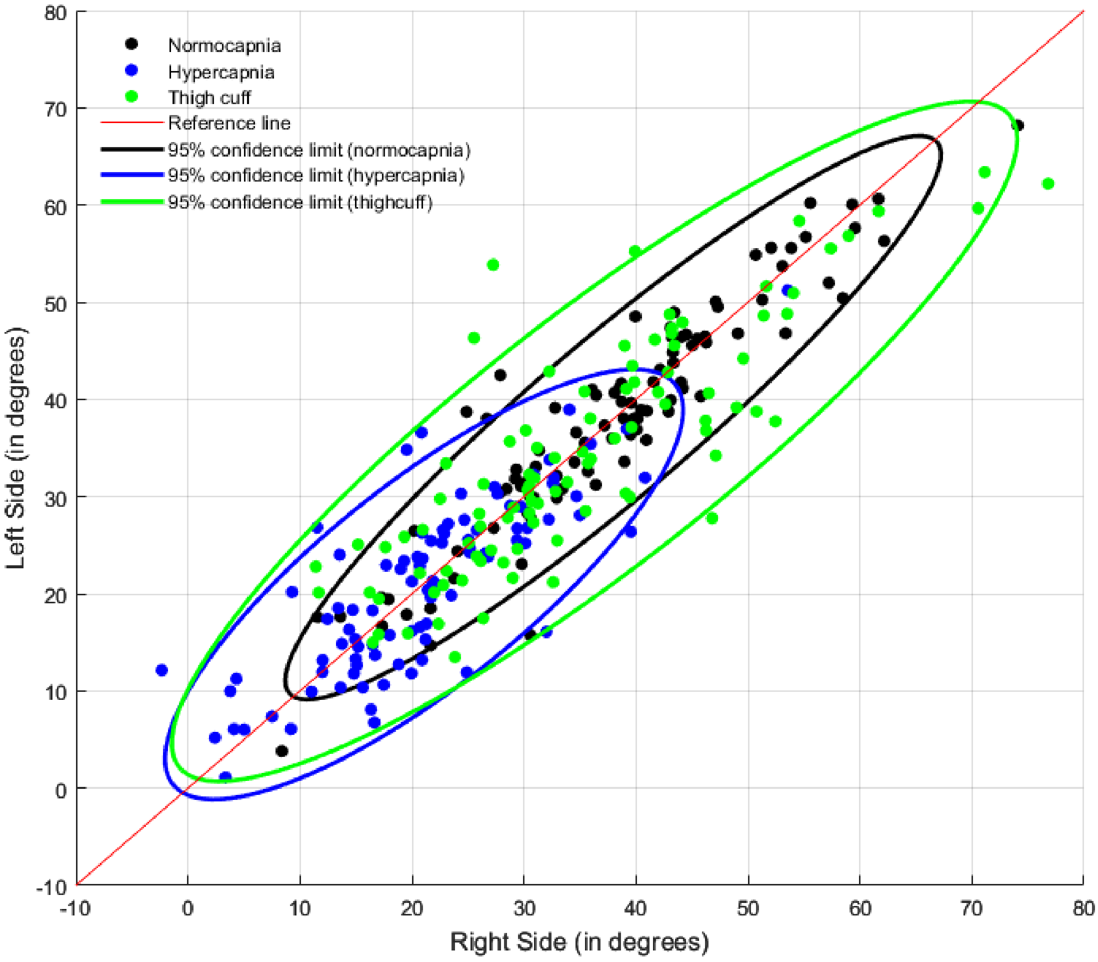

Figure 4-5: Phase variations of both right and left sides across different physiological challenges for all subjects at LF band

The values of measurement variability and subject variability are shown in ***Figure 4-6***, the different rows showing coherence, gain, and phase, and the different columns showing VLF, LF, and HF bands. The different physiological challenges are shown in different colours and the error bars (denoted red) represents the variance differences (standard error) in the results. The standard error shown on each parameter is computed using $\sqrt[2]{n}$ (n = 20, which is the number of all subjects in this study). In every case, the measurement variability is substantially smaller than the subject variability (as can clearly be seen in ***Figure 4-5***).

For coherence and gain, in every frequency band, the hypercapnia condition gives the highest measurement variability, whereas, for phase, the thigh cuff condition gives the highest measurement variability. In all cases, the normocapnia condition gives a lower measurement variability than that computed from the thigh cuff condition. There are fewer consistent trends in the subject variability values across the different parameter values and conditions. However, LF phase (which is one of the most used parameters to quantify dCA) does show much lower measurement variability in the hypercapnia condition, with the thigh-cuff condition yielding a much higher subject variability than the normocapnia condition. A complete list of the measurement and subject variabilities are listed in ***Table S-4*** in the Appendix for reference.

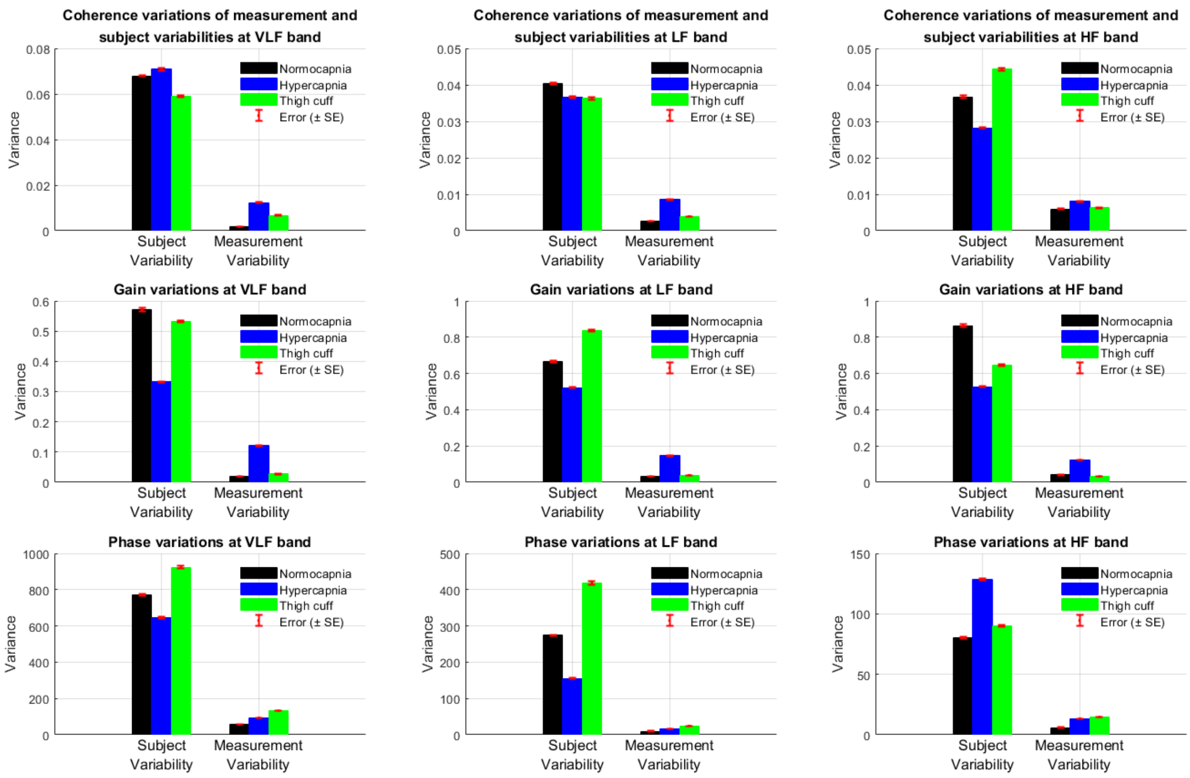

Figure 4-6: TFA parameters variations of measurement and subject variabilities across all conditions at all frequency bands. Bars (black, blue, and green) represent the mean-variance values of all subjects. Error bars (red) represent the standard error (SE) computed using $\sqrt[2]{n}$.

4.6. Discussion

The results in ***Figure 4-3***, the upper two plots representing both the right and left sides results variations at normocapnia condition show that coherence at the LF band has the highest coherence results compared to the HF and VLF bands. Then, the HF band coherence comes second, lower than the LF coherence and higher than the VLF coherence. But in brain injured cases, TFA results shows that coherence and phase resulted in the VLF are significantly correlated with autoregulation index and patient outcome [78].

The middle two plots show gain variations at normocapnia condition across the 3 frequency bands where both LF and HF demonstrate close variation patterns compared to the VLF band, which appear as the lowest in this analysis. However, a study suggested that gain at the LF and VLF bands could be used to evaluate dCA and there are limited number of studies discussed gain at VLF band [79]. Also, further studies are needed to understand dCA behaviour in gender and age differences to understand the significant correlation between gain variation and gender in elderly health subjects [80].

The lower two plots show both the right and left sides phase variation at normocapnia across all frequency bands. The HF band appear to be the lowest value with lowest variation levels compared to other bands. Then the LF band shows a higher magnitude with a larger variation than HF results whereas the VLF band demonstrate the highest phase values and variations compared to the other frequency bands. But it’s suggested that dCA mechanism might not be active in the HF band in hypercapnia condition [81]. Even with the higher coherence levels at the LF band, the VLF band results could assist in understanding autoregulation physiology and the nonstationary nature of dCA [82].

The reproducibility analysis performed by calculating ICC values for all univariate TFA parameters in different conditions as shown in ***Figure 4-4*** demonstrate that the thigh cuff condition has the highest ICC values compared to normocapnia and hypercapnia conditions. It’s worth noting that hypercapnia ICC values has the lowest values compared to the other conditions. This could explain the lower variability results found in the thigh cuff condition when analysing the covariances of TFA parameter. Also, a study found that calculating ICC for univariate TFA parameters appeared significantly higher than calculating ICC for ARI which was less than 0.5 [33].

The covariance analysis performed as shown in ***Figure 4-6*** illustrate different behaviour of univariate TFA parameters in different conditions across all frequency bands. Focusing on measurement variabilities, the thigh cuff coherence variability at the LF band demonstrate the lowest variation in the measurement variability compared to the other conditions whereas normocapnia condition appear to be the lowest at VLF and HF bands. For the gain variations, normocapnia and thigh cuff conditions display close variation levels across all frequency bands. The phase variation of normocapnia condition appear as the lowest compared to hypercapnia and thigh cuff conditions across all frequency bands.

Also, the thigh cuff technique is used to incite rapid changes in *ABP* which has been highlighted as safe technique that improves the detection of dCA impairment and decrease variability [83] . As well, using the autoregressive-moving average (ARMA) modelling has previously shown that dCA variability is significantly reduced with improved temporal resolution [34]. It has been found that dCA variability could be inconsistent in healthy elder group [84].

However, the results presented here show that each condition (normocapnia, hypercapnia and thigh cuff) exhibits different levels of variability in the TFA parameters (both measurement and subject variabilities). This variability is due to the physiological processes that govern the control of *CBv*; for example, in hypercapnia, a certain amount of time is required for CO_2 to enter the bloodstream via the lungs whereas the thigh cuff condition should have a faster response time since it induces changes in *ABP* levels once the cuff is deflated. Since *CBv* is influenced by *ABP* alterations, this will produce different levels of variability and hence reproducibility according to the physiological challenge applied during the recording.

Importantly, the analysis that has been performed here shows clearly that the measurement variability is much smaller than the subject variability, which also indicates that traditional methods to compute measurement-variability may provide an overestimate of the true value (through measuring a mixture of measurement and subject variabilities). The use of multiple recordings in each subject enables the provision of a truer estimate of the actual sources of variability, although the analysis is based on several assumptions that should be tested in more detail in the future.

The thigh cuff condition seems to be more rapid in changing *CBv* gain compared to the other two conditions [33]. Also, the values range from -15 – 30 but most of the phase shift values are between -10 and 10 degrees in the HF band whereas in some studies, phase shifts appear to result in positive range values [85].

One of the few similar previous studies showed that the LF band is a good starting point for further investigation compared to HF and VLF bands and suggested that including both healthy subjects and patients might yield higher levels of ICC. However, the study conducted the Lower Body Negative Pressure (LBNP) technique to induce changes in *ABP* and found that the consistency of phase measurements at the LF band was significantly improved. Additionally, the study suggested that this technique does influence the *ABP* and reduces both *HR* and CO_2 levels [57].

There are a number of limitations to this study. The assumption that dCA is a linear system is used here to simplify the assessment process, even though other studies have shown that dCA does exhibit non-linear behaviour [5]. Of potentially greater significance, the analysis did not consider the influence of other parameters on dCA, in particular CO_2. This has been shown to have a significant effect on the estimates of coherence, gain, and phase, as measured using multivariate TFA [55]. Univariate TFA was performed here for two reasons; first, this enabled the use of a standardised TFA code and thus provide guidance for other studies that use this in future; second, univariate analysis remains the most popular approach. However, the effect of including additional variables will be examined in future work.

4.7. Conclusion

In this study, measurement and subject variabilities were quantified in dCA using univariate TFA under three different physiological challenges. Using a novel approach, it has been found that TFA parameters in the LF band show the best grouping around the reference state among the right and left sides of the brain compared to the HF and VLF bands. The results show that the thigh cuff condition exhibits the best formation and encirclement around the reference state among all TFA parameters at the LF frequency band. It was noted that there is clear variability in the results between the different physiological challenges. The thigh cuff condition shows the lowest variability levels compared to normocapnia and hypercapnia conditions. This also means that variability reaches higher levels in hypercapnia conditions and even higher levels at normocapnia in some frequency bands. However, since the thigh cuff is a physiological challenge that cannot always be used, future work is needed to understand the low variability levels found in the thigh cuff condition observed in the nonstationary behaviour of dCA based on these results.

5. Multivariate Transfer Function Analysis

5.1. Introduction

The previous chapter has highlighted the variability using a univariate model which was the first step in assessing the variability of TFA outputs. Since there are other modalities available in the datasets and according to several studies findings and recommendations [62], it is valuable to assess the variability of TFA outputs in more detailed manner which allow comparison of univariate and multivariate results and should provide better understanding of variability in dCA. Adding more inputs to TFA (multivariate analysis) thus better quantifies the variability. The quantification of dCA is influenced by noise in the signals which could result in different levels of dCA outputs [86].

However, in multivariate analysis, there is a risk of overfitting the model [6], so there is an upper limit of how much can be added due to the fact that unrelated noise is usually present with measurements in real life [5] which imposes a limitation on how further variability can be explained [5]. It worth noting that it is expected for coherence results in the multivariate analysis to increase compared to the univariate analysis [55] but it can be difficult to calculate the statistical significance of this increase.

This chapter will discuss the methods and materials used in the analysis processes of this study. There are 4 parts that will be covered within this chapter: methods; Multivariate Transfer Function Analysis (MTFA); and results across the frequency band spectrum including reproducibility, covariance analysis, significance analysis and results comparison. Methods will describe the approaches used to analyse the recordings datasets. MTFA will provide an explanation about the analysis techniques and algorithms. Results from Sections 5.4, 5.5, and 5.6 will explain the analysis application on the datasets and the results extracted from this analysis. Next, the comparison of UTFA and MTFA will demonstrate outcomes behaviour.

5.2. Methods

In this chapter, the dataset will be analysed using the MTFA technique. Code was developed to study dCA behaviour and to understand the association between *ABP*, CO_2, *HR* (inputs) and *CBv* (output). However, endeavouring to explain the variability as much as possible, the dCA assessment will be primarily based on analysing 2-inputs (*ABP* and either CO_2 or *HR*) and 3-inputs (*ABP*, CO_2, and *HR*) measurements throughout the investigation since this chapter is assessing transfer function results on a multivariate basis (using 2 or more inputs). This means that it will analyse the *ABP* and CO_2 (2-inputs) then it will analyse the *ABP* and *HR* (2-inputs) afterwards it will analyse the *ABP*, CO_2, and *HR* (3-inputs) relationships with the output (*CBv*). Each dataset is a recording of *ABP*, *CBv* (right and left sides), CO_2, and *HR* as well as mean recordings for *ABP* and both sides of *CBv*.

Furthermore, ICC analysis will be performed on the MTFA outputs to evaluate the relationship of MTFA outputs within each subject's recordings and overall participating subjects. ICC results will show the strength level of MTFA outputs resemblances of each subject's recording and overall subjects' recordings. Next, covariance analysis will be applied to measure MTFA outputs variations of all subjects (measurement variability and subject variability) on both 2-inputs cases as well as the 3-inputs case. Later, a statistical analysis will be conducted to examine each MTFA output dependency and view their significance through p-value calculation.

5.3. Multivariate Transfer Function Analysis (MTFA)

This section will look at the MTFA application used in the analysis. This application produces TFA outputs as the following: multiple coherence, multiple gains, separate gains, and separate phases. The multiple values of coherence and gain will show the combined effect of inputs (*ABP*, CO_2…etc) in a single graph (either a line graph or bar graph) and the separate values ones will display the influence of each input in a separate figure. Both multiple and separate outputs display the results for both the right and left sides of the brain across a frequency spectrum of 0 – 0.5 Hz. MTFA analysis will be performed on all subjects' recordings at each physiological challenge (normocapnia, hypercapnia, and thigh cuff). This will result in 8 outputs per subject per visit per physiological challenge across the frequency spectrum (4 outputs for each side of the brain).

Figure 5-1 shows a sample of the MTFA results displaying both multiple gains and separate gains of a subject's visit. The multiple gains are the gains resulted from calculating both inputs (*ABP* & CO_2) in the TFA, i.e., displaying the combined effect of both inputs, where the separate gains display the results of each input separately (for further comparison and clearer display, additional figures of separate gains are listed in the Appendix to compare normalised vs non-normalised gain to ease comparison of indices using each input combinations across all three conditions). It's worth noting, as mentioned in section 1.3, that this thesis is aiming to validate previously developed MTFA technique and investigate the inputs influences on the results. The idea is to compare/display multiple output with separate outputs, not to investigate, which clearly shows that multiple output makes it difficult to measure each input influence on the output.

The upper plot shows the multiple gains waveform (blue line shows the right side and red shows the left side) with the combined effect of two inputs (*ABP* and CO_2) for each side. The left lower plot shows the separate gains waveform for the left side and the right lower shows the separate gains waveform for the right side of the brain. Note that the separate gains illustrate the separate effect of each input (*ABP* and CO_2) influence in the MTFA application (blue line is resulted by the *ABP* input influence and the red line is resulted by the CO_2 input influence).

The next section will present variation of MTFA parameters and the frequency spectrum at normocapnia, hypercapnia and thigh cuff conditions. Also, the upcoming sections will present ICC analysis for all participating subjects, the covariance analysis, and the paired t-test analysis of all subjects at all conditions using different combinations of inputs, *ABP* + CO_2 (2-inputs), *ABP* + *HR* (2-inputs), and *ABP* + CO_2 + *HR* (3-inputs) combinations.

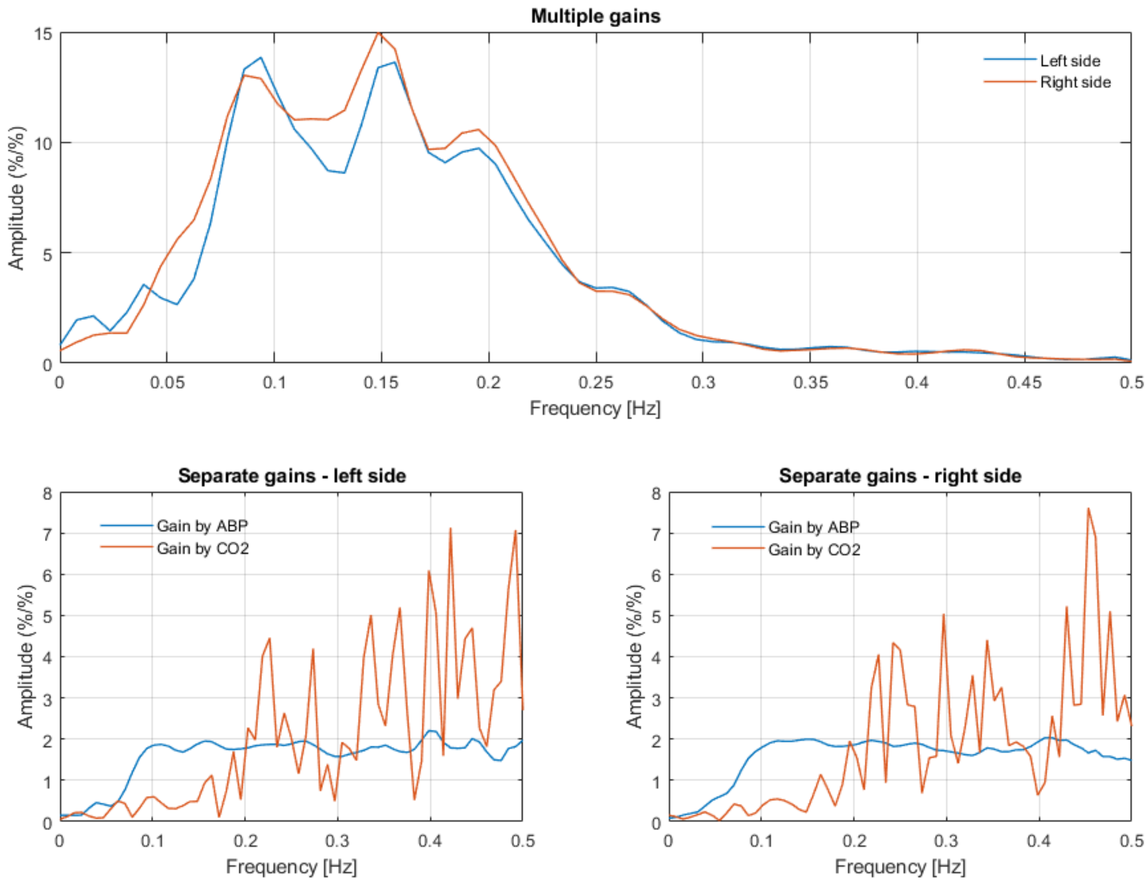

Figure 5-1: Sample of one recording from one subject showing multiple and separate gains for both right and left sides

5.4. Results using *ABP* and CO_2 inputs

This section describes how the results are generated and presented during the analysis process. After executing the MTFA code on all subjects on both right and left sides, a list of MTFA outputs is generated including the multiple coherence, multiple gain, separate gains and separate phases parameters [55] of each recording in each physiological challenge for all subjects over the frequency spectrum. Equation (5) in Section 2.7 represents the multiple coherence mathematically. Multiple gain parameter could be represented by defining the input signals cross and auto spectra in a matrix as:

$$G_i = \begin{bmatrix} G_{PP} & G_{PC} \\ G_{CP} & G_{CC} \end{bmatrix} \tag{10}$$

Then, calculate the cross-spectra between inputs and output (*CBv*) matrix as:

$$G_o = \begin{bmatrix} G_{pv} \\ G_{cv} \end{bmatrix} \tag{11}$$

The partial transfer function could be written as:

$$H = \begin{bmatrix} H_{pv} \\ H_{cv} \end{bmatrix} \tag{12}$$

where H_{pv} is the transfer function between *ABP* and *CBv*, and H_{cv} is the transfer function between CO_2 and *CBv*.

To calculate the multiple gain is by taking the absolute values of the partial transfer function which could be represented mathematically in equation (13) as:

$$Multiple\ Gains = |H| \tag{13}$$

Separate gains parameter is the presented through solving 2-inputs and 2-outputs system. After solving the matrix [87] considering that y_j is the output where $j \in [1,2]$, x_1, and x_2 are the first and second inputs respectively, the transfer functions for the 2-inputs, 2-outputs systems could be mathematically presented as:

$$H_{y_j X_1}(f) = \frac{G_{x_1 y_j}(f) * \left[1 - \frac{G_{x_1 x_2}(f) * G_{x_2 y_j}(f)}{G_{x_2 x_2}(f) * G_{x_1 y_j}(f)}\right]}{G_{x_1\, x_1}(f) * \left[1 - \gamma^2_{x_1 x_2}(f)\right]} \tag{14}$$

$$H_{y_j X_2}(f) = \frac{G_{x_2 y_j}(f) * \left[1 - \frac{G_{x_2 x_1}(f) * G_{x_1 y_j}(f)}{G_{x_1 x_1}(f) * G_{x_2 y_j}(f)}\right]}{G_{x_2\, x_2}(f) * \left[1 - \gamma^2_{x_1 x_2}(f)\right]} \tag{15}$$

From equations (14) and (15) the separate gains could be written as:

$$Separate\ Gains\ = \begin{cases} \left|H_{y_j X_1}(f)\right| \\ \left|H_{y_j X_2}(f)\right| \end{cases} \tag{16}$$

These parameters are listed in a table to plot them and visualize their variations as well as use them in the ICC analysis to measure their reproducibility levels. The ICC values were calculated for each subject and overall subject at different physiological challenges [88]. The ICC values results were plotted on a scatter plot to visualize the variation of these values for all subjects at different conditions over the frequency spectrum.

Furthermore, this thesis will measure the results' covariance to examine the variability of MTFA outputs within-subject (measurement variability recordings during their 5 visits) and subject variability' recordings (between all subjects' recordings) by comparing the measurements of both right and left sides as previously shown in ***Figure 4-2***. This is to evaluate *CBv* output variability on both sides of the brain across all subjects across the frequency spectrum at normocapnia, hypercapnia and thigh cuff conditions.

Next, this thesis will perform a paired t-test analysis to find and compare the p-values of different physiological challenges to investigate the significance of changing conditions/physiological challenges on MTFA parameters. This should show whether MTFA parameter variations are depending on the conditions under which the data are acquired or are independent, i.e., this will explain the association between each MTFA parameter and different conditions and whether associations will change in different conditions.

The next subsections will examine the MTFA outputs using different combinations of inputs (both 2-inputs and 3-inputs). Also, this study will quantify the variability levels of subjects' measurements and will visualize them at normocapnia, hypercapnia and thigh cuff conditions. This should enable the visualization of what is causing the variability of MTFA parameters under different conditions and physiological challenges. This visualization will be enhanced after calculating ICC and p-values of all parameters at different conditions. Besides, calculating MTFA outputs using different input combinations should provide a better understanding of outputs behaviour across the frequency spectrum under all conditions.

The following subsections will show the MTFA results for each condition/physiological challenge using the *ABP* and CO_2 inputs in the analysis across the frequency spectrum. To ease reading the tables listing mean and standard deviation values of each parameter on both sides, the tables will be in grey colour for normocapnia condition, blue colour for the hypercapnia condition, and green colour for the thigh cuff condition. Next, will display the ICC results, covariance analysis results, and the paired t-test analysis results comparing between conditions. It's worth noting that each bar represents the mean variation value for each condition (normocapnia in black, hypercapnia in blue, and thigh cuff in green). The small error bars (red) represent the standard error from each mean variation value above each bar.

5.4.1. Normocapnia condition

This subsection will illustrate the MTFA results of all subjects at normocapnia condition and using both *ABP* and CO_2 inputs. ***Figure 5-2*** shows MTFA outputs of all subjects at normocapnia conditions across the frequency spectrum using *ABP* and CO_2 inputs. The top left plot shows the multiple coherence with the combined effect of the two inputs (*ABP* & CO_2) on both the right and left sides of the brain. It's worth noting that both right side, blue line, (0.527 ± 0.134) and left side, red line, (0.528 ± 0.133) results are almost equal across the frequency spectrum and start hitting the highest coherence value at 0.1 Hz. The top right plot shows the multiple gains on both sides which seem to incline significantly after 0.1 Hz.

The upper middle left and right plots show the left and right sides respectively of separate gains results given by each MTFA input where the blue line is the gain by the *ABP* input, and the red line is the gain by the CO_2 input. However, the average gain resulting from CO_2 influence is significantly higher across the frequency spectrum compared to the *ABP* one on both the right and left sides. The lower middle plots show the left and right sides respectively of the normalised separate gains which demonstrate that *ABP* influence is significantly higher in the frequency range around 0.05 – 0.18 Hz then CO_2 influence appears higher across other ranges of the frequency spectrum.

Next, the bottom left and right plots show the left and right sides respectively of separate phases results given by each MTFA input where the blue line is the phase by the *ABP* input, and the red line is the phase by the CO_2 input. In this condition, the phase shift resulting from the CO_2 influence seems higher than the *ABP* one on both the right and left sides. ***Table 5-1*** shows the average and standard deviation values of MTFA outputs on both right and left sides at normocapnia condition using *ABP* and CO_2 inputs.

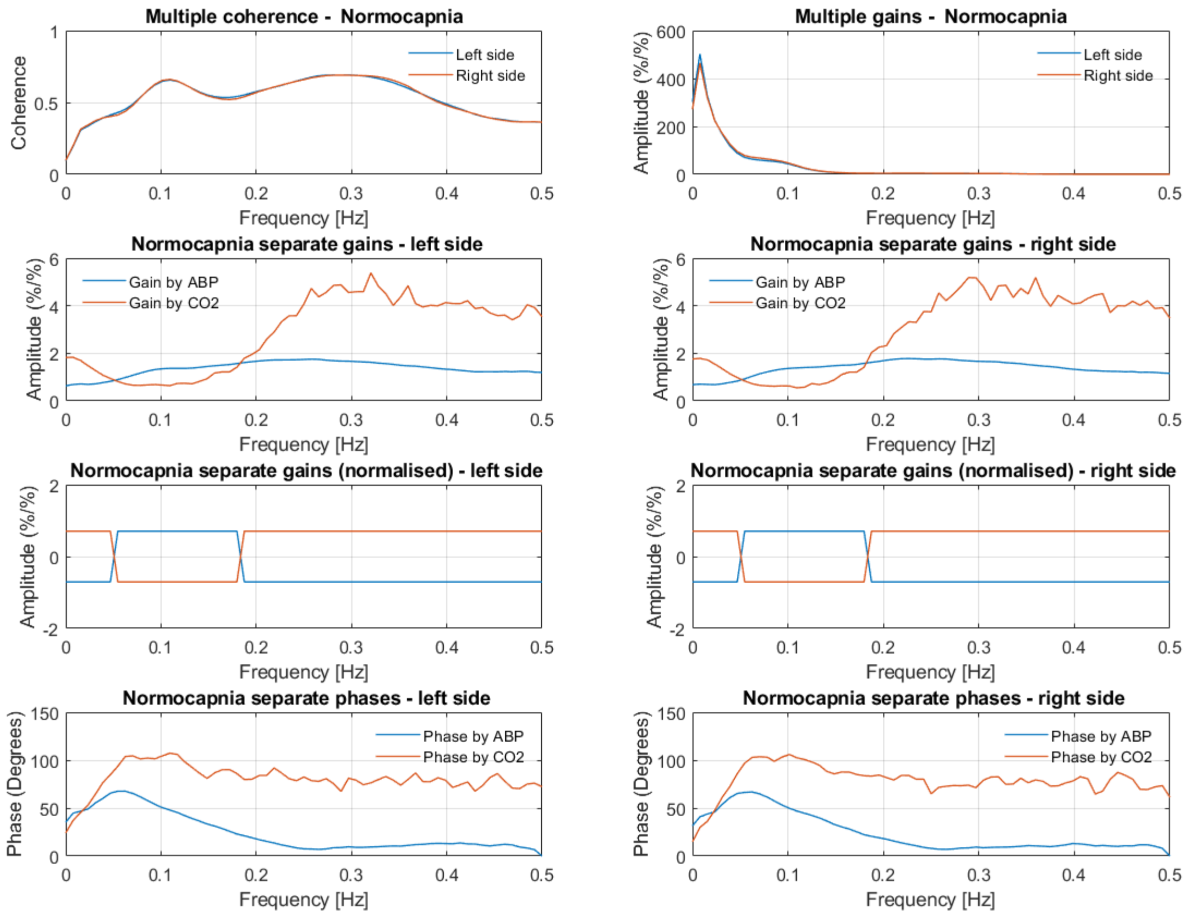

Figure 5-2: MTFA parameters for both right and left sides at normocapnia condition using *ABP* and CO_2 inputs

MTFA output	Multiple Coherence		Multiple Gain		Separate Gains				Separate Phases			
Side	Left	Right	Left	Right	Left		Right		Left		Right	
Input	Combined effect				*ABP*	CO_2	*ABP*	CO_2	*ABP*	CO_2	*ABP*	CO_2
Mean	0.528	0.527	36.160	36.109	1.363	2.851	1.378	2.932	24.342	80.526	23.794	78.752
± Std	0.133	0.134	87.633	83.085	0.303	1.558	0.308	1.621	19.698	14.738	19.435	16.395

Table 5-1: Mean and standard deviation values of MTFA parameters across the frequency spectrum at normocapnia condition using *ABP* and CO_2 inputs

5.4.2. Hypercapnia condition

This subsection will illustrate the MTFA results of all subjects in hypercapnia condition using both *ABP* and CO_2 inputs. ***Figure 5-3*** shows the MTFA outputs of all subjects across the frequency spectrum using *ABP* and CO_2 inputs. The top left plot shows the multiple coherence with the combined effect of the two inputs (*ABP* & CO_2) on both the right and left sides of the brain. Again, it's worth noting that both right and left sides results are significantly alike across the frequency spectrum and start hitting the highest coherence value at 0.1 Hz. The top right plot shows the multiple gains on both sides which start going lower after 0.1 Hz.

The upper middle left and middle right plots show the left and right sides respectively of separate gains results given by each MTFA input where the blue line is the gain by the *ABP* input, and the red line is the gain by the CO_2 input. On both the right and left sides, the gain resulting from CO_2 influence seems significantly higher and alternates across the frequency spectrum whereas the *ABP* one is severely lower with an output of less than 1.5 in gain for both sides. The lower middle plots show the left and right sides respectively of the normalised separate gains which demonstrate that *ABP* influence is significantly lower in the frequency spectrum.

The bottom left and right plots show the left and right sides respectively of separate phases results given by each MTFA input where the blue line is the phase by the *ABP* input, and the red line is the phase by the CO_2 input. Both sides show that the phase shift resulting from CO_2 influence is significantly higher than the phase by *ABP*. ***Table 5-2*** shows the average and standard deviation values of MTFA outputs on both right and left sides at hypercapnia condition using *ABP* and CO_2 inputs.

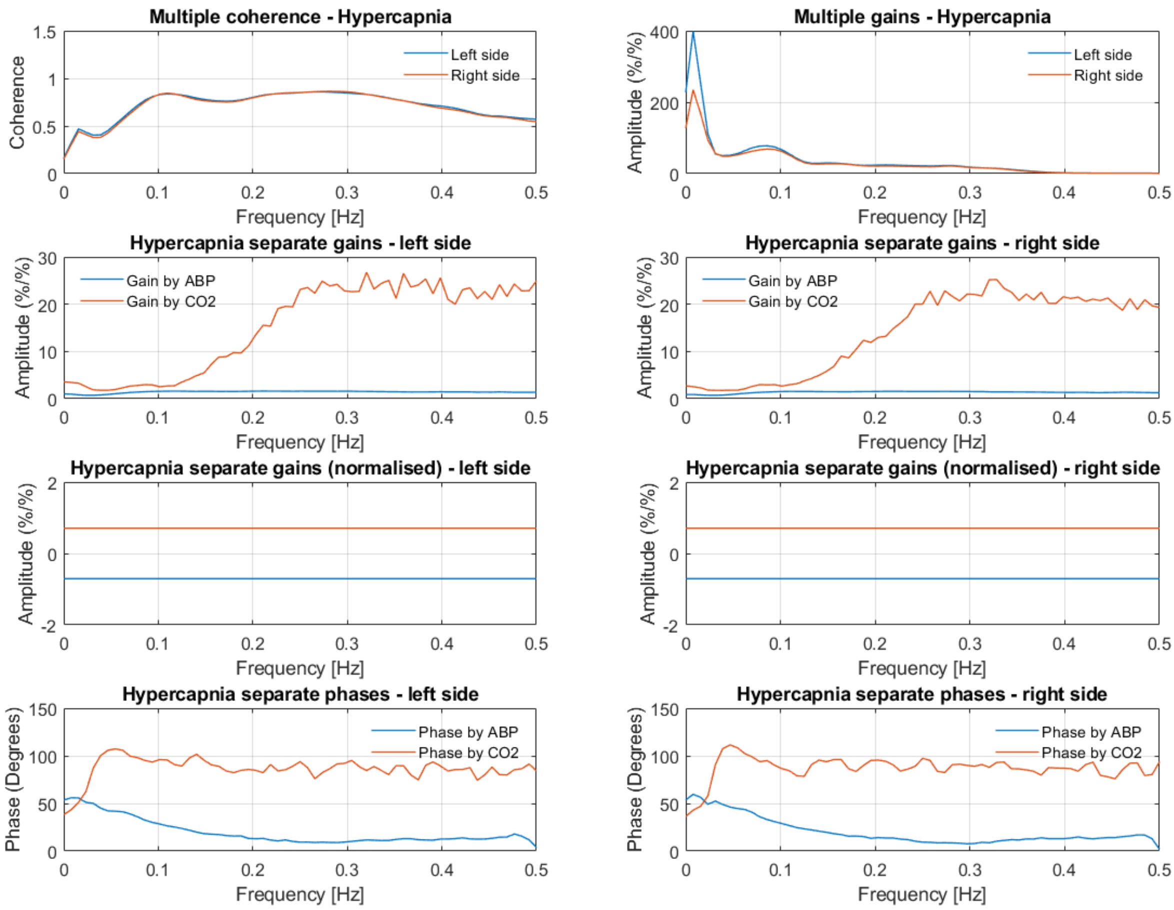

Figure 5-3: MTFA parameters for both right and left sides at hypercapnia condition using *ABP* and CO_2 inputs

MTFA output	Multiple Coherence		Multiple Gain		Separate Gains				Separate Phases			
Side	Left	Right	Left	Right	Left		Right		Left		Right	
Input	Combined effect				*ABP*	CO_2	*ABP*	CO_2	*ABP*	CO_2	*ABP*	CO_2
Mean	0.711	0.703	37.644	30.219	1.425	15.219	1.365	14.073	19.866	86.446	20.294	87.041
± Std	0.151	0.159	63.649	40.044	0.227	9.316	0.222	8.395	13.488	12.195	14.138	12.847

Table 5-2: Mean and standard deviation values of MTFA parameters across the frequency spectrum at hypercapnia condition using *ABP* and CO_2 inputs

5.4.3. Thigh cuff condition

This subsection will highlight the MTFA results of all subjects at the thigh cuff condition and using both *ABP* and CO_2 inputs. ***Figure 5-4*** shows the MTFA outputs of all subjects across the frequency spectrum using *ABP* and CO_2 inputs. The top left plot shows the multiple coherence with the combined effect of the two inputs (*ABP* & CO_2) on both the right and left sides of the brain. Once more, both right and left sides results are significantly alike across the frequency spectrum starting to reach their maximum levels after 0.1 Hz. The top right plot shows the multiple gains on both sides where left side gain starts higher between 0 – 0.01 Hz then both gains start to drop after 0.08 Hz.

The upper middle left and middle right plots show the left and right sides respectively of separate gains results given by each MTFA input where the blue line is the gain by the *ABP* input, and the red line is the gain by the CO_2 input. On both the right and left sides, the gain resulting from CO_2 influence seems significantly higher and alternates across the frequency spectrum whereas the *ABP* one is severely lower with an output of less than 1.7 in gain. The lower middle plots show the left and right sides respectively of the normalised separate gains which demonstrate that CO_2 influence is higher than *ABP* influence across the frequency spectrum but the gain by influence appear to alternate between higher and lower than CO_2 influence around the 0.1 Hz.

The bottom left and right plots show the left and right sides respectively of separate phases results given by each MTFA input where the blue line is the phase by the *ABP* input, and the red line is the phase by the CO_2 input. Both sides show that the phase shift resulting from CO_2 influence is significantly higher than the phase by *ABP*. ***Table 5-3*** shows the average and standard deviation values of MTFA outputs on both right and left sides at the thigh cuff condition using *ABP* and CO_2 inputs.

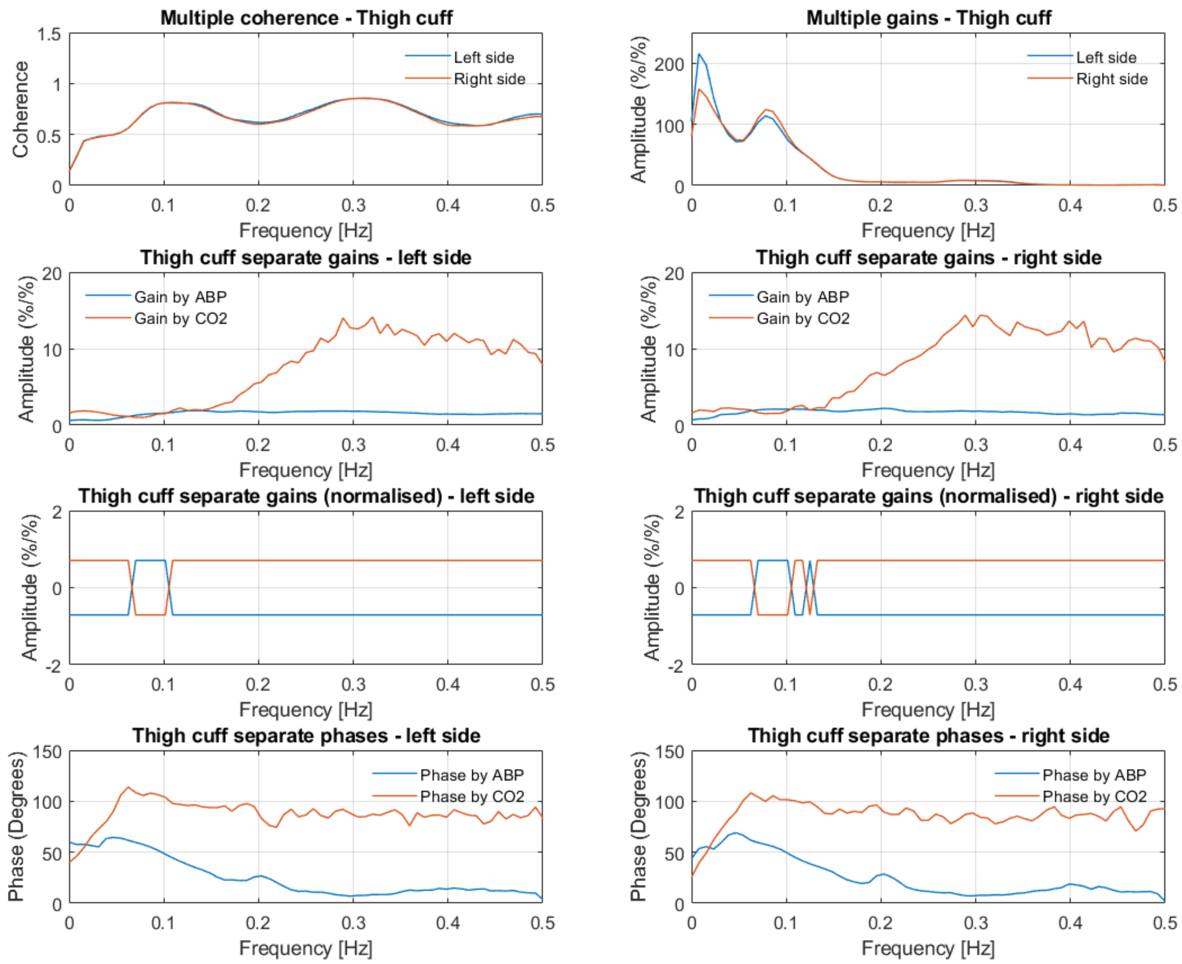

Figure 5-4: MTFA parameters for both right and left sides at thigh cuff condition using *ABP* and CO_2 inputs

MTFA output	Multiple Coherence		Multiple Gain		Separate Gains				Separate Phases			
Side	Left	Right	Left	Right	Left		Right		Left		Right	
Input	Combined effect				*ABP*	CO_2	*ABP*	CO_2	*ABP*	CO_2	*ABP*	CO_2
Mean	0.676	0.668	30.654	29.184	1.519	7.215	1.680	7.884	25.381	87.628	25.476	86.043
± Std	0.137	0.136	48.725	43.464	0.349	4.539	0.324	4.593	19.266	12.725	19.189	13.691

Table 5-3: Mean and standard deviation values of MTFA parameters across the frequency spectrum at thigh cuff condition using *ABP* and CO_2 inputs

5.4.4. Reproducibility analysis

Reproducibility analysis was performed to calculate ICC values for all subjects at normocapnia, hypercapnia and thigh cuff conditions. The result shows significantly moderate reproducibility levels that show a correlation among all subjects under all conditions ranging from 0.51 – 0.68. ***Figure 5-5*** presents a scatterplot of the calculated ICC values for normocapnia, hypercapnia and thigh cuff using both *ABP* and CO_2 inputs.

Obviously, looking at ICC results in each physiological challenge, normocapnia condition has a value of 0.684, hypercapnia condition has a value of 0.514, and thigh cuff condition has a value of 0.617. As discussed in Chapter 2, Section 2.8, this shows that the results are moderately reproducible and have reasonable correlation levels. It's worth noting that normocapnia condition has the highest score compare to the other conditions when using *APB* and CO_2 as inputs in MTFA. ***Table 5-4*** shows the values of ICC results in normocapnia, hypercapnia and thigh cuff at all frequency bands using *ABP* and CO_2 inputs.

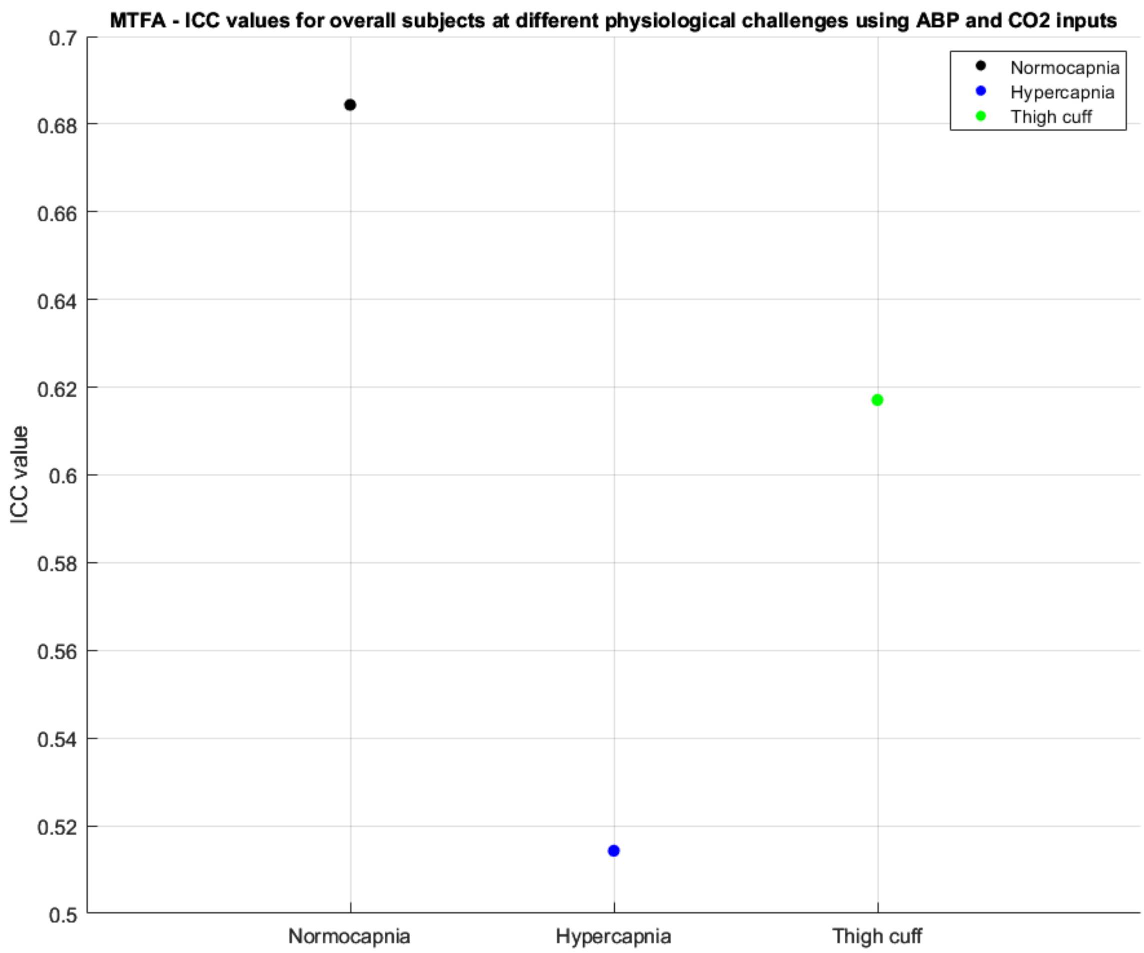

Figure 5-5: Scatterplot shows total ICC values for all subjects at different physiological challenges using *ABP* and CO_2 inputs

Condition	*ICC value*
Normocapnia	0.684
Hypercapnia	0.514
Thigh cuff	0.617

Table 5-4: ICC values for all subjects at different physiological challenges using *ABP* and CO_2 inputs

5.4.5. Covariance analysis

Covariance analysis was performed on the resulted MTFA parameters to study the variation levels between measurement variability and subject variability recording under different physiological challenges. ***Figure 5-6*** shows the analysis results comparing the subject variability with the measurement variability for each MTFA parameter using *ABP* and CO_2 inputs. Overall, all measurement variability results are significantly smaller than the subject variability ones.

The top two plots, from the left to the right, are the multiple coherence and the multiple gains. The multiple coherence in this plot shows that the thigh cuff condition represents the lowest variability level in both measurement and subject variability recordings compared to the other two conditions whereas the multiple gains behave differently and show dissimilar variability among conditions of both measurement and subject variability. For example, hypercapnia subject variability is the highest (which is similar to the behaviour of the separate gain) whereas the thigh cuff measurement variability is the highest compared to the other conditions.

Moreover, the middle two plots in ***Figure 5-6***, from the left to the right, are the separate gains by *ABP* input and the separate gains by CO_2 input. The left plot shows that the thigh cuff condition is the lowest, compared to the other conditions, in the measurement variability but is the highest one, compared to the other conditions, in the subject variability. The middle right plot shows different variation patterns where the thigh cuff is the lowest, compared to the other conditions, in both measurement variability and subject variability but the hypercapnia behaviour in separate gains by CO_2 input is similar to the hypercapnia behaviour in the multiple gains variations.

Additionally, the bottom two plots in ***Figure 5-6***, from the left to the right, are the separate phases by *ABP* input and the separate phases by CO_2 input. In the left plot, by the *ABP* input, the thigh cuff condition is lower than hypercapnia but higher than normocapnia in the measurement variability whereas it shows a different variation patterns in the subject variability side appearing as the highest compared to the other conditions. However, the right plot presenting the phases shift variation levels influenced by CO_2 input shows that the thigh cuff condition appears as the highest compared to the other conditions in both measurement variability and subject variability levels.

Table 5-5 shows the means and standard error of MTFA parameters of both measurement variability and subject variability levels under different conditions using *ABP* and CO_2 inputs.

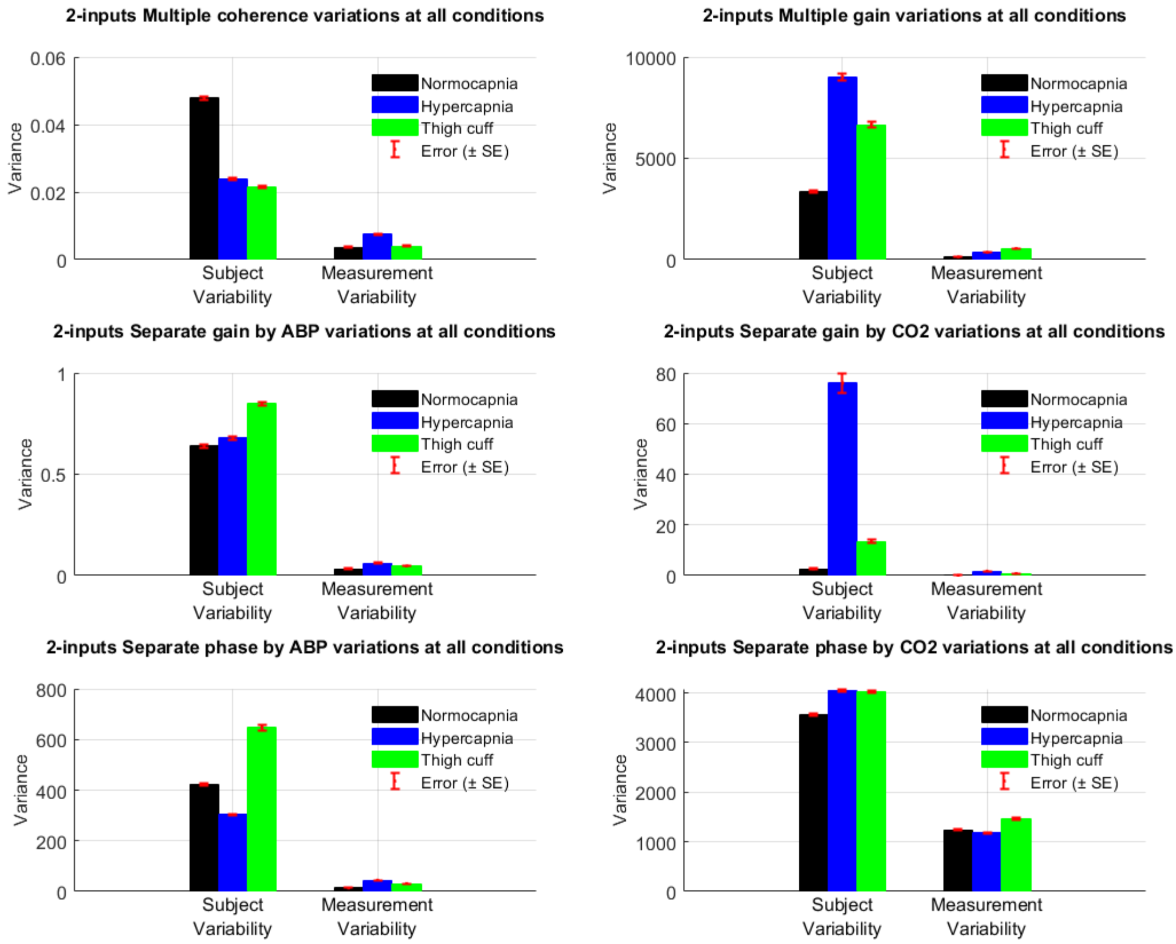

Figure 5-6: MTFA parameters variations of measurement and subject variability in different conditions using *ABP* and CO_2 inputs

MTFA parameter	Variation	Subject variability		Measurement variability	
	Value	Mean	SE	Mean	SE
Multiple coherences	Norm	0.048	0.0007	0.004	< 0.0001
	Hyper	0.024	0.0002	0.007	0.0001
	Thigh	0.021	0.0002	0.004	0.0001
Multiple gains	Norm	3364.079	70.7481	136.173	2.1992
	Hyper	9013.188	148.7184	363.028	8.6505
	Thigh	6663.271	138.8842	549.097	12.8458
Separate gains (*ABP*)	Norm	0.639	0.0069	0.033	0.0004
	Hyper	0.678	0.0069	0.061	0.0009
	Thigh	0.848	0.0080	0.048	0.0007
Separate gains (CO_2)	Norm	2.596	0.1207	0.138	0.0034
	Hyper	76.030	3.8398	1.726	0.0615
	Thigh	13.519	0.6187	0.769	0.0262
Separate phases (*ABP*)	Norm	423.422	4.2396	14.008	0.1567
	Hyper	302.893	2.5180	44.062	1.0963
	Thigh	647.937	10.8919	30.849	0.3826
Separate phases (CO_2)	Norm	3559.190	20.9238	1242.536	11.9967
	Hyper	4054.373	26.8304	1176.866	10.2007
	Thigh	4030.054	21.0982	1465.103	16.1610

Table 5-5: Mean and standard error of MTFA parameters variations of measurement and subject variability in different conditions using *ABP* and CO_2 inputs

5.4.6. Significance analysis

Furthermore to the results, significance analysis was performed by running paired t-test using the Bonferroni correction technique to compute p-values for each MTFA parameter among different conditions (normocapnia, hypercapnia, and thigh cuff) to study each parameter's dependency on the condition or physiological challenge. Since several p-values will be computed in this analysis, the Bonferroni correction method has been selected to minimise potential error in p-values results. Using the Bonferroni correction is essential to avoid type I error especially when running a large number of tests in the absence of planned hypotheses [89].

For statistical accuracy, a paired t-test with Bonferroni correction has been conducted to examine the association of MTFA parameter with other conditions. ***Figure 5-7*** shows bar graphs for each MTFA parameter mean value on the left side using *ABP* and CO_2 inputs topped with super bars (pink line) comparing p-values among conditions. Each pink horizontal line shows the p-value in form of significance which is either not significant (n.s., $p > 0.05$), one star (*, $p < 0.05$), two stars (**, $p < 0.01$), three stars (***, $p < 0.001$), or four stars (****, $p < 0.0001$).

Multiple gains, gain by *CO_2* and phase by *ABP* present significant p-values between conditions whereas the remaining parameters show no significance between conditions. In multiple gains, there is a significant association between normocapnia and hypercapnia conditions as well as a significant association between normocapnia and thigh cuff conditions, $p < 0.0001$ but there is no significant association between hypercapnia and thigh cuff conditions. In gain by *CO_2* input, there is a significant association between normocapnia and hypercapnia, $p < 0.01$ but there are no significant associations between other conditions. In phase by *ABP* input, there is a significant association between normocapnia and hypercapnia conditions similar to the association between hypercapnia and thigh cuff conditions, $p < 0.01$ but there is no significant association between normocapnia and thigh cuff conditions. ***Table 5-6*** lists p-values comparing each MTFA parameter among all conditions on the left side using *ABP* and *CO_2* inputs.

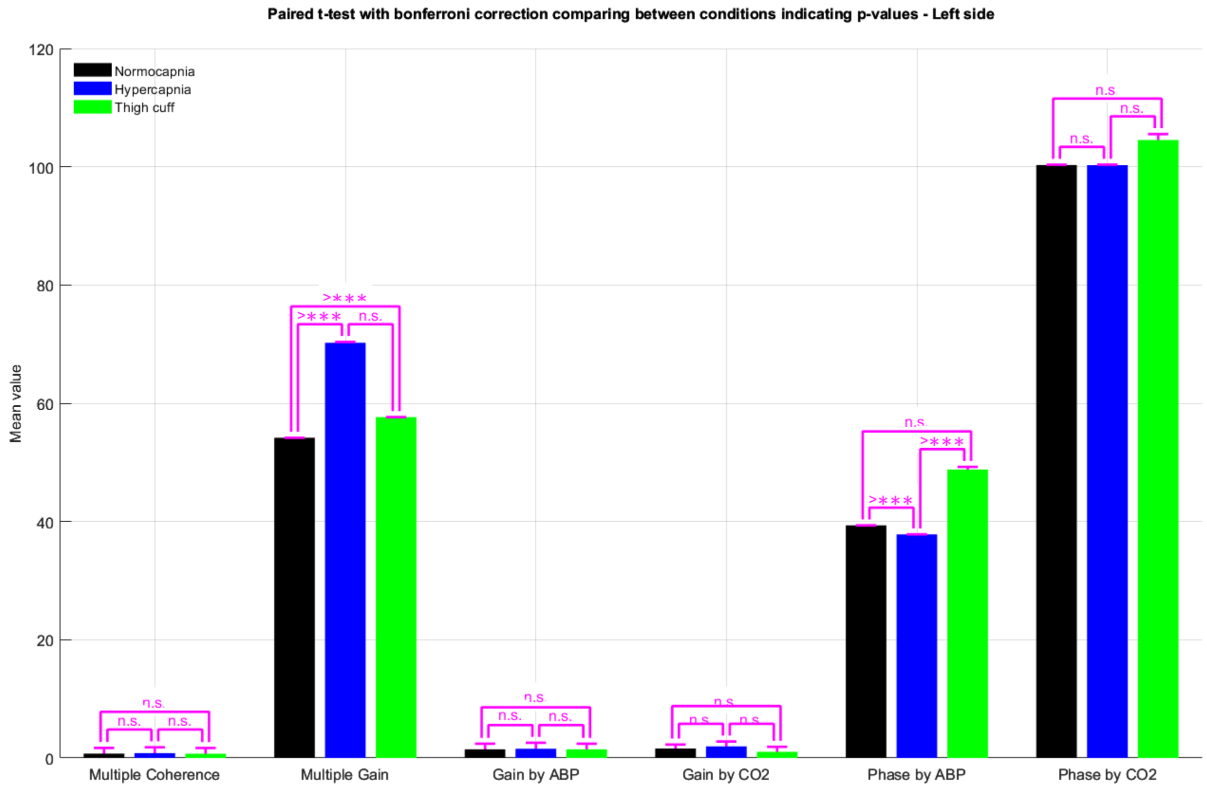

Figure 5-7: Paired t-test analysis with Bonferroni correction to compare p-values of each MTFA parameter in different conditions on the left side using *ABP* and CO_2 inputs (n.s. is no significance, * means p-value is < 0.05, ** < 0.01, *** < 0.001, and **** is < 0.0001)

	P-values left side					
MTFA parameter	Multiple Coherence	Multiple Gain	Gain by *ABP*	Gain by CO_2	Phase by *ABP*	Phase by CO_2
Norm vs Hyper	0.9668	<0.0001	0.9590	0.6765	<0.0001	0.0561
Hyper vs Thigh	0.9966	0.1447	0.9990	0.8144	0.0001	0.0764
Thigh vs Norm	0.9676	<0.0001	0.9538	0.8568	0.4524	0.9986

Table 5-6: Comparing p-values of each MTFA parameter in different conditions on the left side using *ABP* and CO_2 inputs

Contrariwise, ***Figure 5-8*** shows the p-values results on the right side using *ABP* and CO_2 inputs. Both multiple coherence and gain by *ABP* parameters show no significant associations between different conditions. However, both gain and phase by CO_2 inputs show a significant association between normocapnia hypercapnia conditions where $p < 0.001$ for the gain, and $p < 0.05$ for the phase. Likewise, phase by *ABP* input shows a significant association between normocapnia and hypercapnia conditions ($p < 0.01$) and between hypercapnia and thigh cuff conditions ($p < 0.05$). Furtherly, the multiple gains present the significant association between normocapnia and hypercapnia conditions, ($p < 0.001$) and a higher significant association between normocapnia and thigh cuff conditions, ($p < 0.0001$) which is alike to the association between hypercapnia and thigh cuff conditions. ***Table 5-7*** presents p-values comparing each MTFA parameter among different conditions on the right side using *ABP* and CO_2 inputs.

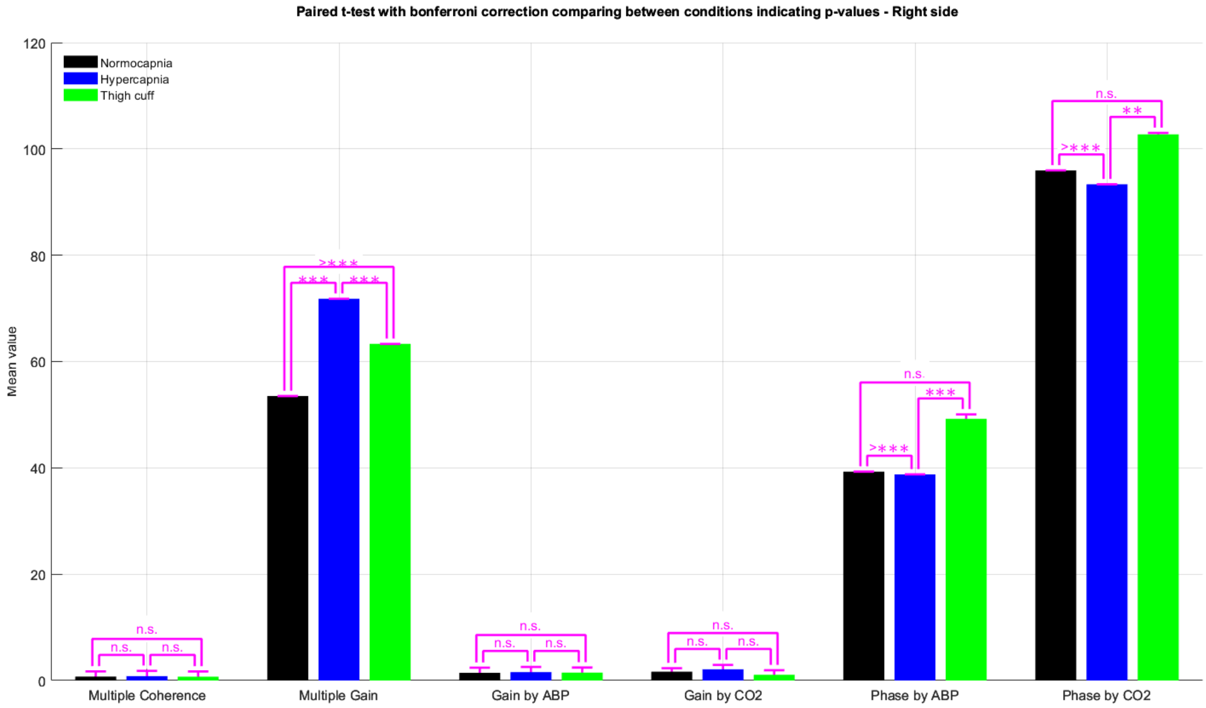

Figure 5-8: Paired t-test analysis with Bonferroni correction to compare p-values of each MTFA parameter in different conditions on the right side using *ABP* and CO_2 inputs (n.s. is no significance, * means p-value is < 0.05, ** < 0.01, *** < 0.001, and **** is < 0.0001)

	P-values right side					
MTFA parameter	Multiple Coherence	Multiple Gain	Gain by *ABP*	Gain by CO_2	Phase by *ABP*	Phase by CO_2
Norm vs Hyper	0.9683	0.0003	0.9715	0.6601	<0.0001	0.0001
Hyper vs Thigh	0.9962	0.0002	0.9838	0.8261	0.0001	0.0090
Thigh vs Norm	0.9731	<0.0001	0.9543	0.8490	0.8282	0.2678

Table 5-7: Comparing p-values of each MTFA parameter in different conditions on the right side using *ABP* and CO_2 inputs

5.5. Results using *ABP* and *HR* inputs

The following subsections will show the MTFA results for each condition/physiological challenge using the *ABP* and *HR* inputs in the analysis across the frequency spectrum. Next, will display the ICC results, covariance analysis results, and the paired t-test analysis results comparing between conditions.

5.5.1. Normocapnia condition

This subsection will illustrate the MTFA results of all subjects at normocapnia condition and using both *ABP* and *HR* inputs. ***Figure 5-9*** shows MTFA outputs of all subjects at normocapnia conditions across the frequency spectrum. The top left plot shows the multiple coherence with the combined effect of the two inputs (*ABP* & *HR*) on both the right and left sides of the brain. It's worth noting that both right (blue line) and left (red line) sides' results are almost equal across the frequency spectrum and start hitting the highest coherence value at 0.1 Hz. The top right plot shows the multiple gains on both sides which seem to decrease dramatically after 0.01 Hz and continue to decrease until 0.15 Hz.

The upper middle left and middle right plots show the left and right sides respectively of separate gains results given by each MTFA input where the blue line is the gain by the *ABP* input, and the red line is the gain by the *HR* input. However, the gain resulting from *HR* influence seems lower across the frequency spectrum compared to the *ABP* one on both the right and left sides. The lower middle plots show the left and right sides respectively of the normalised separate gains which demonstrate that gain by *ABP* influence is significantly higher than gain by CO_2 influence across the frequency spectrum.

Next, the bottom left and right plots show the left and right sides respectively of separate phases results given by each MTFA input where the blue line is the phase by the *ABP* input, and the red line is the phase by the *HR* input. In this condition, the phase shift resulting from the *HR* influence seems higher than the *ABP* one on both the right and left sides. ***Table 5-8*** shows the average and standard deviation values of MTFA outputs on both right and left sides at normocapnia condition using *ABP* and *HR* inputs.

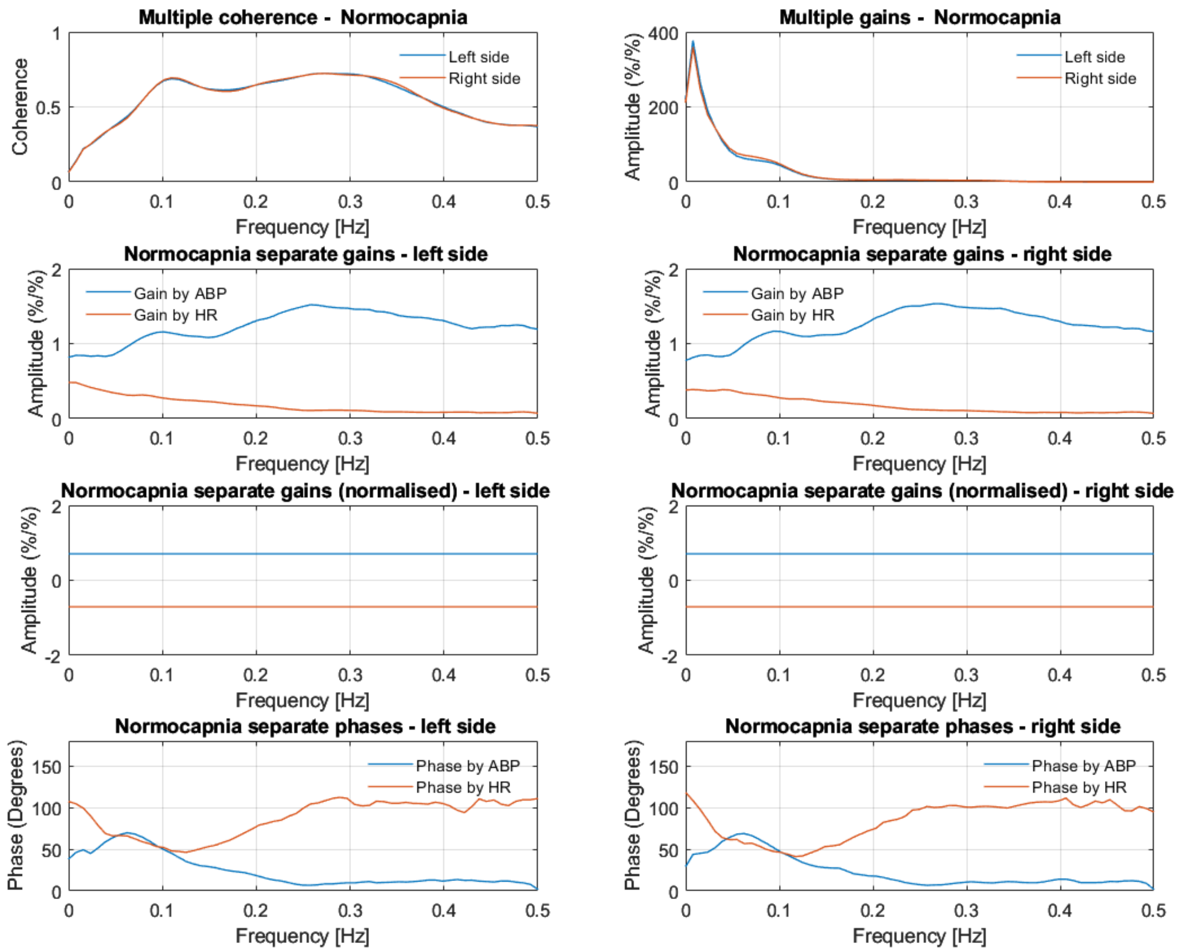

Figure 5-9: MTFA parameters for both right and left sides at normocapnia condition using *ABP* and *HR* inputs

MTFA output	Multiple Coherence		Multiple Gain		Separate Gains				Separate Phases			
Side	Left	Right	Left	Right	Left		Right		Left		Right	
Input	Combined effect				*ABP*	*HR*	*ABP*	*HR*	*ABP*	*HR*	*ABP*	*HR*
Mean	0.547	0.547	31.002	31.282	1.227	0.178	1.237	0.176	23.908	87.663	23.213	84.937
± Std	0.160	0.161	68.351	65.815	0.199	0.114	0.209	0.107	19.385	22.169	18.846	22.934

Table 5-8: Mean and standard deviation values of MTFA parameters across the frequency spectrum at normocapnia condition using *ABP* and *HR* inputs

5.5.2. Hypercapnia condition

This subsection will demonstrate the MTFA results of all subjects in hypercapnia condition using both *ABP* and *HR* inputs. ***Figure 5-10*** shows the MTFA outputs of all subjects across the frequency spectrum. The top left plot shows the multiple coherence with the combined effect of the two inputs (*ABP* & *HR*) on both the right and left sides of the brain. Yet again, both right and left sides results are significantly alike across the frequency spectrum and start hitting the highest coherence value at 0.1 Hz. The top right plot shows the multiple gains on both sides which start dropping lower after 0.1 Hz.

The upper middle left and middle right plots show the left and right sides respectively of separate gains results given by each MTFA input where the blue line is the gain by the *ABP* input, and the red line is the gain by the *HR* input. On both the right and left sides, the gain resulting from *HR* influence seems significantly lower across the frequency spectrum than the *ABP* one. The lower middle plots show the left and right sides respectively of the normalised separate gains which demonstrate that gain by *ABP* influence is significantly higher than gain by CO_2 influence across the frequency spectrum.

The bottom left and middle right plots show the left and right sides respectively of separate phases results given by each MTFA input where the blue line is the phase by the *ABP* input, and the red line is the phase by the *HR* input. Both sides show that the phase shift resulting from *HR* influence is significantly higher than the phase by *ABP*. ***Table 5-9*** shows the average and standard deviation values of MTFA outputs on both right and left sides at hypercapnia condition using *ABP* and *HR* inputs.

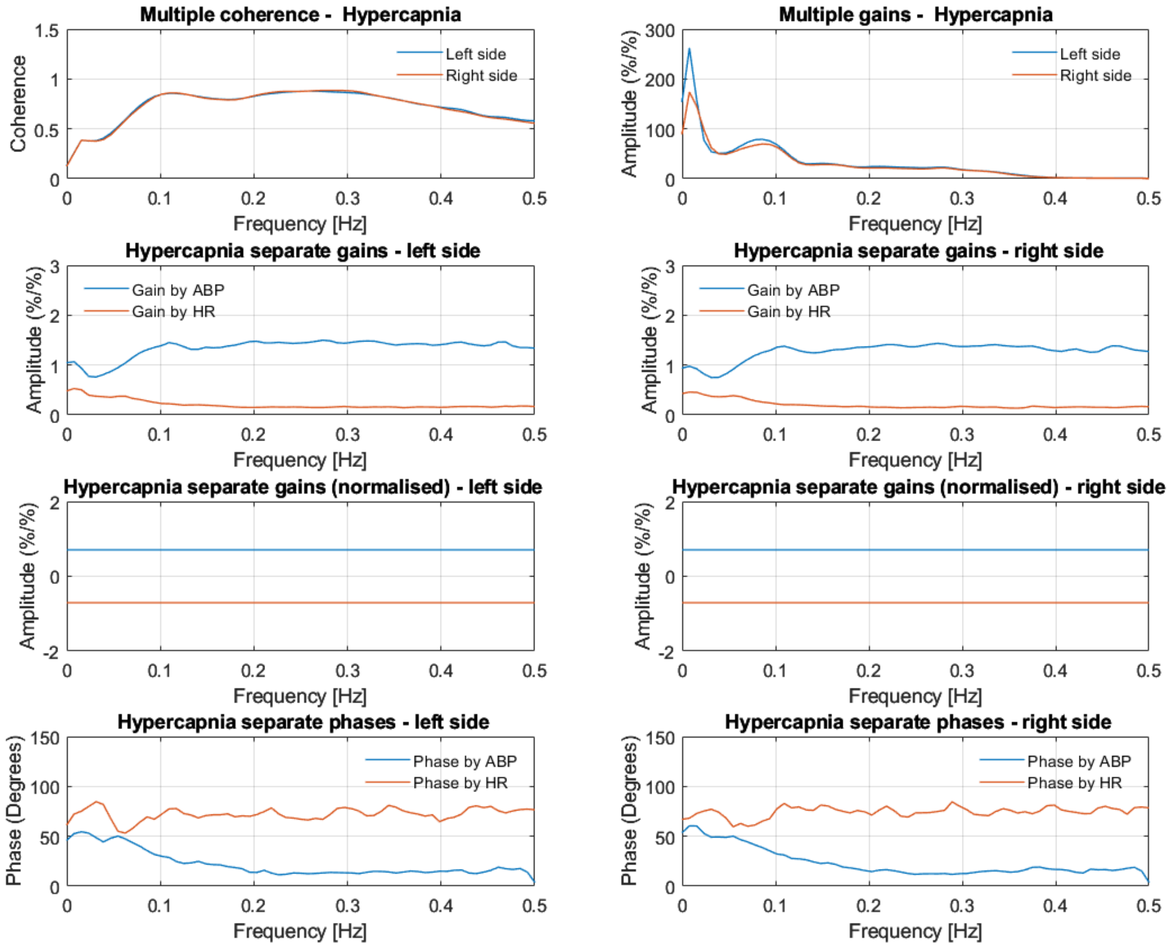

Figure 5-10: MTFA parameters for both right and left sides at hypercapnia condition using *ABP* and *HR* inputs

MTFA output	**Multiple Coherence**		**Multiple Gain**		**Separate Gains**				**Separate Phases**			
Side	Left	Right	Left	Right	Left		Right		Left		Right	
Input	Combined effect				*ABP*	*HR*	*ABP*	*HR*	*ABP*	*HR*	*ABP*	*HR*
Mean	0.724	0.721	32.745	28.832	1.341	0.209	1.273	0.202	22.010	72.265	23.306	74.414
± Std	0.167	0.172	43.131	33.205	0.186	0.094	0.173	0.087	13.036	6.064	13.922	5.221

Table 5-9: Mean and standard deviation values of MTFA parameters across the frequency spectrum at hypercapnia condition using *ABP* and *HR* inputs

5.5.3. Thigh cuff condition

This subsection will highlight the MTFA results of all subjects at the thigh cuff condition and using both *ABP* and *HR* inputs. ***Figure 5-11*** shows the MTFA outputs of all subjects across the frequency spectrum. The top left plot shows the multiple coherence with the combined effect of the two inputs (*ABP* & *HR*) on both the right and left sides of the brain. Once more, both right and left sides results are significantly alike across the frequency spectrum starting to reach their maximum levels after 0.1 Hz. The top right plot shows the multiple gains on both sides which start dropping lower after 0.08 Hz where gain left side starts higher between 0 – 0.02 Hz then both gains start to drop after 0.08 Hz.

The upper middle left and middle right plots show the left and right sides respectively of separate gains results given by each MTFA input where the blue line is the gain by the *ABP* input, and the red line is the gain by the *HR* input. On both the right and left sides, the gain resulting from *HR* influence seems significantly lower across the frequency spectrum whereas than the *ABP* one. However, the right side in this case seems alternating signal compared to the left side. The lower middle plots show the left and right sides respectively of the normalised separate gains which demonstrate that gain by *ABP* influence is significantly higher than gain by CO_2 influence across the frequency spectrum.

The bottom left and middle right plots show the left and right sides respectively of separate phases results given by each MTFA input where the blue line is the phase by the *ABP* input, and the red line is the phase by the *HR* input. Both sides show that the phase shift produced from *HR* influence is significantly lower than the phase by *ABP*. ***Table 5-10*** shows the average and standard deviation values of MTFA outputs on both right and left sides at the thigh cuff condition using *ABP* and *HR* inputs.

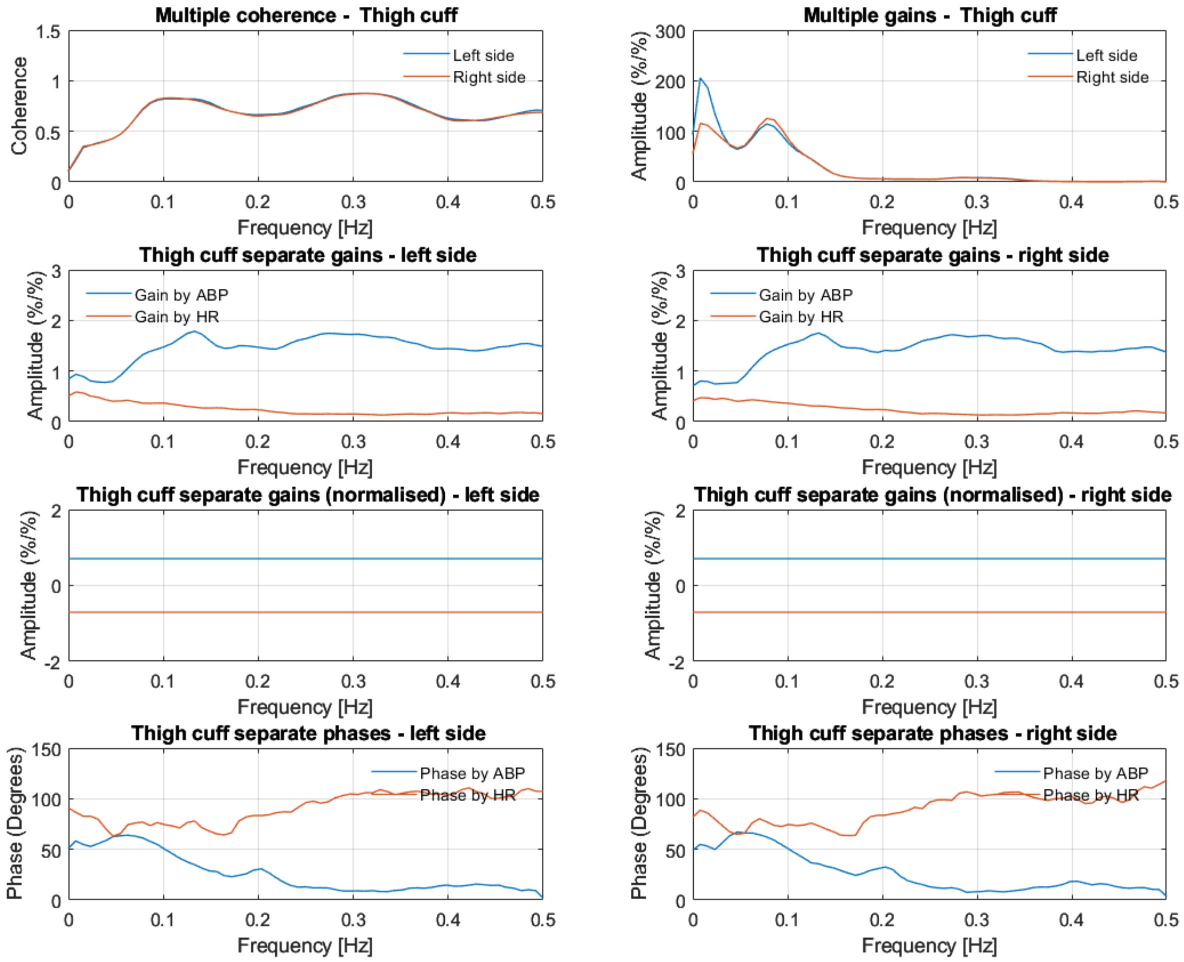

Figure 5-11: MTFA parameters for both right and left sides at thigh cuff condition using *ABP* and *HR* inputs

MTFA output	Multiple Coherence		Multiple Gain		Separate Gains				Separate Phases			
Side	Left	Right	Left	Right	Left		Right		Left		Right	
Input	Combined effect				*ABP*	*HR*	*ABP*	*HR*	*ABP*	*HR*	*ABP*	*HR*
Mean	0.685	0.680	29.827	26.913	1.450	0.243	1.417	0.243	25.796	90.964	26.669	90.022
± Std	0.160	0.157	46.578	38.575	0.266	0.120	0.275	0.108	19.006	15.023	19.126	14.934

Table 5-10: Mean and standard deviation values of MTFA parameters across the frequency spectrum at thigh cuff condition using *ABP* and *HR* inputs

5.5.4. Reproducibility analysis

Reproducibility analysis was performed to calculate ICC values for all subjects at normocapnia, hypercapnia and thigh cuff conditions. The result shows poor to moderate reproducibility levels among all subjects under all conditions ranging from 0.45 – 0.57. ***Figure 5-12*** presents a scatterplot of the calculated ICC values for normocapnia, hypercapnia and thigh cuff using both *ABP* and *HR* inputs.

Obviously, looking at ICC results in each physiological challenge, normocapnia condition has a value of 0.489, hypercapnia condition has a value of 0.446, and thigh cuff condition has a value of 0.570. This demonstrate that the results are moderately reproducible for the thigh cuff condition and poorly reproducible for both normocapnia and hypercapnia conditions. ***Table 5-11*** shows the values of ICC results in normocapnia, hypercapnia and thigh cuff using *ABP* and *HR* as inputs in the MTFA.

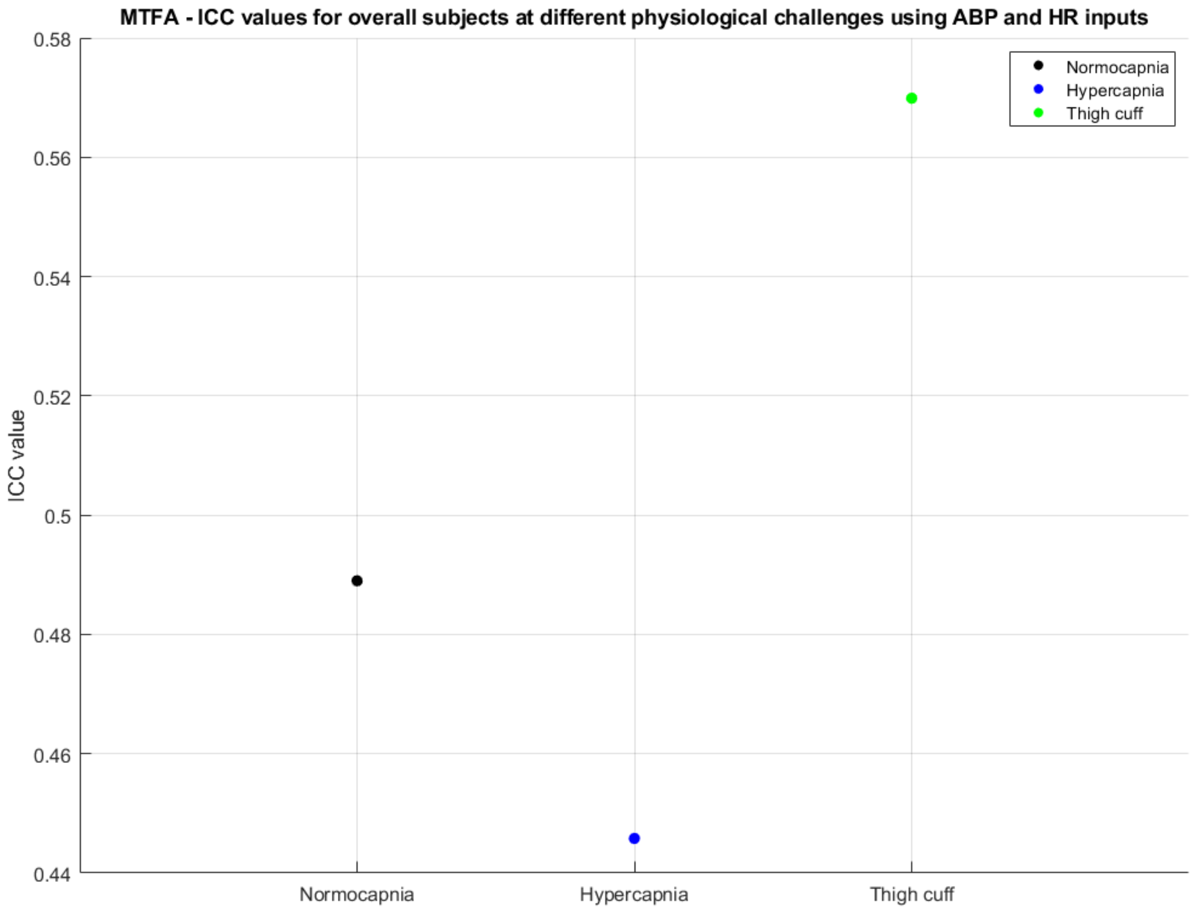

Figure 5-12: Scatterplot shows total ICC values for all subjects at different physiological challenges using *ABP* and *HR* inputs

Condition	*ICC value*
Normocapnia	0.489
Hypercapnia	0.446
Thigh cuff	0.570

Table 5-11: ICC values for all subjects at different physiological challenges using *ABP* and *HR* inputs

5.5.5. Covariance analysis

Covariance analysis was performed on the resulted MTFA parameters to study the variation levels between measurement variability and subject variability recording under different physiological challenges. ***Figure 5-13*** shows the analysis results comparing the subject variability with the measurement variability for each MTFA parameter. Overall, all measurement variability results are significantly smaller than the subject variability ones.

The top two plots, from the left to the right, are the multiple coherence and the multiple gain. The multiple coherence in this plot shows that the thigh cuff condition represents the lowest variability level in both measurement and subject variability recordings compared to the other two conditions whereas the multiple gains behave differently and show dissimilar variability among conditions of both measurement and subject variability. For example, hypercapnia subject variability is the highest (which is similar to the behaviour of the separate gain) whereas the normocapnia measurement variability and subject variability are the highest compared to the other conditions.

Moreover, the middle two plots in ***Figure 5-13***, from the left to the right, are the separate gains by *ABP* input and the separate gains by *HR* input. The left plot shows that the normocapnia condition is the lowest, compared to the other conditions, in the measurement variability and subject variability. But the thigh cuff is the highest one, compared to the other conditions, in the subject variability. The middle right plot shows different variation patterns where the normocapnia is the lowest, compared to the other conditions, in both measurement variability and subject variability but the hypercapnia behaviour in separate gains by *HR* input is the highest, similar to the hypercapnia behaviour in the multiple gains variations.

Additionally, the bottom two plots in ***Figure 5-13***, from the left to the right, are the separate phases by *ABP* input and the separate phases by *HR* input. In the left plot, by the *ABP* input, the thigh cuff condition is lower than hypercapnia but higher than normocapnia in the measurement variability whereas it shows a different variation patterns in the subject variability side appearing as the highest compared to the other conditions. However, the right plot presenting the phase shift variation levels influenced by *HR* input shows that the hypercapnia condition appears as the highest compared to the other conditions in measurement variability whereas the thigh cuff in subject variability levels appears as the lowest variation compared to other conditions.

Table 5-12 shows the means and standard error of MTFA parameters of both measurement variability and subject variability levels under different conditions using *ABP* and *HR* inputs.

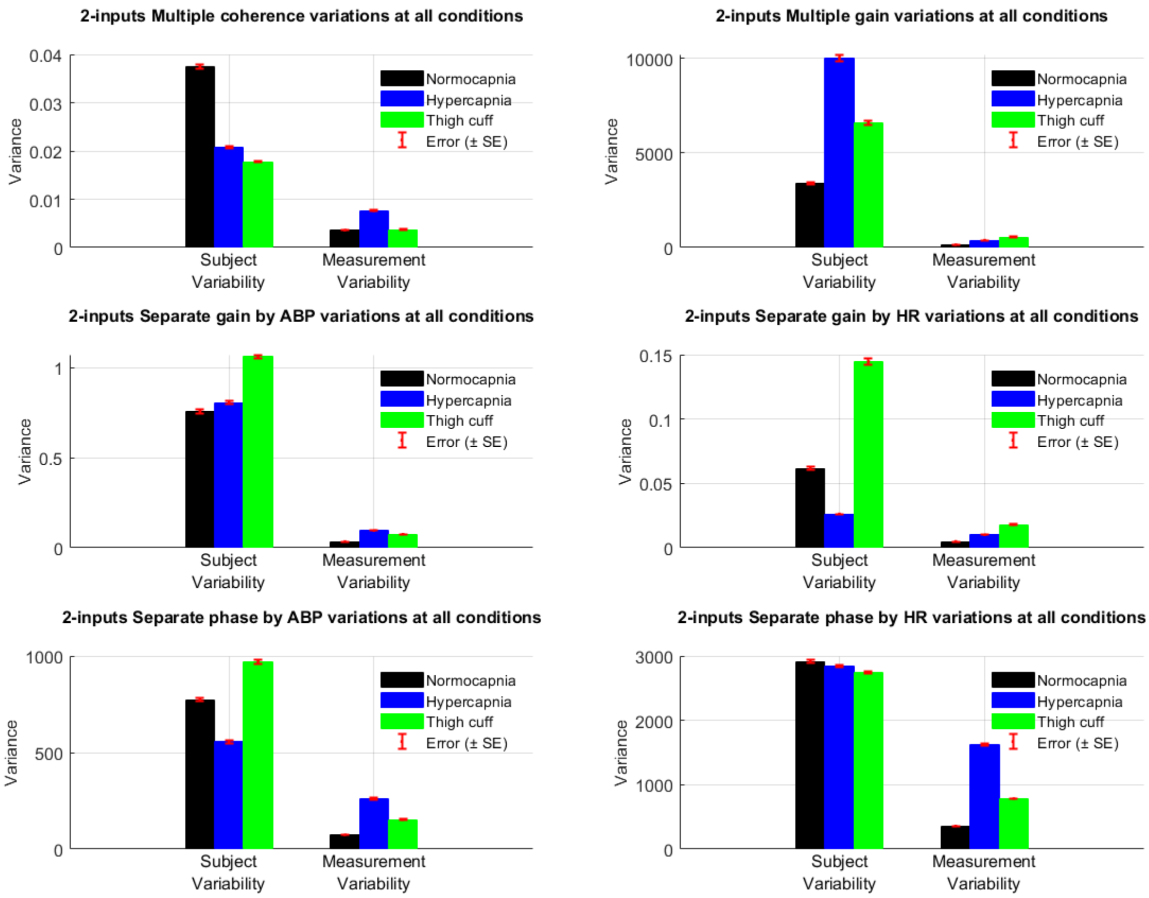

Figure 5-13: MTFA parameters variations of measurement and subject variability in different conditions using *ABP* and *HR* inputs

MTFA parameter	Variation	Subject variability		Measurement variability	
	Value	Mean	SE	Mean	SE
Multiple coherences	Norm	0.037	0.0004	0.004	< 0.0001
	Hyper	0.021	0.0003	0.008	0.0001
	Thigh	0.018	0.0002	0.004	0.0001
Multiple gains	Norm	3389.854	68.7292	144.221	2.3221
	Hyper	10040.982	173.1559	380.081	8.8012
	Thigh	6594.010	136.6657	554.637	12.5145
Separate gains (*ABP*)	Norm	0.757	0.0102	0.034	0.0004
	Hyper	0.808	0.0084	0.096	0.0011
	Thigh	1.061	0.0117	0.075	0.0011
Separate gains (*HR*)	Norm	0.062	0.0013	0.005	< 0.0001
	Hyper	0.026	0.0002	0.010	0.0001
	Thigh	0.145	0.0023	0.018	0.0003
Separate phases (*ABP*)	Norm	773.577	7.2607	73.965	1.2384
	Hyper	555.910	6.8888	259.945	7.0358
	Thigh	969.313	12.5283	151.932	2.5474
Separate phases (*HR*)	Norm	2915.154	23.8870	356.554	5.3300
	Hyper	2847.512	19.0803	1620.472	17.6977
	Thigh	2738.948	16.4307	783.091	7.9436

Table 5-12: Mean and standard error of MTFA parameters variations of measurement and subject variability in different conditions using *ABP* and *HR* inputs

5.5.6. Significance analysis

Similarly to Subsection 5.4.6, significance analysis was performed by running paired t-test using the Bonferroni correction technique to compute p-values for each MTFA parameter among different conditions (normocapnia, hypercapnia, and thigh cuff) to study each parameter's dependency on the condition or physiological challenge. Since several p-values will be computed in this analysis, the Bonferroni correction method has been selected to minimise potential error in p-values results.

Again, a paired t-test with Bonferroni correction has been conducted to examine the association of MTFA parameter with other conditions. ***Figure 5-14*** shows bar graphs for each MTFA parameter mean value on the left side using *ABP* and *HR* inputs topped with super bars (pink line) comparing p-values among conditions. Again, each pink horizontal line shows the p-value in form of significance which is either not significant (n.s., $p > 0.05$), one star (*, $p < 0.05$), two stars (**, $p < 0.01$), three stars (***, $p < 0.001$), or four stars (****, $p < 0.0001$).

Multiple gains, phase by *ABP*, and phase by *HR* present significant p-values between conditions whereas the remaining parameters show no significance between conditions. In multiple gain, there is a significant association between normocapnia and hypercapnia conditions as well as a significant association between normocapnia and thigh cuff conditions, $p < 0.0001$ but there is no significant association between hypercapnia and thigh cuff conditions.

In phase by *ABP* input, there is a significant association between normocapnia and hypercapnia conditions, $p < 0.01$, and significant association between hypercapnia and thigh cuff conditions, $p < 0.05$ but there is no significant association between normocapnia and thigh cuff conditions. In phase by *HR* there is a significant association between normocapnia and hypercapnia conditions, $p < 0.01$ and a significant association between normocapnia and thigh cuff conditions, $p < 0.001$ but there is no significant association between hypercapnia and thigh cuff conditions. ***Table 5-13*** lists p-values comparing each MTFA parameter among all conditions on the left side using *ABP* and *HR* inputs.

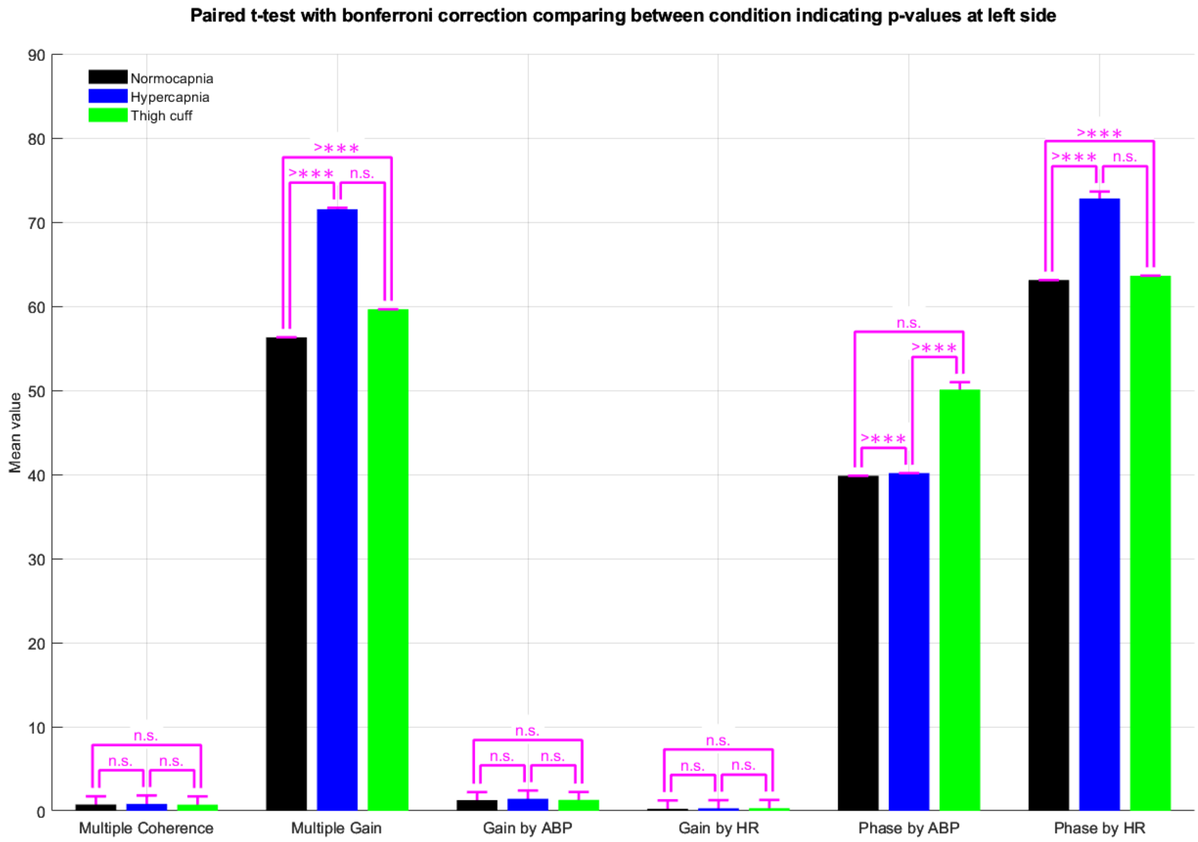

Figure 5-14: Paired t-test analysis with Bonferroni correction to compare p-values of each MTFA parameter in different conditions on the left side using *ABP* and *HR* inputs (n.s. is no significance, * means p-value is < 0.05, ** < 0.01, *** < 0.001, and **** is < 0.0001)

	P-values left side					
MTFA parameter	Multiple Coherence	Multiple Gain	Gain by *ABP*	Gain by *HR*	Phase by *ABP*	Phase by *HR*
Norm vs Hyper	0.9698	<0.0001	0.9580	0.9915	<0.0001	<0.0001
Hyper vs Thigh	0.9956	0.1615	0.9863	0.9766	<0.0001	0.8281
Thigh vs Norm	0.9703	<0.0001	0.9342	0.9811	0.8703	<0.0001

Table 5-13: Comparing p-values of each MTFA parameter in different conditions on the left side using *ABP* and *HR* inputs

On the other hand, ***Figure 5-15*** shows the p-values results on the right side where multiple coherence and gain by *ABP* and *HR* parameters show no significant associations between different conditions. However, multiple gain shows significant association between normocapnia and hypercapnia conditions similar to the significant association between normocapnia and thigh cuff conditions, $p < 0.0001$. In addition, there is a significant association between hypercapnia and thigh cuff conditions, $p < 0.001$.

Moreover, in phase by *ABP* input there is a significant association between normocapnia hypercapnia conditions as well as hypercapnia and thigh cuff conditions, $p < 0.05$ but there is no significant association between normocapnia and thigh cuff in this parameter. Likewise, phase by *HR* input shows a significant association between normocapnia and hypercapnia conditions ($p < 0.0001$) and between normocapnia and thigh cuff conditions ($p < 0.0001$) but there is no significant association between hypercapnia and thigh cuff conditions. Furtherly, the multiple gains present the significant association between normocapnia and hypercapnia conditions, ($p < 0.001$) and a higher significant association between normocapnia and thigh cuff conditions, ($p < 0.0001$) which is alike to the association between hypercapnia and thigh cuff conditions. ***Table 5-14*** presents p-values comparing each MTFA parameter among different conditions on the right side.

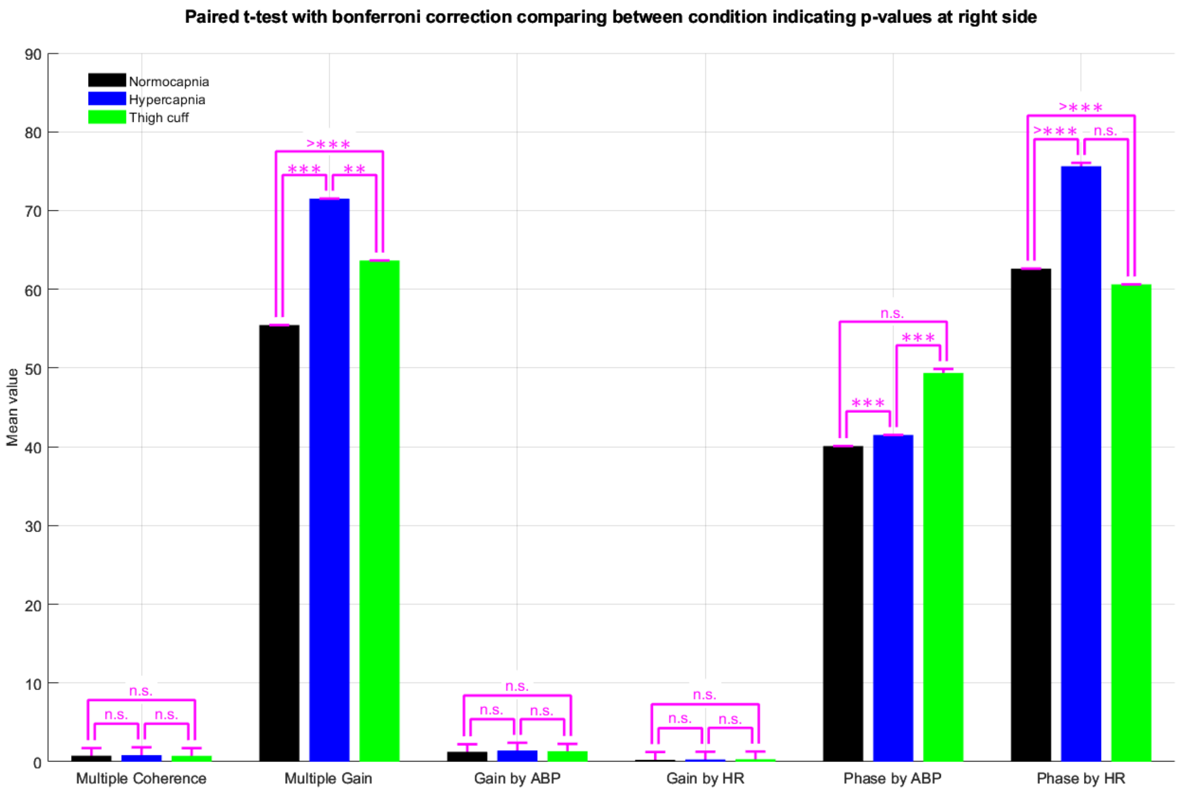

Figure 5-15: Paired t-test analysis with Bonferroni correction to compare p-values of each MTFA parameter in different conditions on the right side using *ABP* and *HR* inputs (n.s. is no significance, * means p-value is < 0.05, ** < 0.01, *** < 0.001, and **** is < 0.0001)

MTFA parameter	P-values right side					
	Multiple Coherence	Multiple Gain	Gain by *ABP*	Gain by *HR*	Phase by *ABP*	Phase by *HR*
Norm vs Hyper	0.9710	0.0006	0.9651	0.9904	0.0005	<0.0001
Hyper vs Thigh	0.9961	0.0012	0.9766	0.9774	0.0002	0.4287
Thigh vs Norm	0.9739	<0.0001	0.9356	0.9836	0.5114	<0.0001

Table 5-14: Comparing p-values of each MTFA parameter in different conditions on the right side using *ABP* and *HR* inputs

5.6. Results using *ABP*, CO_2, and *HR* inputs

The following subsections will show the MTFA results for each condition/physiological challenge using the *ABP*, CO_2, and *HR* inputs (3-inputs) in the analysis across the frequency spectrum. Next, will display the ICC results, covariance analysis results, and the paired t-test analysis results comparing between conditions.

5.6.1. Normocapnia condition

This subsection will illustrate the MTFA results of all subjects at normocapnia condition and using 3-inputs. ***Figure 5-16*** shows MTFA outputs of all subjects at normocapnia conditions across the frequency spectrum using 3-inputs. The top left plot shows the multiple coherence with the combined effect of the 3-inputs (*ABP*, CO_2, & *HR*) on both the right and left sides of the brain. It's worth noting that both right (blue line) and left (red line) sides' results are almost equal across the frequency spectrum and start hitting the highest coherence value at 0.1 Hz. The top right plot shows the multiple gains on both right and left sides which seem to incline significantly after 0.1 Hz.

The upper middle left and right plots show the left and right sides respectively of separate gains results given by each MTFA inputs where the blue line is the gain by the *ABP* input, the red line is the gain by the CO_2 input, and the yellow line is the gain by the *HR* input. However, the gain resulting from CO_2 influence seems higher across most of the frequency spectrum compared to the other inputs on both the right and left sides. The lower middle plots show the left and right sides respectively of the normalised separate gains which demonstrate that gain by *ABP* influence is significantly higher than gain influenced by other inputs between 0.05 –

0.15 Hz where gain by *HR* influence is continuously lower than gain by other inputs across the frequency spectrum.

Next, the bottom left and right plots show the left and right sides respectively of separate phases results given by each MTFA input where the blue line is the phase by the *ABP* input, the red line is the phase by the CO_2 input, and the yellow line is the phase by *HR* input. In this condition, the phase shift resulting from the CO_2 influence seems higher than other phases on both the right and left sides at 0.1 Hz. Then, phase by *HR* increases above the CO_2 phase after 0.2 Hz whereas the *ABP* phase continue decreasing after 0.1 Hz. ***Table 5-15*** shows the average and standard deviation values of MTFA outputs on both right and left sides at normocapnia condition using 3-inputs.

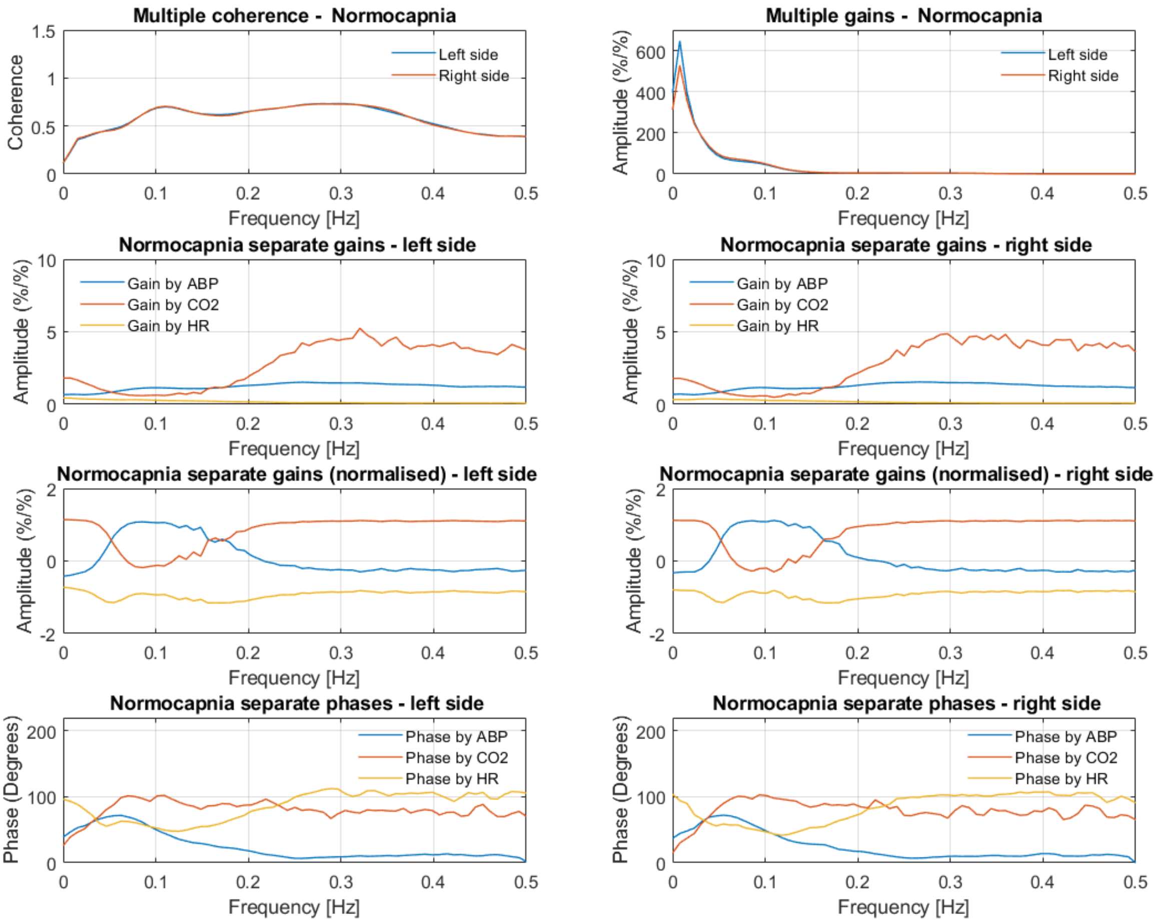

Figure 5-16: MTFA parameters for both right and left sides at normocapnia condition using 3-inputs

MTFA output	Multiple Coherence		Multiple Gain		Separate Gains						Separate Phases					
Side	Left	Right	Left	Right	Left			Right			Left			Right		
Input	Combined effect				*ABP*	CO_2	*HR*	*ABP*	CO_2	*HR*	*ABP*	CO_2	*HR*	*ABP*	CO_2	*HR*
Mean	0.57	0.57	42.33	39.70	1.21	2.77	0.17	1.22	2.84	0.17	24.53	80.12	86.02	24.12	78.78	83.66
± Std	0.14	0.14	109.26	93.35	0.23	1.53	0.10	0.24	1.59	0.10	20.80	13.71	21.80	20.38	16.03	22.51

Table 5-15: Mean and standard deviation values of MTFA parameters across the frequency spectrum at normocapnia condition using 3-inputs

5.6.2. Hypercapnia condition

This subsection will illustrate the MTFA results of all subjects in hypercapnia condition using 3-inputs. ***Figure 5-17*** shows the MTFA outputs of all subjects across the frequency spectrum using 3-inputs. The top left plot shows the multiple coherence with the combined effect of the 3-inputs (*ABP*, CO_2, & *HR*) on both the right and left sides of the brain. Again, it's worth noting that both right and left sides results are significantly alike across the frequency spectrum and start hitting the highest coherence value at 0.1 Hz. The top right plot shows the multiple gains on both sides which start inclining after 0.02 Hz.

The upper middle left and middle right plots show the left and right sides respectively of separate gains results given by each MTFA input where the blue line is the gain by the *ABP* input, the red line is the gain by the CO_2 input, and the yellow is the gain by *HR* input. On both the right and left sides, the gain resulting from CO_2 influence seems significantly higher and alternates across the frequency spectrum compared to the other inputs. The lower middle plots show the left and right sides respectively of the normalised separate gains which demonstrate that gain by CO_2 influence is the higher than gain by *ABP* and gain by *HR* is lower than gain by ABP influence across the frequency spectrum.

The bottom left and right plots show the left and right sides respectively of separate phases results given by each MTFA input where the blue line is the phase by the *ABP* input, the red line is the phase by the CO_2 input, and the yellow line is the phase by the *HR* input. Both sides show that the phase shift resulting from CO_2 influence is significantly higher than the phase by other inputs. It's worth noting that both *ABP* and *HR* phases starts at higher than CO_2 but at

0.05 Hz CO_2 increase above other inputs levels. ***Table 5-16*** shows the average and standard deviation values of MTFA outputs on both right and left sides at hypercapnia condition using 3-inputs.

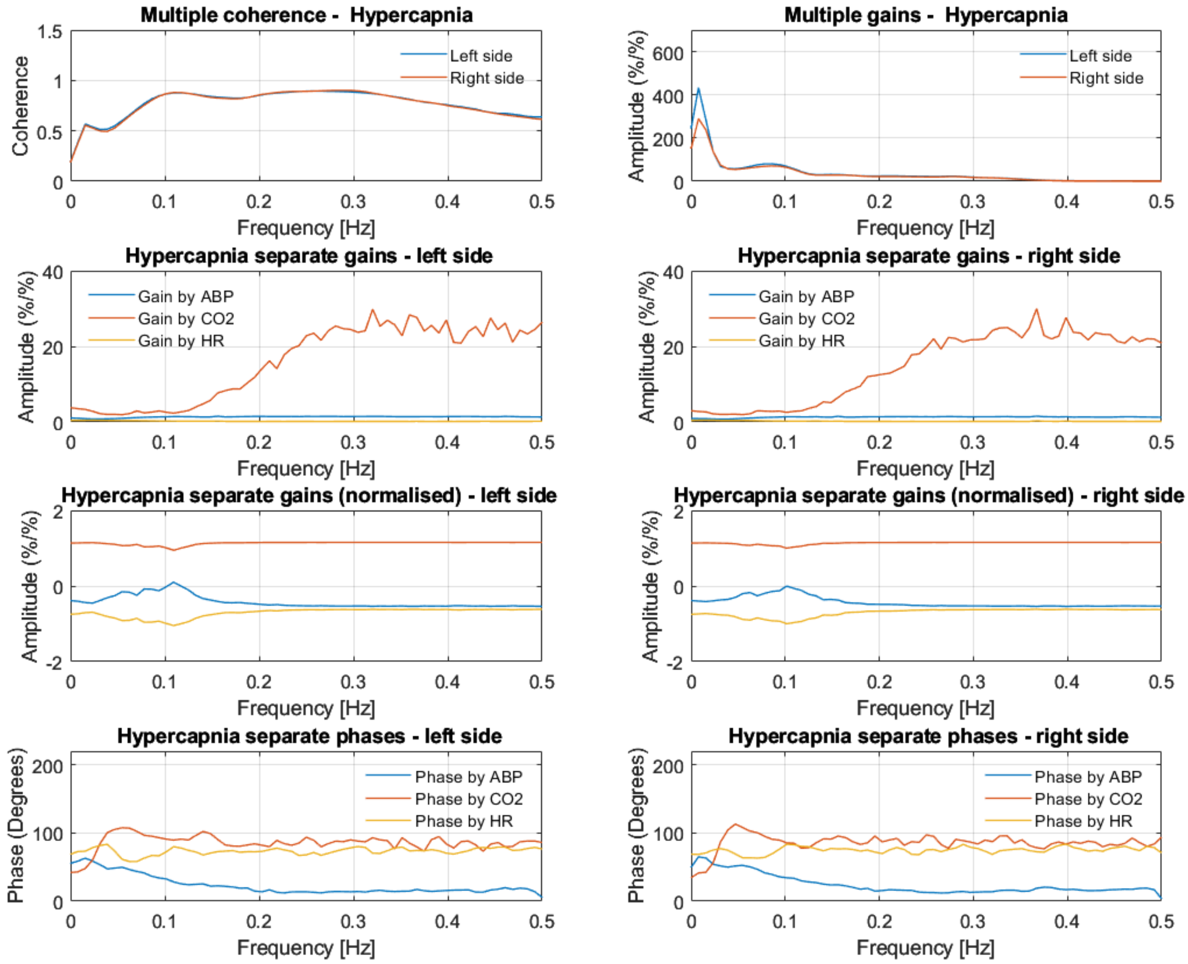

Figure 5-17: MTFA parameters for both right and left sides at hypercapnia condition using 3-inputs

MTFA output	**Multiple Coherence**		**Multiple Gain**		**Separate Gains**						**Separate Phases**					
Side	Left	Right	Left	Right	Left			Right			Left			Right		
Input	Combined effect				*ABP*	CO_2	*HR*	*ABP*	CO_2	*HR*	*ABP*	CO_2	*HR*	*ABP*	CO_2	*HR*
Mean	0.77	0.76	40.45	34.34	1.35	15.85	0.22	1.29	14.74	0.22	23.30	85.75	73.35	24.26	85.79	74.82
± Std	0.14	0.14	69.74	51.01	0.19	9.94	0.09	0.18	9.10	0.10	14.16	12.30	5.13	14.39	13.11	4.77

Table 5-16: Mean and standard deviation values of MTFA parameters across the frequency spectrum at hypercapnia condition using 3-inputs inputs

5.6.3. Thigh cuff condition

This subsection will highlight the MTFA results of all subjects at the thigh cuff condition and using 3-inputs. ***Figure 5-18*** shows the MTFA outputs of all subjects across the frequency spectrum using 3-inputs. The top left plot shows the multiple coherence with the combined effect of the 3-inputs (*ABP*, CO_2, & *HR*) on both the right and left sides of the brain. Again, both right and left sides results are significantly alike across the frequency spectrum starting to reach their maximum levels after 0.1 Hz. The top right plot shows the multiple gains on both sides where it starts higher between 0 – 0.02 Hz then both gains start to drop after 0.15 Hz.

The upper middle left and middle right plots show the left and right sides respectively of separate gains results given by each MTFA input where the blue line is the gain by the *ABP* input, the red line is the gain by the CO_2 input, and the yellow line is the gain by the *HR* input. On both the right and left sides, the gain resulting from CO_2 influence seems significantly higher across the frequency spectrum compared to the other gains. The lower middle plots show the left and right sides respectively of the normalised separate gains which demonstrate that gain by *ABP* influence is significantly higher than gain influenced by other inputs between 0.05 – 0.1 Hz where gain by *HR* influence is continuously lower than gain by other inputs across the frequency spectrum.

The bottom left and right plots show the left and right sides respectively of separate phases results given by each MTFA input where the blue line is the phase by the *ABP* input, the red line is the phase by the CO_2 input, and the yellow is the phase by *HR* input. Both sides show that the phase shift resulting from CO_2 influence is significantly higher than other phases at 0.1 Hz but the *HR* phase start to lead at higher levels after 0.25 Hz. ***Table 5-17*** shows the average and standard deviation values of MTFA outputs on both right and left sides at the thigh cuff condition using 3-inputs.

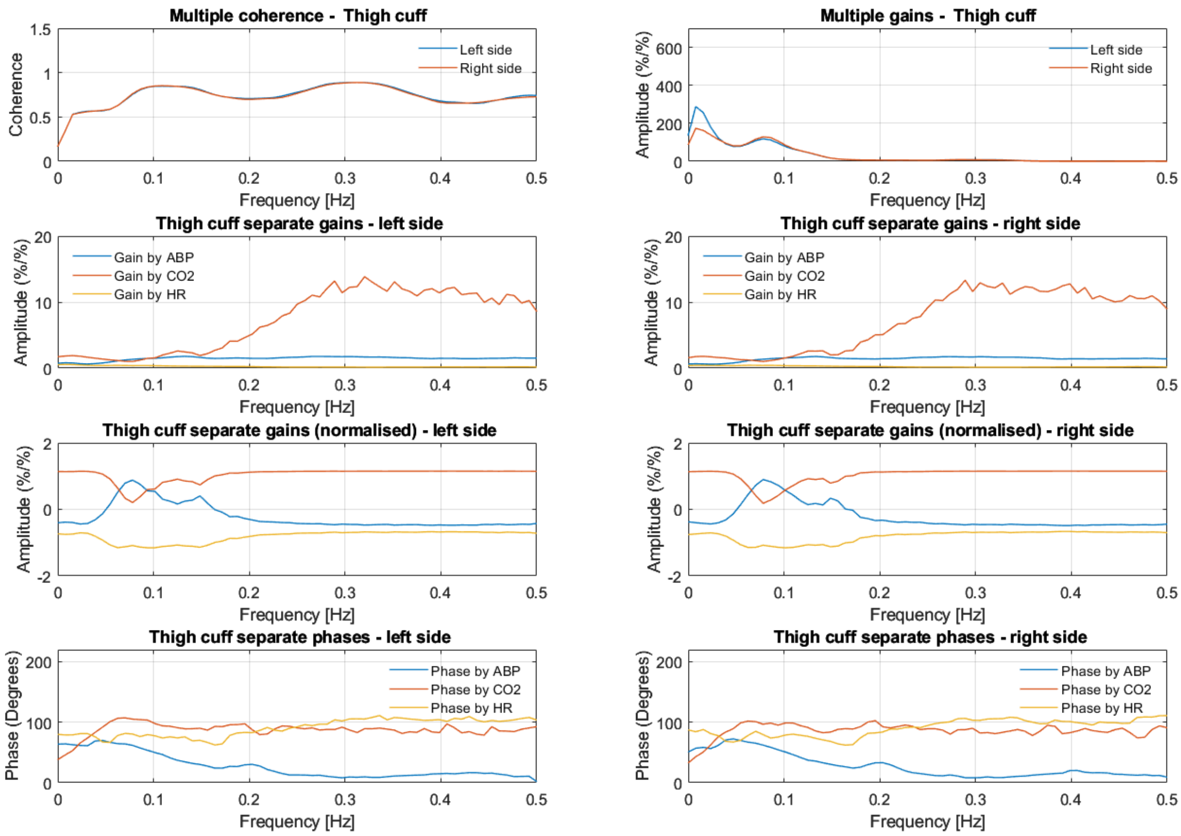

Figure 5-18: MTFA parameters for both right and left sides at thigh cuff condition using 3-inputs

MTFA output	Multiple Coherence		Multiple Gain		Separate Gains						Separate Phases					
Side	Left	Right	Left	Right	Left			Right			Left			Right		
Input	Combined effect				*ABP*	*CO_2*	*HR*	*ABP*	*CO_2*	*HR*	*ABP*	*CO_2*	*HR*	*ABP*	*CO_2*	*HR*
Mean	0.73	0.73	35.11	31.35	1.45	7.25	0.25	1.41	7.20	0.24	27.17	87.50	90.66	27.72	86.22	90.58
± Std	0.13	0.13	59.92	47.01	0.30	4.55	0.11	0.31	4.53	0.10	20.47	11.89	14.27	19.85	12.26	13.94

Table 5-17: Mean and standard deviation values of MTFA parameters across the frequency spectrum at thigh cuff condition using 3-inputs

5.6.4. Reproducibility analysis

In this subsection, reproducibility analysis was performed to calculate ICC values for all subjects at normocapnia, hypercapnia and thigh cuff conditions. The result shows moderate reproducibility levels that show a correlation among all subjects under all conditions ranging from 0.50 – 0.62. ***Figure 5-19*** presents a scatterplot of the calculated ICC values for normocapnia, hypercapnia and thigh cuff using 3-inputs.

Looking at ICC results in each physiological challenge, normocapnia condition has a value of 0.619, hypercapnia condition has a value of 0.504, and thigh cuff condition has a value of 0.598. The figure also demonstrates that normocapnia condition has the highest ICC value, the thigh cuff condition comes second, and the hypercapnia condition represent the lowest when using 3-inputs in the MTFA. ***Table 5-18*** shows the values of ICC results in normocapnia, hypercapnia and thigh cuff at all frequency bands using 3-inputs.

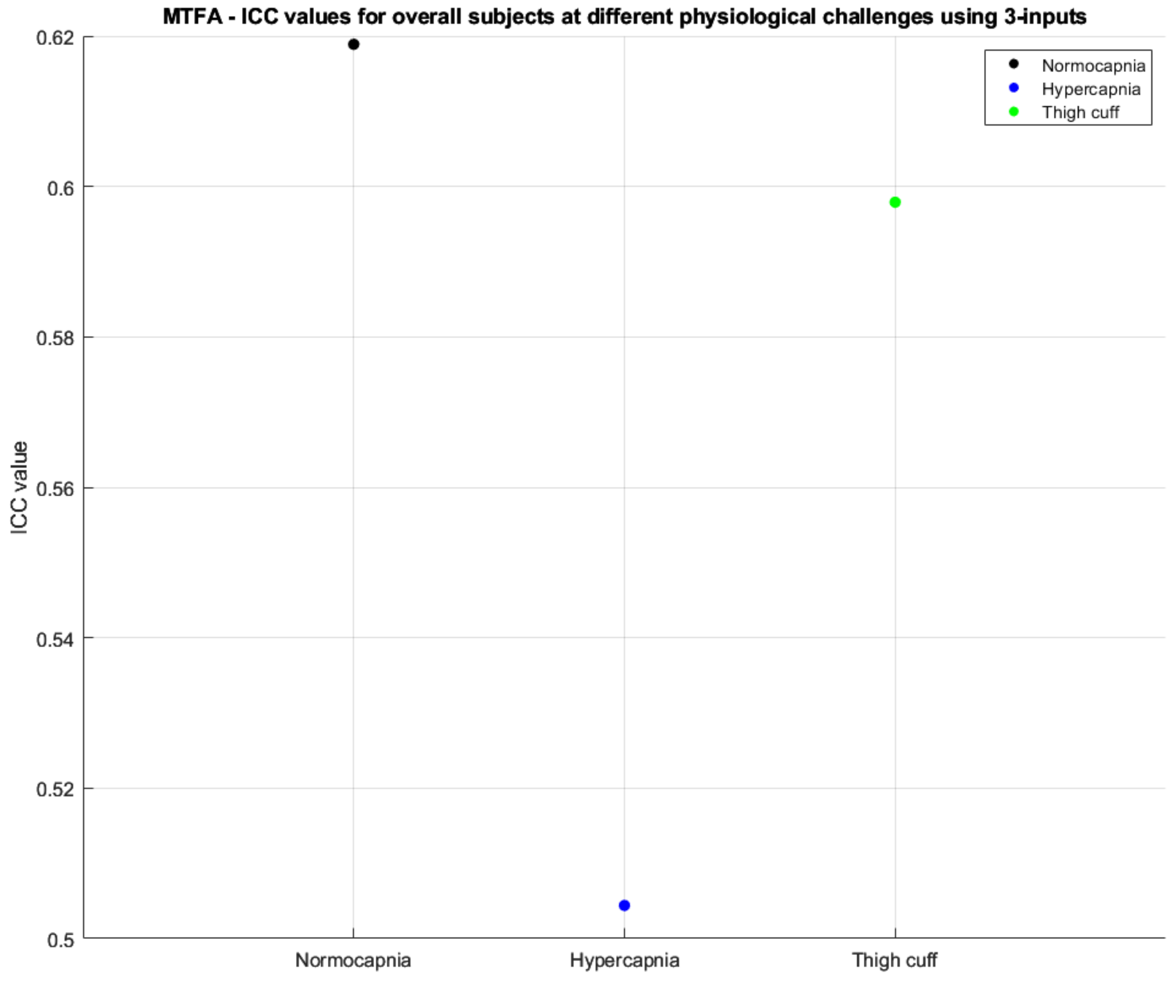

Figure 5-19: Scatterplot shows total ICC values for all subjects at different physiological challenges using 3-inputs

Condition	*ICC value*
Normocapnia	0.619
Hypercapnia	0.504
Thigh cuff	0.598

Table 5-18: ICC values for all subjects at different physiological challenges using 3-inputs

5.6.5. Covariance analysis

Covariance analysis was performed on the resulted MTFA parameters to study the variation levels between measurement variability and subject variability recording under different physiological challenges. ***Figure 5-20*** shows the analysis results comparing the subject variability with the measurement variability for each MTFA parameter using *ABP*, CO_2, and *HR* inputs. Overall, all measurement variability results are significantly smaller than the subject variability ones.

The top two plots, from the left to the right, are the multiple coherence and the multiple gains. The multiple coherence in this plot shows that the thigh cuff condition represents the lowest variability level in both measurement and subject variability recordings compared to the other two conditions whereas the multiple gains behave otherwise and show dissimilar variability among conditions of both measurement and subject variability. For example, hypercapnia subject variability is the highest (which is similar to the behaviour of the separate gain by CO_2) whereas the normocapnia measurement variability is the lowest compared to the other conditions.

Moreover, the second row two plots in ***Figure 5-20***, from the left to the right, are the separate gains by *ABP* input and the separate gains by CO_2 input. The left plot shows that the normocapnia condition is the lowest, compared to the other conditions, in the measurement variability but the thigh cuff is the highest one, compared to the other conditions, in the subject variability. The right plot (gain by CO_2) shows different variation patterns where the normocapnia is the lowest, compared to the other conditions, in both measurement variability and subject variability but the hypercapnia behaviour in separate gains by CO_2 input is similar to the hypercapnia behaviour in the multiple gains variations.

Additionally, the third row two plots in ***Figure 5-20***, from the left to the right, are the separate gain by *HR* input and the separate phases by *ABP* input. In the left plot, by the *HR* input, the normocapnia condition is the lowest compared to other conditions in both the measurement variability and subject variability whereas the thigh cuff is the highest. However, the right plot presenting the phases shift variation levels influenced by *ABP* input shows that the hypercapnia condition appears as the highest compared to the other conditions in measurement variability but the lowest in subject variability.

Furthermore, the bottom two plots in ***Figure 5-20***, from the left to the right, are the separate phase by CO_2 input and separate phase by *HR* input. In the left plot, the thigh cuff condition appears as the lowest in the measurement variability but the highest in subject variability. The right plot, normocapnia condition is the lowest in both subject variability and measurement variability whereas the thigh cuff condition is the highest in subject variability but not in the measurement variability. ***Table 5-19*** shows the means and standard error of MTFA parameters of both measurement variability and subject variability levels under different conditions using 3-inputs.

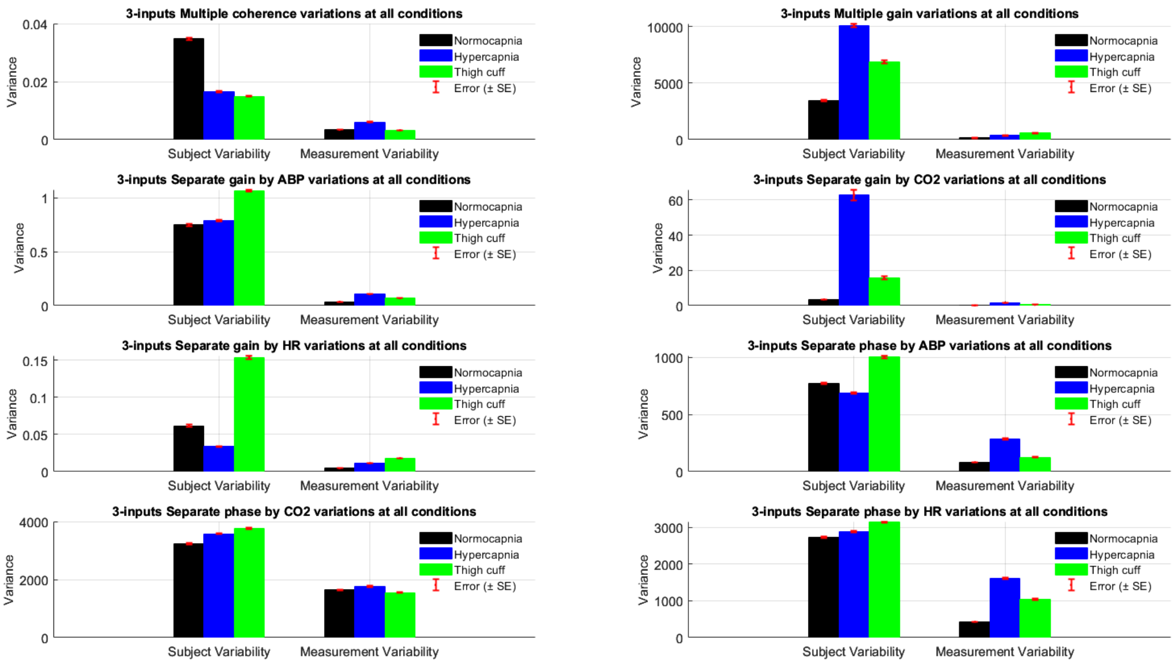

Figure 5-20: MTFA parameters variations of measurement and subject variability in different conditions using 3-inputs

MTFA parameter	Variation	Subject variability		Measurement variability	
	Value	**Mean**	**SE**	**Mean**	**SE**
Multiple coherences	Norm	0.035	0.0004	0.003	< 0.0001
	Hyper	0.017	0.0002	0.006	0.0001
	Thigh	0.015	0.0002	0.003	0.0001
Multiple gains	Norm	3425.793	69.4795	143.293	2.2951
	Hyper	10079.978	173.5560	358.188	8.3861
	Thigh	6863.728	146.5328	572.154	13.0703
Separate gains (*ABP*)	Norm	0.748	0.0106	0.035	0.0004
	Hyper	0.790	0.0079	0.106	0.0013
	Thigh	1.064	0.0111	0.068	0.0008
Separate gains (CO_2)	Norm	3.458	0.1704	0.136	0.0043
	Hyper	62.710	3.1245	1.552	0.0421
	Thigh	15.745	0.7443	0.543	0.0223
Separate gains (*HR*)	Norm	0.062	0.0013	0.005	< 0.0001
	Hyper	0.034	0.0003	0.011	0.0001
	Thigh	0.154	0.0026	0.018	0.0002
Separate phases (*ABP*)	Norm	774.837	7.2043	81.979	1.4305
	Hyper	687.647	7.8318	285.899	6.2899
	Thigh	1003.931	12.4609	125.777	1.5968
Separate phases (CO_2)	Norm	3237.451	19.1702	1640.015	14.7091
	Hyper	3576.957	20.8309	1763.147	16.9818
	Thigh	3767.797	23.3849	1555.461	16.0840
Separate phases (*HR*)	Norm	2735.660	23.2600	429.474	6.9154
	Hyper	2894.379	20.0326	1614.667	13.9282
	Thigh	3142.604	21.0266	1043.172	12.7954

Table 5-19: Mean and standard error of MTFA parameters variations of measurement and subject variability in different conditions using 3-inputs

5.6.6. Significance analysis

Additionally, significance analysis was performed by running paired t-test using the Bonferroni correction technique to compute p-values for each MTFA parameter among different conditions (normocapnia, hypercapnia, and thigh cuff) to study each parameter's dependency on the condition or physiological challenge. Since several p-values will be computed in this analysis, the Bonferroni correction method has been selected to minimise potential error in p-values results.

Nevertheless, a paired t-test with Bonferroni correction has been conducted to examine the association of MTFA parameter with other conditions. ***Figure 5-21*** shows bar graphs for each MTFA parameter mean value on the left side using 3-inputs topped with super bars (pink line) comparing p-values among conditions. Each pink horizontal line shows the p-value in form of significance which is either not significant (n.s., $p > 0.05$), one star (*, $p < 0.05$), two stars (**, $p < 0.01$), three stars (***, $p < 0.001$), or four stars (****, $p < 0.0001$).

Obviously, Multiple gains, gain by CO_2, phase by *ABP*, and phase by *HR* present significant p-values between conditions whereas the remaining parameters show no significance between conditions. In multiple gains, there is a significant association between normocapnia and hypercapnia conditions equivalent to the significant association between normocapnia and thigh cuff conditions, $p < 0.0001$ but there is no significant association between hypercapnia and thigh cuff conditions. In gain by CO_2 input, there is a significant association between normocapnia and hypercapnia, $p < 0.001$, and there is a significant association between normocapnia and thigh cuff conditions, $p < 0.05$.

In phase by *ABP* input, there is a significant association between normocapnia and hypercapnia conditions alike the association between hypercapnia and thigh cuff conditions, $p < 0.05$ but there is no significant association between normocapnia and thigh cuff conditions. Moreover, in phase by *HR*, there is a significant association between normocapnia and hypercapnia conditions, p <0.01, and there is a significant association between normocapnia and thigh cuff conditions, p <0.0001). ***Table 5-20*** lists p-values comparing each MTFA parameter among all conditions on the left side using 3-inputs.

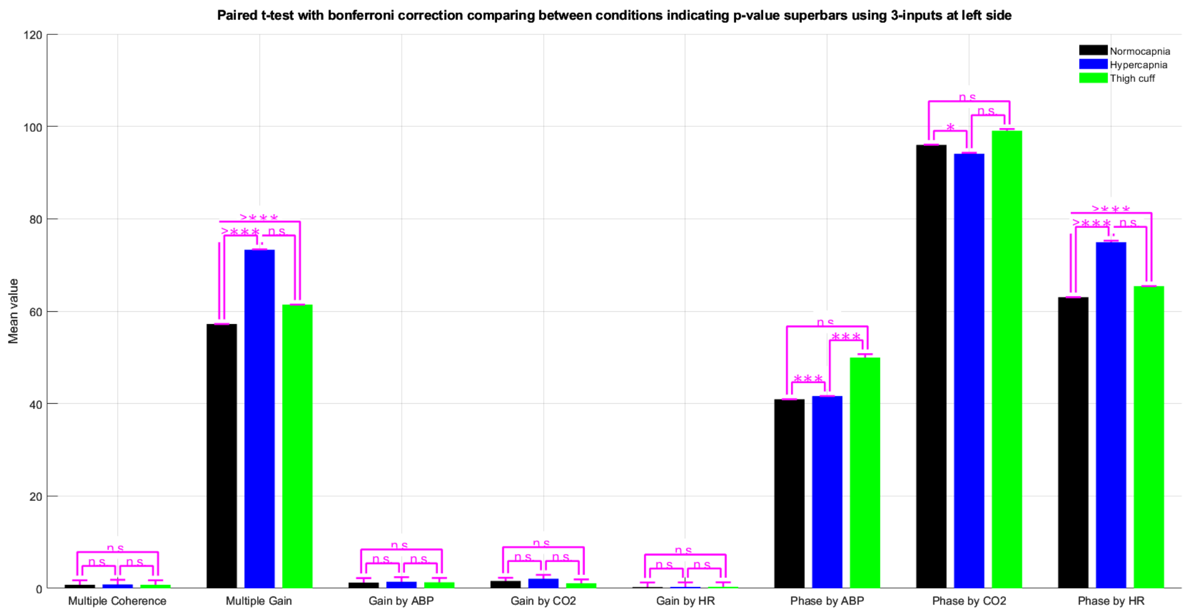

Figure 5-21: Paired t-test analysis with Bonferroni correction to compare p-values of each MTFA parameter in different conditions on the left side using 3-inputs (n.s. is no significance, * means p-value is < 0.05, ** < 0.01, *** < 0.001, and **** is < 0.0001)

		P-values left side						
MTFA parameter	Multiple Coherence	Multiple Gain	Gain by *ABP*	Gain by CO_2	Gain by *HR*	Phase by *ABP*	Phase by CO_2	Phase by *HR*
Norm vs Hyper	0.9698	<0.0001	0.9581	0.6750	0.9945	0.0003	0.0316	<0.0001
Hyper vs Thigh	0.9969	0.0891	0.9823	0.8380	0.9800	0.0003	0.2139	0.3303
Thigh vs Norm	0.9706	<0.0001	0.9337	0.8247	0.9828	0.7426	0.3625	<0.0001

Table 5-20: Comparing p-values of each MTFA parameter in different conditions on the left side using 3-inputs

Contrariwise, ***Figure 5-22*** shows the p-values results on the right side using 3-inputs. Multiple coherence gain by *ABP* and gain by *HR* parameters show no significant associations between different conditions. However, multiple gain shows an equivalent significant association between all 3 conditions where p < 0.0001. In gain by CO_2, there is a significant association between normocapnia and hypercapnia conditions, p < 0.001, and there is a significant association between normocapnia and thigh cuff conditions, $p < 0.05$ but here is no significant association between hypercapnia and thigh cuff conditions.

Likewise, phase by *ABP* input shows a significant association between hypercapnia and thigh cuff conditions ($p < 0.05$) but there are no significant associations between other conditions. Also, the phase by CO_2 presents a significant association between normocapnia and hypercapnia conditions similar to the significant association between hypercapnia and thigh cuff conditions, ($p < 0.05$). For the phase by *HR*, there is a significant association between normocapnia and hypercapnia conditions equivalent to the significant association between normocapnia and thigh cuff, $p < 0.0001$.

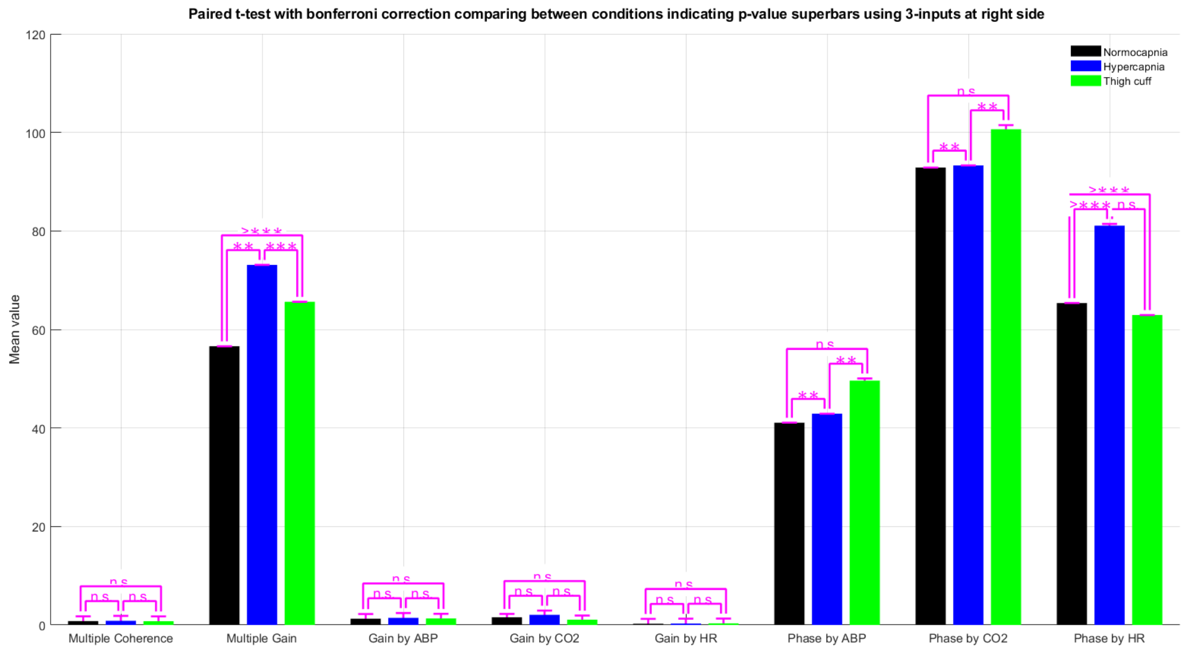

Figure 5-22: Paired t-test analysis with Bonferroni correction to compare p-values of each MTFA parameter in different conditions on the right side using 3-inputs (n.s. is no significance, * means p-value is < 0.05, ** < 0.01, *** < 0.001, and **** is < 0.0001)

		P-values right side						
MTFA parameter	Multiple Coherence	Multiple Gain	Gain by *ABP*	Gain by CO_2	Gain by *HR*	Phase by *ABP*	Phase by CO_2	Phase by *HR*
Norm vs Hyper	0.9714	0.0019	0.9595	0.6813	0.9921	0.0053	0.0023	<0.0001
Hyper vs Thigh	0.9964	0.0005	0.9798	0.8520	0.9781	0.0011	0.0029	0.3486
Thigh vs Norm	0.9746	<0.0001	0.9358	0.8298	0.9837	0.4362	0.8531	<0.0001

Table 5-21: Comparing p-values of each MTFA parameter in different conditions on the right side using 3-inputs

5.7. Comparing univariate and multivariate results

This section will provide an overview of some results comparing between univariate and multivariate analyses. ***Figure 5-23*** shows the resulted coherence outputs from both single subject and average of all subjects using univariate and multivariate analyses using 3 different combination of inputs (*ABP*+CO_2, *ABP*+*HR*, and *ABP*+CO_2+*HR*) where the solid black line represents the univariate coherence, the dotted green line represents the multivariate using *ABP*+CO_2, the dotted-dashed pink line represents the multivariate using *ABP*+*HR*, and the dashed blue line represents the multivariate using all 3-inputs. Clearly, using 3-inputs on MTFA has increased the resulted coherence output across the frequency spectrum. ***Table 5-22*** lists means and standard deviations of all subjects' coherences in univariate and multivariate analyses.

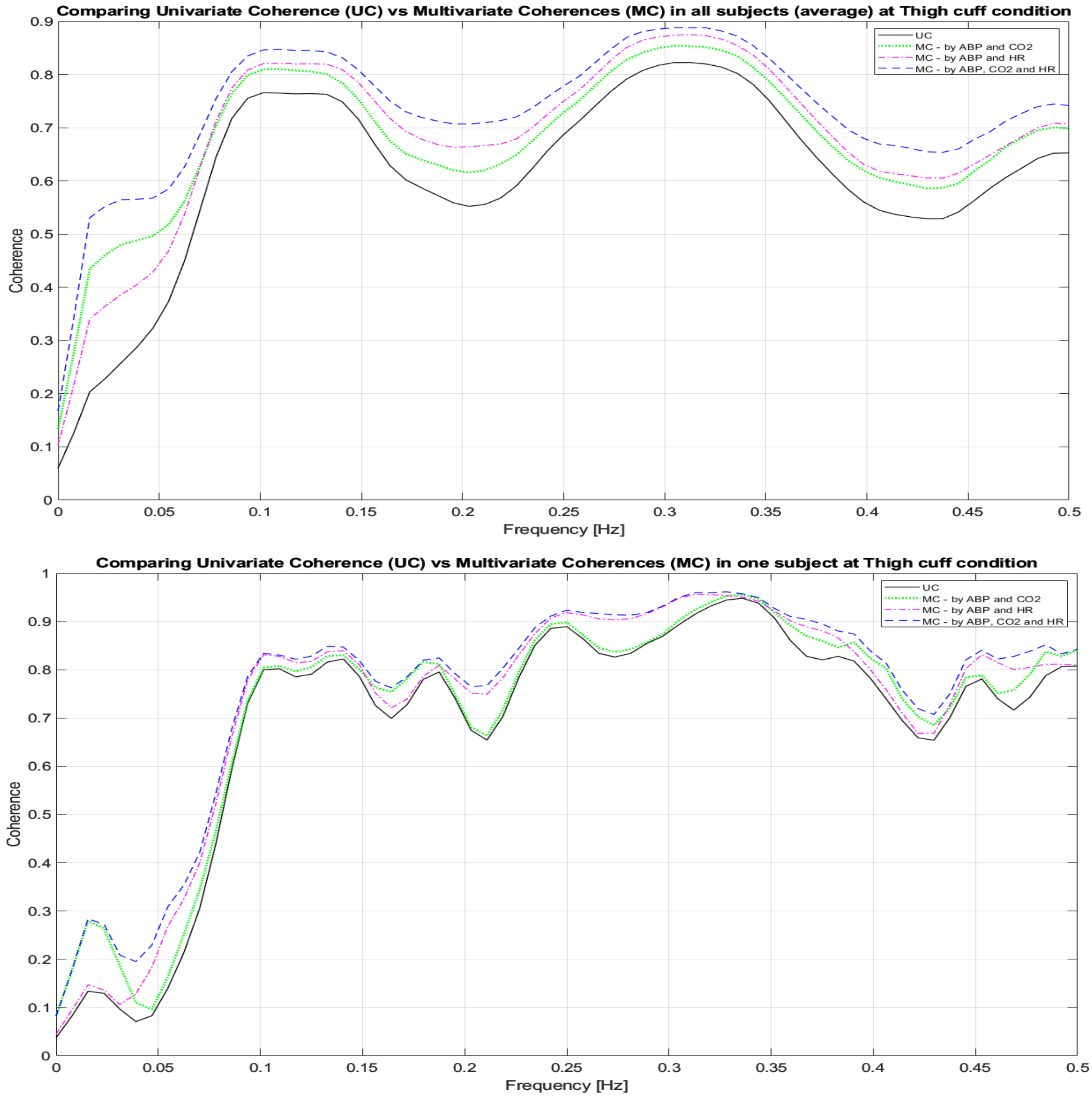

Figure 5-23: Comparison of coherence outputs from both single subject and average of all subjects in univariate and multivariate analyses across the frequency spectrum

Multiple coherences	*ABP* only	*ABP* + CO_2	*ABP* + *HR*	*ABP* + CO_2 + *HR*
Mean	0.611	0.676	0.685	0.732
Std +/-	0.174	0.137	0.160	0.128

Table 5-22: Means and standard deviations of all subjects' coherences in univariate and multivariate analyses

Furthermore, ***Figure 5-24*** shows a bar graph of all MTFA parameters when adding *HR* variable as an input to the MTFA (3-inputs) coloured purple and when removing *HR* variable from the transfer function (2-inputs) coloured green on both sides under different conditions. The figure displays different behaviour of some MTFA parameters under different conditions. For example, despite consistent behaviour of multiple gain phase by CO_2 on all plots, phase by *ABP* in normocapnia on both sides decreased when adding *HR* input but clearly increased in hypercapnia and thigh cuff conditions. ***Table 5-23*** list means and standard deviations values of MTFA parameters on both right and left sides under different conditions when adding and removing *HR* input from the transfer function.

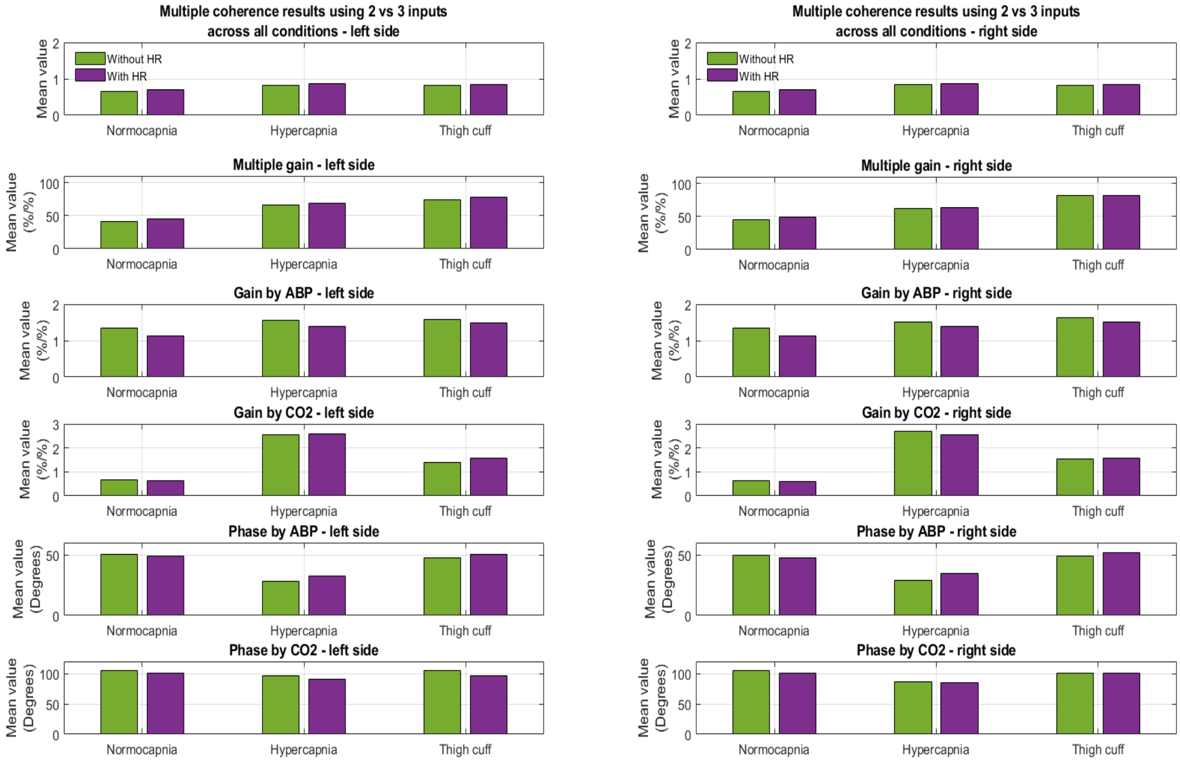

Figure 5-24: Comparison of MTFA parameter with and without adding *HR* variable as input on both right and left sides under different conditions

MTFA Parameter	2 vs 3 inputs	Condition	Normocapnia				Hypercapnia				Thigh cuff			
		Side	Left side		Right side		Left side		Right side		Left side		Right side	
		Value	Mean	Std +/-	Mean	Std +/-	Mean	Std +/-	Mean	Std +/-	Mean	Std +/-	Mean	Std +/-
Multiple Coherence	without *HR*	merged	0.645	0.16	0.65	0.161	0.83	0.133	0.834	0.117	0.81	0.11	0.81	0.117
	with *HR*	merged	0.691	0.14	0.697	0.137	0.866	0.112	0.869	0.1	0.847	0.088	0.845	0.101
Multiple Gain	without *HR*	merged	41.583	37.3	45.017	45.8	66.73	69.14	62	67.84	73.72	52.84	81.62	67.92
	with *HR*	merged	45.342	37.7	49.084	46.89	69.11	73.23	64.08	71.29	77.5	52.98	82.132	66.8
Separate Gains	without *HR*	by *ABP*	1.34	0.54	1.354	0.611	1.568	0.619	1.52	0.598	1.574	0.643	1.625	0.702
	with *HR*	by *ABP*	1.137	0.62	1.141	0.645	1.381	0.711	1.385	0.627	1.49	0.716	1.518	0.733
	without *HR*	by CO_2	0.679	1.22	0.637	1.15	2.533	5.678	2.676	6.751	1.409	2.239	1.537	2.793
	with *HR*	by CO_2	0.632	1.35	0.58	1.371	2.581	5.611	2.556	5.731	1.572	2.731	1.585	3.103
Separate Phases	without *HR*	by *ABP*	50.309	15.3	49.743	14.5	28.38	13.38	28.84	12.97	47.27	16.84	48.717	17.34
	with *HR*	by *ABP*	49.262	20.9	47.791	21.03	32.6	20.72	34.35	23.33	50.66	23.64	51.433	24.16
	without *HR*	by CO_2	104.53	47	105.36	51.1	96.03	51.69	86.55	50.59	104.5	48.95	100.12	54.15
	with *HR*	by CO_2	101	47.6	100.2	51.14	91	51.05	85.53	52.29	97.13	49.25	101.07	53.61

Table 5-23: Means and standard deviations of MTFA parameter with and without adding HR variable as input on both right and left sides under different conditions

In addition, reproducibility studies conducted on each case from the previous subsections were compared with each other to examine ICC results behaviour under different conditions using different combinations of inputs on the transfer function. ***Figure 5-25*** is a scatterplot shows ICC results behaviour under different conditions when using 1, 2, and 3-inputs to the TFA.

The ICC resulted from using *ABP* only as input to the UTFA is denoted red, the ICC resulted from using *ABP* and CO_2 as inputs is denoted yellow, the ICC resulted from using *ABP* and *HR* as inputs is denoted green, and the ICC resulted from using *ABP*, CO_2, and *HR* as inputs is denoted blue. The figure demonstrates that adding *HR* input to the TFA has resulted to a lower level of reproducibility than using $ABP+CO_2$ inputs. It worth noting that ICC resulted from UTFA is significantly lower in hypercapnia and thigh cuff conditions than ICC resulted from MTFA except normocapnia condition which is slightly higher than ICC from $ABP+HR$ despite the poor reproducibility. ***Table 5-24*** list overall subjects ICC values under different conditions using different combinations of TFA inputs.

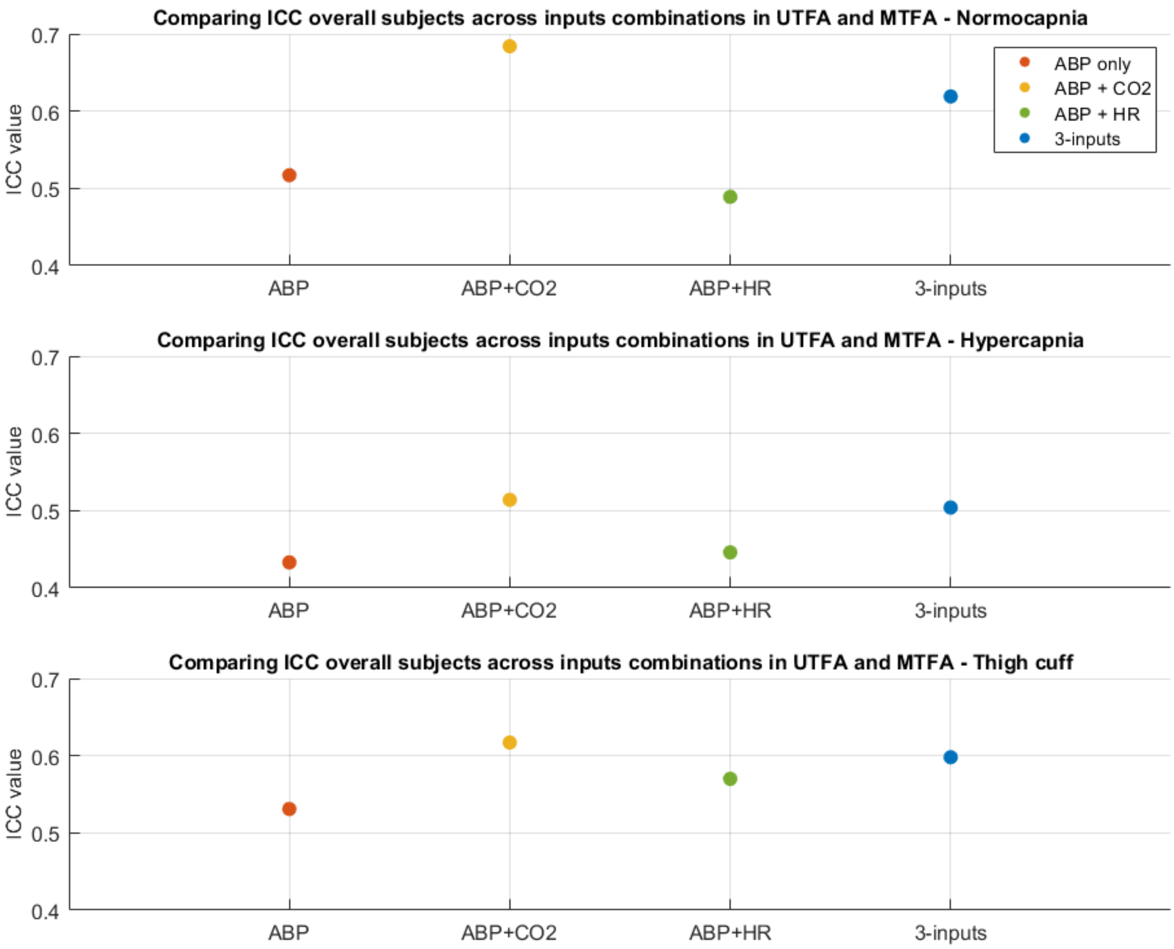

Figure 5-25: Comparing ICC results using all combinations of inputs across all conditions in UTFA and MTFA

Value	ICC values at Normocapnia				ICC values at Hypercapnia				ICC values at Thigh cuff			
	Univariate	Multivariate			Univariate	Multivariate			Univariate	Multivariate		
	1-input	*ABP + CO_2*	*ABP + HR*	3-inputs	1-input	*ABP + CO_2*	*ABP + HR*	3-inputs	1-input	*ABP + CO_2*	*ABP + HR*	3-inputs
Overall	**0.517**	**0.684**	**0.489**	**0.619**	**0.433**	**0.514**	**0.446**	**0.504**	**0.531**	**0.617**	**0.570**	**0.598**

Table 5-24: ICC results using all combinations of inputs across all conditions in UTFA and MTFA

Nevertheless, paired t-test analysis was performed to measure the statistical significance of *HR* input influence to the MTFA under different conditions/physiological challenges. ***Figure 5-26*** show a bar graph of both right and left sides comparing p-values of MTFA parameters among different conditions with *HR* input influence. Obviously, there is no significant association on all MTFA parameters between *HR* influence and different conditions, $p > 0.05$. ***Table 5-25*** lists p-values of each MTFA parameter in different conditions on both right and left sides when adding/removing *HR* input.

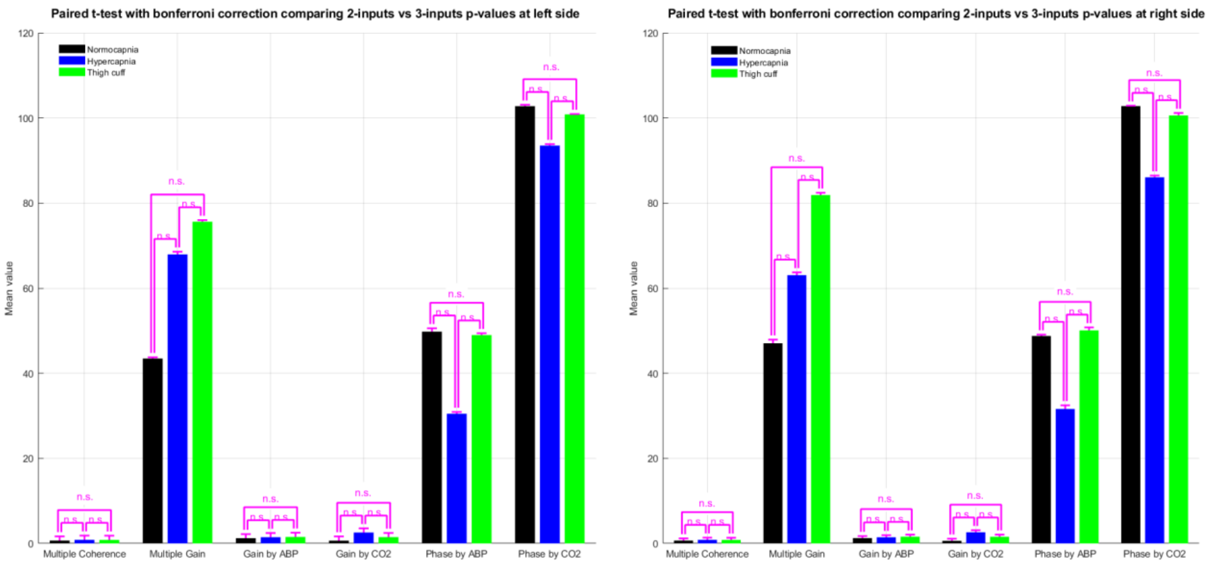

Figure 5-26: Paired t-test analysis with Bonferroni correction to compare p-values of each MTFA parameter under different conditions on both right and left sides when adding/removing *HR* input (n.s. is no significance, * means p-value is < 0.05, ** < 0.01, *** < 0.001, and **** is < 0.0001)

MTFA parameter	Left side			Right side		
	Norm vs Hyper	Hyper vs Thigh	Thigh vs Norm	Norm vs Hyper	Hyper vs Thigh	Thigh vs Norm
Multiple Coherence	0.505	0.503	0.503	0.505	0.503	0.503
Multiple Gain	0.850	0.680	0.804	0.840	0.660	0.539
Gain by *ABP*	0.478	0.485	0.492	0.479	0.489	0.492
Gain by CO_2	0.495	0.504	0.515	0.494	0.490	0.504
Phase by *ABP*	0.386	0.797	0.779	0.317	0.863	0.700
Phase by CO_2	0.165	0.161	0.047	0.104	0.420	0.573

Table 5-25: P-values of each MTFA parameter in different conditions on both right and left sides when adding/removing *HR* input

5.8. Discussion

The results of TFA on both univariate and multivariate scales have shown different variability behaviour of TFA parameters using different inputs, as would be expected. In the univariate analysis, the thigh cuff condition, particularly in the LF band, appears in most cases to exhibit the lowest variation levels compared to the normocapnia and hypercapnia conditions. A previous study suggested that the thigh cuff method is the most suitable technique in studying dCA [3]. This is because the thigh cuff technique has a faster influence on *ABP* and even in impaired dCA, hence thigh cuff testing shows a faster recovery of *CBv* in some major arteries in the brain [3].

Looking at the univariate analysis results, the thigh cuff condition demonstrates the highest ICC values compared to other conditions. The covariance analysis shows that the thigh cuff condition has the lowest coherence and gain variations compared to other conditions but not for the phase shift parameter. A previous study has shown that thigh cuff testing could cause relatively high measurement variability, but that this could be tackled by the sit-stand technique which has lowered the measurement variability results. The study presents the sit-stand technique as an appropriate measure when using ARI values in dCA assessment [90].

In contrast with previous research work, a previous study found that the LF band is a good starting point for further investigation compared to HF and VLF bands. The study suggested that including healthy and patient subjects in future work might deliver higher levels of ICC. However, the study conducted the Lower Body Negative Pressure (LBNP) technique to induce changes in *ABP* and found that the consistency of phase measurements at the LF band was significantly improved. This study suggested that this technique does influence *ABP* and reduce both heart rate and CO_2 levels [57].

Moreover, adding CO_2 and *HR* inputs has shown different variability behaviour of the results using the same datasets in the multivariate analysis. As expected, adding CO_2 and *HR* inputs to the MTFA does increase coherence results. Perhaps surprisingly, adding *HR* as a second input to MTFA appears to increase the coherence more compared to adding CO_2 as a second input. Using 3-inputs in the MTFA has increased coherence results compared to the other two inputs (*ABP* + CO_2 and *ABP* + *HR*). A previous study has previously explored the inclusion of CO_2 and O_2 as inputs to the MTFA [55], other studies investigated the influence of *HR* input using nonlinear models [11] [12], but this study now presents the use of *HR* as a 2nd and 3rd input to the MTFA.

Using $ABP+CO_2$ inputs, this study displayed the output of MTFA parameters using the combination of inputs in each condition (normocapnia, hypercapnia, and thigh cuff) for both the right and left sides of the brain. Then, calculated ICC values of each condition using this combination and it has shown a moderate reproducibility level (between 0.5 – 0.7) for all conditions. Also, a covariance analysis has been performed to calculate the variances of each MTFA parameter across all conditions using $ABP+CO_2$ inputs. Finally, significance analysis was performed using a paired t-test to calculate p values and measure the association between each MTFA parameter with each condition on both the right and left sides.

As a result of using the combination of $ABP+CO_2$ inputs, multiple coherence in the hypercapnia condition shows the highest mean values on both sides compared to other conditions (left, 0.711 ±0.15 and right, 0.703 ±0.16). Moreover, the average MTFA output of the separate gain and phase influenced by CO_2 input is significantly higher on both the right and left sides compared to the gain resulted from *ABP* influence across all conditions. However, the significance analysis shows, in general, no significant associations between MTFA parameters and different conditions except for multiple gain and phase results by *ABP* input on the left side which shows a significant association between MTFA parameters and different conditions. Also, the phase for the CO_2 input on the right side shows a significant association between MTFA parameters and different conditions.

Using the combination of *ABP+HR* inputs, this study overviewed the MTFA parameters outputs, reproducibility, covariance, and significance results. Again, multiple coherence in the hypercapnia condition shows the highest mean values on both sides compared to other conditions (left, 0.724 ±0.17 and right, 0.721 ±0.17). But the average MTFA output of the separate gain influenced by *ABP* input is significantly higher on both the right and left sides compared to the *HR* influence across all conditions whereas the opposite case is for the separate phase parameter across all conditions. However, significance analysis shows a significant association between MTFA parameters and different conditions except for multiple coherence and separate gains on both the right and left sides.

In the case of using 3-inputs (*ABP*+CO_2+*HR*) in the analysis, this study applied the same analyses in the previous combinations of inputs (*ABP*+CO_2 and *ABP*+*HR*). The multiple coherence in the hypercapnia condition shows the highest mean values on both sides compared to other conditions (left, 0.766 ±0.14 and right, 0.762 ±0.14). Interestingly, the average separate gain influenced by CO_2 input is significantly higher on both the right and left sides compared to the other inputs' influence across all conditions. Also, the average phase by *HR* input is significantly higher than other inputs' influences on both sides in normocapnia and thigh cuff conditions whereas the separate phase average by CO_2 input is the highest in the hypercapnia condition only.

The significance analysis using 3-inputs shows a significant association between parameters and different conditions except for multiple coherence and separate gains on both the right and left sides. It's worth noting that in reproducibility analysis using UTFA, the thigh cuff condition demonstrates the highest ICC mean values compared to the other conditions (0.531). The normocapnia condition exhibit the highest value when using 3-inputs (0.619) compared to other combination of inputs, and persistently, the *ABP*+CO_2 input has the highest ICC values compared to the UTFA and other combination of inputs in the MTFA across all conditions (normocapnia: 0.684, hypercapnia: 0.514, and thigh cuff: 0.617). Also, covariance analysis demonstrates that multiple coherence in the thigh cuff condition has the lowest variability levels in both measurement and subject variabilities across combinations of inputs.

This thesis also compared the univariate (*ABP* only) with multivariate (all inputs combinations) coherences in the thigh cuff condition to examine the behaviour of coherences using different input combinations as shown in ***Figure 5-23***. The results show that univariate coherence has the lowest mean value, and multiple coherence calculated using the 3-inputs have the highest mean value where the *ABP*+CO_2 comes higher than univariate coherence then *ABP*+*HR* is just lower than 3-inputs as shown in ***Table 5-22***. Even more, this study compared MTFA parameters with and without *HR* as an input to the TFA across all conditions and found that adding *HR* to the analysis significantly increases the coherence of the results.

It's worth noting that the contribution of ABP, CO_2 and *HR* inputs to *CBv* in terms of gain and phase could be described physiologically as the influence amplitude of each input to changes in CBv, i.e. the amount of each input influence to CBv (gain) and the angle shift, in degrees, determine which input occurred first in influencing changes in CBv, i.e. the order of input influence (phase).

Likewise, comparing ICC values in univariate and multivariate analyses using different combinations of inputs across all conditions, the results show that using *ABP*+*HR* inputs in the TFA demonstrated the highest ICC mean values compared to all other inputs combinations across all conditions as shown in ***Figure 5-25*** and ***Table 5-24***. Also, the significance analysis of adding or removing the *HR* input from the MTFA shows no significant association on all MTFA parameters between *HR* influence and different conditions, $p > 0.05$ on both the right and left sides.

Importantly, comparing univariate with multivariate coherences, the results shows that 3-inputs coherence has the highest mean value across the spectrum. But when using every combination of inputs to the MTFA, it has been found that using *ABP*+*HR* inputs result in a higher value with a lower variability compared to the results from using *ABP*+CO_2. Looking at ***Table 5-23*** the resulted multiple coherence from using 2-inputs or 3-inputs in both hypercapnia and thigh cuff conditions are significantly higher than normocapnia condition. These results may suggest that using 3-inputs and comparing hypercapnia and thigh cuff conditions results could be beneficial for future research to investigate multivariate analysis and hence to quantify variabilities.

However, although previous studies have suggested that further multivariate analysis should be considered in future work to assess dCA [4 58 59 60] this study conducted both univariate and multivariate analyses and compared some parameters results from both analyses to observe the changes in resulting parameters from both UTFA and MTFA. The resulted ICC values from the thigh cuff condition appears higher than other conditions in every combination of input to the TFA which would align with the study suggesting that inducing oscillation to *ABP* improves coherence results [91].

The limitations of the results presented in this chapter include the assumption that dCA is a linear system despite the known non-linearity behaviour nature of the dCA [5]. Also, multiple coherence results show the combined influences of all inputs whereas some studies present the partial coherence results to show the coherence output influenced by each input to the MTFA [92 93]. Besides, reproducibility analysis presents ICC results in this research for overall participants' MTFA parameters on both sides, but the analysis could be applied to present the ICC value for each MTFA parameter as performed in a previous study [60].

5.9. Conclusion

This chapter discussed methods, MTFA, and results including reproducibility, covariance analysis, and significance analysis in different conditions as well as results comparison. Next, covariance analysis was performed to calculate both the measurement and subject variabilities in the results. Then, a statistical significance analysis was conducted to compute the p-value and measure the association between MTFA parameters with different conditions after each covariance analysis. Finally, comparisons of some univariate and multivariate results were performed to overview parameters behaviour using different combinations under different conditions.

From this chapter it could be concluded that, as expected, MTFA has improved coherence results and using 3-inputs into the MTFA will present the highest coherence values compared to univariate and 2-input combinations. In another word, adding *HR* input as a 3rd input has increased coherence outcomes on both sides across all conditions. Also, the thigh cuff condition demonstrate the highest ICC values compared to other conditions and there is no significant association between MTFA parameters and different conditions, $p > 0.05$.

6. Dynamic CA assessment: one-side vs two-side

6.1. Introduction

This chapter will examine the results from MTFA parameters on each side and their average separately. The examination of each case (right side, left side, average of both sides) will be comparing MTFA parameters across hypercapnia vs thigh cuff conditions. These examinations should show the difference between MTFA outcomes on each side and their average. That might assist in choosing a case for future analysis.

First, right side will be examined, MTFA parameters results presented, and covariance analysis performed. Second, left side will be examined, MTFA parameters results presented, and covariance analysis performed. Then, the average of both sides (right and left) will be examined, MTFA parameters results presented, and covariance analysis performed. Finally, an autoregulatory parameters significance analysis will be presented to examine the MTFA parameters behaviour in each side (right and left) and their average across different conditions. It's worth noting that each bar figure in covariance results represents the mean variance value ($ABP+CO_2$ is yellow, $ABP+HR$ is green, and 3-inputs is orange) and the error bar (black) represents the standard error from the mean on the top of each bar.

6.2. Testing right side outcomes

This section will present the results of MTFA parameters and covariance analyses on the right side. The results here are comparing MTFA parameters from the hypercapnia versus the cuff conditions. The covariance analysis will plot the variations of each MTFA parameter using different input combinations across hypercapnia and thigh cuff conditions on the right side.

6.2.1. MTFA results

This subsection explains the results of executing the MTFA on the right side of the brain. ***Figure 6-1*** illustrate MTFA parameters across hypercapnia and thigh cuff conditions using both *ABP* and CO_2 inputs on the right side. The left top plot shows the multiple coherence with the combined effect of *ABP* and CO_2 inputs across hypercapnia and thigh cuff conditions on the right side of the brain. It's worth noting that the blue line represents hypercapnia condition, and the red line represents the thigh cuff condition. In average, the hypercapnia condition appears larger than thigh cuff results where both conditions results behave unequally across the frequency spectrum starting to reach their maximum levels after 0.1 Hz. The top right plot shows the multiple gains for both conditions where it starts higher between 0 – 0.02 Hz then both gains start to drop after 0.15 Hz.

The upper middle left and middle right plots show the hypercapnia and thigh cuff conditions respectively of separate gains results given by each MTFA input on the right side where the blue line is the gain by the *ABP* input, the red line is the gain by the CO_2 input, and the yellow line is the gain by *HR* input. On both conditions, the gain resulting from CO_2 influence seems significantly higher across the frequency spectrum compared to the gain resulted by *ABP* and *HR* influences especially in hypercapnia condition.

The lower middle plots show the hypercapnia and thigh cuff conditions respectively of the normalised separate gains on the right side which demonstrate that gain by CO_2 influence is significantly higher than gain influenced by other inputs across the frequency spectrum in hypercapnia at the right side. In Thigh cuff condition the gain by CO_2 is mostly higher than other gains across the spectrum (gain by *HR* is the lowest) except at the frequency 0.075 Hz the gain by *ABP* rise above other gains then return to be in the middle between gains across the spectrum.

The bottom left and right plots show the hypercapnia and thigh cuff conditions respectively of separate phases results given by each MTFA input where the blue line is the phase by the *ABP* input, the red line is the phase by the CO_2 input, and the yellow line is the phase by *HR* input. Both conditions show that the phase shift resulting from CO_2 influence is significantly higher than the phase resulted from *ABP* influence at 0.1 Hz. But the thigh cuff condition (lower right plot) show higher phase level by the *HR* input after 0.25 Hz than the other inputs. ***Table 6-1*** MTFA parameters mean and standard deviation across hypercapnia and thigh cuff conditions using both *ABP* and CO_2 inputs on the right side.

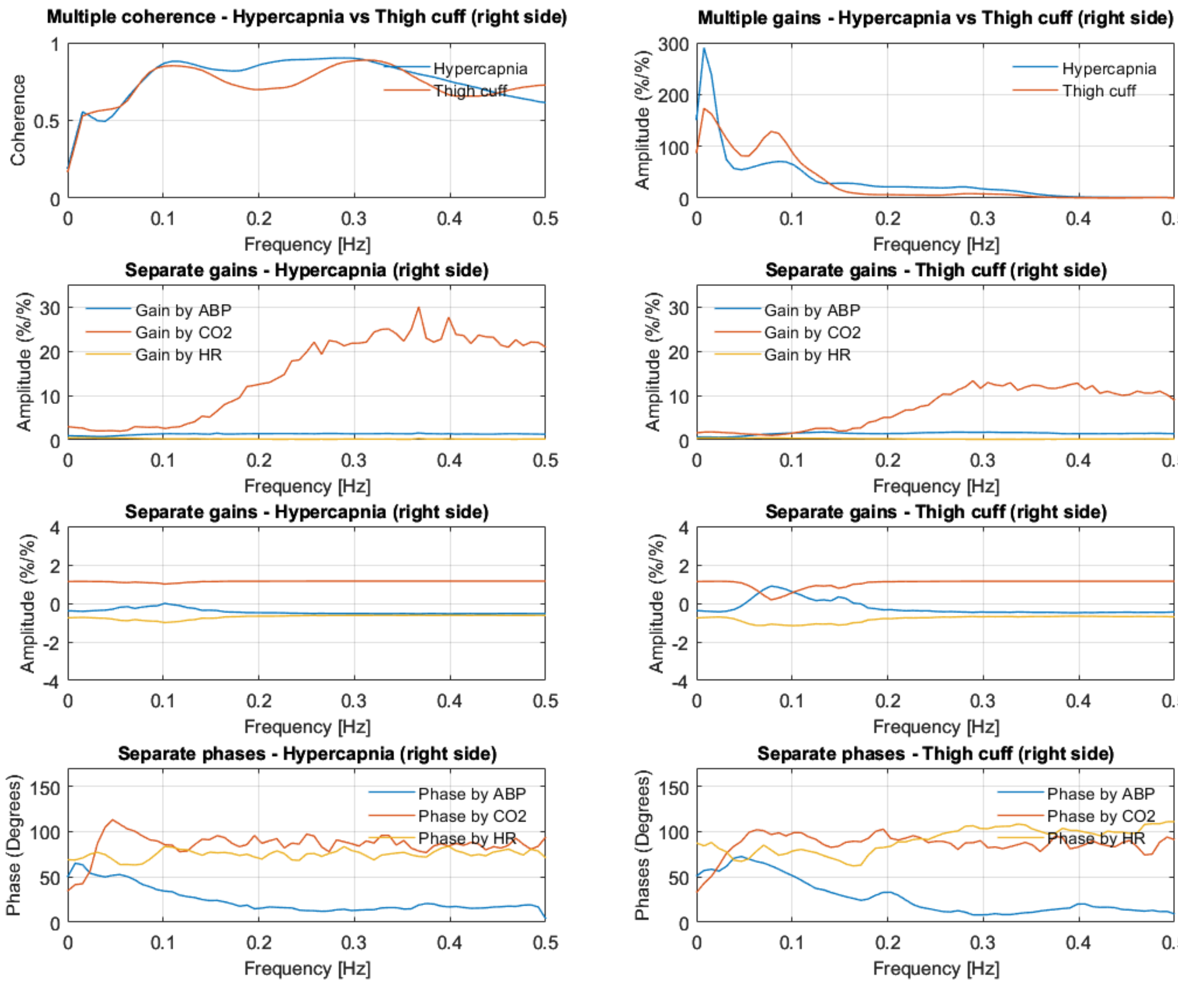

Figure 6-1: MTFA parameters results across hypercapnia and thigh cuff conditions using 3-inputs on the right side

MTFA parameter	Condition	Mean	Std (+/-)
Multiple coherences	Hyper	0.762	0.145
	Thigh	0.728	0.127
Multiple gains	Hyper	34.339	51.011
	Thigh	31.351	47.008
Separate gains (*ABP*)	Hyper	1.290	0.184
	Thigh	14.738	9.103
Separate gains (CO_2)	Hyper	0.222	0.096
	Thigh	1.415	0.306
Separate gains (*HR*)	Hyper	7.196	4.527
	Thigh	0.245	0.099
Separate phases (*ABP*)	Hyper	24.264	14.391
	Thigh	85.787	13.109
Separate phases (CO_2)	Hyper	74.816	4.766
	Thigh	27.725	19.853
Separate phases (*HR*)	Hyper	86.224	12.258
	Thigh	90.578	13.940

Table 6-1: MTFA parameters mean and standard deviation across hypercapnia and thigh cuff conditions using 3-inputs on the right side

6.2.2. Covariance analysis

Covariance analysis was performed on the resulted MTFA parameters to study the variation levels between measurement variability and subject variability recording across hypercapnia and thigh cuff conditions using different combinations of inputs on the right side. ***Figure 6-2*** shows the analysis results comparing the subject variability with the measurement variability for each MTFA parameter influenced by each input (*ABP*, CO_2, and *HR*). Overall, all measurement variability results are significantly smaller than the subject variability ones.

The top two plots, from the left to the right, are the multiple coherence and the multiple gain variations. The multiple coherence in this plot shows that the using 3-inputs in the MTFA is the lowest variability level in both measurement and subject variability recordings compared to the other input combinations whereas the multiple gain behave otherwise and show dissimilar variability across input combinations for both measurement and subject variability. For example, 3-inputs subject variability is the highest (which is similar to the behaviour of the separate gain by *ABP*) whereas the 3-inputs measurement variability is the lowest compared to the other input combinations.

Moreover, the second row two plots in ***Figure 6-2***, from the left to the right, are the separate gains by *ABP* input and the separate gains by CO_2 input. The left plot shows that the *ABP*+CO_2 input is the lowest, compared to the other input combinations, in both subject and measurement variability. The 3-inputs shows the highest subject variability but not the measurement variability. The right plot (gain by CO_2) shows different variation patterns where the *ABP*+CO_2 is the lowest in measurement variability but the highest in subject variability whereas the 3-input variations behave the opposite across the two groups.

Additionally, the third row two plots in ***Figure 6-2***, from the left to the right, are the separate gain by *HR* input and the separate phases by *ABP* input. In the left plot, by the *HR* input, the *ABP+HR* variation is the lowest the measurement variability but not in the subject variability whereas the 3-inputs behave the opposite across the 2 groups of variation. However, the right plot presents the phase shift variation levels influenced by *ABP* input shows that the *ABP*+CO_2 input is the highest compared to the other input combinations in both measurement variability and subject variability.

Furthermore, the bottom two plots in ***Figure 6-2***, from the left to the right, are the separate phase by CO_2 input and separate phase by *HR* input. In the left plot, the *ABP*+CO_2 input appears as the lowest in the measurement variability and subject variability. The right plot shows that *ABP+HR* input is the lowest in measurement variability but the opposite in the subject variability. ***Table 6-2*** shows the mean and standard error of MTFA parameters variations of measurement and subject variability in different input combinations across hypercapnia and thigh cuff conditions.

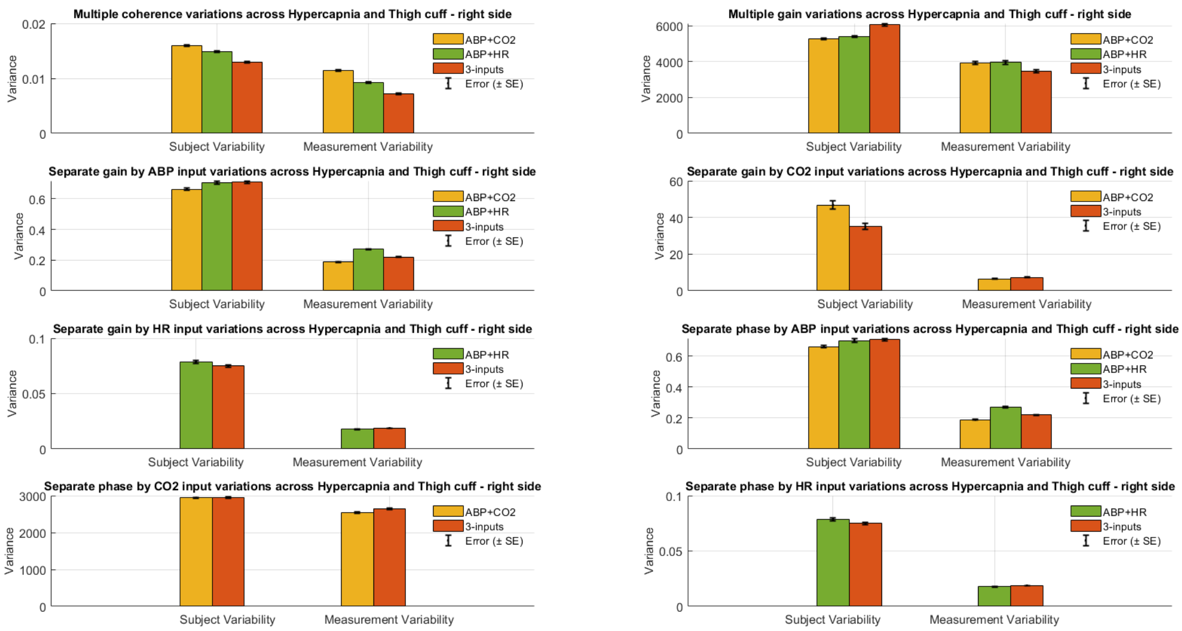

Figure 6-2: MTFA parameters variations of measurement and subject variability in different input combinations across hypercapnia and thigh cuff conditions on the right side

Variation		Subject variability		Measurement variability	
MTFA parameter	**Combination**	**Mean**	**SE (+/-)**	**Mean**	**SE (+/-)**
Multiple coherence	*ABP+CO₂*	0.0159	0.0001	0.0115	0.0001
	ABP+HR	0.0149	0.0001	0.0092	0.0001
	3-inputs	0.0130	0.0001	0.0072	0.0001
Multiple gain	*ABP+CO₂*	5273.5694	33.9457	3934.2426	101.0285
	ABP+HR	5408.8550	50.9894	3956.8598	94.2424
	3-inputs	6071.3216	67.1774	3467.5966	80.3680
Separate gain (by *ABP*)	*ABP+CO₂*	0.6612	0.0077	0.1881	0.0020
	ABP+HR	0.7020	0.0099	0.2704	0.0027
	3-inputs	0.7084	0.0082	0.2203	0.0028
Separate gain (by *CO₂*)	*ABP+CO₂*	46.7936	2.3602	6.5173	0.2726
	3-inputs	35.0226	1.7287	7.3867	0.3422
Separate gain (by *HR*)	*ABP+HR*	0.0787	0.0014	0.0178	0.0002
	3-inputs	0.0749	0.0010	0.0188	0.0002
Separate phase (by *ABP*)	*ABP+CO₂*	308.3996	3.5621	160.0218	1.2215
	ABP+HR	668.9419	5.8148	429.2784	6.3853
	3-inputs	591.2770	3.4355	536.0707	8.9849
Separate phase (by *CO₂*)	*ABP+CO₂*	2944.7255	12.9927	2546.4416	18.4666
	3-inputs	2957.3753	22.2140	2649.4827	19.4379
Separate phase (by *HR*)	*ABP+HR*	2285.2146	13.1844	1694.8350	14.3638
	3-inputs	2579.2255	15.8482	1788.3054	13.6283

Table 6-2: Mean and standard error of MTFA parameters variations of measurement and subject variability in different input combinations across hypercapnia and thigh cuff conditions on the right side

6.3. Testing left side outcomes

This section will present the results of MTFA parameters and covariance analyses on the right side. The results here are comparing MTFA parameters from the hypercapnia versus the cuff conditions. The covariance analysis will plot the variations of each MTFA parameter using different input combinations across hypercapnia and thigh cuff conditions on the left side.

6.3.1. MTFA results

This subsection explains the results of executing the MTFA on the left side of the brain. ***Figure 6-3*** illustrate MTFA parameters across hypercapnia and thigh cuff conditions using both *ABP* and CO_2 inputs on the left side. The left top plot shows the multiple coherence with the combined effect of *ABP* and CO_2 inputs across hypercapnia and thigh cuff conditions on the left side of the brain. In average, the hypercapnia condition appears larger than thigh cuff results where both conditions results behave unequally across the frequency spectrum starting to reach their maximum levels after 0.1 Hz. The top right plot shows the multiple gains for both conditions where it starts higher in the frequency range of 0 – 0.02 Hz then both gains start to drop after 0.15 Hz.

The upper middle left and right plots show the hypercapnia and thigh cuff conditions respectively of separate gains results given by each MTFA input where the blue line is the gain by the *ABP* input, the red line is the gain by the CO_2 input, and the yellow line is the gain by *HR* input. On both conditions, the gain resulting from CO_2 influence seems significantly higher across the frequency spectrum compared to the gain resulted by *ABP* and *HR* influences especially in hypercapnia condition.

The lower middle plots show the hypercapnia and thigh cuff conditions respectively of the normalised separate gains on the right side which demonstrate that gain by CO_2 influence is significantly higher than gain influenced by other inputs across the frequency spectrum in hypercapnia at the right side. In Thigh cuff condition the gain by CO_2 is mostly higher than other gains across the spectrum (gain by *HR* is the lowest) except at the frequency 0.075 Hz the gain by *ABP* rise above other gains then return to be in the middle between gains across the spectrum.

The bottom left and right plots show the hypercapnia and thigh cuff conditions respectively of separate phases results given by each MTFA input where the blue line is the phase by the *ABP* input, the red line is the phase by the CO_2 input, and the yellow line is the phase by *HR* input. Both conditions show that the phase shift resulting from CO_2 influence is significantly higher than the phase resulted from *ABP* influence at 0.1 Hz. But in the thigh cuff condition, the phase by *HR* input appears higher than other inputs after 0.25 Hz. ***Table 6-3*** MTFA parameters mean and standard deviation across hypercapnia and thigh cuff conditions using both *ABP* and CO_2 inputs on the left side.

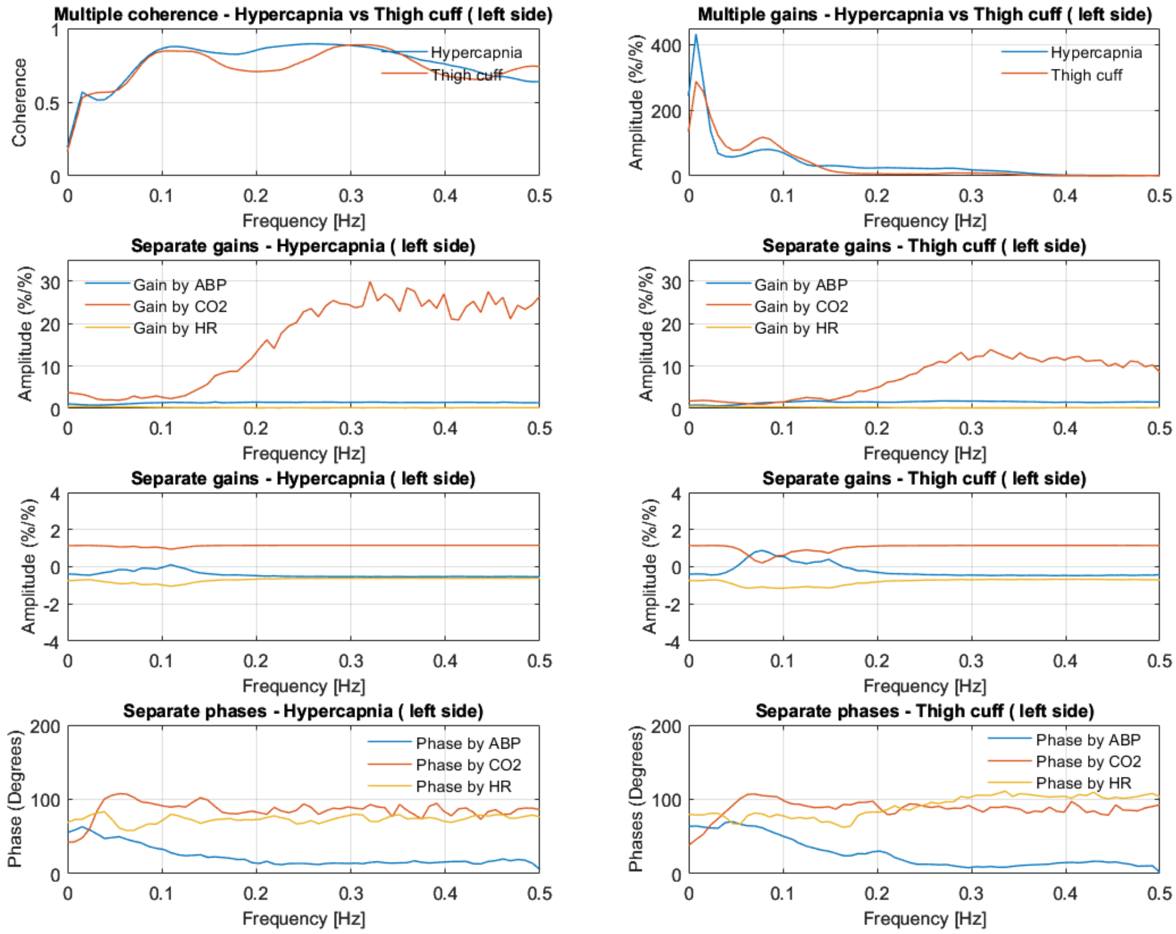

Figure 6-3:MTFA parameters results across hypercapnia and thigh cuff conditions using 3-inputs on the left side

MTFA parameter	Condition	Mean	Std (+/-)
Multiple coherences	Hyper	0.766	0.139
	Thigh	0.733	0.127
Multiple gains	Hyper	40.446	69.744
	Thigh	35.115	59.921
Separate gains (*ABP*)	Hyper	1.347	0.187
	Thigh	15.849	9.939
Separate gains (*CO_2*)	Hyper	0.221	0.091
	Thigh	1.452	0.297
Separate gains (*HR*)	Hyper	7.252	4.553
	Thigh	0.247	0.112
Separate phases (*ABP*)	Hyper	23.304	14.159
	Thigh	85.752	12.301
Separate phases (*CO_2*)	Hyper	73.353	5.130
	Thigh	27.166	20.465
Separate phases (*HR*)	Hyper	87.502	11.887
	Thigh	90.660	14.266

Table 6-3: MTFA parameters mean and standard deviation across hypercapnia and thigh cuff conditions using 3-inputs on the left side

6.3.2. Covariance analysis

Covariance analysis was performed on the resulted MTFA parameters to study the variation levels between measurement variability and subject variability recording across hypercapnia and thigh cuff conditions using different combinations of inputs on the left side. ***Figure 6-4*** shows the analysis results comparing the subject variability with the measurement variability for each MTFA parameter using *ABP*, CO_2, and *HR* inputs. Again, all measurement variability results are significantly smaller than the subject variability ones.

The top two plots, from the left to the right, are the multiple coherence and the multiple gain variations. The multiple coherence in this plot shows that the using 3-inputs in the MTFA is the lowest variability level in both measurement and subject variability recordings compared to the other input combinations whereas the multiple gain behave otherwise and show dissimilar variability across input combinations for both measurement and subject variability. For example, 3-inputs subject variability is the highest (which is similar to the behaviour of the separate gain by *ABP*, gain by *HR*, and separate phases) whereas the 3-inputs measurement variability is the lowest compared to the other input combinations.

Moreover, the second row two plots in ***Figure 6-4***, from the left to the right, are the separate gains by *ABP* input and the separate gains by CO_2 input. The left plot shows that the $ABP+CO_2$ input is the lowest, compared to the other input combinations, in both subject and measurement variability. The 3-inputs is the highest in subject variability but not in the measurement variability. The right plot (gain by CO_2) shows different variation patterns where the $ABP+CO_2$ is the lowest in measurement variability but the highest in subject variability whereas the 3-input variations behave the opposite across the two groups.

Additionally, the third row two plots in ***Figure 6-4***, from the left to the right, are the separate gain by *HR* input and the separate phases by *ABP* input. In the left plot, by the *HR* input, the

ABP+HR variation is the lowest in both measurement and subject variability. However, the right plot presents the phase shift variation levels influenced by *ABP* input shows that the *ABP+CO₂* input is the lowest compared to the other input combinations in both measurement variability and subject variability.

Furthermore, the bottom two plots in ***Figure 6-4***, from the left to the right, are the separate phase by CO_2 input and separate phase by *HR* input. In the left plot, the 3-inputs appears as the lowest in the measurement variability but not in the subject variability. The right plot, *ABP+HR* input is the lowest in both the measurement and the subject variability. ***Table 6-4*** shows the mean and standard error of MTFA parameters variations of measurement and subject variability in different input combinations across hypercapnia and thigh cuff conditions.

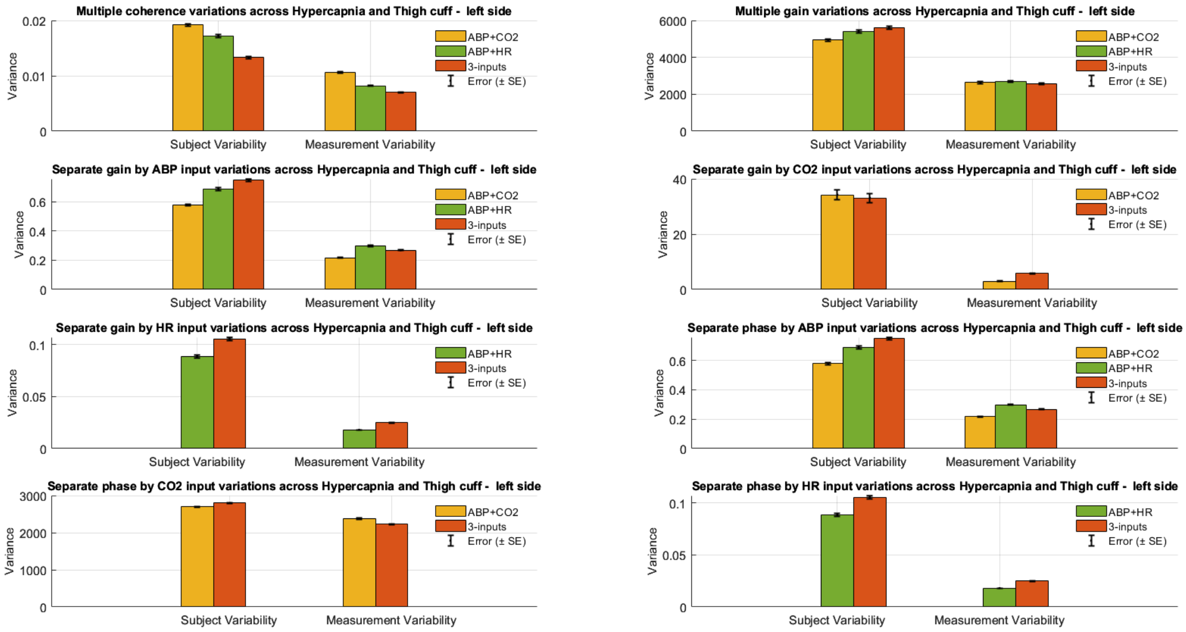

Figure 6-4: MTFA parameters variations of measurement and subject variability in different input combinations across hypercapnia and thigh cuff conditions on the left side

Variation		Subject variability		Measurement variability	
MTFA parameter	**Combination**	**Mean**	**SE (+/-)**	**Mean**	**SE (+/-)**
Multiple coherence	*$ABP+CO_2$*	0.0192	0.0002	0.0106	0.0001
	$ABP+HR$	0.0172	0.0002	0.0082	0.0001
	3-inputs	0.0133	0.0002	0.007	0.0001
Multiple gain	*$ABP+CO_2$*	4933.8684	55.3146	2633.3576	44.7467
	$ABP+HR$	5393.7124	73.2080	2703.9349	45.0755
	3-inputs	5605.3735	74.3354	2559.465	47.0628
Separate gain (by *ABP*)	*$ABP+CO_2$*	0.5786	0.0062	0.2176	0.0021
	$ABP+HR$	0.6887	0.0088	0.2987	0.0029
	3-inputs	0.7496	0.0086	0.2676	0.0025
Separate gain (by *CO_2*)	*$ABP+CO_2$*	34.2338	1.7107	2.9654	0.1165
	3-inputs	33.1201	1.6390	5.7602	0.2587
Separate gain (by *HR*)	*$ABP+HR$*	0.0887	0.0012	0.018	0.0001
	3-inputs	0.1056	0.0017	0.0249	0.0003
Separate phase (by *ABP*)	*$ABP+CO_2$*	292.633	2.5391	169.7855	2.0524
	$ABP+HR$	558.6303	8.0212	319.5025	5.5064
	3-inputs	560.7775	6.6176	426.8056	7.4611
Separate phase (by *CO_2*)	*$ABP+CO_2$*	2697.7692	13.8314	2371.1159	18.8065
	3-inputs	2802.6386	12.5294	2228.518	13.8380
Separate phase (by *HR*)	*$ABP+HR$*	2215.7297	17.5213	1669.2472	10.0155
	3-inputs	2383.7171	14.0951	1849.0014	12.9670

Table 6-4: Means and standard error MTFA parameters variations of measurement and subject variability in different input combinations across hypercapnia and thigh cuff conditions on the left side

6.4. Testing the average of both sides' outcomes

This section will present the results of MTFA parameters and covariance analyses on the right side. The results here are comparing MTFA parameters from the hypercapnia versus the cuff conditions. The covariance analysis will plot the variations of each MTFA parameter using different input combinations across hypercapnia and thigh cuff conditions on the average of both sides.

6.4.1. MTFA results

This subsection explains the results of executing the MTFA on the average of both sides of the brain. ***Figure 6-5*** illustrates MTFA parameters across hypercapnia and thigh cuff conditions using both *ABP* and CO_2 inputs on the average of both sides. The left top plot shows the multiple coherence with the combined effect of *ABP* and CO_2 inputs across hypercapnia and thigh cuff conditions on the average. Overall, the hypercapnia condition appears larger than thigh cuff results where both conditions results behave unequally across the frequency spectrum starting to reach their maximum levels after 0.1 Hz. The top right plot shows the multiple gains for both conditions where it starts higher in the frequency range of 0 – 0.02 Hz then both gains start to drop after 0.15 Hz.

The upper middle left and middle right plots show the hypercapnia and thigh cuff conditions respectively of separate gains results given by each MTFA input where the blue line is the gain by the *ABP* input, the red line is the gain by the CO_2 input, and the yellow line is the gain by *HR* input. On both plots, the gain resulting from CO_2 influence seems significantly higher across the frequency spectrum compared to the gain resulted by *ABP* influence.

The lower middle plots show the hypercapnia and thigh cuff conditions respectively of the normalised separate gains on the right side which demonstrate that gain by CO_2 influence is significantly higher than gain influenced by other inputs across the frequency spectrum in hypercapnia at the right side. In Thigh cuff condition the gain by CO_2 is mostly higher than other gains across the spectrum (gain by *HR* is the lowest) except at the frequency 0.075 Hz, the gain by *ABP* rise above other gains then return to be in the middle between gains across the spectrum.

The bottom left and right plots show the hypercapnia and thigh cuff conditions respectively of separate phases results given by each MTFA input where the blue line is the phase by the *ABP* input, the red line is the phase by the CO_2 input, and the yellow line is the phase by *HR* input. Both plots show that the phase shift resulting from CO_2 influence is significantly higher than the phase resulted from *ABP* influence at 0.1 Hz. But in the thigh cuff condition, the phase by *HR* input increase above the phase by CO_2 input after 0.25 Hz. ***Table 6-5*** MTFA parameters mean and standard deviation across hypercapnia and thigh cuff conditions using both *ABP* and CO_2 inputs on the average of both sides.

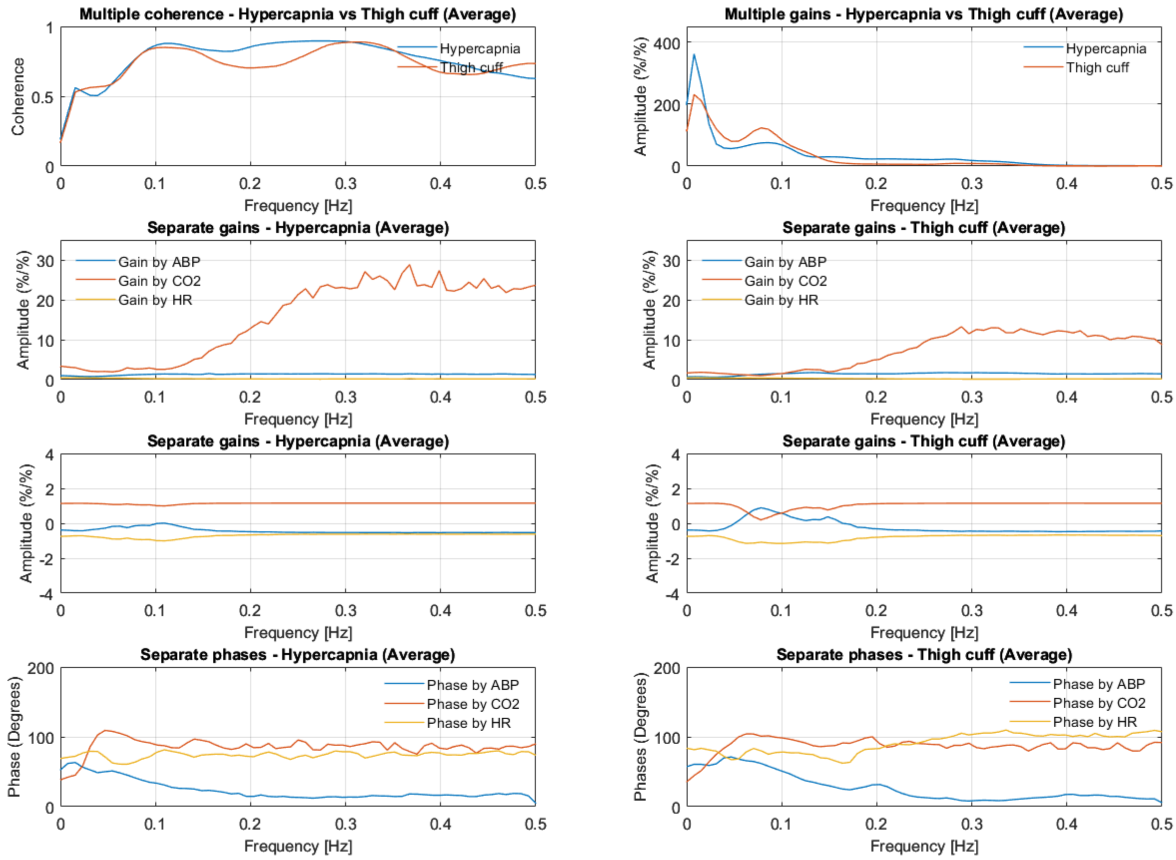

Figure 6-5: MTFA parameters results across hypercapnia and thigh cuff conditions using 3-inputs of both sides average

MTFA parameter	Condition	Mean	Std (+/-)
Multiple coherences	Hyper	0.764	0.142
	Thigh	0.730	0.127
Multiple gains	Hyper	37.392	60.151
	Thigh	33.233	52.913
Separate gains (*ABP*)	Hyper	1.319	0.184
	Thigh	15.293	9.485
Separate gains (CO_2)	Hyper	0.221	0.093
	Thigh	1.433	0.300
Separate gains (*HR*)	Hyper	7.224	4.534
	Thigh	0.246	0.104
Separate phases (*ABP*)	Hyper	23.784	14.230
	Thigh	85.769	12.348
Separate phases (CO_2)	Hyper	74.084	4.434
	Thigh	27.446	20.115
Separate phases (*HR*)	Hyper	86.863	11.807
	Thigh	90.619	13.934

Table 6-5: Means and standard deviations of MTFA parameters results across hypercapnia and thigh cuff conditions using *3*-inputs of both sides average

6.4.2. Covariance analysis

Covariance analysis was performed on the resulted MTFA parameters to study the variation levels between measurement variability and subject variability recordings across the hypercapnia and thigh cuff conditions using different combinations of inputs on both sides' average. ***Figure 6-6*** shows the analysis results comparing the subject variability with the measurement variability for each MTFA parameter using *ABP*, CO_2, and *HR* inputs. Overall, all measurement variability results are significantly smaller than the subject variability ones.

The top two plots, from the left to the right, are the multiple coherence and the multiple gain variations. The multiple coherence in this plot shows that the using 3-inputs in the MTFA is the lowest variability level in both measurement and subject variability recordings compared to the other input combinations whereas the multiple gain behave otherwise and show dissimilar variability across input combinations for both measurement and subject variability. For example, 3-inputs subject variability is the highest (which is similar to the behaviour of the separate gain by *ABP*, gain by *HR*, and separate phases by *ABP* and *HR* inputs) whereas the 3-inputs measurement variability is the lowest compared to the other input combinations.

Moreover, the second row two plots in ***Figure 6-6***, from the left to the right, are the separate gains by *ABP* input and the separate gains by CO_2 input. The left plot shows that the *ABP*+CO_2 input is the lowest, compared to the other input combinations, in both subject and measurement variability. The 3-inputs is the highest in subject variability but not in the measurement variability. The right plot (gain by CO_2) shows different variation patterns where the *ABP*+CO_2 is the lowest in measurement variability but the highest in subject variability whereas the 3-input variations behave the opposite across the two groups.

Additionally, the third row two plots in ***Figure 6-6***, from the left to the right, are the separate gain by *HR* input and the separate phase by *ABP* input. In the left plot, by the *HR* input, the

ABP+HR variation is the lowest in both measurement and subject variability. However, the right plot presents the phase shift variation levels influenced by *ABP* input shows that the *ABP+*CO_2 input is the lowest compared to the other input combinations in both measurement variability and subject variability.

Furthermore, the bottom two plots in ***Figure 6-6***, from the left to the right, are the separate phase by CO_2 input and separate phase by *HR* input. In the left plot, the 3-inputs appears as the lowest in the measurement variability but not in the subject variability. The right plot, *ABP+HR* input is the lowest in both the measurement and the subject variability. ***Table 6-6*** shows the mean and standard error of MTFA parameters variations of measurement and subject variability in different input combinations across hypercapnia and thigh cuff conditions.

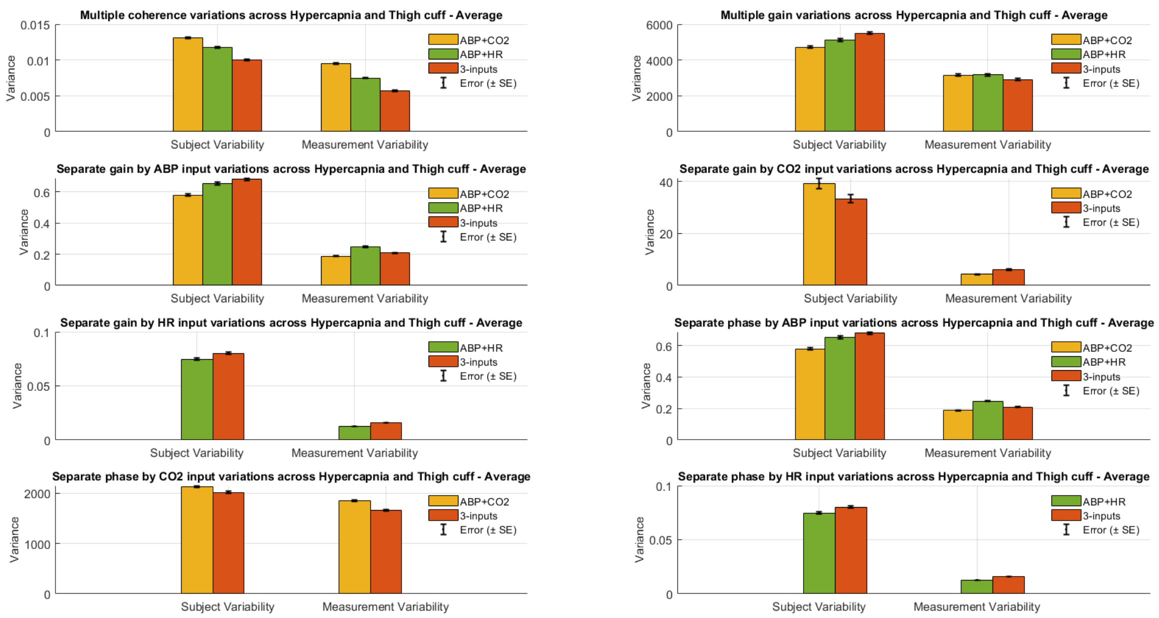

Figure 6-6: MTFA parameters variations of measurement and subject variability in different input combinations across hypercapnia and thigh cuff conditions on both sides' average

Variation		Subject variability		Measurement variability	
MTFA parameter	Combination	Mean	SE (+/-)	Mean	SE (+/-)
Multiple coherence	*ABP+CO2*	0.0131	0.0001	0.0095	0.0001
	ABP+HR	0.0118	0.0001	0.0075	0.0001
	3-inputs	0.01	0.0001	0.0057	0.0001
Multiple gain	*ABP+CO2*	4722.2	50.6823	3152.6736	66.4969
	ABP+HR	5114.5335	69.2857	3176.9199	66.6780
	3-inputs	5501.989	69.2536	2910.5685	64.4417
Separate gain (by *ABP*)	*ABP+CO2*	0.5792	0.0066	0.1877	0.0020
	ABP+HR	0.6538	0.0091	0.247	0.0027
	3-inputs	0.6792	0.0083	0.2085	0.0024
Separate gain (by *CO2*)	*ABP+CO2*	39.3333	1.9881	4.2948	0.1809
	3-inputs	33.3802	1.6682	6.1633	0.2819
Separate gain (by *HR*)	*ABP+HR*	0.0747	0.0011	0.0127	0.0001
	3-inputs	0.0802	0.0012	0.0159	0.0002
Separate phase (by *ABP*)	*ABP+CO2*	283.7477	3.0478	143.2847	1.2277
	ABP+HR	506.6721	6.2142	259.3245	3.2475
	3-inputs	509.6186	6.4292	337.6024	4.1010
Separate phase (by *CO2*)	*ABP+CO2*	2132.5855	19.1799	1855.9262	15.5572
	3-inputs	2019.813	16.2551	1662.2346	8.5922
Separate phase (by *HR*)	*ABP+HR*	1465.487	11.1536	1261.6306	9.6703
	3-inputs	1559.8928	10.5284	1399.6881	8.7613

Table 6-6: Means and standard error of MTFA parameters variations of measurement and subject variability in different input combinations across hypercapnia and thigh cuff conditions on both sides' average

6.5. Autoregulatory parameters significance

In this section, significance analysis was performed by running paired t-test using the Bonferroni correction technique to compute p-values for each MTFA parameter among different conditions (normocapnia, hypercapnia, and thigh cuff) to study each parameter's dependency on the condition or physiological challenge for both sides and their average. Since several p-values will be computed in this analysis, the Bonferroni correction method has been selected to minimise potential error in p-values results.

Nevertheless, a paired t-test has been conducted to compare each MTFA parameter's p-values with the same parameter in other conditions. ***Figure 6-7*** shows 4 by 4 bar graphs for each MTFA parameter mean value using 3-inputs topped with super bars (blue, red, and pink horizontal lines) comparing p-values among conditions. Each horizontal line shows the p-value in form of significance which is either not significant (blank, $p > 0.05$), one star (*, $p < 0.05$), two stars (**, $p < 0.01$), three stars (***, $p < 0.001$), or four stars (****, $p < 0.0001$).

The top and bottom left plots shows the 8 MTFA parameters for both left (blue axis) and right (red axis) sides indicating the significance results of each side that matches the axis colour. The top left plot has 4 parameters (multiple coherence, gain by *ABP*, gain by CO_2, and gain by *HR*) and the bottom left has the remaining 4 parameters (multiple gain, phase by *ABP*, phase by CO_2, phase by *HR*). The top and bottom right plots shows the 8 MTFA parameters for the average of both sides indicating the significance results of each side in pink super bars.

Obviously, the top left and right plots (each side and their average) shows that there is no significant association between 4 of the MTFA parameters (multiple coherence and separate gains by all inputs) and different conditions in each side. However, the remaining MTFA parameters on both sides and their average behave differently. The multiple gain shows significant association, $p < 0.0001$ between normocapnia and hypercapnia on the left side and significant association, $p < 0.01$ on the right side. Also, there is a significant association between hypercapnia and thigh cuff, $p < 0.001$ on the right side but there is no significant association on the left side.

Moreover, the phase by *ABP* input shows significant association across conditions with $p < 0.001$ for the left side and $p < 0.01$ for the right side. The phase by CO_2 input shows significant association between normocapnia and hypercapnia on the left side, $p < 0.05$ but there is no significant association between hypercapnia and thigh cuff. The right side for phase by CO_2 shows equal significant associations across different conditions on the right side, $p < 0.01$. in phase by *HR* input there is a significant association between normocapnia and hypercapnia on both sides, $p < 0.0001$ but there is no significant association between hypercapnia and thigh cuff conditions.

For the top and bottom right plots (average), the multiple coherence and separate gains by all inputs shows no significant association across different conditions. However, in multiple gain, there is a significant association between normocapnia and hypercapnia, $p < 0.0001$, and significant association between hypercapnia and thigh cuff, $p < 0.01$. In phase by *ABP* input, there is a significant association between parameter and different conditions, $p < 0.001$. In phase by CO_2 input, there is a significant association between normocapnia and hypercapnia, $p < 0.01$ and a lower significant association between hypercapnia and thigh cuff, $p < 0.05$. In phase by *HR* input there is a significant association between normocapnia and hypercapnia, $p < 0.0001$ but there is no significant association between hypercapnia and thigh cuff conditions. ***Table 6-7*** lists p-values resulted from the significance analysis of each MTFA parameter across different conditions on the left, right, and average of both sides.

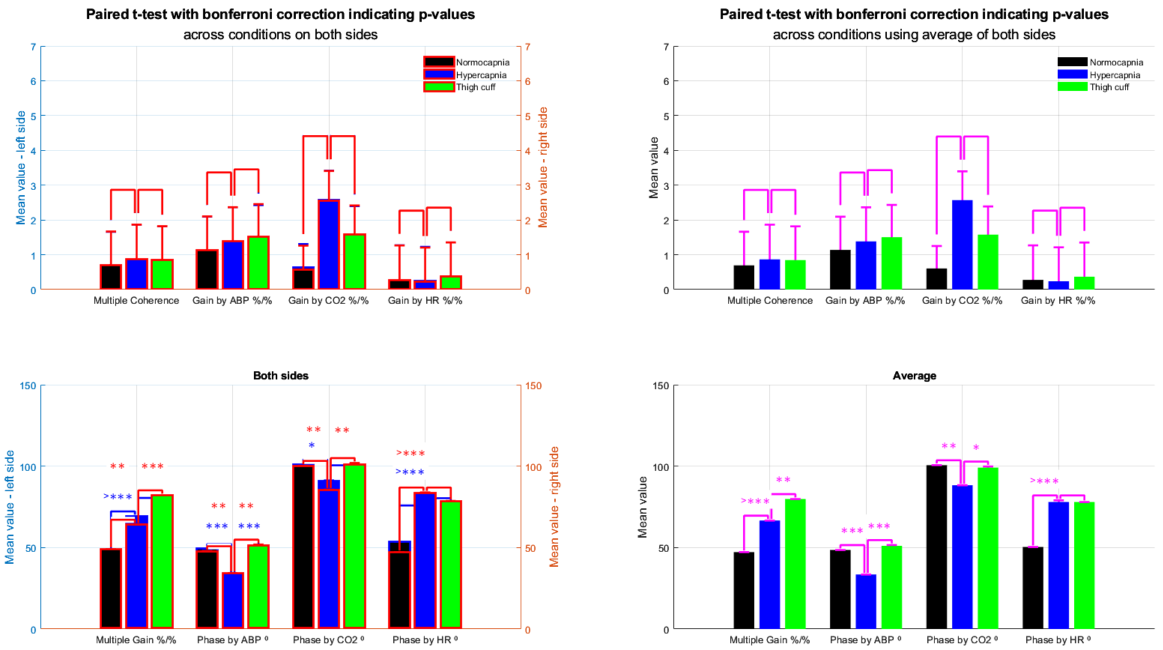

Figure 6-7: Paired t-test analysis with Bonferroni correction to compare p-values of each MTFA parameter across different conditions on both left (blue) and right (red) sides (left plot) and on the average of both sides (right plot). Blank means no significance, * means p-value is < 0.05, ** < 0.01, *** < 0.001, and **** is < 0.0001)

MTFA parameter		Multiple Coherence	Multiple Gain	Gain by *ABP*	Gain by CO_2	Gain by *HR*	Phase by *ABP*	Phase by CO_2	Phase by *HR*
P-value left	Norm vs Hyper	0.9698	<0.0001	0.9581	0.675	0.9945	0.0003	0.0316	<0.0001
	Hyper vs Thigh	0.9969	0.0891	0.9823	0.838	0.98	0.0003	0.2139	0.3303
	Thigh vs Norm	0.9706	<0.0001	0.9337	0.8247	0.9828	0.7426	0.3625	<0.0001
P-value average	Norm vs Hyper	0.9673	<0.0001	0.9541	0.6442	0.9925	0.0004	0.0037	<0.0001
	Hyper vs Thigh	0.9962	0.0039	0.979	0.8288	0.9767	0.0001	0.018	0.9932
	Thigh vs Norm	0.9698	<0.0001	0.9278	0.8091	0.9815	0.5318	0.7094	<0.0001
P-value right	Norm vs Hyper	0.9714	0.0019	0.9595	0.6813	0.9921	0.0053	0.0023	<0.0001
	Hyper vs Thigh	0.9964	0.0005	0.9798	0.852	0.9781	0.0011	0.0029	0.3486
	Thigh vs Norm	0.9746	<0.0001	0.9358	0.8298	0.9837	0.4362	0.8531	<0.0001

Table 6-7:P-values resulted from the significance analysis of each MTFA parameter across different conditions on the left, right, and average of both sides

6.6. Discussion

Most previous studies have investigated MTFA results on both the right and left sides measurements under different physiological challenges [4,45,55,59,61,68,90] and most of their conclusions support the use of multivariate analysis when studying dCA to improve MTFA parameters results. However, no previous study compared MTFA parameters results from each side separately [4,45,55,59,61,68,90]. One previous study did compare the results of their assessment to a few cerebral haemodynamics parameters in the time-domain only [94]. This study provided a comparison of both the left and the right sides and assessed the correlation of both the Mean Velocity Index (Mx) and the Cerebral Oximetry Index (COx) using the average of both the right and left sides [94].

In contrast with previous research work, examining MTFA parameters' behaviour on each side separately provided an overview of what to expect when performing MTFA on healthy participants. The results of each side analysis appear very close (almost alike) in terms of MTFA parameters, covariance, and significance analyses. Since the previous chapter plotted the results of the right side against the left side across different conditions, this chapter plotted the MTFA results, covariance, and significance analyses of the hypercapnia conditions against the thigh cuff condition across different combinations of inputs on the right side, left side, and the average of both sides.

This study displayed MTFA parameters using *ABP*+CO_2 inputs plotting hypercapnia results against the thigh cuff condition on the right side. The covariance analysis was performed to calculate the variances of each MTFA parameter across all combinations of inputs resulting from the hypercapnia and the thigh cuff conditions. The same analyses were also applied to the left side results and the average of both sides' results. Then, significance analysis was performed using a paired t-test to calculate p values and measure the association between each MTFA parameter with each condition in the three cases (right side, left side, and average of both).

On the right side, this study demonstrated the output of MTFA parameters using a combination of *ABP*+CO_2 input across hypercapnia and thigh cuff conditions. Then, a covariance analysis has been performed to calculate the variances of each MTFA parameter using different combinations of inputs (*ABP*+CO_2, *ABP*+*HR*, and *ABP*+CO_2+*HR* as 3-inputs) presenting the hypercapnia condition on the left plots and the thigh cuff conditions in the right plots. The mean value of multiple coherence resulting from the influence of *ABP*+CO_2 inputs in the hypercapnia condition is significantly higher than the thigh cuff condition (hypercapnia: 0703 ±16, thigh cuff: 0668 ±14). However, the mean values of separate gains and phases resulting from the CO_2 input are significantly higher than results from *ABP* input in both hypercapnia and thigh cuff conditions.

Covariance analysis at the right side shows that multiple coherence in both measurement and subject variabilities presents the lowest variance compared to other combinations of inputs across hypercapnia and thigh cuff conditions. Also, the separate phases by *HR* input show that using 3-inputs presents significantly lower variances in both measurement and subject variabilities than using *ABP+HR* inputs across hypercapnia and thigh cuff conditions.

On the left side, this study demonstrated the output of MTFA parameters using a combination of *ABP+*CO_2 input across hypercapnia and thigh cuff conditions. Then, a covariance analysis has been performed to calculate the variances of each MTFA parameter using different combinations of inputs (*ABP+*CO_2, *ABP+HR*, and *ABP+*CO_2*+HR* as 3-inputs) presenting the hypercapnia condition on the left plots and the thigh cuff conditions in the right plots. The mean value of multiple coherence resulting from the influence of *ABP+*CO_2 inputs in the hypercapnia condition is significantly higher than the thigh cuff condition (hypercapnia: 0711 ±15, thigh cuff: 0676 ±14). However, the mean values of separate gains and phases resulting from the CO_2 input are significantly higher than results from *ABP* input in both hypercapnia and thigh cuff conditions.

Covariance analysis at the left side shows that multiple coherence in both measurement and subject variabilities presents the lowest variance compared to other combinations of inputs across hypercapnia and thigh cuff conditions. Also, the separate phases by *HR* input show that using *ABP+HR* inputs present significantly lower variances in both measurement and subject variabilities than using 3-inputs across hypercapnia and thigh cuff conditions.

Using the average of both sides, this study demonstrated the output of MTFA parameters using a combination of *ABP+*CO_2 input across hypercapnia and thigh cuff conditions. Then, a covariance analysis has been performed to calculate the variances of each MTFA parameter using different combinations of inputs (*ABP+*CO_2, *ABP+HR*, and *ABP+*CO_2*+HR* as 3-inputs) presenting the hypercapnia condition on the left plots and the thigh cuff conditions in the right plots. The mean value of multiple coherence resulting from the influence of *ABP+*CO_2 inputs in the hypercapnia condition is significantly higher than the thigh cuff condition (hypercapnia:

0707 ±16, thigh cuff: 0672 ±14). However, the mean values of separate gains and phases resulting from the CO_2 input are significantly higher than results from *ABP* input in both hypercapnia and thigh cuff conditions.

Covariance analysis of the average of both sides shows that multiple coherence in both measurement and subject variabilities presents the lowest variance compared to other combinations of inputs across hypercapnia and thigh cuff conditions. Again, the separate phases by *HR* input show that using *ABP+HR* inputs present significantly lower variances in both measurement and subject variabilities than using 3-inputs across hypercapnia and thigh cuff conditions.

Finally, the significance analysis is shown in ***Figure 6-7*** where both the right and left sides results are illustrated on the left side plots and the average of both sides on the right side plots. The top plots are shows multiple coherence and separate gains by each MTFA input with no significant association between different conditions and those parameters. Conversely, both lower plots show the multiple gain and separate phases by each MTFA input with significant associations between different conditions and those parameters except for phase by *HR* input that shows no significant association between hypercapnia and thigh cuff.

A previous study applied UTFA on right-handed healthy subjects to compare coherences and spectral power distributions of both sides (right and left) separately [95] but this study applied MTFA on each side and their average separately to compare between parameters resulted from each case (right, left, and average). However, the absence of significant association of phase by *HR* input between hypercapnia and thigh cuff conditions could be due to the steady variance of phase by *HR* input (variance of *ABP+HR* inputs is lower than 3-inputs) in both left side and average.

Despite the detailed work made on each side and their average in separate approaches but the analyses performed in this chapter are limited to comparing the results across hypercapnia and thigh cuff conditions. Also, multiple coherence results show the combined influences of all inputs whereas some studies present the partial coherence results to show the coherence output influenced by each input to the MTFA [92 93].

From this chapter it may be concluded that both right and left sides' results are significantly close (in some cases they are alike) and therefore using the average of both sides could well be beneficial for future work. ***Table 6-8*** show a comparison of both left and right sides MTFA parameters means and standard deviations across hypercapnia and thigh cuff conditions using both *ABP* and CO_2 inputs. For example, hypercapnia multiple coherence has a mean difference of 0.008 (±0.008) between both left and right sides.

		Left side		**Right side**	
MTFA parameter	**Condition**	**Mean**	**Std (+/-)**	**Mean**	**Std (+/-)**
Multiple coherences	Hyper	0.766	0.139	0.762	0.145
	Thigh	0.733	0.127	0.728	0.127
Multiple gains	Hyper	40.446	69.744	34.339	51.011
	Thigh	35.115	59.921	31.351	47.008
Separate gains (*ABP*)	Hyper	1.347	0.187	1.290	0.184
	Thigh	15.849	9.939	14.738	9.103
Separate gains (CO_2)	Hyper	0.221	0.091	0.222	0.096
	Thigh	1.452	0.297	1.415	0.306
Separate gains (*HR*)	Hyper	7.252	4.553	7.196	4.527
	Thigh	0.247	0.112	0.245	0.099
Separate phases (*ABP*)	Hyper	23.304	14.159	24.264	14.391
	Thigh	85.752	12.301	85.787	13.109
Separate phases (CO_2)	Hyper	73.353	5.130	74.816	4.766
	Thigh	27.166	20.465	27.725	19.853
Separate phases (*HR*)	Hyper	87.502	11.887	86.224	12.258
	Thigh	90.660	14.266	90.578	13.940

Table 6-8: Comparing both left and right sides MTFA parameters means and standard deviations across hypercapnia and thigh cuff conditions using 3-inputs

6.7. Conclusion

This chapter tested the results from MTFA parameters on each side and their average separately. First, right side was tested, presented MTFA parameters results, and performed covariance analysis. Secondly, left side was tested, presented MTFA parameters results, and performed covariance analysis. Then, the average of both sides (right and left) was tested, presented MTFA parameters, and performed covariance analysis. Finally, the autoregulatory parameters significance analysis was presented to examine the MTFA parameters behaviour in each side (right and left) and their average across different conditions.

7. Conclusion

7.1. Introduction

This chapter will conclude this report, describe future work and limitations of this study. The summary section will wind up the study and summarize the major findings. The future work section will describe upcoming research activities towards the title of this report. Finally, limitations of the study will describe this work boundaries and limits points that were not considered in this work for future researchers to consider in their investigation.

7.2. Summary

This study applied the UTFA technique to examine the nonstationary behaviour of dCA. This was achieved by using *ABP* as the input and examining the output (*CBv*) response under different physiological challenges (normocapnia, hypercapnia and thigh cuff) which is considered a univariate method of UTFA. Then, UTFA parameters (coherence, gain and phase) were analysed for each subject's visit at 3 conventional frequency bands which are HF, LF and VLF bands. Nonetheless, reproducibility analysis was applied by calculating the ICC values of each and overall participating subjects using UTFA parameters results for each visit. Also, covariance analysis highlighted the variability of UTFA outputs of measurement and subject variabilities among different physiological challenges at all frequency bands.

In brief, UTFA parameters at the LF bands show the best grouping form around the reference line among the right and left sides of the brain compared to the HF and VLF bands (***Figure 4-3***, ***Figure 4-4***, and ***Figure 4-5***). Also, these 3 figures show that the thigh cuff condition exhibits the best formation and encirclement around the reference line among all UTFA parameters at the LF frequency band. However, since it is known that blood gas levels affect autoregulation at low frequencies, the starting point for future work will be applying the multivariate analysis method by including CO_2 as an input along with *ABP*.

Besides, there is clear variability in outputs among different physiological challenges. The thigh cuff condition shows the lowest variability levels compared to normocapnia and hypercapnia conditions as shown in ***Figure 4-6*** This also means that variability reaches higher levels in hypercapnia condition and even higher levels at normocapnia in some frequency bands. Though, considering that the thigh cuff is a physiological challenge that could be greater than hypercapnia, future work is needed to understand the low variability levels in thigh cuff condition which is also essential in examining the nonstationary behaviour of dCA.

Until now, this research explored *CBv* outputs (MTFA parameters) behaviour under different physiological challenges at the frequency spectrum (0 – 0.5 Hz) focusing on the 0.1 Hz results under different conditions with additional focus on the thigh cuff condition. The results *CBv* parameters using MTFA displayed different behaviour and increased values among all inputs. For example, ***Figure 5-23*** demonstrate how coherence outputs increased as more inputs are added to the TFA were the lowest was in the univariate results and the highest appeared in the 3-inputs MTFA. As well, reproducibility analysis presented higher ICC values as shown in ***Figure 5-25*** and ***Table 5-24*** compared to the univariate analysis results. This study recommends the use of CO_2 and *HR* as additional inputs in transfer function analysis.

In summary, from reproducibility findings in UTFA, the results support further investigations focusing on LF and thigh cuff condition (ICC = 0.53). From the reproducibility findings in MTFA, the results suggest further exploration of MTFA using 3-inputs under the thigh cuff condition (ICC = 0.60) and further investigation of using 3-inputs under the normocapnia condition (ICC = 0.62). Moreover, further investigation is suggested to understand the persistent higher moderate reliability found in $ABP+CO_2$ input in normocapnia (ICC = 0.68), hypercapnia (ICC = 0.51), and thigh cuff (ICC = 0.62) than *ABP+HR* input which are poorly reliable (ICC < 0.5) except in the thigh cuff condition (ICC = 0.57). it worth noting that according to a reliability testing guideline that were developed earlier by a study suggested that

ICC values less than 0.4 represents poor reliability where ICC values between 0.4 – 0.59 represents fair reliability, and values between 0.6 and 0.74 represents good reliability [96].

However, coherence results were improved using 3-inputs MTFA compared to the 2-inputs MTFA and to univariate analysis. Moreover, the ICC results showed better reproducibility levels in the MTFA compared with the univariate analysis results. Whereas the covariance analysis showed alike variability levels to the univariate results but using 3-inputs MTFA has lower the variability levels in the results. For the significance analysis, the results show that Multiple gain and Gain by *ABP* parameters have no significant association with different conditions, but Multiple gain showed the lowest p-values among all MTFA results using different combinations of inputs. Other parameters showed significant associations with different conditions that varies in p-values using different combinations of inputs to the MTFA.

Obviously, adding *HR* input to the MTFA (3-inputs) has increased the coherence and separate phase outputs across the frequency spectrum compared to the 2-inputs results, especially in thigh cuff condition. Also, adding *HR* as a second input has significantly increased the coherence compared to adding CO_2 as the second input. As well, adding *HR* input has increased ICC results compared to the univariate analysis but there is no significance association between adding *HR* input with different conditions.

It's worth noting that this thesis compared univariate TFA with adding *HR* as additional input using multivariate TFA which demonstrate different results and dissimilar comparison from the work done by different study that compared univariate TFA results with nonlinear ARMA model results [11]. Also, the conclusion in this thesis is comparable with the results from previous study used PDM (nonlinear model) to analyse *HR* as a third input [12].

Moreover, the thesis examined each side (right and left) measurements and their average separately across hypercapnia and thigh cuff conditions. First, right side MTFA parameters and covariance analysis were examined. Then, examined left side MTFA parameters and covariance analysis. Both sides were examined separately testing MTFA parameters results across hypercapnia and thigh cuff conditions. Also, in covariance analysis, each side variations of measurement and subject variability were calculated using different input combinations across hypercapnia and thigh cuff conditions.

Furthermore, the average of both sides was used to examine MTFA parameter outputs in ***Figure 6-5*** and calculate the variation of measurement and subject variability as shown in ***Figure 6-6***. In all cases (right, left, and average) multiple coherence variations appeared at the lowest levels in both measurement and subject variabilities when using 3-inputs in the MTFA. Other MTFA parameters varies in their variations across different combinations of inputs but, in general, all cases demonstrate similar variations of the remaining parameters.

In addition, significance analysis was performed on MTFA parameters for right side, left side, and their average to compare p-values of each MTFA parameter across different conditions as shown in ***Figure 6-7***. The results show significant similarity between right and left sides as well as their average in their mean values and p values results which could be beneficial for future researcher when studying dCA on healthy subjects.

7.3. Study limitations

This subsection will describe the potential limitations of this study. A major limitation is the assumption that dCA is a linear system despite the nonlinear behaviour of this mechanism [4]. Additional limitation is that one of the problems when computing ICC, especially when the mean value decreases, ICC appear to be larger which is a biased manner to compare among different conditions. A study suggested that the F-test could be used to examine the presence of biases in ICC analysis [97].

Similarly, it is worth highlighting a limitation of this study's method is that non-invasive blood pressure measurement is a less accurate measurement of a subject's haemodynamics [98] despite its accuracy in detecting blood flow and volume displacement which is a more accurate approach in measuring the pressure causing the flow [99]. The actual differences between invasive and non-invasive measurements could be argued to the complex nature of haemodynamics behaviour [100]. Both invasive and non-invasive measurements could be used for dCA estimation and both methods will lead to comparable results, but the invasive method is still preferable for patients with critical conditions [101].

Besides, using the thigh cuff across participants, in both univariate and multivariate analyses, appears to increase the variability and spread out the results of subject variability. Moreover, this study assumed that all participants are normally distributed, the noise and artefacts associated with recorded signals are assumed absent (noise-free recordings). It's worth noting that noise level associated with recordings could results into different dCA outputs [90].

On the other hand, the univariate analysis focused on presenting UTFA parameters of all subjects at LF band (≈ 0.1 Hz). Previous studies investigated TFA parameters VLF and LF bands and discussed the correlation between the two bands in both univariate and multivariate scales [78 102 103]. Although, the results in this research demonstrate different behaviour of UTFA parameters in the VLF, LF and HF bands but a correlation between UTFA parameters in different frequency bands were not performed.

On the multivariate analysis, the results of MTFA parameters, ICC analyses, covariance and significance analyses were focused on presenting the results at 0.1 Hz (where multiple coherence start reaching high levels) but there are, sometimes, other higher frequencies that reach same or acceptable levels that were not included in this research. Additionally, there are other input variables not included in this thesis that could be included in the MTFA (such as

ICP and temperature) which was recommended by other studies to include in future multivariate analysis [4 55].

A further limitation of this study is the absence of squat-stand manoeuvres (SSM) which has been suggested to be a noninvasively effective approach in assessing dCA [104] but performing SSM during hypercapnia condition could be potentially harmful for participating subjects and further caution should be exercised [91]. The repeated SSM method has been shown to shed light on the importance of considering the changes of *ABP* direction (changes of directional blood pressure) and on the excellent ICC results from reproducibility analysis [105]. A study found that dCA assessment depends on the *ABP* change direction and further studies are required to confirm their findings [106]. SSM protocol enables the assessment of dCA at low frequencies, especially when using thigh cuff technique to induce rapid changes in *ABP* [107].

It's worth noting that CO_2 is sampled/recorded during breathing/respiration process and the limit for CO_2 Nyquist sampling frequency is around 0.1 Hz. Chest movement during respiration is happening during the sampling process but this movement is not likely changing the sampling results. It has been found that most fluctuations in CO_2 signal fall in the range of 0 – 0.1 Hz, respiration signals in the range of 0.1 – 0.3 Hz, and HR between 0.5 – 2 Hz. This shows that CO_2 analysis above 0.1 Hz is interfered by the fluctuations in the respiration signals. This means that CO_2 analysis in the frequency domain is challenged to understand where signal aliasing is expected in this case [108].

7.4. Future work

Forthcoming research in quantifying dCA variability and examining the nonstationary behaviour of dCA should be based on expanding the analysis techniques used and expanding the datasets analysed. Since dCA is a complex mechanism that is associated with several variable factors, multivariate analysis is recommended by several studies in the field [1 3 4].

Particularly, a study examined the nonstationary behaviour of dCA which suggest that developing and validating a multivariate time-varying method is a key priority for future research. The study suggested that multivariate analysis should reduce the effect of many co-variates contributing to the nonstationary behaviour of dCA [4].

However, although dCA behaviour is not yet fully understood, understanding the nonstationary behaviour of dCA is essential in this work and would be a very significant starting point in analysing dCA in diseased conditions [3]. There are confounding issues associated with the topic such as signal noise, artefact, and other influences (such as CO_2) as well as the variability of recordings across participating subjects [4]. This would make the work challenging but a need for further research to tackle them one by one to quantify the variability found from the analysis. Then, this should answer both questions, how much variability resulted from the nonstationary behaviour and how much is due to other sources.

This research has studied *CBv* outputs behaviour in different physiological challenges at all frequency bands by applying univariate and multivariate TFA, measuring the reproducibility of the results, and testing the differences in TFA parameters variability for measurement and subject variability recordings. Consequently, the results demonstrate that each *CBv* output for each physiological challenge behaves differently across the frequency spectrum. Also, the reproducibility measurement demonstrates moderate levels of ICC for both normocapnia and thigh cuff conditions where the thigh cuff condition presents the highest level in univariate scale and appears even higher when adding 2-inputs to the TFA. it's worth noting that normocapnia condition demonstrate the highest ICC results when using 3-inputs compared to other conditions. As well, the results demonstrate that TFA parameters variations of measurement variability are much lower than the variations of subject variability for all physiological challenges at all frequency bands in both univariate and multivariate analyses.

The research expanded the work to examine differences between both right and left sides as well as their average. This included examining MTFA parameters outputs and variability measurement in each case (right, left, and average). The significance results show that there is a significant similarity in all three cases in terms of results (both mean and p values). This could assist future researcher in designing their methodology when applying multivariate system studying health subjects.

The work done in this research shows that dCA mechanism perform in different approaches under different physiological challenges and TFA parameters, in both univariate and multivariate analyses, behave dissimilarly under different conditions. The generally moderate levels of reproducibility shown in this research ($\approx 0.5 > ICC > 0.7$) and the quantification of measurement and subject variabilities variances in TFA parameters could assist future researchers in identifying dCA metrics. Also, it could assist future researchers in setting up a unified standard to identify metrics that leads to quantify dCA mechanism.

Future research should consider examining and understanding the source of nonstationary behaviour by expanding techniques used when applying multivariate analysis with a recommendation to add CO_2 and HR as additional inputs. Also, it is significant to examine and understand the variability found in participants (measurement and subject variabilities). Likewise, it is significant to analyse dCA in diseased conditions and investigate results variability in stroke patient.

In addition, future research should also consider the application of nonlinear models to assess dCA and understand its dynamics. One study has suggested that nonlinear models can reduce gain results and better explain the dCA mechanism [109]. Using the same datasets on linear and nonlinear models, it has been found that nonlinear approach significantly enhances the accuracy of model and the explanation of results [95]. The nonstationary nature of physiological variables such as *ABP* and *CBv* suggest analysing them through designing a multi-modal or a nonlinear model to estimate dCA which shows better reproducibility than conventional ARI, better presentation of input-output (*ABP* and *CBv)* relation, better reliability in dCA assessment [110], and significant statistical reduction in error of the predicted results [12].

References

1. Payne S. *Cerebral Blood Flow and Metabolism: A Quantitative Approach.* 1st Edition ed. World Scientific Publishing Company; 2017

2. Tiecks FP, Lam AM, Aaslid R, Newell DW. Comparison of static and dynamic cerebral autoregulation measurements. *Stroke.* 1995;26(6):1014-1019

3. Payne S. *Cerebral autoregulation: control of blood flow in the brain.* Vol 1. Springer; 2016

4. Panerai RB. Nonstationarity of dynamic cerebral autoregulation. *Med Eng Phys.* 2014;36(5):576-584

5. Jurgen AHR Claassen, Aisha SS Meel-van den Abeelen, David M Simpson and Ronney B Panerai, on behalf of the international Cerebral Autoregulation Research Network (CARNet). Transfer function analysis of dynamic cerebral autoregulation: A white paper from the International Cerebral Autoregulation Research Network. *Journal of cerebral blood flow and metabolism.* 2016;36(4):665-680. https://www.narcis.nl/publication/RecordID/oai:cris.maastrichtuniversity.nl:publications%2Fc79531da-fcd5-4093-a283-57b027cd3c89

6. Beishon L, Minhas J, Nogueira R, et al. INFOMATAS multi-center systematic review and meta-analysis individual patient data of dynamic cerebral autoregulation in ischemic stroke. *International journal of stroke.* 2020;15(7):174749302090700-812. doi:10.1177/1747493020907003

7. Kennedy McConnell F, Payne S. The Dual Role of Cerebral Autoregulation and Collateral Flow in the Circle of Willis After Major Vessel Occlusion. *TBME.* 2017;64(8):1793-1802. doi:10.1109/TBME.2016.2623710

8. Guo Z, Shao A, Tong L, Sun W, Liu J, Yang Y. The Role of Nitric Oxide and Sympathetic Control in Cerebral Autoregulation in the Setting of Subarachnoid Hemorrhage and Traumatic Brain Injury. *Mol Neurobiol.* 2016;53(6):3606-3615. doi:10.1007/s12035-015-9308-x

9. Guo W, Ma H, Liu J, Guo Z, Yang Y. Dynamic Cerebral Autoregulation Remains Stable During the Daytime (8 a.m. to 8 p.m.) in Healthy Adults. *Front Physiol.* 2018;9. doi:10.3389/fphys.2018.01642

10. Bryant JED, Birch AA, Panerai RB, Nikolic D, Bulters D, Simpson DM. Estimating confidence intervals for cerebral autoregulation: a parametric bootstrap approach. *PMEA.* 2021;42(10):104004. doi:10.1088/1361-6579/ac27b8

11. Panerai RB, Batterham A, Robinson TG, Haunton VJ. Determinants of cerebral blood flow velocity change during squat-stand maneuvers. *American Journal of Physiology-Regulatory, Integrative and Comparative Physiology.* 2021;320(4):R452. doi:10.1152/ajpregu.00291.2020

12. Marmarelis VZ, Mitsis GD, Shin DC, Zhang R. Multiple-input nonlinear modelling of cerebral haemodynamics using spontaneous arterial blood pressure, end-tidal CO2 and heart rate measurements. *Proc R Soc A.* 2016;374(2067). doi:10.1098/rsta.2015.0180

13. Fantini S, Sassaroli A, Tgavalekos KT, Kornbluth J. Cerebral blood flow and autoregulation: current measurement techniques and prospects for noninvasive optical methods. *Neurophotonics (Print).* 2016;3(3):031411. doi:10.1117/1.NPh.3.3.031411

14. Ogedegbe G, MD, Pickering, Thomas, MD, DPhil. Principles and Techniques of Blood Pressure Measurement. *Cardiology clinics.* 2010;28(4):571-586. doi:10.1016/j.ccl.2010.07.006

15. Goodman CT, Kitchen GB. Measuring arterial blood pressure. *Anaesthesia and intensive care medicine.* 2021;22(1):49-53. doi:10.1016/j.mpaic.2020.11.007

16. Calamante F, Thomas DL, Pell GS, Wiersma J, Turner R. Measuring Cerebral Blood Flow Using Magnetic Resonance Imaging Techniques. *Journal of Cerebral Blood Flow & Metabolism.* 1999;19(7):701-735. doi:10.1097/00004647-199907000-00001

17. Cenic A, Nabavi DG, Craen RA, Gelb AW, Lee T. Dynamic CT Measurement of Cerebral Blood Flow: A Validation Study. *American journal of neuroradiology : AJNR.* 1999;20(1):63-73. http://www.ajnr.org/cgi/content/abstract/20/1/63

18. Pham T, Tgavalekos K, Sassaroli A, Blaney G, Fantini S. Quantitative measurements of cerebral blood flow with near-infrared spectroscopy. *Biomedical optics express.* 2019;10(4):2117-2134. doi:10.1364/BOE.10.002117

19. Groen D, Richardson RA, Coy R, et al. Validation of Patient-Specific Cerebral Blood Flow Simulation Using Transcranial Doppler Measurements. *Front Physiol.* 2018;9. doi:10.3389/fphys.2018.00721

20. Mahinrad S, Tan CO, Ma Y, et al. Intracranial Blood Flow Quantification by Accelerated Dual- venc 4D Flow MRI : Comparison With Transcranial Doppler Ultrasound. *Magnetic Resonance Imaging.* 2022;56(4):1256. doi:10.1002/jmri.28115

21. ACHTEN J, JEUKENDRUP AE. Heart Rate Monitoring: Applications and Limitations. *Sports Medicine.* 2003;33(7):517-538. doi:10.2165/00007256-200333070-00004

22. GIARDINO ND, LEHRER PM, EDELBERG R. Comparison of finger plethysmograph to ECG in the measurement of heart rate variability. *Psychophysiology.* 2002;39(2):246-253. doi:10.1111/1469-8986.3920246

23. Kranjec J, Beguš S, Geršak G, Drnovšek J. Non-contact heart rate and heart rate variability measurements: A review. *Biomedical signal processing and control.* 2014;13:102-112. doi:10.1016/j.bspc.2014.03.004

24. Passler S, Müller N, Senner V. In-Ear Pulse Rate Measurement: A Valid Alternative to Heart Rate Derived from Electrocardiography? *Sensors (Basel, Switzerland).* 2019;19(17):3641. doi:10.3390/s19173641

25. Capnography for Monitoring End-Tidal CO 2 in Hospital and Pre-hospital Settings: A Health Technology Assessment. 2016

26. Kugelman A, Zeiger-Aginsky D, Bader D, Shoris I, Riskin A. A Novel Method of Distal End-Tidal CO2 Capnography in Intubated Infants: Comparison With Arterial CO2 and With Proximal Mainstream End-Tidal CO2. *Pediatrics (Evanston).* 2008;122(6):e1219-e1224. doi:10.1542/peds.2008-1300

27. BARTON C, CALLAHAM M. Lack of correlation between end-tidal carbon dioxide concentrations and Paco2 in cardiac arrest. *Critical care medicine.* 1991;19(1):108-110. doi:10.1097/00003246-199101000-00023

28. Cinar O, MD, Acar YA, MD, Arziman İ, MD, Kilic E, MD, Eyi YE, MD, Ocal R, MD. Can mainstream end-tidal carbon dioxide measurement accurately predict the arterial carbon dioxide level of patients with acute dyspnea in ED. *The American journal of emergency medicine.* 2012;30(2):358-361. doi:10.1016/j.ajem.2010.12.014

29. Duyu M, Bektas AD, Karakaya Z, et al. Comparing the novel microstream and the traditional mainstream method of end-tidal CO2 monitoring with respect to PaCO2 as gold

standard in intubated critically ill children. *Scientific reports.* 2020;10(1):22042. doi:10.1038/s41598-020-79054-y

30. Lewis LM, Stothert J, Standeven J, Chandel B, Kurtz M, Fortney J. Correlation of end-tidal CO2 to cerebral perfusion during CPR. *Annals of Emergency Medicine.* 1992;21(9):1131. doi:10.1016/s0196-0644(05)80658-4

31. Aaslid R, Lindegaard KF, Sorteberg W, Nornes H. Cerebral autoregulation dynamics in humans. *Stroke (1970).* 1989;20(1):45-52. doi:10.1161/01.str.20.1.45

32. Panerai RB, Sammons EL, Smith SM, et al. Continuous estimates of dynamic cerebral autoregulation: influence of non-invasive arterial blood pressure measurements. *Physiological measurement.* 2008;29(4):497-513. doi:10.1088/0967-3334/29/4/006

33. Brodie FG, Atkins ER, Robinson TG, Panerai RB. Reliability of dynamic cerebral autoregulation measurement using spontaneous fluctuations in blood pressure. *Clin Sci (Lond).* 2009;116(6):513-520. doi:10.1042/CS20080236

34. R B Panerai, P J Eames, J F Potter. Physiological Measurement Variability of time-domain indices of dynamic cerebral autoregulation. *PHYSIOLOGICAL MEASUREMENT.* 2003

35. LIU Y, ALLEN R. Analysis of dynamic cerebral autoregulation using an ARX model based on arterial blood pressure and middle cerebral artery velocity simulation. *Medical & biological engineering & computing.* 2002;40(5):600-605. doi:10.1007/BF02345461

36. Liu Y, Birch AA, Allen R. Dynamic cerebral autoregulation assessment using an ARX model: comparative study using step response and phase shift analysis. *Medical Engineering & Physics.* 2003;25(8):647. doi:10.1016/s1350-4533(03)00015-8

37. R B Panerai, S T Deverson, P Mahony, P Hayes, D H Evans. Effect of CO 2 on dynamic cerebral autoregulation measurement. 1999

38. Czosnyka M, Smielewski P, Kirkpatrick P, Menon DK, Pickard JD. Monitoring of Cerebral Autoregulation in Head-Injured Patients. *Stroke.* 1996;27(10):1829-1834. doi:10.1161/01.STR.27.10.1829

39. STEINMEIER R, HOFMANN RP, BAUHUF C, HÜBNER U, FAHLBUSCH R. Continuous Cerebral Autoregulation Monitoring by Cross-Correlation Analysis. *Journal of neurotrauma.* 2002;19(10):1127-1138. doi:10.1089/08977150260337949

40. Chiu C, Yeh S. Assessment of cerebral autoregulation using time-domain cross-correlation analysis. *Computers in Biology and Medicine.* 2001;31(6):471. doi:10.1016/s0010-4825(01)00015-4

41. CHRIST M, NOACK F, SCHROEDER T, et al. Continuous cerebral autoregulation monitoring by improved cross-correlation analysis: comparison with the cuff deflation test. *Intensive care medicine.* 2007;33(2):246-254. doi:10.1007/s00134-006-0451-8

42. Cole A. Giller. 1990 The frequency-dependent behavior of cerebral autoregulation. 1990

43. Giller C, Gerardo Lacopino D. Use of middle cerebral velocity and blood pressure for the analysis of cerebral autoregulation at various frequencies: The coherence index. *Neurological Research.* 1997;19(6). doi:10.1080/01616412.1997.11740873

44. Zhang R, Zuckerman JH, Giller CA, Levine BD. Transfer function analysis of dynamic cerebral autoregulation in humans. *American journal of physiology. Heart and circulatory physiology*. 1998;274(1):H233-H241. doi:10.1152/ajpheart.1998.274.1.h233

45. van den Abeelen A, Beek AHEA, Slump CH, Panerai RB, Claassen JAHR. Transfer function analysis for the assessment of cerebral autoregulation using spontaneous oscillations in blood pressure and cerebral blood flow. *Medical engineering & physics.* 2014;36(5):563-575. https://www.narcis.nl/publication/RecordID/oai:ris.utwente.nl:publications%2F66904743-0cae-43ee-8f88-52713eadecdd

46. Jachan M, Reinhard M, Spindeler L, Hetzel A, Schelter B, Timmer J. Parametric Versus Nonparametric Transfer Function Estimation of Cerebral Autoregulation from Spontaneous Blood-Pressure Oscillations. *Cardiovasc Eng.* 2009;9(2):72-82. doi:10.1007/s10558-009-9072-5

47. Deegan BM, Serrador JM, Nakagawa K, Jones E, Sorond FA, ÓLaighin G. The effect of blood pressure calibrations and transcranial Doppler signal loss on transfer function estimates of cerebral autoregulation. *Medical engineering & physics.* 2011;33(5):553-562. doi:10.1016/j.medengphy.2010.12.007

48. Birch AA, Dirnhuber MJ, Hartley-Davies R, Iannotti F, Neil-Dwyer G. Assessment of Autoregulation by Means of Periodic Changes in Blood Pressure. *Stroke.* 1995;26(5):834-837. doi:10.1161/01.STR.26.5.834

49. Liu J, Simpson MD, Yan J, Allen R. Tracking time-varying cerebral autoregulation in response to changes in respiratory PaCO2. *Physiological measurement.* 2010;31(10):1291-1307. doi:10.1088/0967-3334/31/10/001

50. Aoi MC, Matzuka BJ, Olufsen MS. Toward online, noninvasive, nonlinear assessment of cerebral autoregulation. *2011 Annual International Conference of the IEEE Engineering in Medicine and Biology Society*. 2011. doi:10.1109/iembs.2011.6090671

51. Noack F, Christ M, May S, Steinmeier R, Morgenstern U. Assessment of dynamic changes in cerebral autoregulation. *Biomedizinische Technik*. 2007;52(1):31-36. doi:10.1515/BMT.2007.007

52. Panerai RB, Simpson DM, Deverson ST, Mahony P, Hayes P, Evans DH. Audio Production Techniques for Video. *The Technology Teacher*. 1987;47(2):40. https://search.proquest.com/docview/2190101350

53. Liu J, Simpson D, Kouchakpour H, et al. Rapid pressure-to-flow dynamics of cerebral autoregulation induced by instantaneous changes of arterial CO sub(2). *Medical engineering & physics*. 2014;36(12):1636-1643. doi:10.1016/j.medengphy.2014.09.005

54. Novak V, Yang ACC, Lepicovsky L, Goldberger AL, Lipsitz LA, Peng C. Multimodal pressure-flow method to assess dynamics of cerebral autoregulation in stroke and hypertension. *BioMedical Engineering OnLine*. 2004;3(1):39. doi:10.1186/1475-925X-3-39

55. Peng T, Peng T, Rowley A, et al. Multivariate System Identification for Cerebral Autoregulation. *Ann Biomed Eng*. 2008;36(2):308-320. doi:10.1007/s10439-007-9412-9

56. Elucimed.com. Transfer function analysis. 2019. https://elucimed.com/ensemble-r/extract/pf-transfer-function/. Accessed Aug 10, 2020

57. Nikolic D, Birch AA, Panerai RB, Simpson DM. Assessing cerebral blood flow control from variability in blood pressure and arterial CO2 levels. EEE Engineering in Medicine and Biology Society (EMBC); 2015

58. Sanders ML, Claassen JAHR, Aries M, et al. Reproducibility of dynamic cerebral autoregulation parameters: a multi-centre, multi-method study. *Physiological measurement.* 2018;39(12):125002. doi:10.1088/1361-6579/aae9fd

59. Sanders ML, Elting JWJ, Panerai RB, et al. Dynamic Cerebral Autoregulation Reproducibility Is Affected by Physiological Variability. *Frontiers in Physiology.* 2019;10. doi:10.3389/fphys.2019.00865

60. Elting JW, Sanders ML, Panerai RB, et al. Assessment of dynamic cerebral autoregulation in humans: Is reproducibility dependent on blood pressure variability? *PloS one.* 2020;15(1):e0227651. doi:10.1371/journal.pone.0227651

61. Panerai RB, Brassard P, Burma JS, et al. Transfer function analysis of dynamic cerebral autoregulation: a CARNet white paper 2022 update. *Journal of Cerebral Blood Flow & Metabolism.* 2022:271678X221119760. doi:10.1177/0271678X221119760

62. B Panerai R, Hanby MF, Robinson TG, Haunton VJ. Alternative representation of neural activation in multivariate models of neurovascular coupling in humans. *Journal of neurophysiology.* 2019;122(2):833-843. doi:10.1152/jn.00175.2019

63. Nogueira RC, Aries M, Minhas JS, et al. Review of studies on dynamic cerebral autoregulation in the acute phase of stroke and the relationship with clinical outcome. *Journal of Cerebral Blood Flow & Metabolism.* 2022;42(3):430-453. doi:10.1177/0271678X211045222

64. Chi N, Hu H, Wang C, et al. Dynamic Cerebral Autoregulation Is an Independent Functional Outcome Predictor of Mild Acute Ischemic Stroke. *Stroke.* 2018;49(11):2605-2611. doi:10.1161/STROKEAHA.118.022481

65. Otite F, Mink S, Tan CO, et al. Impaired Cerebral Autoregulation Is Associated With Vasospasm and Delayed Cerebral Ischemia in Subarachnoid Hemorrhage. *Stroke.* 2014;45(3):677-682. doi:10.1161/STROKEAHA.113.002630

66. Di Virgilio V, Barbieri R, Mainardi L, Strano S, Cerutti S. A multivariate time-variant AR method for the analysis of heart rate and arterial blood pressure. *Medical Engineering & Physics.* 1997;19(2):109-124. doi:10.1016/S1350-4533(96)00058-6

67. Barbieri R, Di Virgilio V, Cerutti S, Saul JP. Multivariate Time-Variant Autoregressive Techniques for Closed-loop Cardiovascular Control using Simulations and Comparisons. *Frontiers of Blood Pressure and Heart Rate Analysis.* 1997:101-114. doi:10.3233/978-1-60750-879-3-101

68. Kostoglou K, Debert CT, Poulin MJ, Mitsis GD. Nonstationary multivariate modeling of cerebral autoregulation during hypercapnia. *Medical Engineering and Physics.* 2013;36(5):592-600. doi:10.1016/j.medengphy.2013.10.011

69. Labmate I. What is the Difference Between Repeatability and Reproducibility? Labmate Online Web site. https://www.labmate-online.com/news/news-and-views/5/breaking-news/what-is-the-difference-between-repeatability-and-reproducibility/30638. Accessed Aug 18, 2020

70. Koo TK, Li MY. A Guideline of Selecting and Reporting Intraclass Correlation Coefficients for Reliability Research. *Journal of chiropractic medicine.* 2016;15(2):155-163. doi:10.1016/j.jcm.2016.02.012

71. Bruton A, Conway JH, Holgate ST. Reliability - What is it and how is it measured? *Physiotherapy, Elsevier.* 2000

72. ATKINSON G, NEVILL AM. Statistical Methods For Assessing Measurement Error (Reliability) in Variables Relevant to Sports Medicine. *Sports Medicine.* 1998;26(4):217-238. doi:10.2165/00007256-199826040-00002

73. Chinn S. Statistics in respiratory medicine. 2. Repeatability and method comparison. *Thorax.* 1991;46(6):454-456. doi:10.1136/thx.46.6.454

74. Bobak CA, Barr PJ, O'malley AJ. Estimation of an inter-rater intra-class correlation coefficient that overcomes common assumption violations in the assessment of health measurement scales. *BMC Medical Research Methodology.* 2018;18. doi:10.1186/s12874-018-0550-6

75. Mahdi A, Nikolic D, Birch AA, et al. Increased blood pressure variability upon standing up improves reproducibility of cerebral autoregulation indices. *Medical Engineering and Physics.* 2017;47:151-158. doi:10.1016/j.medengphy.2017.06.006

76. Gommer E, Shijaku E, Mess W, Reulen J. Dynamic cerebral autoregulation: different signal processing methods without influence on results and reproducibility. *Med Biol Eng Comput.* 2010;48(12):1243-1250. doi:10.1007/s11517-010-0706-y

77. Minhas JS, Syed NF, Haunton VJ, Panerai RB, Robinson TG, Mistri AK. Is dynamic cerebral autoregulation measurement using transcranial Doppler ultrasound reproducible in the presence of high concentration oxygen and carbon dioxide? *Physiological measurement.* 2016;37(5):673-682. doi:10.1088/0967-3334/37/5/673

78. Liu X, Czosnyka M, Donnelly J, et al. Comparison of Frequency and Time Domain Methods of Assessment of Cerebral Autoregulation in Traumatic Brain Injury. *Journal of cerebral blood flow and metabolism.* 2015;35(2):248-256. doi:10.1038/jcbfm.2014.192

79. Vittrup A, Sofie A, Simonsen A, et al. Assessing low-frequency oscillations in cerebrovascular diseases and related conditions with near-infrared spectroscopy: a plausible method for evaluating cerebral autoregulation? "Assessing low-frequency oscillations in cerebrovascular diseases and related conditions with near- infrared spectroscopy: a plausible method for evaluating cerebral autoregulation? Assessing low-frequency oscillations in cerebrovascular diseases and related conditions with near-infrared spectroscopy: a plausible method for evaluating cerebral autoregulation? *Neurophoton.* 2018;5(3)

80. Brian M. Deegan, Farzaneh A. Sorond, Lewis A. Lipsitz, Gearóid ÓLaighin, Jorge M. Serrador. 2009 Gender related differences in cerebral autoregulation in older healthy subjects. 2009

81. Liu J, Simpson DM, Panerai RB. Point-Counterpoint: Transfer function analysis of dynamic cerebral autoregulation: To band or not to band? *J Cereb Blood Flow Metab.* 2022. doi:10.1177/0271678x221098448

82. Latka M, Turalska M, Glaubic-Latka M, et al. Phase dynamics in cerebral autoregulation Downloaded from journals.physiology.org/journal/ajpheart at Oxford Univ Bodleian Lib. *Am J Physiol Heart Circ Physiol.* 2005;289

83. Katsogridakis E, Bush G, Fan L, et al. Detection of Impaired Cerebral Autoregulation Improves by Increasing Arterial Blood Pressure Variability. *Journal of cerebral blood flow and metabolism.* 2013;33(4):519-523. doi:10.1038/jcbfm.2012.191

84. Liu J, Tseng BY, Khan MA, et al. Individual variability of cerebral autoregulation, posterior cerebral circulation and white matter hyperintensity. *J Physiol.* 2016;594(11):3141. doi:10.1113/jp271068

85. Peng T, Rowley AB, Ainslie PN, Poulin MJ, Payne SJ. Wavelet Phase Synchronization Analysis of Cerebral Blood Flow Autoregulation. *TBME.* 2010;57(4):960-968. doi:10.1109/TBME.2009.2024265

86. Liu X, Czosnyka M, Donnelly J, et al. Assessment of cerebral autoregulation indices – a modelling perspective. *Sci Rep.* 2020;10(1):1-11. doi:10.1038/s41598-020-66346-6

87. 1999 Multiple-input, multiple-output system identification for characterization of limb stiffness dynamics.

88. Kevin Brownhill. Intraclass correlation coefficients, https://uk.mathworks.com/matlabcentral/fileexchange/21501-intraclass-correlation-coefficients, visited July 2020. Math Works Web site. https://uk.mathworks.com/matlabcentral/fileexchange/21501-intraclass-correlation-coefficients. Updated 2020. Accessed July, 2020

89. Armstrong RA. When to use the Bonferroni correction. *Ophthalmic & physiological optics.* 2014;34(5):502-508. doi:10.1111/opo.12131

90. Sorond FA, Serrador JM, Jones RN, Shaffer ML, Lipsitz LA. The Sit-to-Stand Technique for the Measurement of Dynamic Cerebral Autoregulation. *Ultrasound in Medicine & Biology.* 2009;35(1):21-29. doi:10.1016/j.ultrasmedbio.2008.08.001

91. Barnes SC, Haunton VJ, Beishon L, Llwyd O, Robinson TG, Panerai RB. Extremes of cerebral blood flow during hypercapnic squat-stand maneuvers. *Physiological Reports.* 2021;9(19). doi:10.14814/phy2.15021

92. De Smet D, Jacobs J, Ameye L, et al. The Partial Coherence Method for Assessment of Impaired Cerebral Autoregulation using Near-infrared Spectroscopy: Potential and

Limitations. *Advances in Experimental Medicine and Biology*. 2009:219. doi:10.1007/978-1-4419-1241-1_31

93. Katsogridakis E, Simpson DM, Bush G, et al. Revisiting the frequency domain: the multiple and partial coherence of cerebral blood flow velocity in the assessment of dynamic cerebral autoregulation. *Physiol Meas.* 2016;37(7):1056. doi:10.1088/0967-3334/37/7/1056

94. Rivera-Lara L, Geocadin R, Zorrilla-Vaca A, et al. Validation of Near-Infrared Spectroscopy for Monitoring Cerebral Autoregulation in Comatose Patients. *Neurocrit Care.* 2017;27(3):362-369. doi:10.1007/s12028-017-0421-8

95. Panerai RB. Cerebral Autoregulation: From Models to Clinical Applications. *Cardiovasc Eng.* 2008;8(1):42-59. doi:10.1007/s10558-007-9044-6

96. Cicchetti DV. Guidelines, Criteria, and Rules of Thumb for Evaluating Normed and Standardized Assessment Instruments in Psychology. *Psychological assessment.* 1994;6(4):284-290. doi:10.1037/1040-3590.6.4.284

97. Liljequist D, Elfving B, Skavberg Roaldsen K. Intraclass correlation – A discussion and demonstration of basic features. *PLoS One.* 2019;14(7):e0219854. doi:10.1371/journal.pone.0219854

98. Yartsev A. Invasive and non-invasive measurement of blood pressure | Deranged Physiology. https://derangedphysiology.com/main/cicm-primary-exam/required-reading/cardiovascular-system/Chapter 752/invasive-and-non-invasive-measurement-blood-pressure. Accessed May 9, 2023

99. Murray WB, Gorven AM. Invasive v. non-invasive blood pressure measurements--the influence of the pressure contour. *S Afr Med J.* 1991;79(3):134-139

100. Pinna GD, Maestri R, Mortara A. Estimation of arterial blood pressure variability by spectral analysis: comparison between Finapres and invasive measurements. *Physiol Meas.* 1996;17(3):147. doi:10.1088/0967-3334/17/3/002

101. Petersen NH, Ortega-Gutierrez S, Reccius A, Masurkar A, Huang A, Marshall RS. Comparison of Non-invasive and Invasive Arterial Blood Pressure Measurement for Assessment of Dynamic Cerebral Autoregulation. *Neurocrit Care.* 2014;20(1):60-68. doi:10.1007/s12028-013-9898-y

102. Tzeng YC, Ainslie PN, Cooke WH, et al. Assessment of cerebral autoregulation: the quandary of quantification. *American Journal of Physiology - Heart and Circulatory Physiology.* 2012;303(6):658-671. doi:10.1152/ajpheart.00328.2012

103. Liu X, Czosnyka M, Donnelly J, et al. Assessment of cerebral autoregulation indices – a modelling perspective. *Sci Rep.* 2020;10(1). doi:10.1038/s41598-020-66346-6

104. Barnes SC, Ball N, Panerai RB, Robinson TG, Haunton VJ. Random squat/stand maneuvers: a novel approach for assessment of dynamic cerebral autoregulation? *Journal of Applied Physiology.* 2017;123(3):558. doi:10.1152/japplphysiol.00316.2017

105. Labrecque L, Smirl JD, Brassard P. Utilization of the repeated squat-stand model for studying the directional sensitivity of the cerebral pressure-flow relationship. *Journal of applied physiology (1985).* 2021;131(3):927-936. doi:10.1152/japplphysiol.00269.2021

106. Ronney X, Panerai B, Barnes SC, et al. Directional sensitivity of dynamic cerebral autoregulation in squat-stand maneuvers. *Am J Physiol Regul Integr Comp Physiol.* 2018;315:730

107. Claassen C. African Archaeological Journals and Social Issues 2014–2021. *Humans.* 2023;3(1):25-35. doi:10.3390/humans3010004

108. Wise RG, Ide K, Poulin MJ, Tracey I. Resting fluctuations in arterial carbon dioxide induce significant low frequency variations in BOLD signal. *NeuroImage (Orlando, Fla.).* 2004;21(4):1652-1664. doi:10.1016/j.neuroimage.2003.11.025

109. Mitsis GD, Zhang R, Levine BD, Marmarelis VZ. Modeling of Nonlinear Physiological Systems with Fast and Slow Dynamics. II. Application to Cerebral Autoregulation. . doi:10.1114/1.1477448

110. Hu K, Peng CK, Czosnyka M, Zhao P, Novak V. Nonlinear Assessment of Cerebral Autoregulation from Spontaneous Blood Pressure and Cerebral Blood Flow Fluctuations. *Cardiovasc Eng.* 2008;8(1):60-71. doi:10.1007/s10558-007-9045-5

S. Appendix

a. Tables

Subject	Visit	Normocapnia									
		Mean *ABP* (mmHg)		Mean *CBv* Right (cm/s)		Mean *CBv* Left (cm/s)		*HR* (beat/min)		*CO2* (mmHg)	
		Mean	Standard deviation	Mean	Standard deviation	Mean	Standard deviation	Mean	Standard deviation	Mean	Standard deviation
1	1	-	-	-	-	-	-	-	-	-	-
	2	-	-	-	-	-	-	-	-	-	-
	3	76.65	2.24	55.71	2.61	59.44	2.53	70.40	5.32	39.32	1.02
	4	67.11	3.17	55.10	2.86	63.02	3.51	56.92	4.66	38.11	1.41
	5	-	-	-	-	-	-	-	-	-	-
2	1	82.68	9.77	54.84	5.02	66.30	6.02	62.44	7.48	35.91	1.50
	2	83.54	5.60	77.61	6.20	64.03	6.23	60.28	6.98	36.38	1.31
	3	76.57	6.24	84.04	6.51	62.92	4.85	60.27	7.28	35.37	1.60
	4	73.01	6.20	82.92	6.89	66.16	5.63	55.95	7.10	35.22	1.71
	5	67.55	5.94	52.16	3.88	59.77	5.50	55.41	8.26	36.47	1.65
3	1	70.95	3.88	54.51	4.43	56.39	5.04	64.56	6.06	38.95	1.60
	2	72.81	4.38	48.15	4.10	63.74	5.14	76.64	4.61	39.38	1.17
	3	75.65	6.03	40.81	11.36	54.56	4.98	55.71	4.51	39.67	1.89
	4	84.89	4.63	51.84	3.58	57.58	3.82	69.98	4.87	36.90	1.18
	5	85.26	4.60	45.11	4.17	61.97	5.89	77.63	5.91	38.12	1.30
4	1	80.83	3.75	77.16	3.11	65.52	2.46	54.86	2.44	42.27	1.12
	2	64.48	9.01	65.80	3.94	53.87	3.07	59.39	11.81	41.71	0.81
	3	77.31	2.84	64.00	3.36	59.63	2.83	60.58	3.28	39.19	1.43
	4	79.53	4.53	59.40	2.98	55.63	2.78	62.31	3.34	42.66	2.36
	5	80.94	3.93	61.58	3.61	56.38	3.04	62.88	3.83	40.10	1.00
5	1	76.99	3.30	90.69	5.35	96.60	5.69	68.41	5.02	41.83	1.10
	2	77.90	5.34	81.36	4.54	86.19	5.20	68.98	4.69	38.39	1.50
	3	76.85	4.61	90.15	4.70	94.54	5.12	64.47	5.74	41.24	1.08
	4	84.84	6.66	81.93	4.76	85.86	5.07	77.36	6.00	40.69	1.24
	5	87.02	10.51	91.23	7.59	89.27	6.68	65.94	12.52	41.62	1.82
6	1	67.55	4.75	76.69	5.91	80.88	7.39	57.86	2.47	39.90	1.60
	2	71.29	5.63	75.06	4.91	69.46	5.47	53.90	2.39	39.95	1.67
	3	69.71	3.11	70.00	3.00	68.87	2.15	76.56	5.02	34.05	1.55
	4	64.65	5.75	77.29	6.86	71.22	6.20	60.05	2.41	40.35	1.69
	5	72.61	5.73	59.49	5.11	70.33	5.26	79.42	5.98	36.76	2.50
7	1	81.81	2.39	67.35	6.82	79.24	8.12	82.23	5.34	38.86	2.74
	2	73.53	4.20	64.51	7.27	71.21	8.81	62.84	4.98	37.70	2.40
	3	78.08	4.56	69.56	9.14	70.56	10.00	62.00	4.47	37.42	2.83
	4	72.46	4.84	64.61	8.52	69.99	8.73	62.12	5.40	32.48	2.70
	5	81.34	5.36	66.30	7.79	68.32	8.68	71.71	4.64	33.07	2.01
8	1	76.75	2.45	72.12	4.93	78.41	5.23	50.77	3.80	34.75	1.25

	2	72.59	1.74	74.81	5.99	78.61	6.40	51.33	3.82	35.14	1.51
	3	76.59	3.08	79.57	5.99	86.79	5.95	58.21	6.12	37.47	1.82
	4	71.34	2.47	78.51	4.82	82.52	5.44	54.89	4.39	36.22	1.90
	5	76.81	2.05	77.47	7.26	90.82	6.86	53.71	4.58	35.08	1.83
9	1	79.06	2.22	101.37	7.04	99.96	6.51	70.85	3.28	37.97	1.06
	2	70.49	2.14	91.96	4.80	92.22	4.77	70.71	2.82	36.19	1.05
	3	63.76	1.52	79.57	4.00	96.41	5.24	70.53	3.17	37.27	0.95
	4	83.16	4.54	104.22	5.74	94.92	5.20	75.28	3.89	36.45	0.95
	5	69.43	1.51	110.59	9.10	100.15	8.37	74.54	4.01	37.08	1.18
10	1	86.18	16.79	71.48	3.60	74.90	3.15	67.63	5.48	33.94	0.86
	2	65.32	1.19	76.14	3.99	66.71	3.21	68.77	4.76	34.01	1.14
	3	60.70	4.36	78.49	4.21	67.17	3.34	64.07	5.24	34.08	0.97
	4	67.42	1.90	77.68	6.35	69.60	4.94	71.08	4.66	34.61	1.45
	5	70.28	2.43	81.61	5.41	72.52	4.51	75.94	4.28	33.46	1.50
11	1	69.71	2.91	76.76	5.90	80.95	6.03	59.83	5.24	38.52	2.36
	2	76.94	2.99	78.63	5.87	83.18	6.27	71.74	5.06	38.39	1.24
	3	74.84	3.38	73.42	9.78	77.41	10.95	57.66	4.62	34.05	3.01
	4	68.81	3.16	59.30	5.51	72.63	14.09	58.17	4.47	35.50	2.20
	5	74.44	4.07	81.61	6.84	76.04	6.36	57.53	4.32	37.82	1.93
12	1	75.24	2.89	89.37	7.67	79.44	7.65	68.41	5.80	32.65	1.42
	2	78.65	2.91	101.18	7.78	79.31	6.05	60.41	4.08	29.66	1.40
	3	79.72	2.81	96.93	6.84	80.52	6.19	54.87	5.09	31.51	1.33
	4	77.01	3.89	79.36	6.42	70.05	5.90	67.52	5.69	30.19	1.27
	5	75.70	3.26	73.52	6.03	80.82	7.44	62.66	5.18	32.49	1.57
13	1	84.97	2.96	73.64	4.07	77.69	3.12	71.74	5.14	31.90	0.93
	2	84.23	3.45	79.19	4.22	83.76	3.95	78.79	6.45	34.83	1.58
	3	80.90	2.44	67.34	4.35	77.14	4.08	75.65	6.12	33.59	1.12
	4	79.99	3.27	68.69	4.28	76.71	4.91	65.58	5.85	35.38	1.23
	5	79.23	4.32	77.23	4.70	81.59	5.14	75.78	5.85	34.64	1.32
14	1	73.27	3.11	64.15	3.15	71.18	3.28	59.51	2.65	36.65	1.18
	2	77.65	2.18	59.00	5.49	68.86	5.32	58.07	3.12	39.69	1.61
	3	70.48	8.19	56.03	3.26	69.47	3.07	68.08	4.11	45.29	1.37
	4	74.30	2.11	57.36	2.50	68.97	3.15	74.22	4.44	40.75	1.05
	5	80.20	2.45	61.21	2.82	70.44	3.19	62.87	3.15	36.44	1.79
15	1	73.31	2.75	52.63	2.32	64.35	2.71	60.91	3.55	39.40	1.54
	2	69.01	4.00	55.63	3.52	62.14	4.14	62.46	4.98	38.80	2.09
	3	72.22	2.67	65.27	5.90	65.05	5.37	58.72	4.77	42.57	2.07
	4	71.26	3.48	69.42	6.72	71.49	6.30	64.05	5.52	40.16	1.75
	5	70.23	2.90	59.48	5.55	71.38	5.83	62.45	3.98	39.34	1.90
16	1	82.94	1.93	85.56	5.66	80.27	4.85	71.54	5.20	37.08	1.09
	2	80.00	1.97	93.72	7.12	88.08	5.86	67.48	4.79	35.53	1.66
	3	80.61	1.94	88.95	4.36	83.16	3.57	73.49	5.01	38.95	0.85
	4	81.66	2.08	84.82	6.17	84.82	6.17	78.85	5.17	35.78	1.14
	5	81.19	3.28	88.16	7.08	83.90	6.08	67.71	6.05	34.10	1.56

	1	72.80	2.83	65.17	3.83	63.10	4.01	59.56	3.33	35.83	0.94
	2	69.46	2.57	65.86	3.27	68.29	2.24	56.27	3.90	36.78	1.51
17	3	62.18	4.30	65.33	3.33	63.71	3.41	62.65	4.05	34.01	1.19
	4	65.95	6.08	64.00	3.85	58.77	3.59	64.91	5.44	34.74	0.99
	5	72.54	2.14	64.89	3.19	63.18	3.35	63.54	3.62	36.56	1.28
	1	81.22	2.06	74.31	4.11	77.89	4.62	66.77	9.11	35.59	1.50
	2	85.68	3.09	72.07	4.29	74.57	4.69	64.40	10.32	34.54	1.24
18	3	73.28	3.17	82.26	6.77	85.63	9.17	70.53	11.06	38.26	2.11
	4	81.64	4.14	86.00	7.46	87.22	7.32	58.58	6.42	39.56	2.11
	5	74.46	2.03	71.95	3.12	79.48	3.39	78.88	6.31	33.99	1.27
	1	77.62	2.71	85.03	7.45	74.90	5.78	60.08	6.21	35.77	1.34
	2	82.32	2.41	82.49	7.69	74.02	7.78	50.97	6.84	38.16	1.60
19	3	72.70	3.88	79.92	9.82	76.36	8.95	53.38	5.95	36.94	2.13
	4	81.61	2.75	64.72	7.64	62.97	7.40	55.26	6.79	34.20	2.36
	5	70.21	5.86	81.63	10.04	77.78	9.96	53.42	6.14	34.50	2.11
	1	68.27	2.05	74.68	3.06	77.27	3.22	60.96	5.15	40.07	0.94
	2	68.13	1.68	63.73	4.83	66.82	4.18	61.61	5.11	38.75	0.87
20	3	64.34	1.85	51.07	45.77	69.34	3.05	56.98	4.48	34.49	1.03
	4	66.14	1.94	67.64	3.09	69.51	3.12	59.79	4.65	35.12	1.04
	5	66.87	2.42	64.04	3.62	69.24	2.76	68.74	4.76	37.55	0.94
Total mean		75.08	3.79	72.75	5.80	73.94	5.36	64.56	5.20	36.92	1.52
Total SD ±		6.24	2.22	13.54	4.53	10.74	2.13	7.64	1.82	2.93	0.49

Table S-1: Mean and standard deviation values of key parameters, *ABP*, *CBv* (right and left sides), *HR* and *CO*2 for all subject recordings at normocapnia condition

Subject	Visit	Hypercapnia									
		Mean *ABP* (mmHg)		Mean *CBv* Right (cm/s)		Mean *CBv* Left (cm/s)		Heart rate (beat/min)		*CO2* (mmHg)	
		Mean	Standard deviation	Mean	Standard deviation	Mean	Standard deviation	Mean	Standard deviation	Mean	Standard deviation
1	1	70.94	2.63	59.67	3.35	65.47	3.26	64.55	7.48	33.86	1.35
	2	72.59	2.11	61.48	3.53	64.26	3.68	54.39	4.37	44.61	1.41
	3	67.17	2.49	-	-	65.32	3.44	55.93	5.69	42.20	1.93
	4	75.49	3.37	61.56	4.42	55.54	4.11	53.95	4.64	49.76	0.90
	5	69.60	2.96	63.10	5.41	71.80	4.79	52.99	4.95	46.99	1.71
2	1	91.05	3.71	72.71	3.44	73.82	4.64	74.32	6.08	43.90	0.56
	2	83.55	4.19	76.63	3.38	72.73	3.06	69.28	7.53	45.88	0.57
	3	81.15	3.72	75.37	2.90	77.68	3.89	68.93	6.66	46.48	0.68
	4	78.16	7.71	82.94	5.88	66.71	5.45	59.44	9.48	44.43	1.34
	5	84.16	5.00	79.53	4.38	67.51	3.74	63.18	8.88	45.56	0.54
3	1	88.21	3.56	67.19	4.89	67.33	4.33	77.07	6.74	47.16	0.63
	2	90.68	5.03	68.29	3.37	73.61	3.75	83.11	5.63	49.03	0.70
	3	76.09	2.69	50.95	2.21	64.57	3.15	67.28	4.86	46.82	0.75
	4	74.61	5.88	-	-	65.88	3.55	73.36	5.35	47.07	0.84
	5	89.08	3.50	55.06	2.66	74.30	3.82	85.03	4.85	47.68	0.72
4	1	86.81	9.05	94.12	6.60	83.81	6.31	63.87	7.62	50.94	1.38
	2	103.82	3.35	85.71	4.81	76.92	5.41	72.11	6.76	49.93	1.46
	3	90.57	5.55	85.99	4.75	72.87	4.68	64.24	5.19	48.67	1.09
	4	84.32	3.62	85.26	8.07	76.42	7.20	67.56	6.61	51.42	1.54
	5	89.05	3.73	81.57	4.32	72.83	4.07	65.25	6.42	49.53	0.65
5	1	80.27	3.40	103.67	5.18	107.96	5.90	71.04	9.36	49.04	1.18
	2	89.61	2.95	97.30	5.27	103.38	5.48	78.11	9.75	46.41	1.14
	3	79.18	2.87	100.35	6.05	108.42	6.90	74.46	10.88	48.55	1.26
	4	80.32	4.53	88.76	6.06	104.37	8.10	76.63	7.58	46.57	2.29
	5	76.57	3.66	100.65	10.71	95.75	9.53	67.88	8.75	46.72	3.43
6	1	81.32	2.90	87.38	4.19	88.76	4.62	59.13	3.61	48.21	0.66
	2	69.59	2.33	89.11	2.71	81.31	3.16	58.63	5.56	51.18	0.60
	3	68.68	4.59	79.35	2.95	76.15	2.71	67.73	6.92	46.53	0.91
	4	68.29	3.30	83.99	3.18	74.18	2.78	63.18	6.29	45.80	0.78
	5	70.37	2.94	71.82	3.36	79.38	2.91	79.01	5.46	47.74	0.56
7	1	85.40	2.19	85.40	3.95	88.73	4.06	84.51	5.08	49.79	0.86
	2	80.93	6.54	79.93	5.06	84.63	4.51	72.19	7.79	49.92	1.05
	3	79.12	2.52	76.50	4.28	88.65	4.32	68.71	7.22	46.21	0.83
	4	89.03	3.58	72.23	5.24	84.66	6.38	70.22	8.35	46.76	1.80
	5	82.84	3.07	78.51	3.44	79.69	3.01	82.53	5.10	41.83	0.65
8	1	109.15	4.63	86.89	7.29	104.04	7.32	62.94	10.80	45.87	0.85
	2	87.09	2.07	106.64	5.16	108.11	5.07	55.42	4.01	46.29	0.87
	3	84.05	2.67	94.57	3.80	105.44	4.58	59.63	6.51	47.00	0.90
	4	78.33	2.36	88.12	4.44	95.81	5.08	57.05	6.77	45.40	0.68

	5	83.82	1.79	109.76	8.05	116.45	7.71	56.85	6.75	45.39	1.23
9	1	78.18	2.94	126.80	7.13	113.60	6.75	89.28	6.27	44.95	0.62
	2	77.05	2.17	119.88	5.71	113.77	5.39	79.56	5.92	45.07	0.80
	3	68.83	3.29	108.10	4.43	115.55	4.77	77.35	5.98	45.66	0.63
	4	73.53	2.64	121.12	5.34	133.26	6.19	80.57	5.48	45.02	0.52
	5	68.36	2.31	137.54	6.82	120.27	5.63	83.41	5.77	45.78	1.44
10	1	75.78	5.01	92.65	4.17	93.84	3.61	75.16	4.97	39.52	0.69
	2	71.30	3.14	98.03	3.49	-	-	78.69	4.54	36.52	0.83
	3	78.41	1.93	87.11	4.41	79.63	3.79	73.38	4.85	38.14	0.75
	4	74.57	2.33	109.66	4.45	98.79	3.70	77.62	5.00	40.80	0.61
	5	73.56	2.13	96.67	4.74	100.66	5.83	81.30	4.87	39.79	1.16
11	1	77.34	3.02	95.35	6.82	99.76	5.85	62.99	9.59	44.64	1.35
	2	84.04	3.64	102.00	6.84	103.81	6.53	68.40	8.74	46.49	1.23
	3	79.96	5.05	88.38	7.60	93.57	6.89	61.55	4.96	41.66	1.96
	4	61.74	196.87	63.02	3.53	92.05	5.55	56.93	7.29	43.83	0.93
	5	68.95	4.38	-	-	-	-	57.78	8.59	44.38	1.80
12	1	84.27	2.35	130.13	4.94	121.03	9.45	76.83	6.77	41.71	0.65
	2	79.33	2.90	129.18	9.86	117.63	8.95	69.55	4.72	40.74	0.61
	3	85.67	2.30	123.00	4.04	110.44	5.25	64.40	4.48	38.01	0.67
	4	86.86	3.13	115.15	5.21	114.88	8.45	71.13	6.08	42.02	1.08
	5	81.53	3.33	110.02	7.35	109.29	9.99	68.88	4.75	43.15	1.37
13	1	102.51	6.03	107.54	8.05	112.23	7.31	106.09	14.83	36.53	1.28
	2	93.97	2.79	97.78	5.44	108.44	4.91	87.56	9.07	40.81	1.57
	3	-	-	-	-	-	-	-	-	-	-
	4	86.63	2.95	95.72	5.05	108.37	5.89	75.76	10.10	46.79	1.46
	5	92.32	4.08	91.59	6.07	104.18	7.31	88.45	10.27	46.73	1.33
14	1	82.08	2.30	19.19	71.04	86.01	8.29	67.26	4.93	47.35	0.96
	2	81.46	1.76	79.89	6.69	80.98	5.84	63.87	6.38	50.75	0.84
	3	75.17	2.61	70.33	3.60	75.41	3.49	67.84	5.30	57.98	1.21
	4	79.05	2.27	0.89	108.29	51.82	52.31	71.02	5.58	54.74	0.87
	5	80.98	2.62	65.68	18.84	78.54	4.72	64.63	4.90	46.79	0.67
15	1	88.10	2.30	58.13	4.57	77.15	4.15	65.45	6.17	45.68	0.83
	2	82.74	2.90	66.60	4.02	76.78	4.59	63.77	5.03	49.00	1.17
	3	71.21	2.26	64.53	4.09	71.67	4.41	61.68	6.22	50.34	1.16
	4	77.12	2.66	78.10	5.98	75.19	5.25	65.44	7.46	48.83	1.41
	5	73.73	2.00	61.19	3.30	77.67	4.17	62.87	4.74	48.62	0.70
16	1	97.97	9.27	74.20	3.73	96.13	4.27	72.18	4.64	43.93	0.73
	2	84.31	5.21	107.50	5.40	103.13	4.95	71.31	4.22	42.97	0.77
	3	80.30	2.19	106.69	5.23	102.52	5.41	78.01	4.07	46.84	0.73
	4	82.98	1.93	114.52	5.86	100.07	5.00	79.99	3.99	45.20	0.90
	5	82.70	2.69	107.87	5.53	111.27	5.95	74.45	4.20	44.90	0.85
17	1	81.77	2.34	89.58	5.40	89.22	4.92	67.83	3.96	46.79	0.55
	2	79.99	2.12	95.98	5.03	97.75	4.41	62.84	3.68	49.89	0.62
	3	78.39	2.82	80.05	4.05	402.15	446.11	68.27	5.12	46.06	0.61

	4	80.65	3.63	83.92	4.65	83.00	5.09	72.97	5.75	46.13	0.75
	5	77.76	2.68	90.17	5.32	91.09	5.79	66.81	4.86	46.77	0.70
18	1	79.64	2.23	-	-	84.60	3.65	78.04	6.85	42.17	1.25
	2	82.24	2.40	85.67	4.94	86.77	4.42	73.07	10.63	45.18	1.19
	3	73.29	2.08	101.26	7.69	105.21	7.74	72.49	9.12	48.55	0.49
	4	78.79	1.89	87.17	4.01	92.93	4.58	76.62	8.22	46.72	0.74
	5	78.87	2.15	88.17	4.43	94.34	5.02	78.42	6.26	46.09	0.89
19	1	87.47	2.36	129.86	9.59	109.62	6.61	72.74	6.85	48.75	1.55
	2	94.07	2.26	134.53	9.93	123.63	9.14	65.13	8.23	50.36	1.28
	3	76.72	3.41	112.65	8.02	110.63	9.69	58.18	7.76	49.94	1.96
	4	78.48	2.45	104.16	6.85	109.69	9.32	64.02	8.88	51.15	1.35
	5	93.45	4.57	118.71	8.13	118.92	6.95	71.26	10.17	50.16	1.15
20	1	70.95	2.67	84.99	3.49	90.03	3.87	74.75	7.22	47.12	0.80
	2	79.22	3.91	85.20	4.85	88.54	12.08	70.06	7.65	47.96	0.82
	3	78.08	2.14	91.64	3.13	98.78	3.33	72.37	6.64	45.84	1.03
	4	70.11	2.20	80.38	6.86	84.12	6.56	69.66	6.82	43.52	2.99
	5	67.58	1.98	82.21	3.64	82.34	3.71	69.06	6.23	46.86	0.57
Total mean		80.82	5.28	89.41	7.20	95.03	10.60	70.41	6.59	46.22	1.04
Total SD ±		8.26	19.71	22.40	12.79	36.15	45.45	8.94	2.00	3.57	0.50

Table S-2: Mean and standard deviation values of key parameters, *ABP*, *CBv* (right and left sides), *HR* and *CO*2 for all subject recordings at hypercapnia condition

Subject	Visit	Thigh cuff									
		Mean *ABP* (mmHg)		Mean *CBv* Right (cm/s)		Mean *CBv* Left (cm/s)		*HR* (beat/min)		*CO*2 (mmHg)	
		Mean	Standard deviation	Mean	Standard deviation	Mean	Standard deviation	Mean	Standard deviation	Mean	Standard deviation
1	1	68.77	2.50	63.28	2.82	66.68	2.57	62.52	4.42	34.60	1.59
	2	76.66	2.35	55.77	2.25	57.46	2.65	64.87	5.33	36.41	1.78
	3	80.43	3.54	57.66	2.83	64.64	3.16	55.87	4.79	37.03	1.55
	4	64.73	3.24	53.55	2.99	50.90	2.16	55.35	3.37	38.15	1.65
	5	62.99	2.04	55.70	3.65	64.17	4.76	52.36	3.32	40.13	1.91
2	1	91.15	5.44	56.54	4.32	64.73	5.62	60.24	5.53	35.70	0.90
	2	80.79	6.70	74.10	6.16	62.88	5.41	56.23	6.54	36.00	0.95
	3	109.43	5.55	78.16	6.60	67.46	6.30	56.16	6.70	37.08	1.16
	4	67.72	14.37	81.44	6.24	58.13	6.08	53.34	8.38	35.25	2.09
	5	68.69	9.23	58.19	3.94	58.65	3.80	48.84	5.67	36.32	1.19
3	1	56.27	11.81	52.55	3.04	56.35	3.28	68.76	4.23	37.26	0.90
	2	70.65	5.42	43.10	2.21	54.66	3.27	77.83	5.50	37.99	0.60
	3	63.38	4.86	47.11	3.47	52.05	2.48	59.98	4.50	38.07	0.98
	4	74.66	3.95	52.00	2.87	52.71	2.97	64.90	3.88	37.20	0.80
	5	71.99	4.13	44.04	1.99	59.83	2.87	78.49	5.86	37.49	0.75
4	1	84.94	3.65	74.63	4.37	67.61	3.17	59.32	4.48	42.32	0.78
	2	72.36	7.54	67.04	3.12	54.58	2.74	61.28	3.34	40.53	0.88
	3	82.77	3.53	65.26	2.71	59.72	2.33	63.13	3.45	39.63	0.97
	4	77.62	3.21	57.26	3.10	55.69	2.91	67.07	4.20	39.17	0.65
	5	87.96	7.89	61.23	3.57	58.72	3.13	65.90	4.46	40.29	1.01
5	1	75.25	3.03	93.05	6.25	98.26	6.52	65.66	4.73	39.86	2.08
	2	83.77	3.45	84.36	3.96	91.43	3.93	63.72	4.01	40.28	0.87
	3	77.27	6.23	89.49	5.00	92.56	5.73	64.39	6.61	41.43	0.92
	4	78.18	3.87	81.16	4.08	87.13	4.58	72.60	3.72	39.10	1.22
	5	75.17	2.95	92.03	7.13	86.61	7.15	57.28	4.63	40.59	1.87
6	1	73.24	2.93	77.01	3.74	72.27	3.04	58.70	1.03	37.98	0.89
	2	71.60	4.83	71.85	3.63	69.66	3.99	54.73	3.91	38.23	1.37
	3	72.12	2.22	69.41	4.01	67.00	2.90	63.95	6.41	34.83	1.07
	4	71.27	5.16	71.52	5.27	65.44	4.11	62.21	4.24	37.62	1.52
	5	68.71	5.71	56.52	4.08	62.42	4.09	75.61	2.56	36.58	0.79
7	1	78.97	2.83	64.77	4.37	74.50	4.70	76.59	7.45	37.03	1.45
	2	74.45	3.27	60.22	4.21	63.87	4.35	62.46	5.72	36.36	2.32
	3	78.47	2.34	64.41	4.35	63.76	4.33	60.41	4.82	35.34	1.12
	4	80.35	4.27	62.61	5.64	66.88	6.00	62.60	6.07	33.33	1.15
	5	78.51	3.76	61.41	4.39	60.97	4.27	67.55	5.76	32.08	0.80
8	1	76.73	2.76	77.76	6.00	85.20	5.99	49.56	3.88	34.02	3.41
	2	74.89	3.23	78.99	7.16	84.33	7.73	49.52	3.78	35.93	1.83
	3	78.31	3.15	81.02	5.74	87.62	5.62	54.67	6.38	36.90	2.13
	4	72.51	1.99	73.34	5.74	78.83	6.27	52.58	3.78	35.17	2.12
	5	74.83	1.86	85.48	6.91	98.70	8.06	51.03	4.49	35.27	1.89

	1	77.79	1.98	103.25	7.63	93.82	5.81	69.33	2.97	36.90	0.75
	2	67.14	2.00	82.84	6.81	85.50	7.17	66.47	3.80	34.23	1.36
9	3	67.60	2.22	82.08	5.37	98.24	6.07	66.43	3.18	37.67	0.74
	4	72.19	2.32	104.38	6.16	96.98	5.73	71.84	2.83	36.79	0.46
	5	68.99	1.92	103.94	5.22	91.71	4.23	73.43	3.73	36.10	0.63
	1	79.67	6.82	77.88	4.89	79.32	4.67	69.53	5.50	34.23	0.92
	2	72.24	2.08	82.44	5.73	71.13	5.27	65.31	5.73	30.50	1.30
10	3	74.82	3.55	75.96	4.82	69.07	4.09	65.06	5.54	34.00	1.20
	4	56.84	8.36	82.41	6.26	74.90	5.44	69.27	4.87	34.09	1.20
	5	78.97	2.06	86.29	5.10	76.48	4.44	75.86	4.38	33.98	1.16
	1	67.20	2.19	65.51	4.62	65.97	4.78	56.12	4.96	32.35	1.39
	2	78.72	3.45	65.04	4.58	71.42	5.48	70.80	8.62	31.17	2.39
11	3	69.10	2.45	57.94	3.95	61.09	4.11	59.61	5.08	27.68	1.17
	4	81.50	3.74	60.63	5.14	73.36	5.04	56.26	5.63	35.83	1.41
	5	68.23	3.20	62.82	5.23	61.39	5.19	53.80	5.80	29.57	1.34
	1	80.19	2.23	90.35	7.83	75.82	9.54	67.23	3.75	32.97	1.39
	2	78.83	2.74	103.01	9.88	82.85	7.58	60.60	4.86	30.76	1.21
12	3	85.10	3.59	97.29	8.83	83.53	8.08	51.37	5.50	32.54	1.16
	4	76.98	2.06	79.86	6.53	72.14	6.56	63.31	3.88	30.56	1.01
	5	71.27	2.45	68.15	7.53	77.59	6.89	59.76	4.07	32.27	2.18
	1	78.00	3.06	63.34	3.70	71.42	3.81	69.90	5.08	32.23	0.80
	2	79.46	3.05	81.69	5.96	85.03	5.78	77.28	5.80	34.67	1.26
13	3	76.54	3.14	65.55	3.89	77.76	4.16	74.78	6.88	31.34	1.06
	4	72.18	3.38	70.80	4.65	76.61	5.37	59.16	6.46	34.78	0.84
	5	70.79	3.49	81.02	6.15	80.18	5.72	71.80	5.88	34.13	1.01
	1	83.65	2.16	69.98	3.75	70.72	3.35	57.63	3.38	36.33	0.98
	2	79.28	1.53	48.64	3.54	67.91	3.23	59.94	3.33	38.96	1.28
14	3	76.57	1.66	59.28	3.31	64.78	3.03	65.61	3.10	46.68	1.32
	4	75.71	1.59	58.81	3.05	68.40	3.39	71.83	3.69	41.24	0.83
	5	64.81	5.33	57.75	2.99	71.50	3.37	62.22	2.88	38.62	1.02
	1	78.49	4.46	51.03	3.48	61.61	4.01	60.17	4.31	37.16	1.46
	2	76.32	3.32	52.42	3.66	62.13	4.70	62.09	4.85	39.13	1.37
15	3	77.53	2.99	60.43	6.06	63.35	5.15	58.79	4.22	40.33	4.49
	4	73.87	2.83	64.05	4.73	63.27	4.91	61.85	4.68	35.08	1.99
	5	70.01	2.78	61.35	4.15	63.09	4.65	59.32	2.80	41.52	0.91
	1	80.73	1.95	81.52	3.62	78.25	3.38	67.23	4.59	37.54	0.54
	2	76.85	1.78	90.83	4.62	85.71	3.58	66.24	4.89	37.70	0.85
16	3	80.19	1.67	89.08	3.64	81.95	3.01	66.28	5.78	39.15	0.70
	4	78.17	2.16	76.13	4.46	78.92	4.11	72.94	5.26	35.51	0.90
	5	72.93	1.99	82.83	4.31	84.08	3.86	66.80	5.82	35.23	0.77
	1	71.85	2.29	66.08	3.41	66.29	3.68	58.37	2.47	35.70	0.88
17	2	73.66	2.36	70.32	3.51	70.75	3.72	54.21	3.47	38.58	1.09
	3	71.29	1.53	65.07	3.48	65.10	3.53	57.98	2.46	34.87	0.96
	4	66.03	2.26	62.34	3.50	57.95	3.57	60.85	2.72	36.58	0.63

	5	73.57	2.15	64.87	3.20	63.78	3.28	60.72	2.77	36.82	0.73
18	1	73.08	1.55	95.06	55.21	76.87	0.88	67.95	7.67	36.89	0.70
	2	82.22	2.10	69.65	3.76	71.72	3.88	60.59	4.46	34.74	0.64
	3	67.43	3.48	79.71	5.32	87.08	5.89	72.54	7.07	38.77	1.12
	4	80.01	2.90	82.55	5.92	87.55	6.57	57.83	3.68	41.74	1.27
	5	69.31	2.87	70.92	6.48	79.57	6.11	64.08	9.48	36.89	1.22
19	1	75.37	2.59	78.09	5.18	72.42	4.65	59.48	5.30	35.73	0.96
	2	80.57	2.39	80.67	6.90	69.95	5.84	49.47	7.36	38.56	0.95
	3	73.52	3.24	73.51	5.32	73.07	5.83	51.93	5.08	36.94	1.32
	4	73.98	3.03	63.54	6.04	63.95	5.48	55.44	6.37	35.39	1.70
	5	74.02	3.24	79.17	4.50	74.07	4.73	51.09	4.27	35.63	0.91
20	1	66.48	1.61	78.16	4.41	74.28	4.28	60.28	6.05	40.99	1.02
	2	64.86	3.10	67.41	2.89	71.49	2.92	59.75	4.30	38.81	0.57
	3	65.16	2.83	66.81	3.51	69.70	3.71	58.83	5.94	35.04	0.79
	4	60.18	1.54	64.84	3.23	71.03	3.27	58.88	3.66	35.42	0.60
	5	66.01	2.67	67.01	4.10	70.21	3.48	63.43	5.73	38.45	0.68
Total mean		74.56	3.48	71.64	5.25	72.21	4.63	62.43	4.80	36.51	1.20
Total SD ±		7.26	2.10	13.70	5.31	11.36	1.50	7.17	1.47	3.08	0.59

Table S-3: Mean and standard deviation values of key parameters, *ABP*, *CBv* (right and left sides), *HR* and *CO*2 for all subject recordings at thigh cuff condition

TFA output	Condition	Measurement variability		Subject variability	
		Mean	SE	Mean	SE
VLF Coherence	Normocapnia	0.068	0.0003	0.0017	< 0.0001
	Hypercapnia	0.0709	0.0006	0.0123	0.0002
	Thigh cuff	0.0589	0.0003	0.0068	0.0001
VLF Gain	Normocapnia	0.571	0.0054	0.0195	0.0002
	Hypercapnia	0.3318	0.0023	0.1214	0.0012
	Thigh cuff	0.5315	0.0030	0.0274	0.0003
VLF Phase (in degrees)	Normocapnia	770.7302	5.5893	56.0128	0.5420
	Hypercapnia	644.6319	5.5174	93.8909	0.9010
	Thigh cuff	923.4395	6.5033	132.5179	1.9247
LF Coherence	Normocapnia	0.0404	0.0003	0.0026	< 0.0001
	Hypercapnia	0.0366	0.0002	0.0085	0.0001
	Thigh cuff	0.0363	0.0004	0.0039	< 0.0001
LF Gain	Normocapnia	0.6651	0.0058	0.0324	0.0003
	Hypercapnia	0.5214	0.0020	0.1461	0.0014
	Thigh cuff	0.837	0.0048	0.0384	0.0003
LF Phase (in degrees)	Normocapnia	273.2061	2.1544	10.0688	0.6381
	Hypercapnia	154.9904	1.4349	16.0933	0.1581
	Thigh cuff	417.7729	4.8467	24.3715	0.2139
HF Coherence	Normocapnia	0.006	< 0.0001	0.0367	0.0003
	Hypercapnia	0.008	0.0001	0.0282	0.0002
	Thigh cuff	0.0063	0.0001	0.0443	0.0003
HF Gain	Normocapnia	0.0404	0.0004	0.862	0.0072
	Hypercapnia	0.1225	0.0014	0.5261	0.0035
	Thigh cuff	0.0327	0.0002	0.6439	0.0046
HF Phase (in degrees)	Normocapnia	6.0202	0.0254	79.9874	0.8968
	Hypercapnia	13.4055	0.1205	128.6226	0.9016
	Thigh cuff	14.6518	0.2254	89.8816	1.0609

Table S-4: Mean and standard error (SE) of TFA parameters variations of measurement and subject variability in different conditions at frequency bands

Parameter	Description
Function	tfa_out = tfa_car (ABP,CBFV,fs,params)
	Inputs
ABP	Arterial blood pressure (assumed to be in mmHg)
CBFV	Cerebral blood flow velocity (assumed to be in cm/s)
fs	Sampling frequency (assumed to be in Hz)
params	A series of parameters that control TFA analysis (window-length, frequency bands …). If this is not provided, default values, corresponding to those recommended in the white paper, will be used. These default values are given below for each parameter.
params.vlf	[0.02,0.07]: Limits of very low frequency band (in Hz).
params.lf	[0.07,0.2]: Limits of low frequency band (in Hz).
params.hf	[0.2,0.5]: Limits of high frequency band (in Hz).
	Outputs
tfa_out.Mean_abp	Mean ABP
tfa_out.Std_abp	Standard deviation of ABP
tfa_out.Mean_cbfv	Mean CBFV
tfa_out.Std_cbfv	Standard deviation of CBFV
tfa_out.Gain_vlf	average gain in very low frequency band
tfa_out.Phase_vlf	average phase (in degrees) in very low frequency band
tfa_out.Coh^2_vlf	average magnitude-squared coherence in very low frequency band
tfa_out. P_abp_vlf	ABP power in very low frequency band
tfa_out.P_cbfv_vlf	CBFV power in very low frequency band
tfa_out.Gain_lf	average gain in low frequency band
tfa_out.Phase_lf	average phase (in degrees) in low frequency band
tfa_out.Coh^2_lf	average magnitude-squared coherence in low frequency band
tfa_out.P_abp_lf	ABP power in very low frequency band
tfa_out.P_cbfv_lf	CBFV power in very low frequency band
tfa_out.Gain_hf	average gain in high frequency band
tfa_out.Phase_hf	average phase (in degrees) in high frequency band
tfa_out.Coh^2_hf	average magnitude-squared coherence in high frequency band
tfa_out.P_abp_hf	ABP power in high frequency band
tfa_out.P_cbfv_hf	CBFV power in high frequency band

Table S-5*:* List of MATLAB function's inputs and outputs as mentioned in the documentation prepared by David Simpson, reproduced with permission and layout changes [5]

b. Figures

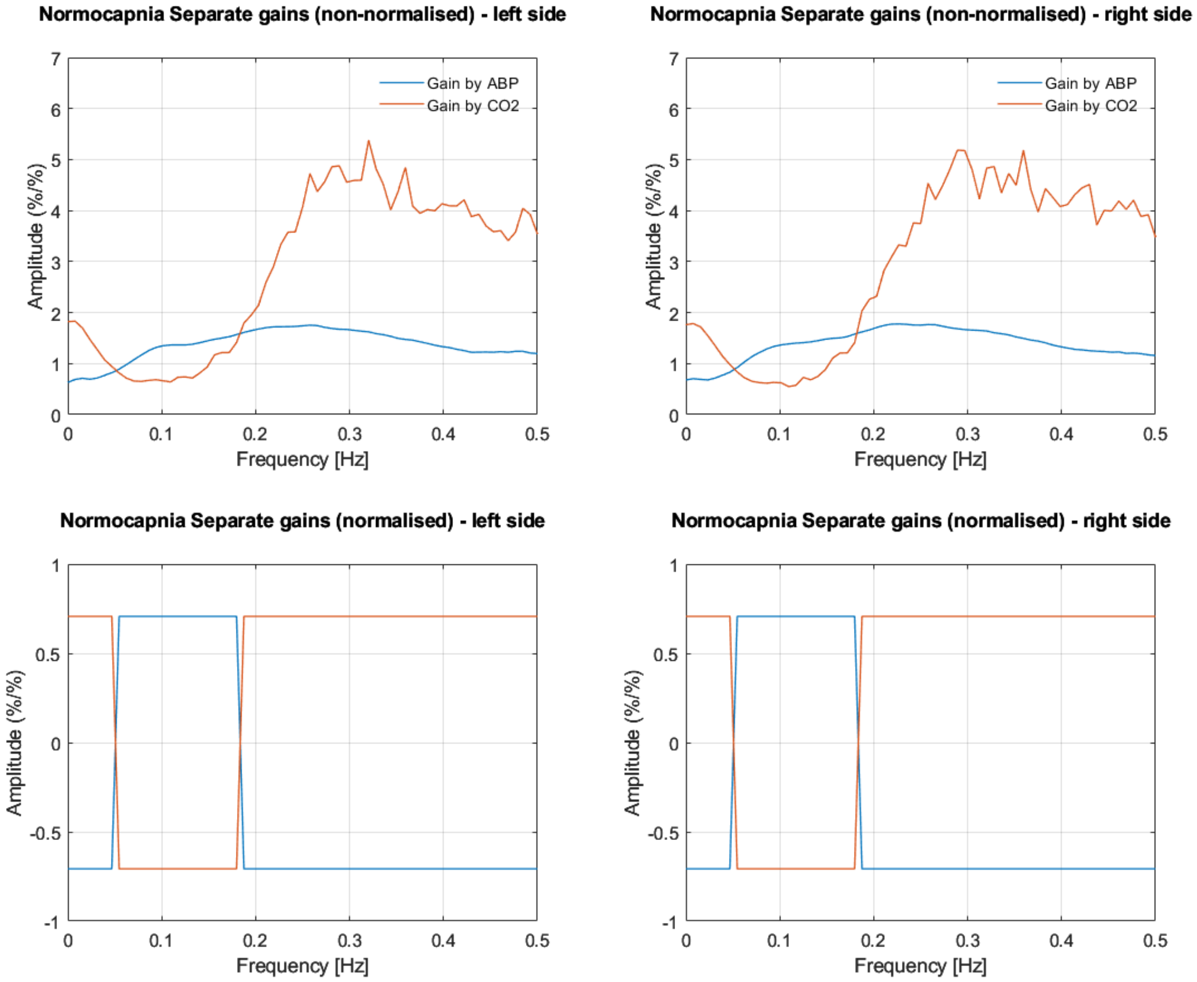

Figure S-1: Normalised vs non-normalised separate gains for both right and left sides at normocapnia condition using *ABP* and CO_2 inputs

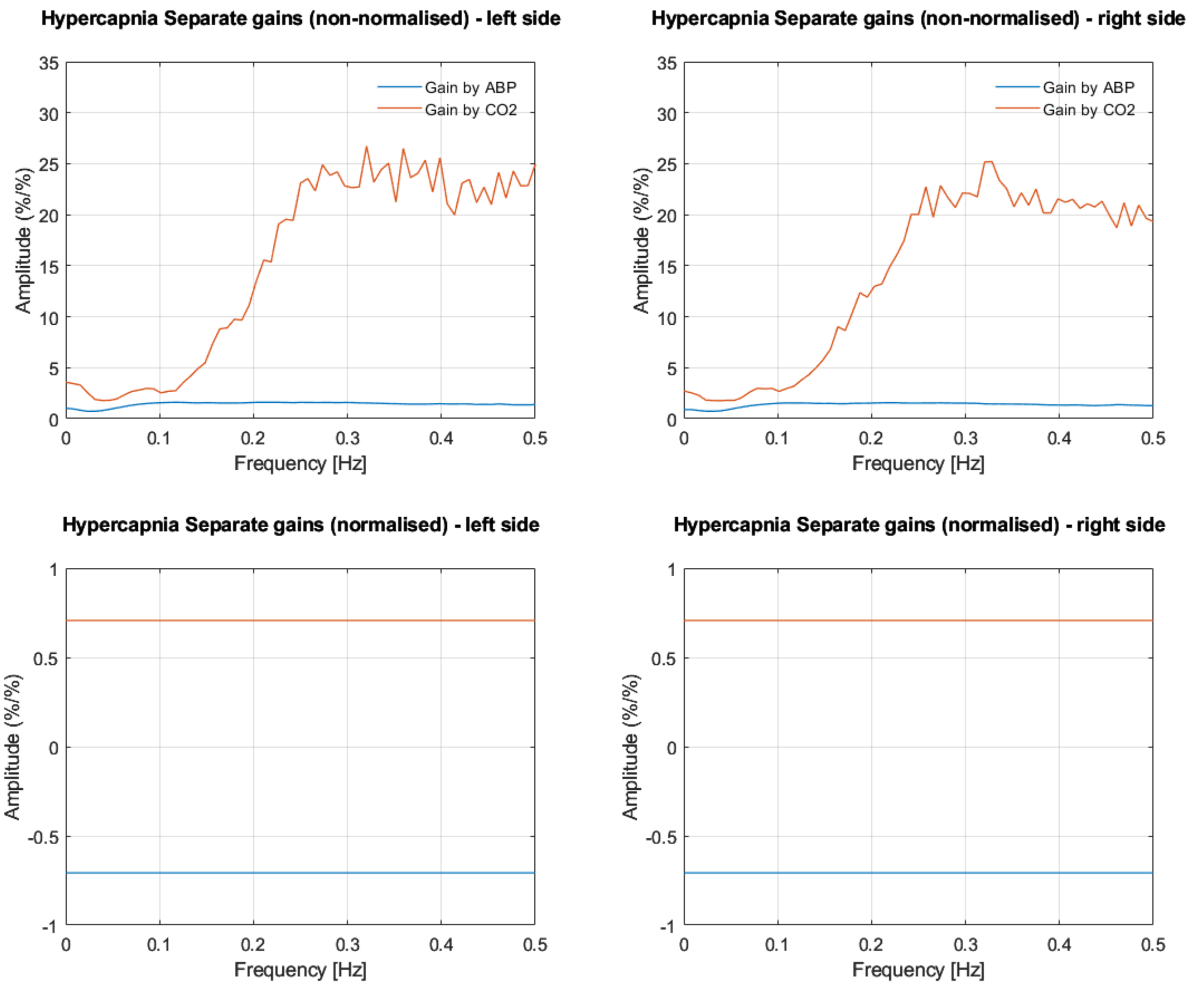

Figure S-2: Normalised vs non-normalised separate gains for both right and left sides at hypercapnia condition using *ABP* and CO_2 inputs

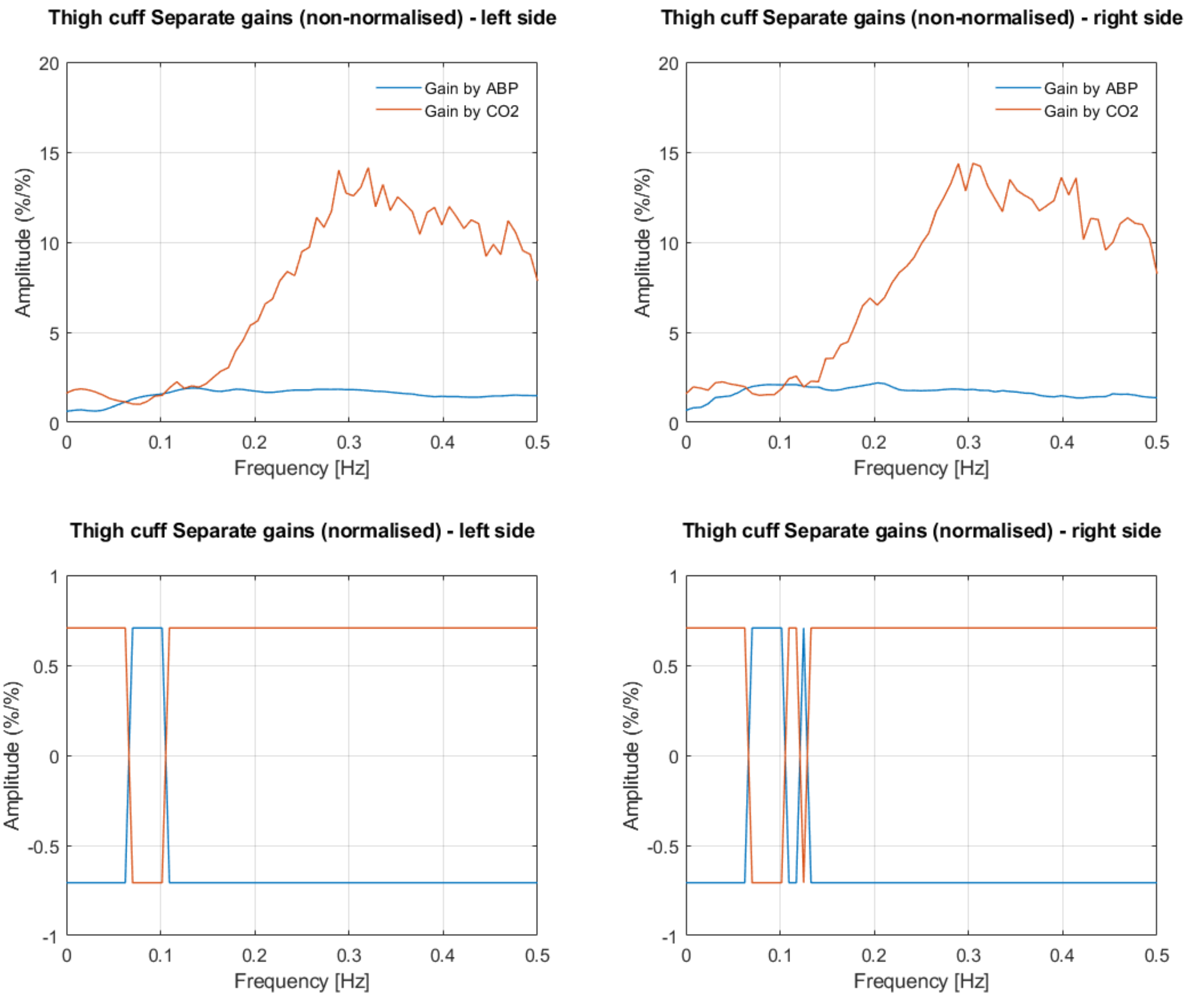

Figure S-3: Normalised vs non-normalised separate gains for both right and left sides at thigh cuff condition using *ABP* and CO_2 inputs

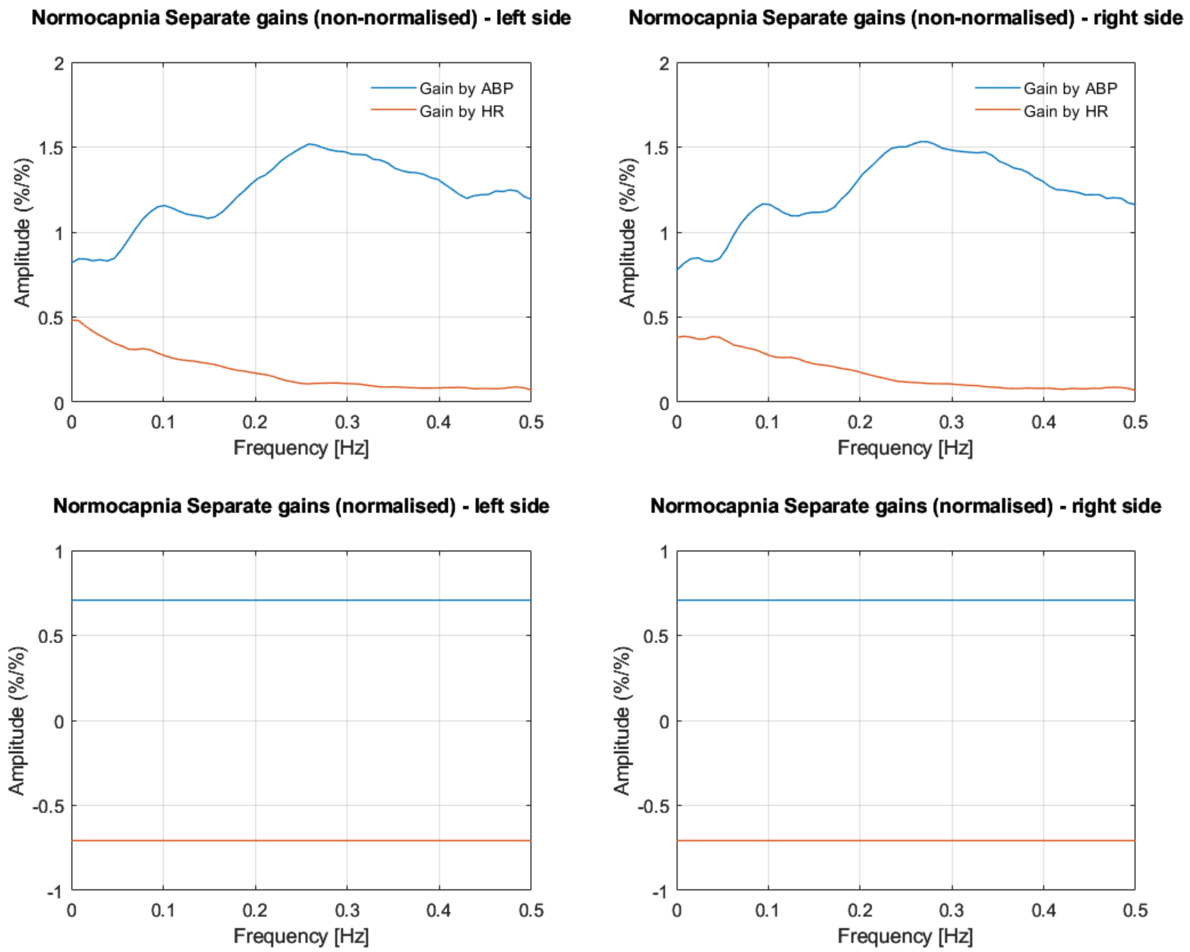

Figure S-4: Normalised vs non-normalised separate gains for both right and left sides at normocapnia condition using *ABP* and *HR* inputs

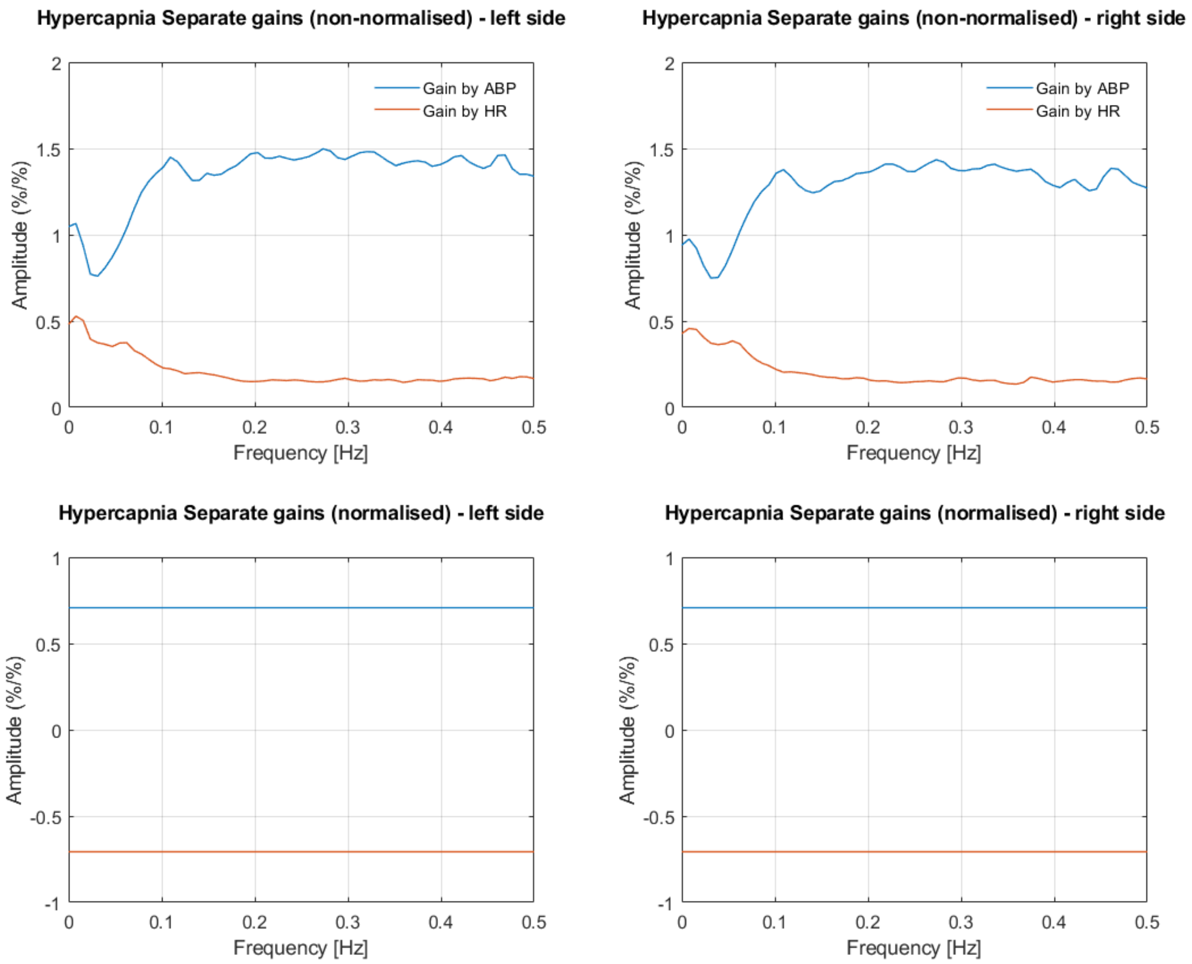

Figure S-5: Normalised vs non-normalised separate gains for both right and left sides at hypercapnia condition using *ABP* and *HR* inputs

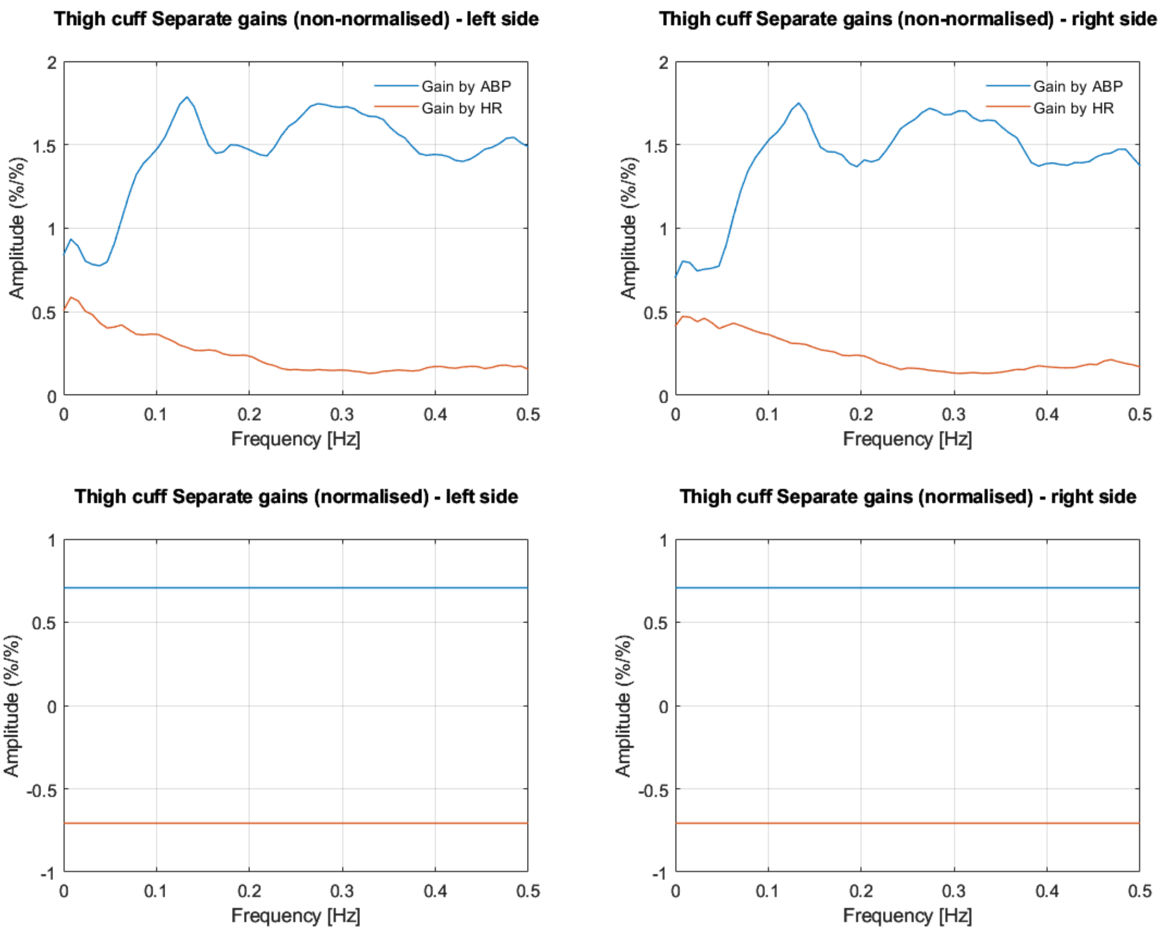

Figure S-6: Normalised vs non-normalised separate gains for both right and left sides at hypercapnia condition using *ABP* and *HR* inputs

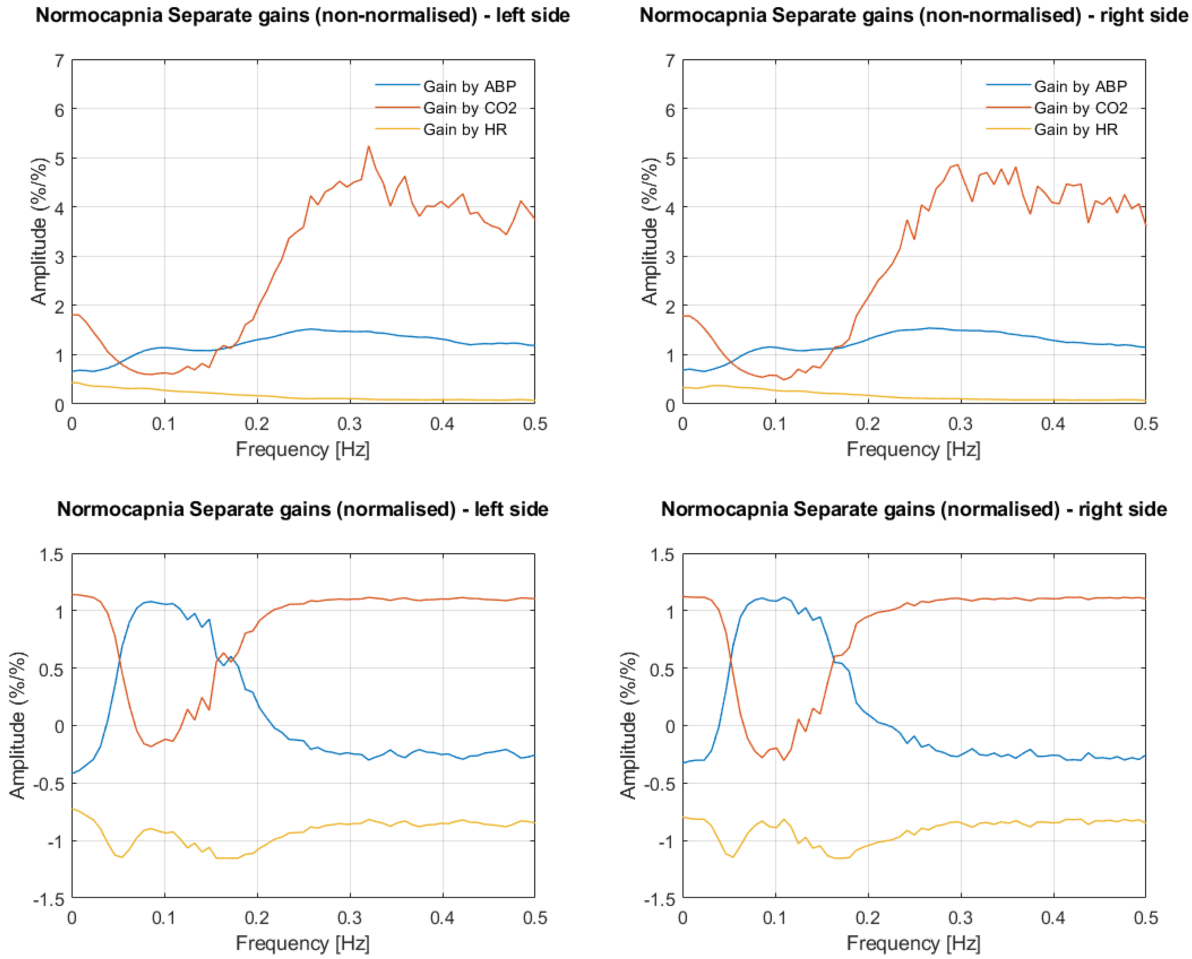

Figure S-7: Normalised vs non-normalised separate gain for both right and left sides at normocapnia condition using 3-inputs

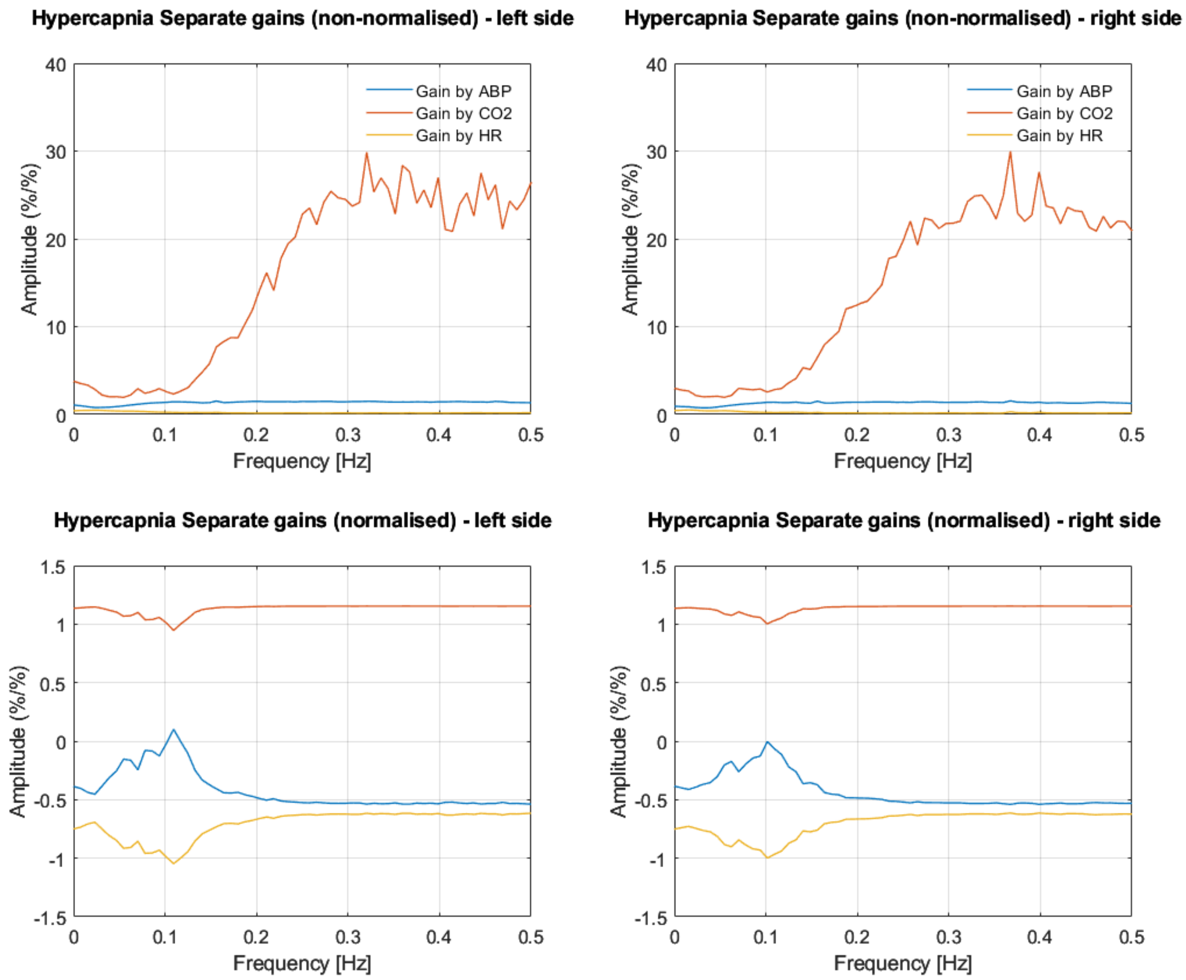

Figure S-8: Normalised vs non-normalised separate gain for both right and left sides at hypercapnia condition using 3-inputs

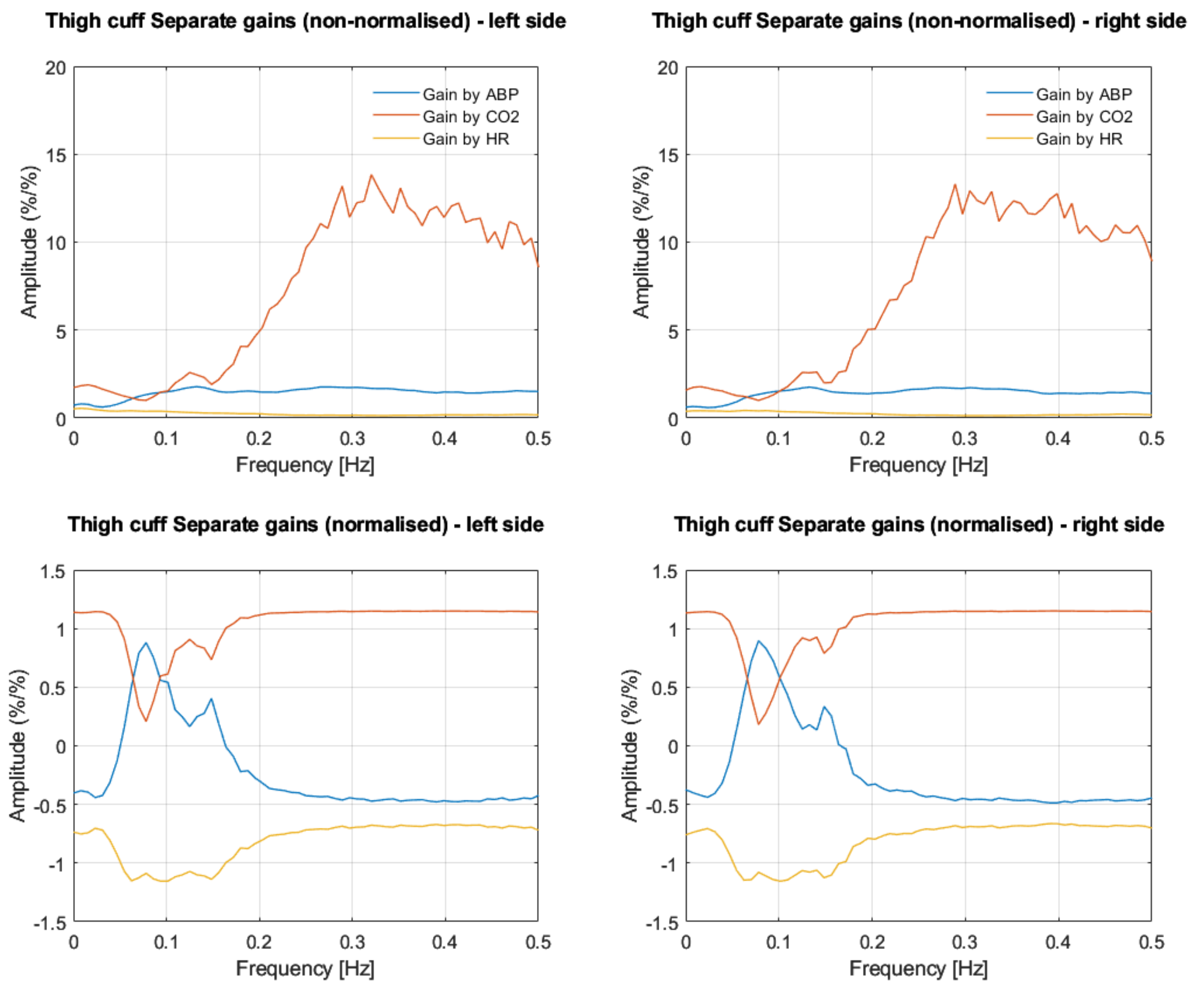

Figure S-9: Normalised vs non-normalised separate gain for both right and left sides at hypercapnia condition using 3-inputs

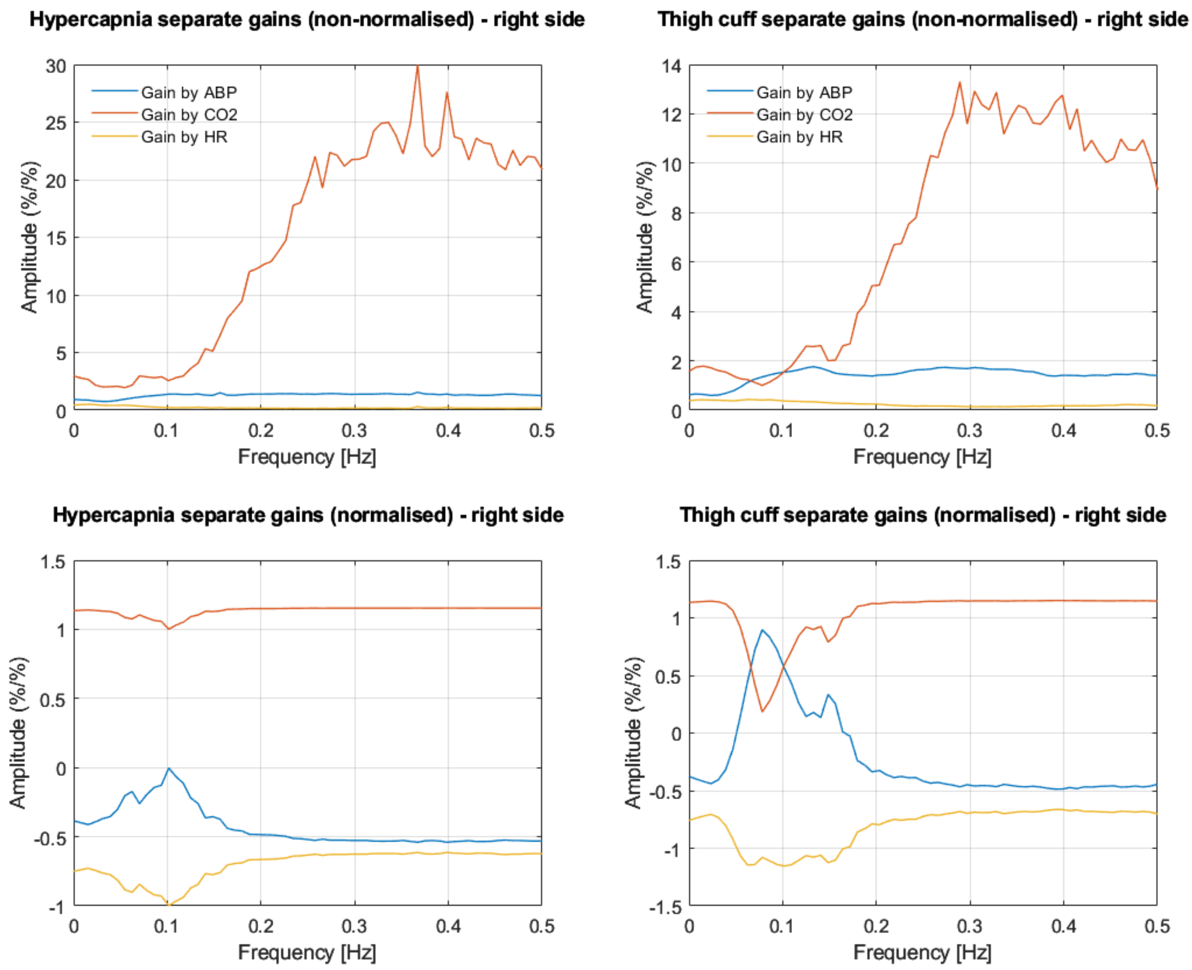

Figure S-10: Normalised vs non-normalised separate gain for both hypercapnia and thigh cuff conditions at the right side using 3-inputs

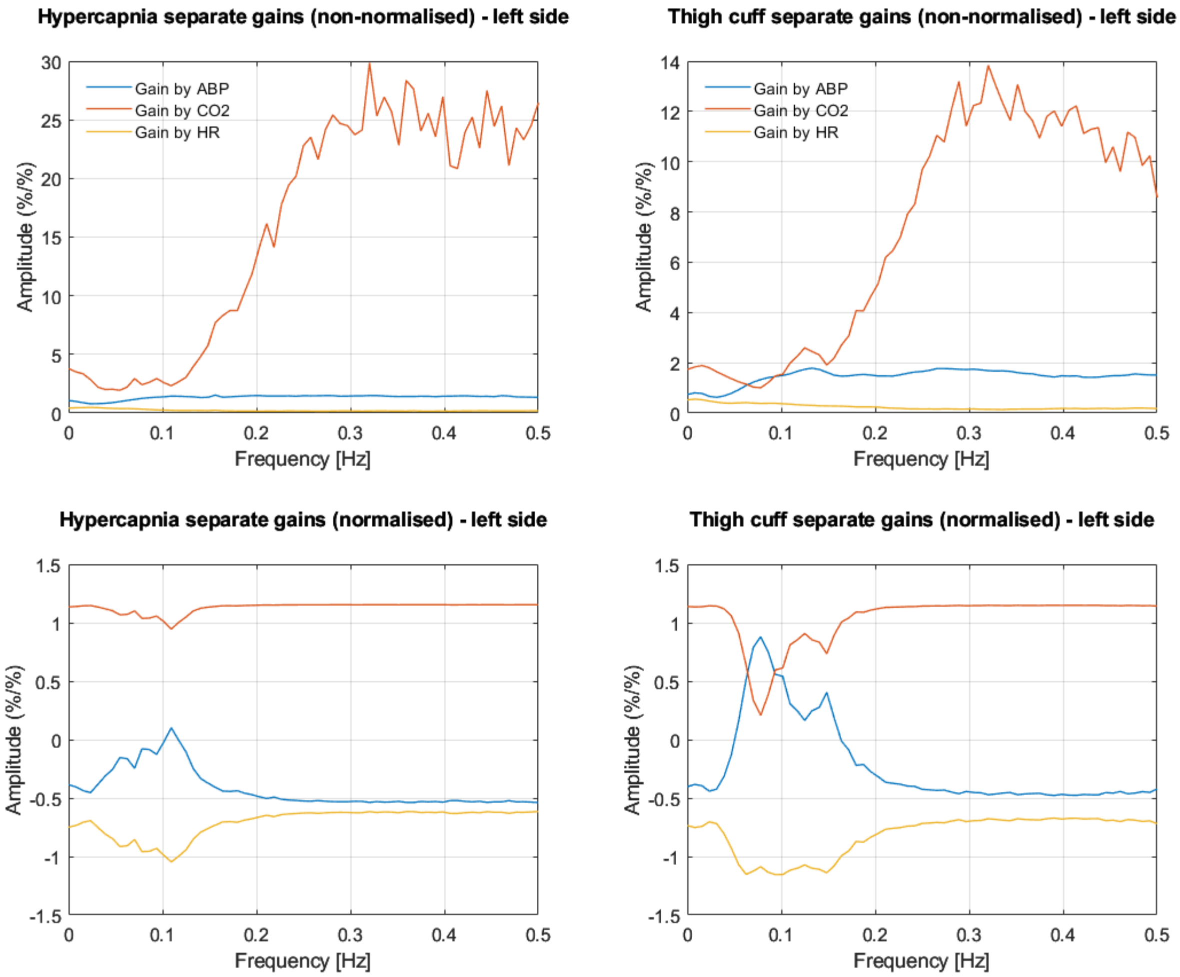

Figure S-11: Normalised vs non-normalised separate gain for both hypercapnia and thigh cuff conditions at the left side using 3-inputs

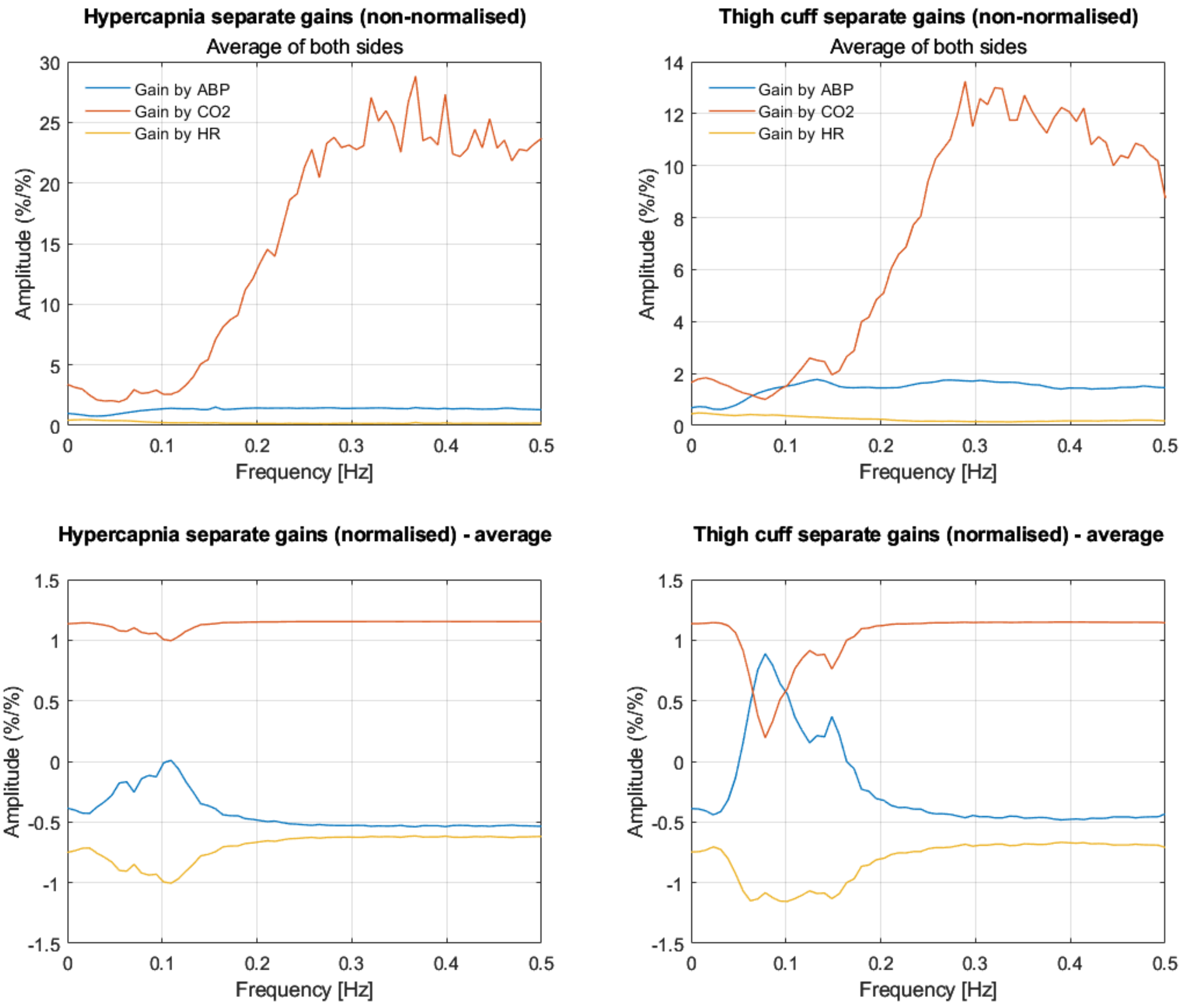

Figure S-12: Normalised vs non-normalised separate gain for both hypercapnia and thigh cuff conditions on the average of both right and left sides using 3-inputs

List of Figures

List of Tables